Characterization of Human Spinal Cord Stem Cells to Improve the Translation of Cell Therapies for Spinal Cord Injury

Ahmad Galuta

Thesis submitted to the University of Ottawa in partial fulfillment of the requirements for the

Doctorate in Philosophy, Neuroscience

Department of Cellular and Molecular Medicine

Faculty of Medicine

University of Ottawa

Abstract

Stem cell treatments for spinal cord injury (SCI) are effective in pre-clinical animal model research but not yet for humans. Two promising stem cell repair strategies involve (1) endogenous neural stem/progenitor cells (NSPCs) and (2) induced pluripotent stem cells (iPSCs). Delineating species differences in spinal cord NSPC biology is essential to inform human SCI endogenous regeneration and repair. Understanding the phenotypic differences between iPSC-derived NSPCs and primary spinal cord NSPCs would also improve the clinical application of iPSC-derived NSPC therapy in human SCI.

To directly compare the molecular and functional attributes of spinal cord NSPCs between humans and animal models of SCI, we designed an in vitro model that allows the characterization of primary human, pig, and rat NSPCs under identical conditions. We found an enrichment of transcription factors in NSPCs of either species that may underlie their differentiation and proliferation potentials. Specifically, human NSPCs are neurogenic, whereas pig and rat NSPCs are gliogenic. Also, the proliferation rate of human and pig NSPCs is less than rat NSPCs. Subsequently, we expanded our in vitro model to examine the responses of NSPCs to inflammation and regenerative factors. Surprisingly, inflammation had induced glial scarring mechanisms from pig and rat NSPCs but potentiated neurogenesis of human NSPCs. We also found species-specific responses to regenerative factors that depend on the type of factor used, concentration, and duration of treatment.

To assess the extent that iPSC-derived NSPCs phenocopy primary spinal cord NSPCs, we created iPSC-derived NSPCs with a previously reported brain or spinal cord phenotype and directly compared them with isogenic primary NSPCs. We found that iPSC-derived NSPCs exhibit an earlier developmental stage and a greater proliferation rate. We also found that primary NSPCs

possess a unique differentiation potential and regional polarity along the rostral-caudal and dorsoventral axes.

In summary, we discovered that species differences in NSPC biology exist between human and animal primary spinal cord NSPCs and that iPSC-derived NSPCs do not recapitulate the transcriptional nor functional attributes of primary spinal cord NSPCs. This thesis highlights the translational gap between pre-clinical research and the clinical application of stem cell treatments that target endogenous NSPCs or transplant iPSC-derived NSPCs.

Acknowledgements

I would like to take a moment to express my sincerest appreciation for the support and guidance that I received throughout my doctoral odyssey.

Foremost, I am grateful to my supervisor, Dr. Eve Tsai, whose confidence in me from the outset and provision of an opportunity to engage in a unique and impactful research project proved instrumental in the successful culmination of my efforts. Her trust in my abilities empowered me to make informed decisions and pursue my research interests. I am also thankful for the opportunities to travel, attend conferences, and network. Without her invaluable support, I would not have been able to attain the level of achievement that I did.

I would like to extend my gratitude to my thesis advisory committee members, Dr. Jing Wang and Dr. Patrice Smith, for their sagacious feedback, constructive critique, and kindness. Dr. Wang's specific technical advice proved vital for my experiments' success on many occasions. Dr. Smith's unwavering encouragement boosted my confidence and propelled me forward with every meeting, keeping me motivated throughout my journey. I also thank Dr. Yun Li for agreeing to attend my defence. Your external review and insightful feedback are deeply appreciated.

I thank all the lab members, collaborators, and students whose collaborative efforts and support have contributed to a productive and enjoyable research experience. A special shout-out to Jason and Ryan for their impressive brain power, help with the overnight shifts, and the exquisitely entertaining company that propelled my research project and experience to new heights. To my friends, Basel, Amir, Grishma, and Alex, I am grateful for the support that you've shown in your own ways and the positive energy you've brought into my life.

I would like to express my sincere gratitude to Yasmine, Karim, Andrée. Your unwavering support, encouragement, and assistance have kept me motivated and focused, even during the most challenging times. Thank you for being there for me and for believing in me.

Lastly, my mother, father, and sister, whose unwavering love, patience, and understanding have kept me strong, deserve my deepest gratitude. Their encouragement has been a beacon of hope throughout my doctoral journey, and I treasure their presence in my life.

Table of Contents

List of Publications

Chapter 2: A Guide to Extract Spinal Cord for Translational Stem Cell Biology Research: Comparative Analysis of Adult Human, Porcine, and Rat Spinal Cord Stem Cells

Ahmad Galuta, Ryan Sandarage, Diana Ghinda, Angela M. Auriat, Suzan Chen,

Jason C. S. Kwan, Eve C. Tsai

Published in *Frontiers in Neuroscience*, section *Neurogenesis*, volume 14, Article 607, June 2020, Pages 174-185

doi: 10.3389/fnins.2020.00607

In this manuscript, Ahmad Galuta conducted all of the rat spinal cord harvests, some of the porcine spinal cord harvests, and all of the spinal cord dissections. Ahmad developed and performed all the *in vitro* assays, acquired the immunohistochemistry and immunocytochemistry data, and contributed to the manuscript writing.

Chapter 3: Primary Human, Pig, and Rat Spinal Cord NSPCs are Transcriptionally Unique and Exhibit Distinct Responses to Inflammatory and Regenerative cues

Ahmad Galuta, Diana Ghinda, Ryan Sandarage, Jason C.S. Kwan, Kyle Malone, Santina Temi, Isaac Kim, Ellen McDoney, Lilia Tran, Michael Hildebrand, Eve C. Tsai

In preparation for submission

In this manuscript, Ahmad Galuta designed all of the experiments, conducted most of the *in vitro* functional assays, collected all of the RNA samples for sequencing, acquired most of the

immunocytochemistry data, analyzed most of the *in vitro* functional assay data, and contributed to most of the manuscript writing.

Chapter 4: Isogenic NSPCs derived from the adult human spinal cord and pluripotent stem cells exhibit distinct functional and transcriptional signatures

Ahmad Galuta, Diana Ghinda, Ellen McDoney, Carole Dore, William L. Stanford, Eve C. Tsai

In preparation for submission

In this manuscript, Ahmad Galuta designed all the experiments, conducted all the skin fibroblast cultures, and performed most of the genetic reprogramming into induced pluripotent stem cells (iPSCs). Ahmad performed the iPSC differentiation protocols and the *in vitro* functional assays, collected all the RNA samples for sequencing, acquired all the immunocytochemistry data, analyzed all the *in vitro* functional assay data, and contributed to most of the manuscript writing.

Appendix A: Demographic profile and spinal cord region influence human NSPC function

Ahmad Galuta, Diana Ghinda, Raiff Rached, Eugene Wai, Eve C. Tsai

In preparation for submission

In this manuscript, Ahmad Galuta designed all the experiments, conducted all *in vitro* functional assays, including differentiation, proliferation, primary yield, and doubling time assessments, acquired all of the immunocytochemistry data, analyzed some of the *in vitro* functional assay data, and contributed to most of the manuscript writing.

List of Tables

List of Figures

List of Abbreviations

ACSF	Artificial cerebrospinal fluid
ANOVA	Analysis of variance
ASIA	American Spinal Cord Injury Association
ATP	Adenosine triphosphate
BDNF	Brain-derived neurotrophic factor
BMP	Bone morphogenic protein
BSCB	Blood-spinal cord barrier
CNS	Central nervous system
CSF	Cerebrospinal fluid
CSPG	Chondroitin sulfate proteoglycan
CTNF	Ciliary neurotrophic factor
DAPI	4′,6-diamidino-2-phenylindole
DAPT	tert-Butyl (S)-{(2S)-2-[2-(3,5-difluorophenyl)acetamido]propanamido}phenylacetate
dbcAMP	Dibutyryl cyclic adenosine monophosphate
DE	Differentially expressed
DIV	Days *in vitro*
DMEM	Dulbecco's Modified Eagle Medium
ECM	Extracellular matrix
EFH	EGF, FGF, Heparin
EGF	Epidermal growth factor
EGTA	Egtazic acid
ERG	Ependymoradial glia
FBS	Fetal bovine serum
FDR	False discovery rate
FGF	Fibroblast growth factor
GABA	γ-Aminobutyric acid
GDF	Growth differentiation factor
GDNF	Glial-derived neurotrophic factor
GFAP	Glial fibrillary acidic protein
GFP	Green fluorescent protein
GSEA	Gene set enrichment analysis
GTP	Guanosine-5'-triphosphate
HBSS	Hanks' Balanced Salt Solution
HCl	Hydrochloric acid
HEPES	2-[4-(2-hydroxyethyl)piperazin-1-yl]ethanesulfonic acid
HGF	Hepatocyte growth factor
HOX	Homeobox
ICAM	Intercellular adhesion molecule
IGF	Insulin-like growth factor

LCMD	Laser capture microdissection
LDN 193189	4-[6-[4-(1-Piperazinyl)phenyl]pyrazolo[1,5-a]pyrimidin-3-yl]quinoline dihydrochloride
LIF	Leukemia inhibitory factor
MSC	Mesenchymal stem cell
NCAM	Neural cell adhesion molecule
NDD	Neurological determination of death
NES	Normalized enrichment score
NGS	Normal goat serum
NIM	Neural induction media
NM	Neurobasal-A medium
NMM	Neural maintenance medium
NMP	Neuromesodermal progenitor
NO	Nitric oxide
NSPC	Neural stem/progenitor cell
NT3	Neurotrophin protein 3
OEC	Olfactory ensheathing cell
OPC	Oligodendrocyte progenitor cell
PBS	Phosphate buffer saline
PCA	Principal component analysis
PDGF	Platelet-derived growth factor
PDGFR	Platelet-derived growth factor receptor
PFA	Paraformaldehyde
PS	Penicillin streptomycin
PSC	Pluripotent stem cell
RA	Retinoic acid
ROS	Reactive oxygen species
RQN	RNA quality number
SCI	Spinal cord injury
SFM	Serum free media
SGZ	Subgranular zone
SHH	Sonic hedgehog
SMAD	Suppressor of mothers against decapentaplegic
SVZ	Subventricular zone
TGF	Transforming growth factor
TGLN	Trillium Gift of Life Network
TNF	Tumor necrosis factor
VCAM	Vascular cell adhesion molecule
VEGF	Vascular endothelial growth factor
WNT	Wingless-related integration site

Chapter 1: An Introduction to Spinal Cord Injury and Stem Cell Therapies

1.1 Overview of traumatic spinal cord injury

Spinal cord injury (SCI) is a devastating and debilitating condition that can happen to anyone at anytime, resulting in life-changing consequences. Injury can be induced through physical trauma to the spinal cord, termed traumatic SCI, but also by non-traumatic means such as infections or tumors (Weidner, Rupp, & Tansey, 2017). Symptoms of SCI include partial or complete loss of sensory, motor, and autonomic function below the level of injury (Weidner et al., 2017). To date, clinical trials have failed to demonstrate an effective cure for SCI that restores neurological function resulting in patients experiencing life-enduring consequences (Failli et al., 2021). Furthermore, no two injuries are identical, further complicating the development of an effective treatment.

A significant roadblock in the successful application of clinical trials may be the lack of translational studies that directly investigate human spinal cord tissue and cells. Indeed, acquiring viable human spinal cord tissue for investigation is ethically and technically challenging. Therefore, our understanding of human SCI is mainly based on studies conducted in rodents such as mice and rats (Cheriyan et al., 2014). While larger animal models such as porcine and non-human primate models have been used to advance promising strategies to clinical trials, these strategies are still unsuccessful in humans (Badhiwala, Wilson, Kwon, Casha, & Fehlings, 2018; Kwon et al., 2015). In this thesis, we will address the roadblock in translation by studying spinal cord tissue from human organ donors, focusing on the functional and molecular characterization of stem cells. The objective is to provide novel insights about human spinal cord stem cell

physiology that researchers can harness to improve the translation of regenerative strategies for SCI.

1.1.1 Epidemiology

In Canada, over 86,000 people live with an SCI, and approximately 50% suffer a traumatic injury. Each year, an additional ~1,400 people in Canada will endure a traumatic SCI (Rhscir, 2009). Despite challenges in determining the prevalence and incidence of SCI worldwide, a literature review reported a prevalence of SCI in the range of 490 to 526 people per million in developed countries. A single study reported a prevalence of SCI to be 440 people per million in developing countries. Also, the incidence rate is estimated to be 13.1 to 163.4 per million in developed countries and 13 to 220 per million in developing countries (Y. Kang et al., 2017).

In Canada and worldwide, men are more likely to be affected by traumatic SCI than women considering that many injuries result from motor vehicle accidents, extreme sports, and assaults. In Canada, the male-to-female ratio is approximately 3.5:1. Worldwide, the male-to-female ratio is estimated to be as high as 6.69:1 in developed countries and 7.59:1 in developing countries (Kang et al., 2017; Rhscir, 2009). Most SCIs in Canada are caused by falls (~50%), primarily influenced by an aging population (Rhscir, 2009). The cervical segment of the spinal cord is most likely to be inflicted by trauma, especially during a motor vehicle or sports injury, due to the flexibility of the neck (Cheriyan et al., 2014; Shin et al., 2015).

1.1.2 Classification of SCI

SCIs can be classified according to the type of injury, severity, and localization (Cheriyan et al., 2014; Silva, Sousa, Reis, & Salgado, 2014). Most SCIs are contusions, compressions, distractions, or lacerations (Norenberg, Smith, & Marcillo, 2004). Every kind of SCI varies in how they are

induced and its pathophysiological features. Contusion injuries typically show no disruptions of the surface anatomy, but damage to the underlying parenchyma consists of hemorrhaging and necrosis with disruption of the spinal tracts. Eventually, lesions can transform into cysts (Norenberg et al., 2004). Compressions are typically associated with vertebral body fractures that can macerate the cord. This lesion is characterized by the formation of connective tissue and fibrous scarring over time (Norenberg et al., 2004). Distraction injury occurs when two adjacent vertebrae are pulled apart in the axial plane, causing the spinal cord to stretch (Min-Te Choo et al., 2009). Lacerations result from penetrating objects like sharp bone fragments or missile injuries that disrupt surface anatomy, including the glia limitans. The underlying parenchyma is damaged and characterized by the deposition of collagenous connective tissue (Norenberg et al., 2004). Transections are another type of injury that can be minor or complete. Although rare in humans, complete transections represent an essential paradigm for testing regenerative strategies in animal models (Alizadeh, Dyck, & Karimi-Abdolrezaee, 2019).

Each type of SCI can bear varying degrees of severity that can cause a complete or incomplete injury. Complete injuries are associated with greater injury severity and result in a total loss of sensory, motor, and autonomic function below the level of damage (Weidner et al., 2017). Considering that most clinical cases consist of cervical injuries, a complete injury, in this case, would have horrifying consequences. In Canada, complete injuries compromise almost one-third of all cases (Rhscir, 2009). On the other hand, incomplete injuries result in spared sensory, motor, and autonomic functions below the level of damage (Weidner et al., 2017). The degree of neurological dysfunction today is most often assessed using the American Spinal Cord Injury Association (ASIA) Impairment Scale, which is graded from “A” to “E”. The grade “A” represents

a complete injury, and grade “E” represents a normal sensory and motor function (Kirshblum et al., 2011).

Depending on where an SCI is located will determine the bodily regions affected. Damage to the cervical cord can induce tetraplegia, characterized by impaired neurological function in the arms, trunk, and legs. On the other hand, damage to the thoracic, lumbar, or conus spinal cord induces paraplegia which spares arm function but can produce impairments in the trunk, pelvic organs, or legs depending on how high the injury is located (Kirshblum et al., 2011). Every three in four patients with incomplete paraplegia will likely regain some locomotor function within a year of SCI (Robert L Waters & Adkins, 1994). On the other hand, paraplegic patients with a complete injury have a meager chance of recovering to an incomplete injury, especially if the damage is above T9. Similarly, tetraplegic patients with an incomplete injury are more likely to gain some functional recovery relative to a complete injury (R L Waters, Adkins, & Yakura, 1991).

1.2 SCI Pathophysiology in mammals

1.2.1 Primary injury

Primary injury is the physical impact on the spinal cord, which can be described by the type and severity of the injury mentioned above. All primary injuries cause anatomical disruption, such as axonal damage and demyelination, blood vessel permeabilization and rupture, and cell membrane breakage (Alizadeh et al., 2019; Silva et al., 2014). The type and severity of the primary injury will largely influence the subsequent pathophysiological mechanisms, termed secondary injury, that will determine the outcome of a particular SCI (J. Wilson, Hashimoto, Dettori, & Fehlings, 2011).

1.2.2 Secondary injury

A cascade of molecular and cellular events ensues immediately following a primary injury, prolonging into days (acute phase), months, and even years later (chronic phase). The immediate events tend to exacerbate neurological damage, while the chronic events impede endogenous regeneration. Early evidence demonstrating secondary injury mechanisms and their deleterious effects came from a study in which the removal of hematomyelia acutely following an SCI led to improved outcomes in dogs (Allen, 1911). Since then, studies have sought to elucidate the mechanisms ensuing a primary injury. Although secondary injury mechanisms can differ between SCIs, there is overlap that can consist of vascular changes (e.g., ischemia, edema, and hemorrhage), inflammation, ionic imbalances, excitotoxicity, cell death (e.g., necrosis, necroptosis, apoptosis), axonal degeneration, cyst formation, and scarring (Alizadeh et al., 2019; Oyinbo, 2011; Silva et al., 2014). Considering that primary injuries are only preventable, research that aims to treat SCI has focused on the secondary injury phase to mitigate or reverse unfavorable mechanisms.

1.2.2.1 The acute phase of secondary injury

Within minutes of a primary injury, a cascade of events is triggered that lasts for days (acute) to weeks (sub-acute), causing progressive damage in an outward fashion from the lesion epicenter (Alizadeh et al., 2019; Oyinbo, 2011; Silva et al., 2014). The acute phase is characterized by vascular deterioration, excitotoxicity, ionic imbalances, free radical formation, lipid peroxidation, necrosis, edema, and inflammation. Later, the sub-acute phase displays features of apoptosis, neuronal demyelination and degeneration, extracellular matrix remodeling, and scar formation (Alizadeh et al., 2019; Oyinbo, 2011; Silva et al., 2014).

1.2.2.1.1 Vascular damage, excitotoxicity, and ionic imbalances

Vascular damage occurs within the first few hours of SCI due to a breakdown of the blood-spinal cord barrier (BSCB), leading to hemorrhage and ischemia surrounding the lesion for up to 24 hours (Rivlin & Tator, 1978; Weidner et al., 2017). A breakdown of the BSCB causes destabilization of homeostasis, leading to tissue damage through mechanisms that include glutamate toxicity, oxygen restriction, ionic imbalances, and free radical formation. Furthermore, immune cells and other circulatory elements infiltrate the spinal cord parenchyma, further contributing to secondary injury (Anwar, Al Shehabi, & Eid, 2016; Weidner et al., 2017).

Within half an hour of a primary injury, there is a rise in the extracellular concentration of glutamate that causes significant excitotoxicity (Panter, Yum, & Faden, 1990). Glutamate excitotoxicity can be triggered by ischemia and the breakdown of cell membranes. Extracellular glutamate can bind to ionotropic and metabotropic receptors on neuronal, glial, and endothelial cells, causing ion channels to be open and an influx of Ca^{2+} ions (Káradóttir & Attwell, 2007; Weidner et al., 2017). Increased intracellular Ca^{2+} causes cellular dysfunction via the activation of secondary messengers and potential cell death in part due to mitochondrial calcium overload (S. Li & Stys, 2001). The resulting mitochondrial failure due to calcium overload can lead to protein degradation and oxidative damage over the first week of SCI (S. Li & Stys, 2001). In astrocytes, increased intracellular Ca^{2+} promotes glutamate release and impairs their ability to reuptake glutamate, further exacerbating glutamate-induced excitotoxicity (Weidner et al., 2017). However, glutamate may have beneficial effects on promoting the survival and proliferation of endogenous stem cells in part by attenuating oxidative stress-induced damage (Hachem, Mothe, & Tator, 2016). Endogenous stem cells get activated in response to pathophysiological cues and act to restrict further secondary injury damage.

A downstream consequence of excitotoxicity is an ionic imbalance of cations that can lead to excess neuronal depolarization, mitochondrial failure, and reduced cell membrane permeability (S. Li & Stys, 2001; Stys, Waxman, & Ransom, 1992). Mitochondrial calcium overload results in a depletion of ATP that impairs the sodium-potassium pump, causing an increase in intracellular Na^+ (S. Li & Stys, 2001; Pandya, Nukala, & Sullivan, 2013). Increased intracellular Na^+ impairs the ability of Na^+-dependent glutamate transporter to uptake glutamate from the extracellular space (McAdoo et al., 2005). Increased intracellular Na^+ may also exacerbate Ca^{2+} influx through the dysregulation of sodium-calcium and sodium-hydrogen exchangers (Agrawal & Fehlings, 1996; Stys et al., 1992). As such, molecular strategies to block Na^+ influx (e.g., using Riluzole) have shown promise in mitigating secondary injury damage leading to improved functional outcomes after SCI (Badhiwala et al., 2018; Siddiqui, Khazaei, & Fehlings, 2015).

Another described mechanism of acute secondary injury involves elevated levels of reactive oxygen species (ROS) that last several weeks (Alizadeh et al., 2019; Anwar et al., 2016). ROS induces peroxidation of unsaturated fatty acids in the cell and organelle membranes, disrupting the nature and structure of phospholipids and leading to cell and organelle lysis (Toborek et al., 1999). Furthermore, lipid peroxidation further induces ionic imbalances in Ca^{2+} and Na^+ concentrations by the damage caused to organelles and the by-products of lipid peroxidation (e.g., aldehyde) that impair metabolic enzymes like sodium-potassium ATPase (Alizadeh et al., 2019; Weidner et al., 2017). The result is severe oxidative damage which can impair neuronal function and induce cell death.

1.2.2.1.2 Cell death

Cell death is a significant consequence of primary and secondary injury-induced damage that affects neurons, astrocytes, and oligodendrocytes (Almad, Sahinkaya, & McTigue, 2011; Beattie,

Hermann, Rogers, & Bresnahan, 2002). Two mechanisms of cell death include apoptosis and necrosis, although other mechanisms have been described (Alizadeh et al., 2019; Crowe, Bresnahan, Shuman, Masters, & Beattie, 1997). While necrosis is regarded as accidental and unprogrammed, apoptosis is an energy-dependent, programmed method of cell death (Oyinbo, 2011). Apoptosis and necrosis are induced via a multitude of factors, including ischemia, excitotoxicity, ionic imbalances, ROS, ATP depletion, circulating inflammatory cues, and the action of immune cells (Beattie, Farooqui, & Bresnahan, 2009; Beattie et al., 2002; Gudz, Komuro, & Macklin, 2006; J. L. Takahashi, Giuliani, Power, Imai, & Yong, 2003). In rodents, apoptosis is initiated within a few hours of SCI, peaking after one week, and continues to affect distally located regions over time (Beattie et al., 2009; X. Z. Liu et al., 1997). In human and non-human primates, apoptosis has been observed extending into the chronic phase (Crowe et al., 1997; Guest, Hiester, & Bunge, 2005). Interestingly, oligodendrocytes are highly susceptible to cell death following SCI, which can cause severe impairments in endogenous remyelination. This understanding has led to strategies promoting oligodendrocyte survival and regeneration (Beattie et al., 2009; Soheila Karimi-Abdolrezaee, Schut, Wang, & Fehlings, 2012; X. Z. Liu et al., 1997; Nagoshi et al., 2018).

1.2.2.1.3 Inflammation

A major component of secondary injury is inflammation, which generates detrimental and beneficial consequences (Donnelly & Popovich, 2008). Although inflammation is most profound during the acute phase, it may persist into the chronic phase and even throughout a patient's life (Beck et al., 2010; Norenberg et al., 2004). The detrimental effects of inflammation include further tissue damage and cell death. In contrast, beneficial effects include clearing debris, activating endogenous regenerative mechanisms, and mitigating secondary damage in the chronic phase (Anwar et al., 2016; Ruxandra Covacu & Brundin, 2015). Multiple immune cells are involved and

each cell type influencing SCI outcome in a temporal and injury-dependent manner. Astrocytes, microglia, neutrophils, macrophages, and lymphocytes have all been implicated in the inflammatory response post-SCI. While astrocytes, microglia, and neutrophils constitute the early (0-2 days) inflammatory response, macrophages and lymphocytes play a significant role afterward (Beck et al., 2010; Donnelly & Popovich, 2008; Jones, McDaniel, & Popovich, 2005; Kigerl et al., 2009).

Although astrocytes are not immune cells, they are involved in the inflammatory response by regulating BSCB permeability to allow and restrict the infiltration of circulatory immune cells (Cekanaviciute & Buckwalter, 2016). Astrocytes can upregulate and secrete chemokines (e.g., Il-1, MCP-1, CCL2, CXCL1) after SCI to promote the recruitment of neutrophils and macrophages. Astrocytes also produce adhesion molecules (ICAM and VCAM) necessary for leukocyte leakage into the spinal cord parenchyma (Cekanaviciute & Buckwalter, 2016; Pineau & Lacroix, 2007; Pineau, Sun, Bastien, & Lacroix, 2010). Besides the recruitment of immune cells, astrocytes also activate immune cells via the production of "pro-inflammatory" and "anti-inflammatory" factors (O 'shea, Burda, & Sofroniew, 2017). Thus, astrocytes are important recruiters and regulators of innate and adaptive immune cells. Furthermore, astrocytes upregulate their proliferation and become hypertrophied leading to the formation of a glial scar which hampers the expansion of inflammation from the lesioned area (discussed below in section 1.2.2.2.2). These observations have rendered astrocytes an important clinical target for modulation of the immune response post SCI.

Neutrophils are one of the primary immune responders to SCI that can be detected in the spinal cord within a few hours of injury and attain their peak around 12-24 hours (Neirinckx et al., 2014; Zivkovic, Ayazi, Hammel, & Ren 2021). However, their presence during secondary injury is short-

lived, as they rarely occur in the sub-acute or chronic phase (Neirinckx et al., 2014). The role of neutrophils in secondary injury is controversial. Neutrophils have been regarded as harmful due to their secretion of proteolytic enzymes such as metalloproteinases (MMPs) and ROS that causes damage to neurons, glia, and endothelial cells (Taoka et al., 1997). However, neutrophils may initiate debris clearance through phagocytosis and secrete pro-inflammatory factors that stimulate downstream tissue repair mechanisms. Furthermore, impeding neutrophil extravasation alters the immune response, impairing wound healing (Dorschner et al., 2020; Stirling, Liu, Kubes, & Yong, 2009; Taoka et al., 1997).

Microglia and macrophages are phagocytic immune cells that are recruited during the acute and sub-acute phases, respectively (Beck et al., 2010; Donnelly & Popovich, 2008; Kigerl et al., 2009; Neirinckx et al., 2014; Zivkovic et al., 2021). Microglia reside in the central nervous system (CNS) and populate the injured spinal cord within two to three days, while macrophages are derived from blood-borne monocytes that infiltrate the spinal cord due to a breakdown of the BSCB (Perry & Teeling, 2013; Zhou, He, & Ren, 2014). While microglia surround the lesion perimeter, macrophages occupy the lesion epicenter, reaching a peak around 7-10 days after SCI in mice (Greenhalgh & David, 2014). However, similar to microglia, macrophages can exist in multiple polarized states, including a pro-inflammatory and an anti-inflammatory phenotype, depending on the timing of SCI and environmental cues present (Ginhoux, Lim, Hoeffel, Low, & Huber, 2013).

Initially, microglia and macrophages adopt pro-inflammatory phenotypes that exacerbate secondary injury through the secretion of pro-inflammatory cytokines and chemokines, proteolytic enzymes, radicals, and growth-inhibitory molecules that form the glial scar (Anwar et al., 2016; Kroner et al., 2014; Zhou et al., 2014). Microglia and macrophages switch from a pro-inflammatory to an anti-inflammatory state later during secondary injury to resolve the immune

response (Figure 1.1). Anti-inflammatory microglia and macrophages produce anti-inflammatory and growth factors, promote neurogenesis, cell survival, and axonal regeneration, contribute to ROS clearance, and are typically associated with functional recovery (Chamak, Morandi, & Mallat, 1994; David & Kroner, 2011; Elkabes, DiCicco-Bloom, & Black, 1996; Zhou et al., 2014). However, similar to the adverse effects of pro-inflammatory microglia, prolonged anti-inflammatory activation can induce unfavorable consequences such as fibrotic scarring (Braga, Agudelo, & Camara, 2015; Göritz et al., 2011; Lech & Anders, 2013). Therefore, a balance between pro-inflammatory and anti-inflammatory states, their timing, and duration of activation are essential factors influencing the pathogenesis of SCI (Brennan & Popovich, 2018).

Overall, the spinal cord environment during secondary injury represents a hostile environment for tissue regeneration (Figure 1.1). The combination of vascular deterioration, inflammation, extracellular remodeling, and CNS cell dysfunction exacerbates secondary injury following the initial damage. Understanding these mechanisms has since led to the development of strategies that either mitigate or reverse secondary injury (discussed below in section 1.4).

1.2.2.2 The chronic phase of secondary injury

Following an intense phase of cell damage and debris clearance, a period of tissue remodeling and stabilization, termed the chronic phase, persists for weeks, months, and even years following the primary injury (Alizadeh et al., 2019; Norenberg et al., 2004). Mechanisms include white matter demyelination, connective tissue deposition, reactive gliosis, fibrotic and glial scarring, neuronal circuit reorganization, and cyst cavity formation (Bradbury & Burnside, 2019; Hagg & Oudega, 2006; O ’shea et al., 2017). The outcome is a lesion that is characterized by two distinct regions: (1) a non-neural lesion core and (2) an astrocytic scar border enclosing the lesion core (O ’shea et al., 2017; Silva et al., 2014) (Figure 1.1).

1.2.2.2.1 Non-neural lesion core

The lesion core is devoid of neural tissue and is marked by the presence of immune cells, stromal cells, fibroblasts, pericytes, glia, and newly formed blood vessels entrapped in connective tissue (Dias et al., 2018; Klapka & Müller, 2006) termed the fibrotic scar (Figure 1.1). These cells deposit connective tissue proteins such as collagen and laminin. They also secrete molecules into the extracellular matrix, including chondroitin sulfate proteoglycans (CSPGs) that have potent growth-inhibitory properties (O 'shea et al., 2017). Studies in rodents and non-human primates have demonstrated axons' difficulty in regenerating through the CSPG extracellular matrix and impaired action potential conduction and axonal remyelination (Dyck et al., 2018; Hunanyan et al., 2010; Lau et al., 2012; Pendleton et al., 2013). Indeed, the degradation of CSPGs from the fibrotic scar using the enzyme chondroitinase ABC results in an improvement of axonal regeneration and sprouting of ascending and descending tracts through the lesion (Bradbury et al., 2002; Cafferty, Yang, Duffy, Li, & Strittmatter, 2007; S. Karimi-Abdolrezaee, Eftekharpour, Wang, Schut, & Fehlings, 2010; Soheila Karimi-Abdolrezaee et al., 2012; Petrosyan et al., 2013). Other inhibitory molecules are also found in the lesion core, including myelin-associated proteins like Nogo-A and myelin-associated glycoprotein that cause neuronal growth cones to collapse via the activation of Rho-kinase (Bradbury & Burnside, 2019; Kucher et al., 2018). Consequently, inhibiting Rho-kinase or antagonism of myelin-associated proteins has improved axonal regeneration through the lesion core and minimized secondary damage (J. K. Lee et al., 2010; McKerracher & Guertin, 2013).

However, some components of the lesion core may benefit regeneration and cell survival. Ependymal-derived astrocytes and oligodendrocytes found inside and surrounding the lesion core can contribute to remyelination and secretion of growth factors such as ciliary neurotrophic factor

(CTNF), hepatocyte growth factor (HGF), and insulin-like growth factor-1 (IGF1) (Barnabé-Heider et al., 2010; Meletis et al., 2008; Sabelström et al., 2013). Furthermore, eliminating ependymal-derived progeny results in reduced cell survival and an enlargement of the lesion core, likely due to the loss of growth factors (Cusimano et al., 2018; Sabelström et al., 2013). Similarly, type-A pericytes in the vasculature migrate to the lesion core and differentiate into stromal cells, aiding connective tissue deposition. Eliminating pericyte-derived stromal cells leads to an enlarged lesion due to a failure to seal the lesion (Göritz et al., 2011). However, reducing pericyte-derived fibrosis without complete elimination improves sensorimotor recovery and axonal regeneration through the lesion core (Dias et al., 2018). Overall, the lesion core represents a cellular and molecular environment that provides neuroprotection and acts as a physical and chemical barrier for endogenous regeneration. As such, the lesion core should be carefully targeted for SCI repair.

1.2.2.2.2 The astrocytic glial scar

The astrocytic scar, also termed the glial scar, has been a primary target for SCI repair strategies. It is characterized by $GFAP^+$ reactive hypertrophic astrocytes with interwoven processes surrounding the lesion core (O 'shea et al., 2017) (Figure 1.1). The glial scar initiates within the first week after SCI and is fully formed by two to three weeks, consisting primarily of newly formed astrocytes derived from resident astrocytes (O 'shea et al., 2017; Wanner et al., 2013). Initially, the glial scar was viewed as an impediment to regeneration due to its production of inhibitory CSPCs (Silver & Miller, 2004; Windle, Clemente, & Chambers, 1952). However, later studies have demonstrated the importance of the glial scar for regulating the immune response and restricting secondary damage beyond the lesion core. Preventing the formation of the glial scar or removing the chronic glial scar results in an enlarged lesion core coincident with reduced

spontaneous axonal regeneration and worsened functional outcomes (M. A. Anderson et al., 2016; Faulkner et al., 2004; Herrmann et al., 2008; Wanner et al., 2013).

Furthermore, glial scar astrocytes produce extracellular matrix molecules such as laminin, which supports axonal growth after SCI (M. A. Anderson et al., 2016; J. Frisén et al., 1995). Also, axonal regeneration through the glial scar has been achieved by appropriately stimulating intrinsic growth programs in neurons using growth factors, genetic manipulations, or cell transplants (M. A. Anderson et al., 2016; Kadoya et al., 2016; Kawaja & Gage, 1991; Zukor et al., 2013). Given this evidence, it is likely that the failure of axons to regenerate beyond the glial scar is a combination of inhibitory molecules and the lack of cell-intrinsic growth program activation in neurons (O 'shea et al., 2017). Therefore, to target the glial scar as a therapeutic option for SCI repair, a combinatorial strategy may be needed that minimizes the detrimental effects of the glial scar while activating endogenous repair mechanisms.

1.3 SCI Pathophysiology in regeneration-competent species

Secondary injury mechanisms in some lower vertebrates, such as axolotls and zebrafish, are different than in mammals, which permit spinal cord regeneration after injury. Even in the case of a complete spinal cord transection, these animals can restore anatomical and functional outcomes (Becker, Becker, & Hugnot, 2018). Based on these remarkable observations, a great deal of research has been conducted to understand the cellular and molecular underpinnings that differentiate regeneration-competent species from mammals in hopes of recapitulating these mechanisms in mammals to regenerate the spinal cord. For instance, some microRNAs are conserved between axolotls and rodents but show significant differences in their temporal expression post-SCI. By mimicking the expression of one of these microRNAs in rats, namely

miRNA125b, to recapitulate the expression and timing observed in axolotls, it was possible to enhance post-injury functional recovery in rats in part through the downregulation of glial scarring mechanisms (Diaz Quiroz, Tsai, Coyle, Sehm, & Echeverri, 2014).

A necessary contributor to spinal cord repair in lower vertebrates involves resident spinal cord stem cells (Hui, Nag, & Ghosh, 2015; Sîrbulescu & Zupanc, 2010; F. Zhang, Clarke, & Ferretti, 2000). These stem cells, also termed ependymo-radial glial cells (ERGs), are in the ependymal niche and express markers for stem cells (Sox2) and ependymal cells (FoxJ1) similar to mammals (Fei et al., 2014; Ribeiro, Monteiro, Certal, Cristovão, & Saúde, 2017). They also express markers for astrocytes (GFAP and GLAST) and radial glial cells (BLBP) since ERGs fulfill the dual role of astrocytes and ependymal cells in anamniotes (Hui et al., 2015). This contrasts with mammals that possess free astrocytes in the parenchyma, which have separate roles from ependymal cells (Becker et al., 2018). Furthermore, ERGs in the ependymal layer of anamniotes extend radial filament-rich processes that form endfeet at the pia. This feature is vital for neurogenesis during CNS development and possibly post-SCI. However, this feature is absent in adult mammals and is speculated to be a result of the increased size of the spinal cord parenchyma (Becker et al., 2018).

ERGs can repair the spinal cord by inducing neurogenesis, secreting trophic factors and extracellular matrix molecules, and providing anatomical support for axonal regeneration (Becker et al., 2018; Sîrbulescu & Zupanc, 2010). FGF signaling is an essential inducer of ERG-mediated regeneration post-SCI (F. Zhang et al., 2000). Initially, FGF signaling induces the activation of ERGs, which require the transcription factor Sox2 to maintain their proliferative state (Hui et al., 2015; Ogai et al., 2014). FGF signals are also needed for directing ERGs to form a "glial bridge" across the lesion site that connects the rostral and caudal ends of the severed spinal cord (Goldshmit et al., 2012). The glial bridge, consisting of $GFAP^+$ astrocyte-like cells, could act as a scaffold for

regenerating axons (Goldshmit et al., 2012; Mokalled et al., 2016; Wehner et al., 2017). Furthermore, cells of the glial bridge produce connective tissue growth factors and FGF proteins that promote axon regeneration of severed neurons by activating intrinsic growth programs (Goldshmit et al., 2012; Mokalled et al., 2016). Therefore, unlike mammalian $GFAP^+$ scar-forming astrocytes, the ERG-derived glial bridge is conducive to axonal regeneration across the lesion following an SCI.

In addition, neurogenesis post-SCI is widely apparent in anamniotes, including the generation of motor neurons, serotonergic interneurons, V2-like interneurons, and other interneuronal populations (Kuscha, Barreiro-Iglesias, Becker, & Becker, 2012; Kuscha, Frazer, et al., 2012; Reimer et al., 2008). These newly generated neurons can relay by connecting severed axons across the lesion (Goldshmit et al., 2012). Importantly, genetic lineage tracing experiments under the GFAP promotor demonstrated that ERGs contribute to *de novo* neurogenesis following injury by producing HuC^+ neurons (Briona, Poulain, Mosimann, & Dorsky, 2015). However, in mammals, endogenous stem cells do not generate new neurons, and very few neurons, if any, are observed post-SCI (reviewed in more detail in section 1.6.3.2). Such differences in the molecular and cellular pathophysiology between lower vertebrates and mammals may underly the inability of mammals to repair the injured spinal cord.

1.4 Clinically tested treatments

There are no treatments for SCI, although many strategies have been attempted or are currently being investigated (Badhiwala et al., 2018; Bradbury & Burnside, 2019; Yamazaki, Kawabori, Seki, & Houkin, 2020). Considering the various mechanisms involved in the acute and chronic phases of secondary injury, it is proposed that a multifaceted approach should prove to be the most

successful. As such, strategies have been developed to either mitigate acute secondary damage or enhance regeneration in the chronic phase, and the combination of such strategies has usually been more successful than the application of either one alone (Chhabra & Sarda, 2017a; Failli et al., 2021; S. Karimi-Abdolrezaee et al., 2010; Ramer, Ramer, & Bradbury, 2014).

1.4.1 Mitigating secondary injury

The discovery of secondary injury mechanisms has led to numerous strategies that could minimize the extent of damage post-SCI. Some of these strategies have been tested or are currently being evaluated for clinical safety and efficacy (Badhiwala et al., 2018; Failli et al., 2021; Yamazaki et al., 2020).

Early surgical decompression (within 24 hours of injury onset) has recently gathered strong evidence for improving sensorimotor recovery at one year, particularly in cervical injuries (Ramakonar & Fehlings, 2021). However, this procedure is not feasible for all patients, with only less than 50% of patients in Canada being eligible (Glennie et al., 2017).

Other strategies involve the use of pharmacological and chemical agents (e.g., methylprednisolone, riluzole, minocycline, ganglioside GM1, naloxone, myelin inhibitors, Rho-kinase inhibitors, ion channel blockers, thyrotropin-releasing hormone) as a means to reduce vascular damage, inflammation, excitotoxicity, ion imbalances, and lipid peroxidation and to promote cell survival and protection (Badhiwala et al., 2018; Fehlings et al., 2021; Silva et al., 2014). These agents may be more feasible than surgical decompression. However, it must be reasoned whether the benefits of treatment will outweigh the potential adverse side effects, which are difficult to determine during the acute phase of SCI. Identifying biomarkers that can predict injury outcomes is under

investigation and will likely help apply pharmacological and chemical interventions acutely following injury (Dalkilic et al., 2018; Kwon et al., 2017).

Other strategies that avoid surgical or pharmacological interventions are being investigated, such as hypothermia and dietary modifications (Ramer et al., 2014; J. Wang & Pearse, 2015). These strategies have garnered interest due to their safety profiles and neuroprotective effects in experimental and human studies. Hypothermia can slow metabolism and secondary injury processes and promote angiogenesis and neurogenesis (Ramer et al., 2014; J. Wang & Pearse, 2015). However, questions remain regarding its optimal use and the potential of combining this with other strategies. Meanwhile, fasting and high-fat ketogenic diets have demonstrated improved SCI outcomes, but the extent of their effectiveness is limited (W. L. Huang et al., 2007; S. N. Lim, Huang, Hall, Michael-Titus, & Priestley, 2013; Streijger et al., 2013).

1.4.2 Bypassing lesion-induced loss of function

Most SCI patients live with chronic neurological deficits that require alternative methods for regaining functional outcomes. The most common and effective modality for chronic SCI patients today is physical rehabilitation (Fehlings et al., 2017; Nas, Yazmalar, Şah, Aydin, & Öneş, 2015; Navarrete-Opazo, Alcayaga, Sepúlveda, Rojas, & Astudillo, 2017). Although rehabilitation is applied during the acute phases to minimize secondary complications (e.g., muscle atrophy and joint contractures), its application for regaining functional recovery requires a patient's injury to stabilize first (Nas et al., 2015). However, functional recovery induced by intense rehabilitation programs will eventually plateau, suggesting that rehabilitation alone is insufficient for SCI repair (Failli et al., 2021). Therefore, combinations of treatments are being applied or tested along with rehabilitation (Edgerton, Tillakaratne, Bigbee, De Leon, & Roy, 2004; Navarrete-Opazo et al., 2017).

One such strategy, termed epidural stimulation, involves the application of a direct current below the level of injury (Courtine & Sofroniew, 2019). This method of epidural stimulation requires the implantation of an array of electrodes in the epidural space. Importantly, this strategy can be applied to chronically injured patients (Ramer et al., 2014). Epidural stimulation coupled with rehabilitation can restore volitional movement after motor-complete SCI and restore some autonomic processes such as cardiovascular, bladder, and sexual function (Gill et al., 2018; Netoff et al., 2019; Wagner et al., 2018). Proposed mechanisms of functional improvements include the activation of large diameter afferents that can induce the excitability of caudal circuits and the recruitment of spared descending tracts (Courtine & Sofroniew, 2019; Ramer et al., 2014).

Elsewhere, technological innovations have paved new avenues for the functional recovery of SCI (Bonizzato & Martinez, 2021; Courtine & Sofroniew, 2019; Inanici, Brighton, Samejima, Hofstetter, & Moritz, 2021; Jovanovic et al., 2021; Musk, 2019). For example, a neuroprosthesis implanted into the motor cortex of rats could improve voluntary control of locomotion following training (Bonizzato & Martinez, 2021). A transcutaneous electrical stimulator was recently developed that allowed rapid and sustained control of movement in the hands and arms of chronic SCI patients (Inanici et al., 2021). Unlike epidural stimulation, which is invasive and affects walking ability, the transcutaneous electrical stimulator is placed directly on a patient's skin and improves upper extremity function.

Brain-computer interface technology and robotic devices have also emerged as non-invasive methods for initiating and controlling basic motor commands (Dunkelberger, Schearer, & O'Malley, 2020; Jovanovic et al., 2021; Long, Federico, & Perez, 2017). On a similar front, Elon Musk's recent venture, "Neuralink," is a brain-machine interface device developed to allow tetraplegic patients to control their computer or phone devices by simply thinking (Musk, 2019).

These technologies may enable chronic SCI patients to regain control of certain aspects of their lives without needing neurological repair.

1.4.3 Promoting regeneration

The mammalian spinal cord exhibits an inhibitory environment for neuronal regeneration. This understanding was elegantly demonstrated by David and Aguayo (1981), in which CNS axons that would not normally regenerate following transection could do so when bridged using a peripheral nerve graft. On the other hand, peripheral nerve axons that are transected can regrow over long distances and innervate their targets (Huebner & Strittmatter, 2009). It's been shown that a combination of anatomical support by glial cells, including Schwann cells and astrocytes, and their secreted trophic factors are responsible for peripheral nerve regeneration by activating regeneration-associated genes in neurons (Giger, Hollis, & Tuszynski, 2010; Huebner & Strittmatter, 2009). In addition, Schwann cells remyelinate axons and provide a permissive substrate for axonal regeneration, including the extracellular deposition of matrix proteins collagen and laminin (Toyota, Carbonetto, & David, 1990). Therefore, achieving axonal regeneration within the spinal cord after injury may require remodeling the extracellular environment from an inhibitory to a permissive one and simultaneously activating intrinsic neuronal growth mechanisms (Bhowmick & Abdul-Muneer, 2021; Giger et al., 2010).

Depending on whether an SCI is complete or incomplete will likely influence the optimal strategy for inducing axonal regeneration. Anatomically incomplete SCI, which spares axons, may benefit from remyelination strategies to improve neuronal conduction across the lesion site. Such methods may involve the supply of trophic factors that promote oligodendrocyte differentiation and survival, and cell transplants containing oligodendrocyte progenitor cells (OPCs), olfactory ensheathing cells (OECs), or Schwann cells (K. D. Anderson et al., 2017; Mackay-Sim et al., 2008;

Manley, Priest, Denham, Wirth, & Lebkowski, 2017). A clinical trial, termed the SCiStar study and led by Asterias Biotherapeutics, has completed phase 1/2a to assess the safety and efficacy of transplanting OPCs into 25 patients with subacute cervical SCI (Global Newswire, 2019; Manley et al., 2017). A 12-month follow-up revealed no adverse side effects in all patients, positive signs of cell engraftment, and improvement in motor function in 95% of patients (Lineage Cell Therapeutics, 2021). Clinical trials have also been conducted using cell transplants of OECs (Mackay-Sim et al., 2008) or Schwann cells (K. D. Anderson et al., 2017). However, these trials have not demonstrated substantial evidence of clinical efficacy.

On the other hand, anatomically complete SCI will likely require re-establishing neuronal circuitry across the lesion (O 'shea et al., 2017). Treating a complete SCI is more complicated and involves the attenuation of inhibitory molecules in the injured spinal cord, provision of anatomical support for axonal regeneration across the lesion, and activation of intrinsic growth programs in neurons (Courtine & Sofroniew, 2019; O 'shea et al., 2017; Silva et al., 2014).

Many strategies have been developed and optimized, while new methods are being investigated for treating complete SCI (Badhiwala et al., 2018; Yamazaki et al., 2020). Attenuation or antagonism of extracellular inhibitory molecules such as CSPGs and myelin-associated proteins has been achieved using digestive enzymes, antibodies, and receptor blockers (Bradbury et al., 2002; Cafferty et al., 2007; S. Karimi-Abdolrezaee et al., 2010; Soheila Karimi-Abdolrezaee et al., 2012; J. K. Lee et al., 2010; McKerracher & Guertin, 2013; Petrosyan et al., 2013). Activation of neuronal intrinsic growth programs can be induced by the supply of trophic factors (e.g., BDNF, GDNF, NT3), growth factors (e.g., EGF and FGF2), and genetic manipulations (e.g., *mTOR*, *PTEN*, *c-Jun*, *ATF-3*) (Badhiwala et al., 2018; Bhowmick & Abdul-Muneer, 2021; Kanno et al., 2012; O 'shea et al., 2017; Raivich et al., 2004; Seijffers, Allchorne, & Woolf, 2006).

To bridge axonal connections, various biomaterials have been developed and implanted into SCI lesions (Hickey, Modulevsky, Cuerrier, & Pelling, 2018; Xiaoran Li et al., 2018, 2013; Xing Li et al., 2017; Marcuzzo et al., 2019; Tsai, Dalton, Shoichet, & Tator, 2004; Z. Xiao et al., 2018). Biomaterials can provide anatomical support and directed channels for guiding axonal regeneration. Biomaterials can also contain extracellular matrix proteins that promote the infiltration of axons and release trophic factors that enhance endogenous regeneration mechanisms (Courtine & Sofroniew, 2019; Xing Li et al., 2017; O 'shea et al., 2017; Tsai, Dalton, Shoichet, & Tator, 2006). The use of biomaterials has progressed to clinical trials (Theodore et al., 2016; Z. Xiao et al., 2018) and continues to be developed ("CelluBridge - Spiderwort").

Cell therapy is a multi-faceted approach that combines the attenuation of inhibitory signals, production of regenerative factors, and restoration of neuronal connectivity across an SCI lesion (Yamazaki et al., 2020). For instance, the transplant of neural stem cells in a rodent SCI model can upregulate the production of trophic factors in the injured spinal cord environment, reduce glial scarring, and form neuronal connections between severed axons (Brock, Graham, Staufenberg, Im, & Tuszynski, 2018; Ceto, Sekiguchi, Takashima, Nimmerjahn, & Tuszynski, 2020; Soheila Karimi-Abdolrezaee et al., 2012; Kumamaru, Lu, Rosenzweig, Kadoya, & Tuszynski, 2019). As such, cell therapy can mediate regeneration via many mechanisms, which may prove to be more fruitful compared to the single application of strategies mentioned above (e.g., digestive enzymes, antibodies, growth factors, biomaterials). However, the injured spinal cord represents a hostile and growth-inhibitory environment that may direct the fate of transplanted stem cells in undesired ways (Cao et al., 2001; Shihabuddin, Horner, Ray, & Gage, 2000b). Therefore, a combination of strategies such as mitigating secondary injury, using biomaterials, and cell therapy may be the best option for treating SCI (Rosenzweig et al., 2018; Silva et al., 2014; Suzuki et al., 2017).

1.5 Stem cells

1.5.1 Overview

Stem cells are promising tools for regenerative medicine due to their inherent ability to self-renew indefinitely and differentiate into specialized cell types (Temple, 2001) (Figure 1.2). Self-renewal is the process of duplicating stem cells to form more stem cells. This feature is essential for embryonic growth and maintaining cell populations in adult tissues where cell replacement is needed (e.g., skin cells, bone-marrow blood cells). Differentiation is the process by which a stem cell acquires specialized features and functions as a specific cell (e.g., neurons, myocytes, adipocytes). Together, self-renewal and differentiation enable the genesis of an entire organism from a single stem cell (Martello & Smith, 2014; Zakrzewski, Dobrzyński, Szymonowicz, & Rybak, 2019).

Stem cells are characterized by their ability to form specialized cells (Figure 1.2). "Totipotent" stem cells can generate every cell type in the body and, ultimately, an entire organism. These cells are derived from the developing embryo after the first few cell divisions (Martello & Smith, 2014; Zakrzewski et al., 2019). "Pluripotent" stem cells are also derived from the developing embryo but at a later stage and cannot form an entire organism. However, they can give rise to all three germ layers and form most, if not all, cell types in the body (Martello & Smith, 2014; Zakrzewski et al., 2019). "Multipotent" stem cells are typically tissue-specific and can only give rise to a discrete number of cells within the tissue they reside. As stem cells get more specialized and approach a terminal differentiation state, they pass an intermediary "progenitor" stage. Progenitor cells are committed to producing one or a few differentiated cell types and have a limited self-renewal ability (Martello & Smith, 2014; Zakrzewski et al., 2019).

1.5.2 Mechanisms of regeneration

There are three described mechanisms by which stem cells can mediate regeneration (Figure 1.3). The primary mechanism involves the direct replacement of dead, damaged, or diseased cells (Temple, 2001; Yamazaki et al., 2020). To achieve this feat, stem cells must differentiate into tissue-specific cells with the same function as the cells being replaced (Quinn, Walters, Vescovi, & Whittemore, 1999). In the context of SCI, oligodendrocyte replacement may be achieved using OPCs and neuronal replacement using neural precursor cells (Kadoya et al., 2016; Manley et al., 2017). In addition to neuronal replacement, neural precursor cells can be used to generate neurons that will form relays between severed axons and restore functional connectivity across an SCI lesion (Bonner & Steward, 2015; Brock et al., 2018; Ceto et al., 2020; Dulin & Lu, 2014).

A second mechanism is that stem cells mediate the supply of trophic factors into the extracellular space (Yamazaki et al., 2020) (Figure 1.3). A variety of stem cells, such as CNS stem cells and mesenchymal stem cells (MSCs), have demonstrated the ability to ameliorate the spinal cord environment to a more growth-permissible one (Lu et al., 2013; O ’shea et al., 2017; Sabelström et al., 2013; Silva et al., 2014; Yamazaki et al., 2020). This includes attenuating inflammation and glial scarring and promoting angiogenesis, neurogenesis, remyelination, cell survival, and axonal regeneration (de Freria, Van Niekerk, Blesch, & Lu, 2021; O ’shea et al., 2017; Yamazaki et al., 2020).

Lastly, stem cells can provide direct anatomical support for regenerating axons, analogous to the glial bridge formed in regeneration-competent species (Yuan et al., 2016) (Figure 1.3). A study by Kadoya, K., and colleagues (2016) demonstrated robust regeneration of corticospinal tracts into stem cell grafts after a transection injury in a rodent model. Importantly, corticospinal tract regeneration required grafts to be in immediate contact with descending fibers, as animals with

grafts that did not contact descending fibers exhibited poor axonal regeneration (Kadoya et al., 2016). This finding suggests that anatomical support provided by stem cells may be of greater importance than diffusible signals, at least for the stem cells and injury model used in that study. Also, it highlights the importance of localizing a cell graft to the injury site, which may be facilitated using biomaterials or other matrices (Assunção-Silva, Gomes, Sousa, Silva, & Salgado, 2015; Courtine & Sofroniew, 2019; Silva et al., 2014).

1.5.3 Application of stem cells

There are two main strategies for using stem cells in regenerative medicine, each with advantages and disadvantages (I. Kulbatski, Mothe, Nomura, & Tator, 2005) (Figure 1.2). The first strategy targets endogenous stem cells in adult tissues (Moreno-Manzano, 2020a). Indeed, this strategy requires that the tissue contains adult stem cells that can be targeted. The second strategy involves transplanting an exogenous source of stem cells (Yamazaki et al., 2020).

The advantages of one strategy typically represent challenges for the other strategy. For instance, transplanting stem cells, especially embryonic stem cells, typically requires more significant ethical consideration than targeting a patient's endogenous stem cells (Assinck, Duncan, Hilton, Plemel, & Tetzlaff, 2017; Hachem, Mothe, & Tator, 2020). However, this could be overcome if the transplanted cells originate from the patient (e.g., autologous bone-marrow MSCs) (Assinck et al., 2017). Also, there may be more significant risks associated with transplant procedures as they are more invasive and may require immunosuppression if allogenic stem cells are used (Yousefifard et al., 2016). However, an advantage of transplant procedures is that different stem cells can achieve various desired outcomes (e.g., OPCs for remyelination vs. neural precursors for neuronal relays) (All et al., 2012; Assinck et al., 2017; Yamazaki et al., 2020). Furthermore, transplantation may be more reproducible since endogenous stem cell function declines with aging.

Therefore, targeting endogenous stem cells in an elderly patient may not be as effective as in a young patient (Xiaofei Li et al., 2016; S. Liu & Chen, 2019). Meanwhile, transplant procedures can use a homogenous source of stem cells from a cell bank that can be applied across different patients (Curtis et al., 2018a; Manley et al., 2017).

1.6 Targeting endogenous CNS stem cells

1.6.1 Discovery of CNS stem cells

The first proposal that neurogenesis occurs in the mammalian brain was in a study by Altman and Das (1965). Two decades later, the laboratory of Fernando Nottebohm provided direct evidence of newly formed and functional neurons in the brain of songbirds (Paton & Nottebohm, 1984). However, it was only within the last three decades that the notion of adult mammalian neurogenesis became widely accepted (Richards, Kilpatrick, & Bartlett, 1992; Weiss et al., 1996). These studies used in vivo labeling techniques to identify newly formed cells (e.g., BrdU, EdU, radioactively labeled thymidine) and neuronal progenitor cells (e.g., DCX and PSA-NCAM).

Using these techniques, neurogenesis was demonstrated in humans for the first time in 1998 by injecting terminal cancer patients with BrdU and detecting newly formed $NeuN^{+}$ neurons in the dentate gyrus (Eriksson, Perrfilieva et al., 1998). Furthermore, the development of cell culture assays for the *in vitro* propagation of CNS stem cells has provided ample evidence for the existence of CNS stem cells (Richards et al., 1992; Weiss et al., 1996). Today, it's understood that several neurogenic niches in the CNS include the brain and spinal cord (Obernier & Alvarez-Buylla, 2019). The discovery of adult neurogenesis in mammals has reshaped our understanding of adult CNS function and has gathered interest in using CNS stem cells for regenerative medicine applications (S. Liu & Chen, 2019; Moreno-Manzano, 2020a).

1.6.2 Stem cells in the brain

There are two well-characterized neurogenic niches within the mammalian brain, including the sub-ventricular zone (SVZ) in the lateral ventricles and the sub-granular zone (SGZ) of the hippocampus (Obernier & Alvarez-Buylla, 2019). Both regions can give rise to newborn neurons that integrate with existing neuronal circuitry throughout the lifespan of an organism, although the rate of neurogenesis tends to decline with age (Boldrini et al., 2018; Obernier & Alvarez-Buylla, 2019; Sorrells et al., 2018a). Furthermore, stem cells in these neurogenic niches are influenced by various niche factors such as stress hormones, growth factors, neurotransmitters, drugs, and behavioral contexts like exercise and social interactions (Kandel et al., 2013). CNS stem cells can also get activated in response to traumatic injuries, stroke, and neurodegenerative diseases, which is likely due to circulating inflammatory and growth factors (R. Covacu, Perez Estrada, Arvidsson, Svensson, & Brundin, 2014; Ruxandra Covacu & Brundin, 2015; Grégoire, Goldenstein, Floriddia, Barnabé-Heider, & Fernandes, 2015)

The SVZ stem cells are described as “type B1” cells and express the proteins GFAP and Sox2 (Obernier & Alvarez-Buylla, 2019; J. Zhang & Jiao, 2015). These stem cells give rise to “type C” transient amplifying neural progenitors, which will generate “type A” neuroblasts that travel along the rostral migratory stream and terminate in the olfactory bulb, where they differentiate into inhibitory interneurons (Lois, García-Verdugo, & Alvarez-Buylla, 1996; Luskin, 1993). SVZ-derived interneurons have been implicated with olfactory memory formation, fine odor discrimination, and odor-reward association (Bergmann, Spalding, & Frisén, 2015; Grelat et al., 2018; W. L. Li et al., 2018; Lledo & Saghatelyan, 2005).

The SGZ stem cells are described as radial glia because they express GFAP and Sox2 like SVZ stem cells (Obernier & Alvarez-Buylla, 2019; J. Zhang & Jiao, 2015). SGZ stem cells migrate a

relatively short distance from the SGZ to the granule cell layer, where they terminally differentiate into excitatory granule cells. Their functional importance is still debated, but there is evidence implicating SGZ neurogenesis in pattern separation, memory consolidation, and other hippocampal-associated memory processes (Denny et al., 2014; Terranova, Ogawa, & Kitamura, 2019).

1.6.3 Stem cells in the spinal cord

Stem cells in the adult mammalian spinal cord were first discovered in 1996 by a Canadian researcher, Samuel Weiss, using *in vitro* culture (Weiss et al., 1996). The ventricular region was micro-dissected, and dissociated cells were cultured in the presence of mitogens epidermal growth factor (EGF) and basic fibroblast growth factor (bFGF or FGF2). These culture conditions have formed the basis of the "Neurosphere assay," which is routinely used today to identify and culture CNS stem cells (Narayanan et al., 2016; Reynolds & Rietze, 2005).

Using this assay, Weiss and colleagues (1996) grew spinal cord stem cells into neurospheres that arise due to the self-renewal activity of a single cell. Weiss and colleagues (1996) were also able to serially passage individual neurospheres, providing evidence for the self-renewal ability of adult spinal cord stem cells. Furthermore, Weiss and colleagues (1996) demonstrated the multi-potency of spinal cord stem cells by differentiating neurospheres into neuronal and glial lineages. Ever since then, a multitude of studies have emerged characterizing the identity and function of spinal cord stem cells, including strategies to target this neurogenic niche for the treatment of neurodegenerative disorders in the spinal cord (Becker et al., 2018; S. Liu & Chen, 2019; Moreno-Manzano, 2020a).

1.6.3.1 Molecular characterization of spinal cord stem cells

In mice, stem cells in the spinal cord are located within the ependymal layer of the central canal (Barnabé-Heider et al., 2010; Cusimano et al., 2018; Meletis et al., 2008; Stenudd et al., 2022). Spinal cord ependymal cells express some markers homogenously, including Sox2, Sox9, Vimentin, FoxJ1, and S100β, amongst other markers (Dromard et al., 2008; Ghazale et al., 2019a; Hamilton, Truong, Bednarczyk, Aumont, & Fernandes, 2009; Marichal, García, Radmilovich, Trujillo-Cenóz, & Russo, 2012; Sabourin et al., 2009a) (Figure 1.5). However, it is unlikely that all ependymal cells are stem cells since they are heterogeneous in their molecular and functional profiles (Hamilton et al., 2009; Sabourin et al., 2009a; Stenudd et al., 2022).

For instance, CD15 and Pax6 are markers for CNS stem cells and are concentrated in the dorsal pole of the central canal (Ghazale et al., 2019a; Sabourin et al., 2009a). Similarly, Nestin is a marker for CNS stem and progenitor cells and is expressed preferentially in the dorsal domain of the rodent central canal (Hamilton et al., 2009; Marichal et al., 2012; Sabourin et al., 2009a). *In vivo* lineage tracing and *in vitro* characterization demonstrate that Nestin$^+$ ependymal cells possess stem cell properties (Cusimano et al., 2018; Meletis et al., 2008; Shu et al., 2021). Furthermore, Nestin becomes upregulated after injury, and Nestin$^+$ cells contribute to the pathophysiological response (Cusimano et al., 2018; Meletis et al., 2008; Shu et al., 2021).

Interestingly, a recent study identified Troy as a marker in a specific subset of ependymal cells in the dorsal central canal, accounting for ~8% of ependymal cells and ~0.1% of all spinal cord cells (Stenudd et al., 2022). Using a transgenic mouse model, the authors argued that Troy$^+$ ependymal cells contained most of the stem cells in the spinal cord, as demonstrated by their self-renewal potential and multi-potency. However, they observed only a slight overlap in Troy and Nestin expression, which contradicts previous findings that implicate Nestin$^+$ cells as a stem cell

population (Cusimano et al., 2018; Meletis et al., 2008; Shu et al., 2021). These contradictions could be explained given that Nestin is also expressed in other cell types, including blood vessel pericytes and meningeal cells, which can contribute to the pathophysiological response after SCI (Birbrair et al., 2014; Decimo et al., 2011).

Another study by Wang, S., and colleagues (2021) argues that PKD2L1^{+} cerebrospinal fluid (CSF)-contacting neurons possess stem cell properties *in vitro* and express neural stem cell markers Sox2, Nestin, and GFAP. However, these findings are yet to be replicated and demonstrated *in vivo*. Therefore, there isn't a consensus regarding the true stem cell population within the ependymal layer. For this reason, ependymal cells have been collectively called "neural stem and progenitor cells" (NSPCs) to reflect the heterogeneity and different lineage potentials of ependymal subsets.

1.6.3.2 Function of NSPCs in the intact and injured spinal cord

The function of spinal cord NSPCs depends on the developmental stage and condition of the spinal cord (Lacroix et al., 2014; Xiaofei Li et al., 2016). During embryonic development and early postnatal stages, NSPCs undergo self-renewal as part of the spinal cord elongation process (Alfaro-Cervello, Soriano-Navarro, Mirzadeh, Alvarez-Buylla, & Garcia-Verdugo, 2012). However, during the adult phase, NSPCs rarely undergo self-renewal and appear quiescent (Blasko et al., 2012; Lacroix et al., 2014; Meletis et al., 2008). In some cases, proliferating NSPCs are observed, but the progeny remain within the ependymal layer and thus are thought to contribute to the maintenance of the ependymal layer and blood-CSF barrier (Barnabé-Heider et al., 2010; Blasko et al., 2012; Lacroix et al., 2014; Paniagua-Torija et al., 2018).

Despite the low self-renewal rate of ependymal cells in the intact spinal cord, a disruption in homeostasis can induce their activation (Barnabé-Heider et al., 2010; Lacroix et al., 2014; Moreno-Manzano et al., 2009). For instance, in response to a traumatic injury, NSPCs upregulate their proliferation to generate progeny that migrate to the site of injury (Barnabé-Heider et al., 2010; Meletis et al., 2008). NSPC activation proceeds rapidly within 24 hours of injury, reaching a peak around three days, and is maintained for several weeks (Lacroix et al., 2014; Meletis et al., 2008). Interestingly, NSPC activation occurs in response to traumatic injuries but not demyelinating injuries, suggesting an influence of specific secondary injury mechanisms of SCI (Lacroix et al., 2014). Furthermore, only NSPCs that are rostral but not caudal to the injury site get activated (Lacroix et al., 2014). Age also plays a role in NSPC activation, as NSPCs from older animals display reduced activation and self-renewal post-SCI (Xiaofei Li et al., 2016).

Following their activation, NSPCs appear to mediate a beneficial response that improves neurological and functional outcomes, but this response is insufficient to repair the spinal cord (Cusimano et al., 2018; Meletis et al., 2008; Moreno-Manzano et al., 2009; Sabelström et al., 2013). However, their exact function is controversial as there are conflicting reports from two labs. Using transgenic mice models (*FoxJ1-CreER* and *Nestin-CreER*) to label and track ependymal cells, the Jonas Frisén Lab has demonstrated over the years that ependymal-derived progeny migrate into the lesion core and the glial scar border where NSPCs differentiate into supporting glia. They observed that most ependymal-derived cells differentiate into GFAP-negative astrocytes which occupy the lesion core and account for ~20% of the lesion core area two weeks post-SCI (Meletis et al., 2008). These astrocytes were shown to produce neurotrophic factors CTNF, HGF, VEGF, LIF, and IGF-1 that enhanced neuronal and oligodendrocyte survival in spared tissue surrounding the lesion (Sabelström et al., 2013). Furthermore, ependymal-derived

astrocytes produced extracellular matrix molecules laminin and fibronectin that were closely associated with axonal sprouting into the lesion core and did not produce inhibitory CSPGs (Meletis et al., 2008). The Jonas Frisén Lab also demonstrated that a small portion (~3%) of ependymal cells differentiated into Olig-2^+ OPCs and APC^+ mature oligodendrocytes, which resided in the glial scar border. Ependymal-derived oligodendrocytes were observed to be closely associated with MBP^+ myelinated axons and may contribute to remyelination post-SCI (Barnabé-Heider et al., 2010; Meletis et al., 2008).

To demonstrate the functional benefits of NSPCs, Sabelström, H. and colleagues (2013) selectively deleted all *Ras* genes in ependymal cells to prevent mitosis and the generation of ependymal-derived progeny. This resulted in an enlarged lesion core concomitant with increased corticospinal tract degeneration and a ~20% reduction in neuronal survival. Several possible compensatory mechanisms to reduce lesion enlargement were also observed, including a larger astrocytic scar border and increased pericyte-derived fibrotic scarring. These observations suggest endogenous-activated NSPCs may reduce fibrotic and glial scarring while supporting neuronal survival and axonal regeneration. A similar study by Cusimano, M., and colleagues (2018) selectively ablated spinal cord NSPCs using a transgenic mouse line carrying thymidine kinase under the control of the Nestin promoter regions. The outcome was worsened anatomical and functional outcomes following SCI, including reduced remyelination, spontaneous recovery, production of trophic factors, and cell survival. Moreover, it was postulated that NSPCs regulated the inflammatory response since NSPC ablation increased pro-inflammatory microglia and expression of pro-inflammatory cytokines.

The controversy regarding the function of spinal cord NSPCs comes from a single report from the Michael V. Sofroniew Lab which argues against the contributions of NSPCs to SCI repair (Ren et

al., 2017). In this study, the authors used a knock-in transgenic mouse model (*FoxJ1*$^{CreERT2:GFP}$) to track ependymal cells and observed that these cells barely gave rise to any GFAP-negative astrocytes following SCI, which is in contrast to previous reports (Barnabé-Heider et al., 2010; Meletis et al., 2008; Sabelström et al., 2013). Furthermore, despite witnessing NSPC activation, they did not observe any migrating ependymal cells except within the direct vicinity of the central canal. The most significant contribution of NSPCs was GFAP$^+$ astrocytes that occupied the glial scar border adjacent to the central canal, accounting for ~20% of all newly proliferated GFAP$^+$ astrocytes in that region.

These discrepancies describing NSPC function after SCI could be attributed to the differences in injury models. While Ren, Y. and colleagues (2017) induced a lateral crush injury, the Frisén Lab used a dorsal midline stab injury that penetrated the ependymal layer and extended rostrally for an entire spinal cord segment (Barnabé-Heider et al., 2010; Meletis et al., 2008; Sabelström et al., 2013). Indeed, when Ren, Y., and colleagues (2017) attempted to replicate the midline stab injury model, they observed an increase in NSPC migration and differentiation but not to the extent seen in previous studies. However, the midline stab injury induced by Ren, Y., and colleagues (2017) was focal and did not extend along the spinal cord axis. Moreover, Meletis, K., and colleagues (2008) induced a stab injury in the lateral spinal cord that did not damage the ependymal layer, resulting in a diminished response from NSPCs. Therefore, the type and severity of the injury and direct ependymal damage may influence the ensuing NSPC response.

1.6.3.3 Effect of inflammation on spinal cord NSPCs

Inflammation is a significant event during secondary SCI that strongly influences the pathophysiology of NSPCs (Ruxandra Covacu & Brundin, 2015; Grégoire et al., 2015). Conversely, activated NSPCs can exert immunomodulatory effects through the secretion of

cytokines and trophic factors that can exacerbate or mitigate the inflammatory response (Kokaia, Martino, Schwartz, & Lindvall, 2012). The interaction between NSPCs and immune cells is dynamic and changes over time depending on the secondary injury phase. As such, cross-talk between immune cells and NSPCs is a critical area of focus for SCI repair strategies that aim to enhance endogenous regeneration and prevent inflammatory damage.

During the acute stage, activated astrocytes and pro-inflammatory microglia and macrophages upregulate the secretion of pro-inflammatory factors such as Il-6, TNFα, Il-β, NO, and ROS (Ruxandra Covacu & Brundin, 2015). The overall effect appears to activate NSPCs from a quiescent to a proliferative state (Lacroix et al., 2014; Xiaofei Li et al., 2016; Moreno-Manzano et al., 2009). The activation of NSPCs is correlated with an upregulation of genes associated with active cell turnover and proliferation, including the Janus kinase/signal transducer and activation of transcription (JAK/STAT) and mitogen-activated protein kinase (MAPK) pathways. While there are many inflammatory factors at play, several have been elucidated, such as Il-6, TNFα, and TGFβ (M. K. Kang & Kang, 2008; Ma, Deng, & Liu, 2019; Monje, Mizumatsu, Fike, & Palmer, 2002; Moreno-Manzano et al., 2009; S. Okada et al., 2004).

Il-6 is a potent cytokine mainly produced by pro-inflammatory microglia and reactive astrocytes acutely following an SCI (Barkho et al., 2006; Ruxandra Covacu & Brundin, 2015; Monje et al., 2002). Il-6 has been associated with adverse outcomes after SCI, and its serum and CSF concentration correlates with long-term functional impairments in humans (Dalkilic et al., 2018; Kwon et al., 2017). It inflicts pleiotropic effects, including the recruitment of inflammatory cells to the lesion, activation, and differentiation of NSPCs, and induction of glial scarring (M. K. Kang & Kang, 2008; Lacroix, Chang, Rose-John, & Tuszynski, 2002; S. Okada et al., 2004). Il-6 has also been shown to have a causal effect on NSPCs by inducing proliferation, inhibiting

neurogenesis, and promoting reactive astrocyte differentiation due to the activation of the JAK/STAT, and MAPK pathways (Heinrich, Behrmann, Müller-Newen, Schaper, & Graeve, 1998; M. K. Kang & Kang, 2008). NSPCs that are treated with Il-6 upregulate Nestin and GFAP expression and exhibit morphological features of hypertrophic astrocytes (M. K. Kang & Kang, 2008; S. Okada et al., 2004).

Similarly, TNFα is produced by pro-inflammatory microglia and has been shown to activate the JAK/STAT and MAPK pathways, which may enhance reactive astrocyte differentiation of NSPCs (Ma et al., 2019). TNFα is also a critical activator of NSPCs following SCI since it increases the proliferation of NSPCs and their expression of Sox2, which is required for self-renewal. Furthermore, microglia-derived TNFα inhibits neuronal differentiation and maturation of NSPCs, and prolonged exposure to TNFα can induce apoptosis (N. Chen et al., 2016; Ma et al., 2019). Overall, the early inflammatory phase of SCI activates NSPCs and primes NSPCs for astrocyte differentiation.

The subacute and chronic secondary injury phase sees a shift in the inflammatory response whereby microglia and macrophages adopt an anti-inflammatory phenotype. Immune cells secrete different factors than during the acute phase, including TGFβ, Il-4, Il-10, and Il-13, which exert pleiotropic effects that can serve as neuroprotective (Ruxandra Covacu & Brundin, 2015; Zhou et al., 2014). For instance, conditioned media from anti-inflammatory microglia reduces Sox2 expression and proliferation of NSPCs while enhancing their neuronal differentiation and maturation (Ma et al., 2019). TGFβ is a pleiotropic cytokine that plays an important role during SCI and is usually associated with astrocyte differentiation and glial scarring (M. F. Azari, Profyris, Zang, Petratos, & Cheema, 2005; Cole, Murray, & Xiao, 2016; Fuller et al., 2007; Q. Xiao, Du, Wu, & Yip, 2010; Yu, Wang, Katagiri, & Geller, 2012). TGFβ can activate JAK/STAT

signaling in NSPCs, promoting reactive astrocyte differentiation and inhibiting the oligodendrocyte lineage (Cole et al., 2016; Q. Xiao et al., 2010). This effect of TGFβ can be enhanced by LIF conditioning (M. F. Azari et al., 2005). TGFβ can also stimulate resident astrocytes in the spinal cord to become reactive and produce CSPGs which form the glial scar (Fuller et al., 2007; Yu et al., 2012). Therefore, NSPCs activated early during secondary injury may be induced to differentiate into reactive astrocytes in part through TGFβ signaling. Ultimately, inflammation in the early phase may be responsible for activating NSPCs, while the late phase is responsible for driving NSPCs into terminal differentiation.

1.6.3.4 Manipulation of spinal cord NSPCs for repair

The observation that endogenous NSPCs get activated following an SCI and recruited to the site of injury has garnered interest in targeting this neurogenic niche (Barnabé-Heider et al., 2010; Becker et al., 2018; Moreno-Manzano, 2020a). This strategy aims to direct the fate of NSPCs towards oligodendrocytes for remyelination, neurons for forming axonal relays, and non-reactive astrocytes for anatomical and paracrine support (Figure 1.3). This strategy is further inspired by regeneration-competent species in which NSPCs are required for the anatomical and functional repair of the injured spinal cord (Becker et al., 2018; Hui et al., 2015). Therefore, understanding the mechanisms underlying NSPC-mediated recovery in regeneration-competent species may allow these mechanisms to be recapitulated in mammals where the NSPC response is insufficient for complete recovery.

To effectively target and manipulate endogenous NSPCs will require their activation, migration to the injury site, and directing their differentiation. This feat will likely require a combination of strategies, including attenuating the hostile and growth-inhibitory environment of the spinal cord, providing a permissive substrate for growth, and promoting regenerative fates in NSPCs (S. Liu

& Chen, 2019; Moreno-Manzano, 2020a; Silva et al., 2014). Inhibitory molecules and matrices in the injured spinal cord can be attenuated with digestive enzymes that can degrade CSPGs and antagonistic molecules of myelin-associated proteins (Bradbury et al., 2002; Cafferty et al., 2007; Petrosyan et al., 2013). For instance, administering chondroitinase ABC to digest CSPGs in the injured spinal cord increases NSPC proliferation and reduces reactive astrocyte differentiation (S. Karimi-Abdolrezaee et al., 2010; Soheila Karimi-Abdolrezaee et al., 2012).

A permissive substrate for growth can be provided using biomaterials, extracellular matrix proteins, or transplanted cells (Courtine & Sofroniew, 2019; Kadoya et al., 2016; O 'shea et al., 2017; Silva et al., 2014). Many studies have demonstrated how scaffolds or extracellular matrix solutions applied at the injury site can enhance neurogenesis and reduce glial scarring leading to improved functional outcomes (Xiaoran Li et al., 2018, 2013; Xing Li et al., 2017). Similarly, transplanting MSCs, dendritic cells, Schwann cells, or OECs can enhance the response of endogenous NSPCs by providing a more permissive and less hostile environment for regeneration (Assinck et al., 2017; Silva et al., 2014).

Directly promoting regenerative fates in NSPC can be achieved by administering exogenous factors or genetic overexpression of lineage-specific transcription factors. For example, the sustained release of EGF and FGF can increase the proliferation of NSPCs, while PDGF-AA can direct oligodendrocyte differentiation (Jimenez Hamann, Tator, & Shoichet, 2005; Soheila Karimi-Abdolrezaee et al., 2012; Kojima & Tator, 2002). Similarly, overexpressing the transcription factor *OLIG2* in NSPCs can increase oligodendrocyte differentiation by 10-fold, improving remyelination and axonal conduction post-SCI (Llorens-Bobadilla et al., 2020).

These strategies have been demonstrated to be effective in targeting and modulating the endogenous NSPC regenerative response but may not be sufficient on their own to completely

repair the injured spinal cord (S. Liu & Chen, 2019; Moreno-Manzano, 2020a). Indeed, the combination of strategies has proven more effective (Silva et al., 2014). For instance, the supply of chondroitinase ABC and growth factors (EGF, FGF2, and PDGF-AA) enhances NSPC proliferation and oligodendrocyte differentiation more than applying either chondroitinase ABC or growth factors alone (Soheila Karimi-Abdolrezaee et al., 2012; Suzuki et al., 2017). Similarly, using a biomaterial scaffold with growth factors and cell transplant produces the best functional recovery outcomes (Soheila Karimi-Abdolrezaee et al., 2012; Xiaoran Li et al., 2018, 2013; Silva et al., 2014). Given the overwhelming possibility of strategies and their combinations, it remains to be determined what the optimal strategy should be. This will depend partly on the type of injury (complete vs. incomplete) and the patient's demographic profile (young vs. elderly).

1.7 Transplanting exogenous stem cells

The idea of transplanting stem cells to treat SCI emerged from the notion that the CNS does not bear the intrinsic capacity for regeneration (Tanaka & Ferretti, 2009). Many experiments have transplanted various stem cells, with some progressing to clinical trials (Badhiwala et al., 2018; Curtis et al., 2018a; Piltti et al., 2017; Silva et al., 2014; Sugai et al., 2021). Most of these trials have demonstrated safety but are yet to demonstrate effectiveness across the board of different SCIs and patient demographics (Yamazaki et al., 2020). Therefore, a great deal of optimization is still required that considers the cell type, cell count, type and location of the injury, intervention phase, method of administration, and co-transplant factors such as immunosuppressants, antibiotics, trophic factors, and biomaterials (Soheila Karimi-Abdolrezaee, Eftekharpour, Wang, Morshead, & Fehlings, 2006; Yousefifard et al., 2016). The following sections will elaborate on the different cell types and the evolution of strategies.

1.7.1 Autologous versus allogeneic cell transplant

Various stem cells have been tested from autologous or allogenic sources and different developmental origins, including embryonic, fetal, and adult tissues (Assinck et al., 2017; Silva et al., 2014; Yamazaki et al., 2020). No two sources are equal, and the type of transplanted cell will largely dictate the mechanisms of regeneration. Autologous cell transplants are derived from adult tissue which includes MSCs derived from bone marrow and adipose tissue, Schwann cells, and OECs (K. D. Anderson et al., 2017; Čížková, Rosocha, Vanický, Jergová, & Čížek, 2006). These options pose less risk for immune rejection but may be more challenging to acquire in sufficient numbers.

MSCs have been the most extensively tested option because they are easy to isolate but have yet to demonstrate clinical efficacy and reproducibility (Hwan Yoon et al., 2007; Silva et al., 2014). MSCs have been proposed to promote beneficial outcomes through the secretion of trophic factors and anti-inflammatory cytokines, but these mechanisms alone may not be sufficient for effective SCI repair. MSCs have also been reported to differentiate into neuronal and glial lineages, but these findings are controversial, and this strategy may not be the most effective for cell replacement (Brazelton, Rossi, Keshet, & Blau, 2000; Mezey, Chandross, Harta, Maki, & McKercher, 2000; Woodbury, Schwarz, Prockop, & Black, 2000, Castro et al., 2002; Terada et al., 2002; Wurmser & Gage, 2002).

Schwann cells have demonstrated the ability to secrete trophic factors, myelinate axons, and provide anatomical support for axonal regeneration (Assinck et al., 2017; Silva et al., 2014). However, transplanting Schwann cells alone without additional co-treatments, such as the blockage of inhibitory molecules or treatment with protective agents, has shown limited benefit (X. Y. Lin et al., 2016). Furthermore, despite the many experimental studies dating back to 1981,

the clinical applications of Schwann cell transplantation are not abundant and have not been convincingly shown to be effective (K. D. Anderson et al., 2017; Duncan, Aguayo, Bunge, & Wood, 1981).

OECs are another experimentally and clinically tested autologous cell type, but their SCI repair mechanisms are poorly understood. Furthermore, there are mixed reports in experimental studies. Clinical trials have also not demonstrated any significant improvements, or they were not adequately designed (e.g., lacking a control group) (Féron et al., 2005, Ramer, Richter, Roskams, Tetzlaff, & Ramer, 2004; Riddell, Enriquez-Denton, Toft, Fairless, & Barnett, 2004; Steward et al., 2006, Lima et al., 2016).

On the other hand, allogeneic cell transplants are at a greater risk of immune rejection but permit the use of cells that can mediate specific mechanisms of regeneration tailored to the type of injury (Assinck et al., 2017; Yamazaki et al., 2020). For instance, OPCs have been used to induce remyelination of denuded axons in incomplete SCI, neural precursor cells to form neuronal relays across large lesions, and glial-restricted precursors to bridge lesions and guide axonal regeneration (All et al., 2012; Ceto et al., 2020; Davies et al., 2006; Yuan et al., 2016). Cells can also be genetically engineered to secrete factors that can stimulate specific means of regeneration (Blesch & Tuszynski, 2007).

A significant clinical advantage of allogenic transplants is that cells can be scaled and preserved until needed, allowing immediate availability for trauma patients. Furthermore, cells could be pre-screened for “ideal” characteristics that would improve treatment efficacy. The reproducibility of transplant treatments could also be improved because the same stock of cells could be used for many patients. Lastly, the elderly population would likely benefit more from an allogenic

transplant due to age-related deficits in autologous cells (Curtis et al., 2018a; I. Kulbatski et al., 2005; Silva et al., 2014).

NSPCs are the most used allogeneic stem cells for the experimental treatment of SCI (Assinck et al., 2017; Yamazaki et al., 2020; Yousefifard et al., 2016). NSPCs are multipotent stem cells that can differentiate into neurons, oligodendrocytes, and astrocytes. Each differentiated cell type can mediate its means of regeneration, including direct cell replacement, the formation of neuronal relays, and remyelination (de Freria et al., 2021; Mortazavi et al., 2015; Yamazaki et al., 2020; Yuan et al., 2016). Furthermore, NSPCs and their progeny can secrete trophic and immunomodulatory factors that can mitigate secondary injury, reduce glial scarring, and promote angiogenesis and axonal regeneration (Assinck et al., 2017; Cusimano et al., 2018; Kumamaru, Lu, Rosenzweig, & Tuszynski, 2018; Sabelström et al., 2013).

Although it is not feasible to acquire autologous NSPCs from adult humans for transplant, they can be generated in large numbers from embryonic or fetal-derived tissue (Bianchi et al., 2018; Kumamaru, Kadoya, et al., 2018; Olmsted et al., 2020; Shimojo et al., 2015). Using embryonic- and fetal-derived NSPCs allows researchers to create a cell bank that can be accessed on demand and administered acutely following injury. The translation of embryonic-derived NSPCs began in 2011 by StemCells Inc., but they have not demonstrated clinical efficacy (A. J. Anderson, Piltti, Hooshmand, Nishi, & Cummings, 2017). However, other clinical trials have been initiated, showing promising results and continuing to be intensely investigated (Curtis et al., 2018a; Manley et al., 2017; Sugai et al., 2021; Yamazaki et al., 2020).

1.7.2 Optimal source of stem cells for SCI

NSPCs are considered the optimal source of cells for transplant in SCI, given their ability to integrate with the host tissue and their multiple modes of mediating regeneration (Ceto et al., 2020; Kadoya et al., 2016; Kumamaru et al., 2019; Kumamaru, Lu et al., 2018; Rosenzweig et al., 2018). However, NSPCs originating from the brain or spinal cord bear different molecular and functional features (Chambers et al., 2009; Kadoya et al., 2016; Kajikawa et al., 2020; Metzis et al., 2018; Shihabuddin, Horner, Ray, & Gage, 2000a). Although both brain- and spinal cord-derived NSPCs have shown promising results in experimental models of SCI, optimal results were obtained using spinal cord-derived NSPCs (Kadoya et al., 2016; Kajikawa et al., 2020; Kumamaru, Kadoya, et al., 2018; Rosenzweig et al., 2018).

Grafts of primary spinal cord-derived NSPCs differentiate into phenotypically appropriate sensory and motor neurons that resemble endogenous spinal cord neurons (Kumamaru, Lu, Rosenzweig, Kadoya, & Tuszynski, 2019). Furthermore, graft-derived neurons effectively integrate with the local neuro-circuitry by forming synapses with host axons rostral and caudal to the lesion (Ceto et al., 2020). Interestingly, synapses between graft-derived motor interneurons and descending motor tracts were formed without additional exogenous guidance (Kumamaru, Lu, Rosenzweig, Kadoya, & Tuszynski, 2019). This led to improved axonal conduction across the lesion and voluntary motor control, likely due to the induced regeneration of corticospinal tract fibers (Ceto et al., 2020; Kumamaru, Lu et al., 2018). Notably, corticospinal tract regeneration occurred only when homotypic spinal cord NSPCs were grafted, not forebrain or hindbrain NSPCs (Kadoya et al., 2016).

These experiments conducted in rodents and non-human primates demonstrated the importance of using NSPCs grafts with a spinal cord phenotype. However, transplanting autologous primary

spinal cord NSPCs for human SCI is not feasible due to the technical limitations of harvesting spinal cord tissue from injured patients. Allogenic spinal cord NSPCs can be harvested from organ donors' tissue to circumvent these limitations, but these opportunities are rare, especially since high-quality NSPCs are needed (Dromard et al., 2008; A. J. Mothe, Zahir, Santaguida, Cook, & Tator, 2011). For these reasons, embryonic- and fetal-derived NSPCs have been preferred in research, but these cells require patient immunosuppression, stringent isolation protocols, and ethical considerations (Nakamura & Okano, 2013; Silva et al., 2014).

Recent advances in cell reprogramming methods have allowed scientists to create autologous, spinal cord-specific NSPCs that could be used instead of primary, embryonic, and fetal tissue (Bianchi et al., 2018; Kumamaru, Kadoya, et al., 2018; Olmsted et al., 2020). These methods have paved a novel way for treating SCI and have entered stages of clinical testing (Sugai et al., 2021).

1.7.3 Creating region-specific CNS stem cells

1.7.3.1 Cell reprogramming overview

In 2006, for the first time, Takahashi, K. and Yamanaka, S. demonstrated the ability to reprogram adult somatic cells into embryonic-like stem cells. The resulting induced pluripotent stem cells (iPSCs) possessed the same general features of embryonic stem cells, including the potential to form all three germ layers (K. Takahashi & Yamanaka, 2006a). Importantly, advances in our knowledge of embryonic and postnatal development have enabled researchers to recapitulate developmental steps in iPSCs to generate tissue-specific cells, including CNS NSPCs (Chambers et al., 2009; Galiakberova & Dashinimaev, 2020) (Figure 1.4). These revolutionary advancements have provided researchers and clinicians unprecedented access to human NSPCs devoid of the technical and ethical limitations imposed by using primary, embryonic, and fetal tissue.

iPSCs are advantageous over embryonic stem cells because they don't require the same ethical considerations since iPSCs can be created from the somatic cells of consulting adults. Somatic cells can be easily obtained via a skin, hair, blood, or urine sample. Furthermore, iPSCs can be created from SCI patients and used for autologous cell transplants (Khazaei, Ahuja, & Fehlings, 2017; Nagoshi, Tsuji, Nakamura, & Okano, 2019).

Another advantage is that iPSCs can self-renew indefinitely, allowing for scaled production for experimental study or transplant (Beers et al., 2015). However, before their clinical use, iPSCs must first be differentiated into adult stem cells that lack pluripotent features, as the presence of pluripotent stem cells can lead to teratoma formation (Kobayashi et al., 2012). Also, the prolonged culture of iPSCs can cause chromosomal abnormalities, which may lead to cellular defects and increase transplant risks. Therefore, stringent differentiation, isolation, and screening protocols are required to safely use iPSCs in a clinical setting (Galiakberova & Dashinimaev, 2020; Kajikawa et al., 2020; Nakamura & Okano, 2013; Sugai et al., 2021).

The original method of generating iPSCs from somatic cells involved the retroviral-mediated genetic integration of defined embryonic transcription factors *OCT3/4*, *SOX2*, *C-MYC*, and *KLF4* (K. Takahashi & Yamanaka, 2006a). Nowadays, alternative means of creating iPSCs have been developed that do not require viral integration and, importantly, allow for the clinical translation of this cellular technology (Figure 1.4). Some of these methods include the transfection of plasmids, synthetic modified messenger RNAs, self-replicating RNAs, or transcription factor proteins (Galiakberova & Dashinimaev, 2020; Seo, Hong, & Do, 2017; Steinle et al., 2019). Other methods not involving transduction or transfection use small molecules that act as epigenetic modifiers (G. Chen et al., 2011). The use of small molecules is considered the safest since it does

not involve introducing foreign genetic material and mitigates cell membrane disruptions accompanying transfection protocols.

Besides reprogramming cells into iPSCs, adult somatic cells can be reprogrammed directly into other adult cell types via a transdifferentiation mechanism (Mertens, Reid, Lau, Kim, & Gage, 2018; Xu, Du, & Deng, 2015) (Figure 1.4). This method can be achieved using lineage-specific transcription factors. For instance, NSPCs can be reprogrammed directly from fibroblasts or astrocytes by overexpressing the transcription factor Sox2 (Su, Niu, Liu, Zou, & Zhang, 2014; D. Xiao et al., 2018). This strategy is advantageous over iPSCs because acquiring the desired reprogrammed cell type requires significantly less time. It can also be mediated *in vivo* to avoid creating pluripotent iPSCs that form teratomas (Su et al., 2014; Xu et al., 2015).

However, direct lineage reprogramming is limited in that it may not produce enough cells for regenerative medicine applications (Gopalakrishnan, Hor, & Ichida, 2017). Furthermore, molecular defects in the original cell may persist into the reprogrammed cell following a transdifferentiation reprogramming but not during iPSC reprogramming (Mertens et al., 2015). While the persistence of molecular defects is advantageous for disease modeling (e.g., studying reprogrammed neurons from Alzheimer's patients or the effect of aging on neuronal function), it may produce undesired cellular phenotypes for cell transplantation. On the other hand, iPSC reprogramming "rejuvenates" the original cell by modifying the epigenetic landscape, which can eradicate the molecular defects in the original cell (Mertens et al., 2015, 2018). Therefore, iPSC reprogramming may be more beneficial for SCI transplant procedures, especially with elderly patients that exhibit age-associated molecular defects.

Given the various methods of reprogramming cells, phenotypically diverse NSPCs can be obtained that portray features of various developmental stages (e.g., embryonic vs. adult) and different

regions of the CNS (e.g., brain vs. spinal cord) (Chambers et al., 2009; Kadoya et al., 2016; Kajikawa et al., 2020; Kumamaru, Kadoya, et al., 2018). However, the true nature of these reprogrammed NSPCs and their homology to endogenous counterparts remains in question. To date, no reports suggest reprogrammed spinal cord NSPCs resemble endogenous spinal cord NSPCs from adult humans at either a molecular or functional level. Therefore, it is unclear whether reprogrammed spinal cord NSPCs will be successful in SCI clinical trials (Sugai et al., 2021). As such, directly comparing reprogrammed spinal cord NSPCs with isogenic human primary spinal cord NSPCs is critical to delineate differences that may impact spinal cord repair in clinical trials.

1.7.3.2 Generating dorsal forebrain NSPCs

Many protocols exist for differentiating iPSCs into NSPCs with a regional brain phenotype (Galiakberova & Dashinimaev, 2020). The most used method involves the dual inhibition of the SMAD pathway to drive neuroectoderm fates (Chambers et al., 2009) (Figure 1.4). In this protocol, iPSCs are treated with two inhibitors of the SMAD signaling pathway, namely Noggin and SB431542, to generate highly enriched populations of $Pax6^{+}$ NSPCs. Noggin inhibits BMP signaling, while SB431542 inhibits TGFβ/Activin/Nodal signaling, and the action of both molecules suppresses iPSC differentiation into mesoderm and endoderm lineages (Chambers et al., 2009).

The resulting population portrays features of anterior NSPCs that express the dorsal forebrain brain markers Otx2, Sox1, Emx1/2, and FoxG1 in addition to canonical NSPC markers Sox2 and Nestin (Galiakberova & Dashinimaev, 2020). Furthermore, anterior-fated NSPCs can generate deep and upper-layer cortical neurons that mirror the differentiation profile of endogenous dorsal forebrain NSPCs (Strano, Tuck, Stubbs, & Livesey, 2020a). Although iPSC-derived NSPCs generated using this method have shown benefits following transplant in SCI models, they are not as effective as

NSPCs with a spinal cord phenotype (Kadoya et al., 2016; Kajikawa et al., 2020; Kumamaru, Kadoya, et al., 2018). Therefore, protocols have been developed to differentiate iPSCs into spinal cord-like NSPCs (Bianchi et al., 2018a; Kajikawa et al., 2020; Kumamaru, Kadoya, et al., 2018; Olmsted et al., 2020).

1.7.3.3 Generating spinal cord NSPCs

The predominant view of CNS development is that all neural cells are derived from ectoderm tissue which is first specified with an anterior identity and then posteriorized to acquire more caudal fates (Sambasivan & Steventon, 2021). Anterior-fated NSPCs that are derived using the dual-SMAD inhibition protocol can be posteriorized using morphogens such as retinoic acid (RA), fibroblast growth factors (FGFs), and growth differentiation factor (GDF) (Shimojo et al., 2015). NSPCs can be further ventralized using sonic hedgehog (Shh) and differentiated to produce $HB9^+$, $Isl1^+$, and $ChAT^+$ motor neurons (Chambers et al., 2009; Galiakberova & Dashinimaev, 2020; Shimojo et al., 2015). However, these morphogens can only activate rostral homeobox (*HOX*) genes (*HOX1-5*) that pertain to the hindbrain and upper cervical regions (Philippidou & Dasen, 2013).

Wnt signaling is another means to induce posterior fates in pluripotent-derived NSPCs by activating the expression of the transcription factor *CDX2* (Kumamaru, Kadoya, et al., 2018). Wnt generates NSPCs with a positional identity that resembles more caudal regions of the CNS, including the thoracic spinal cord (Kumamaru, Kadoya et al., 2018; Metzis et al., 2018). However, NSPCs that have already committed to anterior fates by dual-SMAD inhibition are refractory to Wnt-mediated *CDX2* expression indicating an early time window for posteriorizing Wnt signaling (Metzis et al., 2018). Therefore, early vs. late Wnt signaling suggests distinct developmental pathways for anterior brain vs. posterior spinal cord NSPCs (Metzis et al., 2018).

Indeed, recently, it's been demonstrated that early Wnt signaling generates bipotent neuromesodermal progenitors (NMPs) responsible for developing the posterior neural tissue independent of the anterior neural plate (Tzouanacou, Wegener, Wymeersch, Wilson, & Nicolas, 2009). This evidence contradicts the notion that the spinal cord is generated by posteriorizing anterior neural tissue. NMPs are found at the node-streak border, caudal lateral epiblast, and the chordoneural hinge of elongating embryos and contribute to both the elongation of the spinal cord and adjacent paraxial mesoderm (Cambray & Wilson, 2007; Henrique, Abranches, Verrier, & Storey, 2015; Olivera-Martinez, Harada, Halley, & Storey, 2012).

NMPs are molecularly characterized and maintained in a bipotent state by the co-expression of Sox2 and T/Brachyury (Gouti et al., 2017; Sambasivan & Steventon, 2021). Exposure of pluripotent stem cells to Wnt and FGF signaling induces the expression of Sox2 and T/Brachyury in NMPs by activating *CDX* transcription factors (Henrique et al., 2015). *CDX2* is necessary to upregulate the transcription of more posterior *HOX* genes (*HOX4-10*) and repress hindbrain identity (Kumamaru, Kadoya et al., 2018; Metzis et al., 2018). Fate choice of NMPs into mesoderm or neural lineages is balanced by signaling molecules that regulate Sox2 and T/Brachyury expression. Whereas continued Wnt and FGF signals drive a mesodermal fate by downregulating Sox2, RA promotes a neural fate by downregulating the expression of T/Brachyury (Garriock et al., 2015; Henrique et al., 2015; Metzis et al., 2018; Sambasivan & Steventon, 2021).

According to this recent body of knowledge, many protocols have been developed to differentiate pluripotent stem cells into regionalized spinal cord NSPCs (Bianchi et al., 2018a; Kumamaru, Kadoya, et al., 2018; Olmsted et al., 2020) (Figure 1.4). NSPCs generated using these protocols express posterior spinal cord markers of the thoracic and lumbar regions and canonical NSPC markers (e.g., Sox2 and Nestin). Upon differentiation, NMP-derived NSPCs differentiate into

spinal cord-specific interneurons and motor neurons (Bianchi et al., 2018a; Kumamaru, Kadoya et al., 2018; Olmsted et al., 2020). Notably, the transplant of NMP-derived NSPCs has demonstrated improved anatomical and functional recovery when transplanted into rodent and primate models of SCI compared to the transplant of anterior-fated NSPCs (Kajikawa et al., 2020; Kumamaru, Kadoya, et al., 2018; Rosenzweig et al., 2018). Despite significant improvement in the development of spinal cord-specific NSPCs, whether reprogrammed NMP-derived NSPCs are molecularly and functionally like bona fide spinal cord NSPCs from adult humans remains to be determined.

1.8 The adult human spinal cord stem cell niche

1.8.1 Anatomy and molecular characterization of NSPCs

A handful of studies have characterized the morphological and molecular profiles of adult human spinal cord NSPCs *in situ* using imaging techniques, immunohistochemistry, and RNA sequencing (Cawsey, Duflou, Weickert, & Gorrie, 2015; Dromard et al., 2008; Garcia-Ovejero et al., 2015; Ghazale et al., 2019a; Gonzalez-Fernandez et al., 2017; González et al., 2020; A. J. Mothe et al., 2011; Paniagua-Torija, Arevalo-Martin, Ferrer, Molina-Holgado, & Garcia-Ovejero, 2015; Paniagua-Torija et al., 2018). Among these studies, contradictory observations were described concerning the morphology and organization of ependymal cells in the central canal (Cawsey et al., 2015; Dromard et al., 2008; Garcia-Ovejero et al., 2015; Ghazale et al., 2019a). Specifically, it was observed in some studies that the central canal is not patent but rather is composed of an obliterated structure of condensed ependymal cells (Garcia-Ovejero et al., 2015; Paniagua-Torija et al., 2015, 2018). Garcia-ovejero, D., and colleagues (2015) describe this human-specific feature as “perivascular pseudorosettes” because cells surround a blood vessel instead of a lumen (Figure

1.5). However, these studies also observed central canal patency in some donors, which was more prevalent in younger individuals and the cervical spinal cord. Furthermore, other groups have not reported the absence of a patent central canal in human spinal cord sections (Cawsey et al., 2015; Dromard et al., 2008; Ghazale et al., 2019a). Due to these contradictory results, it's unclear whether central canal patency is a feature exclusive to young individuals that collapse during aging or a post-mortem artifact.

In human spinal cord sections with a patent central canal, ependymal cells are ubiquitously labeled by Vimentin, S100β, FoxJ1, Sox9, and Sox11. Animal models exhibit a similar expression of markers. Ependymal cells are also positive for markers that label NSPCs such as Sox2, Nestin, CD15, CD24, PSA-NCAM, and Pax6 (Cawsey et al., 2015; Dromard et al., 2008; Ghazale et al., 2019a; Hamilton et al., 2009; Marichal et al., 2012; Meletis et al., 2008; Sabourin et al., 2009a) (Figure 1.5). However, some of these markers are not homogenously expressed throughout the ependymal cells, exhibiting dorsal-ventral regionalization. For instance, the dorsal ependymal layer is positive for Pax6, CD15, and Msx1 (Dromard et al., 2008; Ghazale et al., 2019a). Meanwhile, the ventral ependymal layer is positive for Nestin, PSA-NCAM, Arx, and Foxa2 (Cawsey et al., 2015; Dromard et al., 2008; Ghazale et al., 2019a). Moreover, Sox2 is ubiquitously expressed in ependymal cells but exhibits stronger staining in some cells than others (Dromard et al., 2008).

This heterogeneity among ependymal cells may reflect distinct populations of stem and progenitor cells with specific lineage potentials and functions. Interestingly, it's been observed that the ventral sub-ependymal zone consists of a hypocellular region that is negative for GFAP and positive for Nestin which may represent a region of NSPCs in humans (Cawsey et al., 2015; Dromard et al.,

2008). However, this observation contrasts mice in which Nestin and GFAP are co-expressed in the dorsal ependymal domain (Hamilton et al., 2009; Marichal et al., 2012; Sabourin et al., 2009a).

Besides immuno-labeling, the gene expression profile of the human ependymal zone has also been characterized. Using laser capture microdissection (LCMD), two independent groups isolated the ependymal region for RNA analysis (Garcia-Ovejero et al., 2015; Ghazale et al., 2019a; Gonzalez-Fernandez et al., 2017; Paniagua-Torija et al., 2015, 2018). These studies detected an enrichment of genes related to neurogenic niches (e.g., *CD24*, *BDNF*, *PAX6*, and *PAX7*), stem cell maintenance pathways (e.g., smoothened/SHH and Hippo/YAP signaling genes), neurogenesis (e.g., *WNT* and *NOTCH* related genes), and gliogenesis (e.g., *NFIA* and *SOX9*), supporting the notion that the ependymal zone is a neurogenic niche (Garcia-Ovejero et al., 2015; Ghazale et al., 2019a; Gonzalez-Fernandez et al., 2017). The RNA data also confirmed the ependymal nature of cells, as shown by an enrichment of genes involved in cilia formation (e.g., *FOXJ1*) and a high expression of 34 members of the solute carrier family (Ghazale et al., 2019a). Furthermore, Garcia-Ovejero and colleagues (2015) detected an enrichment of spinal cord ependymoma genes compatible with a non-aggressive tumor.

A study by Ghazale and colleagues (2019) discovered 8,733 and 2,122 differentially expressed genes in the ependymal zone from mice and humans, respectively. Interestingly, some markers for CSF-contacting neurons (*PKD1L2*, *PKD2L1*, *CRCT1*, *DCN*, *ESPN*, and *PDZK1IP*) were present in mice but completely absent in humans, in agreement with a lack of immunostaining for these markers in human spinal cord sections (Becker et al., 2018; Ghazale et al., 2019a). Overall, the human spinal cord central canal displays features characteristic of NSPCs, although there are morphological and molecular distinctions with animal models (Figure 1.5).

1.8.2 Pathophysiology of NSPCs in SCI

The role of human spinal cord NSPCs following an SCI is unclear and controversial. At least two independent studies have sought to determine the response of NSPCs following a traumatic SCI with seemingly contradictory results (Cawsey et al., 2015; Paniagua-Torija et al., 2018). A study by Cawsey and colleagues (2015) found a significant increase in the percentage of $Nestin^+$ ependymal cells (~5-6 fold) in people with traumatic CNS injury compared to non-traumatic controls. The increased Nestin expression was not localized but was present at rostral and caudal regions to the injury site, suggesting that circulating factors in the CSF could have led to ependymal activation. Furthermore, Nestin expression was positively correlated with post-injury survival time, which ranged from <30 minutes to 9 months. This data corresponds with rodent models of traumatic SCI in which Nestin is quickly upregulated within the first 24-48 hours and can last up to 13 months (Cizkova et al., 2009; Jonas Frisén, Johansson, Török, Risling, & Lendahl, 1995; Meletis et al., 2008; Namiki & Tator, 1999). Also, rodent NSPCs get activated along the rostral-caudal axis of the spinal cord similarly (Lacroix et al., 2014).

Interestingly, Cawsey and colleagues (2015) did not observe any increase in GFAP staining in trauma patients regardless of patient age, survival time, or post-mortem delay. They also did not observe any reactive astrocytes co-labeled for Nestin and GFAP. The lack of increase in GFAP staining contradicts rodent studies in which a pronounced $GFAP^+/Nestin^+$ glial scar is formed surrounding the lesion following an SCI (M. A. Anderson et al., 2016; O 'shea et al., 2017). Although the study by Cawsey and colleagues (2015) was limited in their patient samples (27 trauma cases), their data suggests that ependymal cells get activated following CNS injury but do not contribute to glial scar-forming astrocytes.

The second study by Paniagua-Torija and colleagues (2018) presents conflicting results. They used three antibodies to stain ependymal cells for proliferation markers (Ki67 and MCM2) in traumatically injured spinal cords. In contrast to Cawsey and colleagues (2015), they did not observe any ependymal cell activation after injury (ranging from 2 days to 6 months) or at any distance rostral or caudal to the injury site. In fact, they calculated a proliferative index of 0.08% in ependymal cells. In rodent models, it is known that ependymal cells in the intact spinal cord are quiescent, but they get activated following a traumatic injury, reaching a proliferative index of ~20% (Blasko et al., 2012; Lacroix et al., 2014). The data from this study suggests that ependymal cells in adult humans do not respond to traumatic SCI and caution against considering these cells as a source of endogenous regeneration.

1.8.3 *In vitro* characterization of NSPCs

For the first time, in 2008, Dromard and colleagues (2008) cultured primary spinal cord NSPCs from organ donors using the Neurosphere assay. The Neurosphere assay has been used routinely since the 1990s to culture and study CNS NSPCs (Reynolds & Rietze, 2005; Weiss et al., 1996). This assay involves culturing cells in serum-free media and in the presence of mitogens (EGF and FGF2), which selects for self-renewing NSPCs. Dromard and colleagues (2008) demonstrated that primary human NSPCs express canonical markers of neural stem (Sox2) and progenitor (Nestin) cells. They also showed the multi-potency of NSPCs by their differentiation into neurons (βiii-tubulin, NF70, Map2ab, NeuN), astrocytes (GFAP), and oligodendrocytes (O4). However, they could not pass primary neurospheres, which raised doubts about whether the NSPCs are self-renewing stem cells.

Three years later, Mothe and colleagues (2011) developed a protocol that allowed for the passage and long-term culture of primary adult human spinal cord NSPCs. They determined that primary

human NSPCs needed to be cultured as an adherent layer which could later be passaged and cultured in suspension to form neurospheres. Using this protocol, Mothe and colleagues (2011) demonstrated that NSPCs self-renew, express canonical markers of stem and progenitor cells, and are multi-potent. However, they noticed that in the absence of differentiation factors, primary human NSPCs exhibited meager rates of differentiation into neuronal (~1.5%) and glial lineages (<1%). Neuronal differentiation could be enhanced 20-fold with the single application of dibutyryl cyclic AMP (dbAMP), but oligodendrocyte differentiation was refractory to platelet-derived growth factor-AA (PDGF-AA) treatment.

To date, these are the only two studies that have characterized primary NSPCs from the adult human thoracic and lumbar spinal cord (Dromard et al., 2008; A. J. Mothe et al., 2011), a reflection of the progress that's been made in translating endogenous NSPC regeneration strategies for SCI. Although these studies represent essential baby steps in the field, they also have limitations. Most importantly, the *in vitro* characterization of NSPCs may not portray their true phenotype since the culture conditions vary significantly from the neurogenic niche *in vivo* (Meletis et al., 2008; Weiss et al., 1996). For this reason, it would be helpful to conduct an *in vitro* characterization of primary human NSPCs in parallel with animal model NSPCs that could be used for cross-reference since animal model NSPCs can be characterized *in vivo*. This would allow researchers to test pre-clinical drug treatments in a side-by-side comparison, which could improve the translation of NSPC-targeted therapies.

1.9 Research goal, hypothesis, and aims

We aim to improve the clinical translation of regenerative strategies that stimulate endogenous NSPCs and transplant reprogrammed NSPCs for SCI repair. We hypothesize that the

transcriptome, differentiation, and proliferation profiles of primary human spinal cord NSPCs are distinct from that of porcine, rodent, and iPSC-derived NSPCs. My research aims to: (1) develop an *in vitro* method that would allow for the molecular and functional characterization of primary spinal cord NSPCs from humans, pigs, and rats in a parallel manner, (2) examine whether the transcriptome, as well as the pathophysiological and regenerative mechanisms, are conserved across species, and (3) determine the molecular and functional homology between bona fide human spinal cord NSPCs and isogenic iPSC-derived NSPCs.

1.10 Study design

1.10.1 Aim 1

In Chapter 2, we will develop an *in vitro* method to directly compare primary spinal cord NSPCs from humans, pigs, and rats under identical culture conditions. We will outline and demonstrate a procedure to harvest spinal cord tissue from organ donors and a large and small animal model of SCI. We will describe a novel means of micro-dissecting the central canal region to minimize contamination of NSPC cultures from the surrounding grey and white matter cells. We will then use identical culture conditions for all species to expand and treat primary NSPCs with single exogenous factors. Finally, we will demonstrate how the differentiation and proliferation profiles of NSPCs from all species can be characterized by using immunocytochemistry.

1.10.2 Aim 2

In Chapter 3, we will examine whether pathophysiological and regenerative mechanisms are conserved across species using the method developed in Chapter 2. Under standardized cell culturing conditions and passage numbers, we will characterize the spontaneous differentiation and proliferation profiles of human, pig, and rat NSPCs. Human NSPC-derived neurons will also

be functionally examined using electrophysiological recordings. Next, we will compare the species-specific responses of NSPCs to inflammatory factors implicated with secondary injury and glial scarring post-SCI. We will also compare the effect of regenerative factors that promote cell-type-specific differentiation and self-renewal among species. Finally, we will perform a transcriptome-wide analysis of primary NSPCs using RNA sequencing to determine differences in gene regulatory networks and transcription factors that could be mediating species-specific functional behavior. These analyses will allow us to understand the critical differences between human and animal primary spinal cord NSPCs and better translate animal therapies to humans.

1.10.3 Aim 3

In Chapter 4, we will determine the molecular and functional homology between bona fide human spinal cord NSPCs and isogenic reprogrammed NSPCs. First, we will use a clinically translatable method of reprogramming donor skin fibroblasts into iPSCs. iPSCs will then be differentiated into regionalized NSPCs with an anterior brain or a posterior spinal cord phenotype. To identify functional differences between iPSC-derived NSPCs and primary spinal cord NSPCs, we will characterize the spontaneous differentiation and proliferation profiles under standardized cell culturing conditions and passage numbers. We will also perform RNA sequencing to identify transcriptome differences that reflect the developmental stage, regionalization, and stem cell features. Importantly, we will characterize reprogrammed NSPCs and primary NSPCs derived from the same donor to establish an isogenic comparison. These analyses will allow us to identify the critical differences between primary human NSPCs and iPSC-derived NSPCs to improve the development of iPSC-derived spinal cord NSPCs towards human spinal cord repair.

1.11 Figures

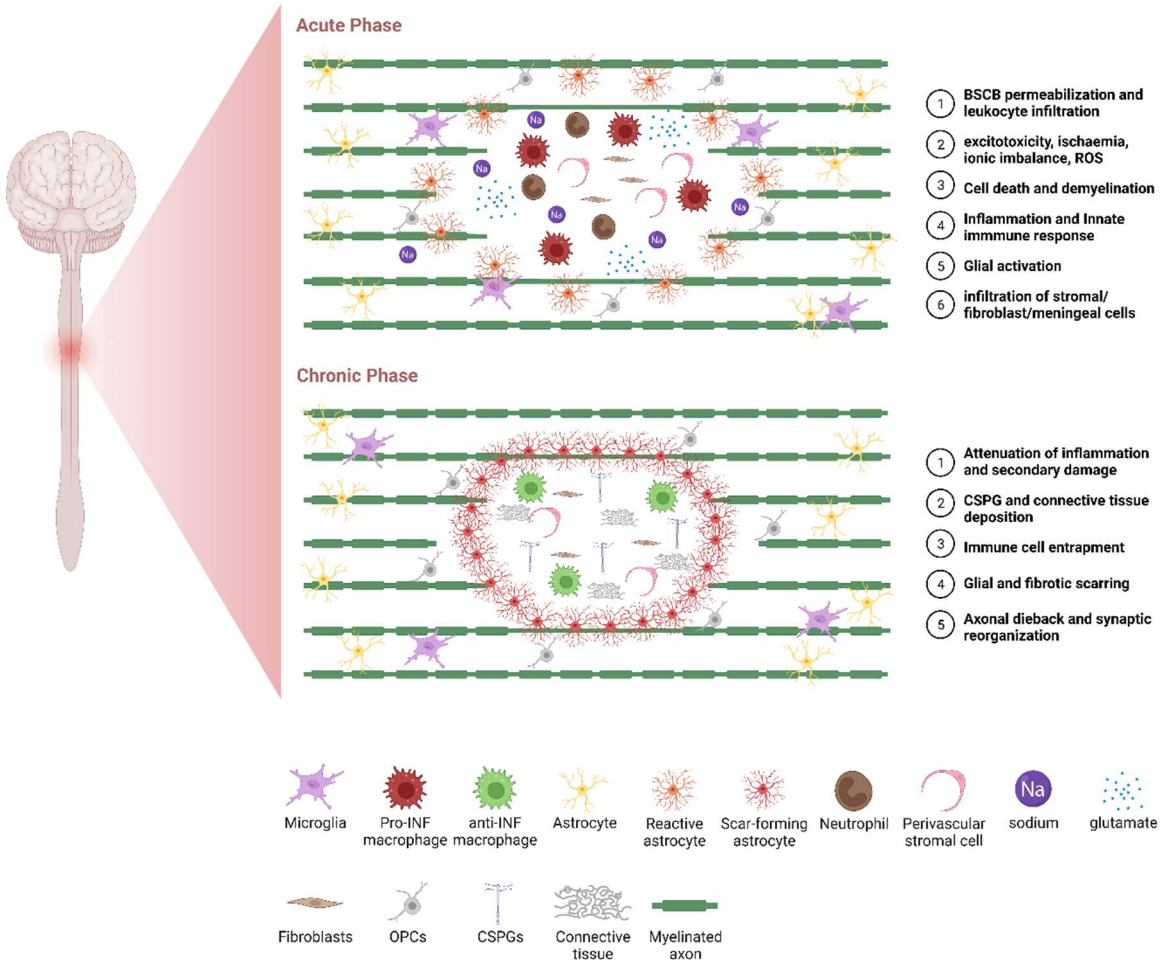

Figure 1.1 Secondary injury mechanisms of SCI in the acute and chronic phases

Secondary injury consists of a series of processes that initiate soon after the primary injury and can last for the entirety of a patient's life. The acute phase starts within minutes and lasts several days and is characterized by pronounced extracellular toxicity, inflammation, infiltration of connective-tissue depositing cells, and glial activation. These events lead to exacerbated cell death and damage. However, the attenuation of acute phase mechanisms in the chronic phase leads to the stabilization and restriction of secondary damage. This period is characterized by an astrocytic

scar bordering a lesion core comprising entrapped cells, connective tissue, and growth-inhibitory molecules. During the chronic phase, little endogenous regeneration and recovery are observed. Thus, experimental strategies include attenuating acute secondary injury mechanisms and promoting regeneration in the chronic phase. BSCB = blood spinal cord barrier, ROS = reactive oxygen species, CSPG = Chondroitin sulfate proteoglycans, INF = inflammatory, OPCs = oligodendrocyte progenitor cells. Created with BioRender.com.

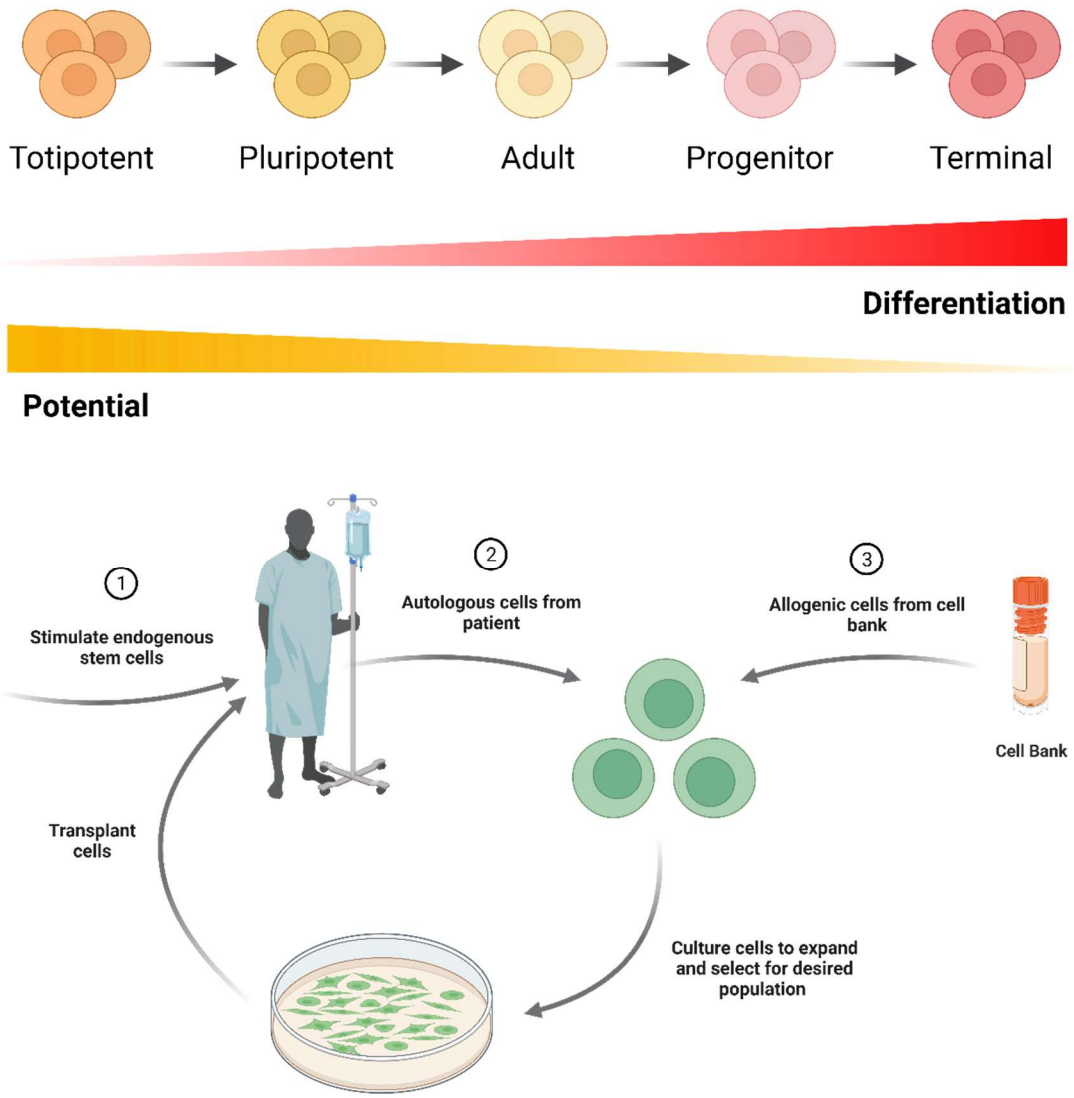

Figure 1.2 Defining stem cells and their application in regenerative medicine

Stem cells are defined by their ability to proliferate and differentiate into specialized cell types. Depending on the potential of stem cells, they can either form an entire organism (totipotent), all three germ layers (pluripotent), tissue-specific cells (adult), or a single cell type (progenitors). Adult, progenitor, or terminally differentiated cells are typically used in regenerative medicine

applications. These cells can be sourced from the patient (autologous) or a cell bank (allogeneic). Regardless of the source, stem cells are expanded *in vitro* to expand and select the desired cell population to be transplanted into the patient. Alternative to cell transplantation, endogenous tissue-specific stem cells can be targeted to promote regeneration. Created with BioRender.com.

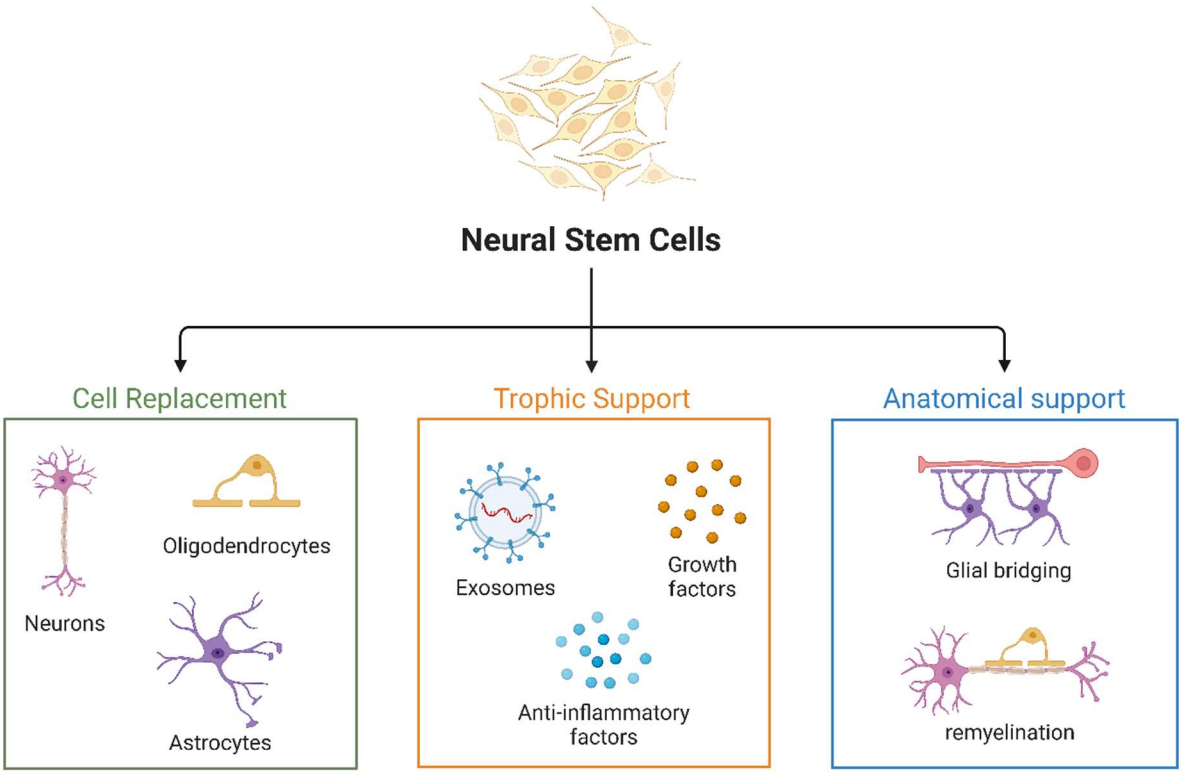

Figure 1.3 Mechanisms of regeneration mediated by neural stem cells

Neural stem cells have multiple modes of inducing regeneration that can be beneficial during the acute and chronic phases of SCI. Through differentiation, neural stem cells can acquire similar phenotypes of the cells that have been damaged or died, thus acting as a source of cell replacement. These mechanisms may be more beneficial in the chronic phase when endogenous regeneration

and cell replacement are low, especially for neurons. Neural stem cells can also secrete pro-growth and anti-inflammatory factors into the injured spinal cord milieu to mitigate the effects of acute secondary injury. Anatomical support provided by neural stem cell-derived progeny is critical for axonal regeneration and functional recovery in lower vertebrates following an SCI. Created with BioRender.com.

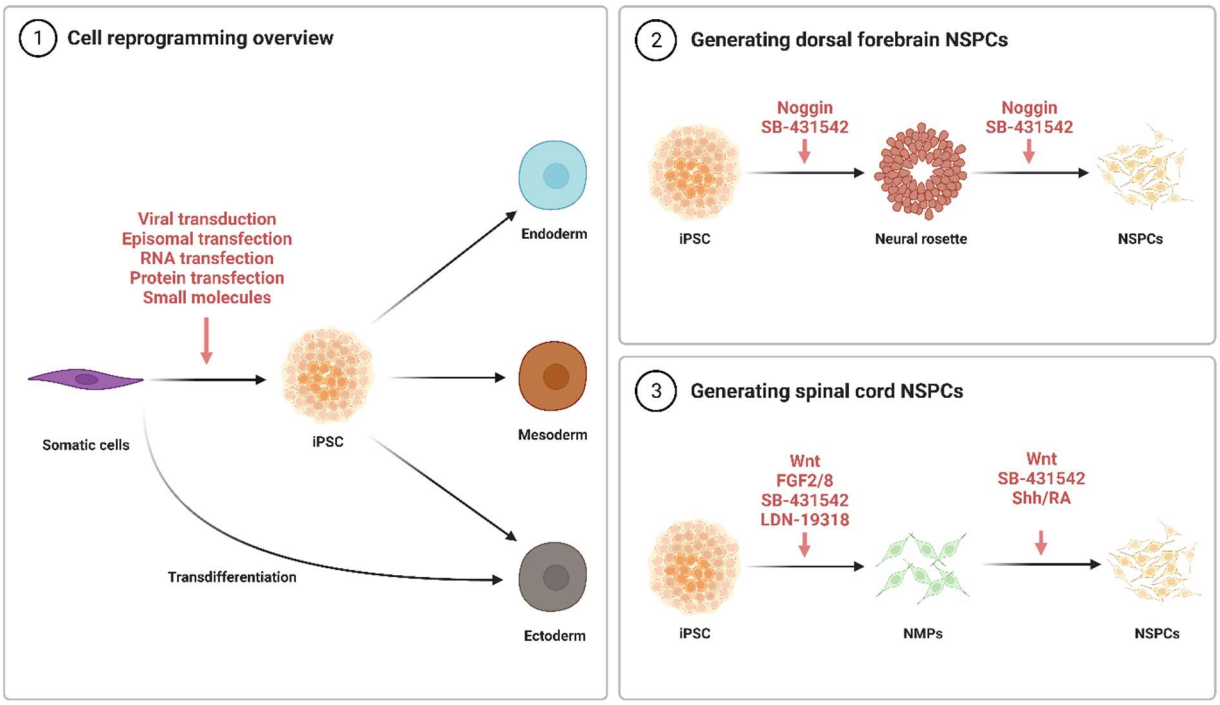

Figure 1.4 Cell reprogramming methods and the differentiation of iPSCs into regional CNS NSPCs

Reprogramming technologies have enabled the transformation of cell phenotypes from one kind to another. This feat can be achieved by reprogramming a cell, such as a somatic fibroblast cell, into a pluripotent state or transdifferentiation. Reprogramming into induced pluripotent stem cells

(iPSCs) enables the formation of any germ layer cell. Meanwhile, transdifferentiation involves a direct lineage conversion between two distinct cellular phenotypes, such as fibroblasts and neurons. Both reprogramming routes can be achieved by the exogenous expression of lineage-specific transcription factors or by using small molecules. Since iPSCs can be differentiated into multiple cell types, it is possible to direct the fate of iPSCs into regionalized CNS NSPCs, including the dorsal forebrain and spinal cord. Dorsal forebrain NSPCs are generated by differentiating iPSCs using dual-SMAD inhibition. Spinal cord NSPCs are created via a neuromesodermal progenitor (NMP) intermediate by activating Wnt and FGF signaling early during iPSC differentiation. Cell reprogramming methods and iPSC differentiation protocols have enabled researchers and clinicians unprecedented access to CNS stem cells for regenerative medicine applications. Created with BioRender.com.

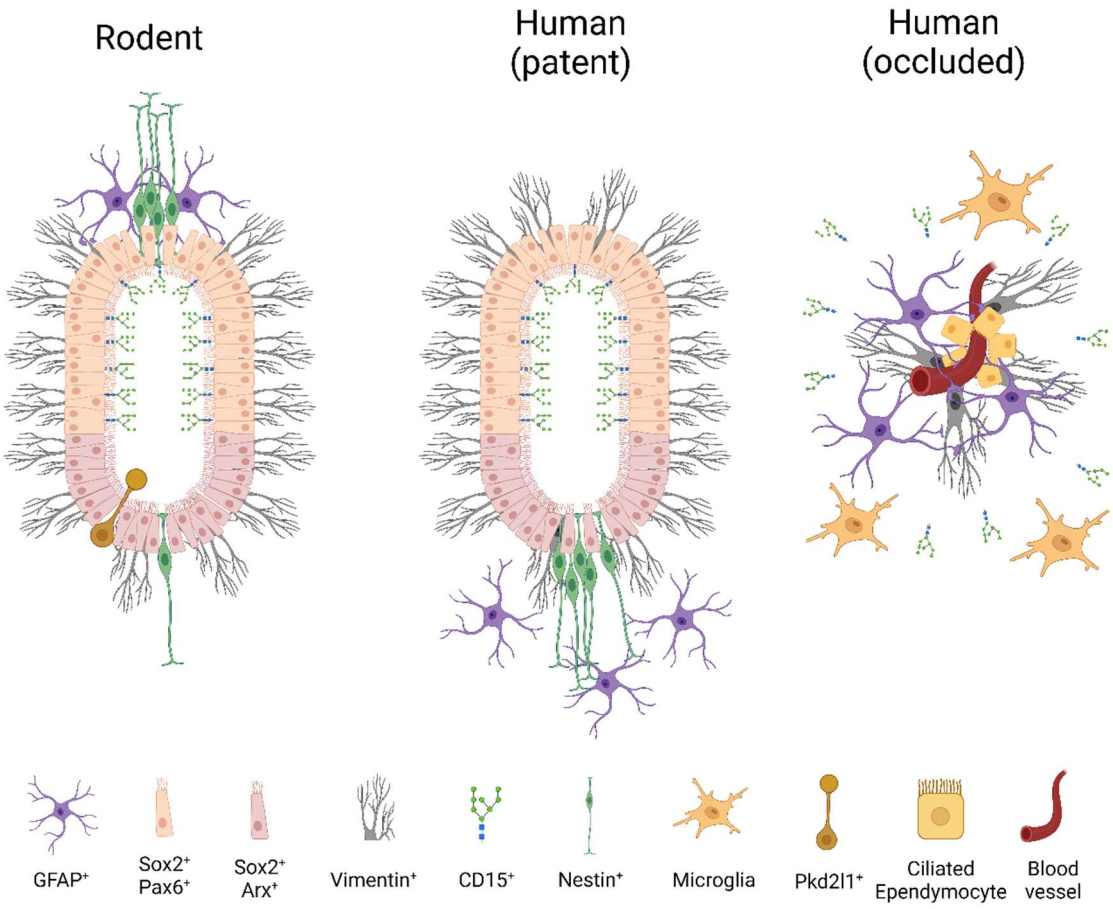

Figure 1.5 Molecular and cellular characterization of the human and rodent spinal cord central canal

The adult human spinal cord exhibits cross-species differences in the central canal's molecular, cellular, and structural components while portraying some similarities. Both human and rodent ependymal cells are all Sox2+ and Vimentin+ in a patent central canal. They also exhibit regionalization with an Arx^+ ventral domain and $Pax6^+/CD15^+$ dorsal domain. In rodents, Nestin is expressed in the dorsal central canal and is intermingled with $GFAP^+$ astrocytes. Meanwhile, in humans, Nestin is expressed in the ventral central canal in a hypocellular region surrounded by

astrocytes. Pkd2l1^{+} cerebrospinal fluid-contacting neurons are found in the rodent but not in the human central canal. Some reports suggest that the central canal becomes occluded and resembles a perivascular pseudorosette in adult humans, especially below the cervical level. In this description, a blood vessel (instead of a canal) is surrounded by GFAP^{+} astrocytes, Vimentin^{+} cells, and ciliated ependymocytes. There are also microglia nearby and CD15^{+} cells surrounding but not within the pseudorosette. Created with BioRender.com.

Chapter 2: A Guide to Extract Spinal Cord for Translational Stem Cell Biology Research: Comparative Analysis of Adult Human, Porcine, and Rat Spinal Cord Stem Cells

2.1 Abstract

Improving the clinical translation of animal-based neural stem/progenitor cell (NSPC) therapies to humans requires understanding intrinsic human and animal cell characteristics. We report a novel *in vitro* method to assess spinal cord NSPCs from a small (rat) and large (pig) animal model compared to human NSPCs. To extract live adult human, pig, and rat spinal cord tissue, we illustrate a strategy using an anterior or posterior approach simulated in a pig model. The initial expansion of primary NSPCs uses the Neurosphere assay, followed by a pharmacological treatment phase. NSPCs derived from humans, pigs, and rats are assessed in parallel using the same cell culture parameters. Using this model, NSPCs from all species demonstrated multi-lineage differentiation and self-renewal. Importantly, these methods provide conditions to directly compare species-dependent cell behavior in response to specific exogenous signals.

2.2 Introduction

Spinal cord injury (SCI) research relies mainly on animal models to understand disease pathogenesis and develop pre-clinical treatment models (Cheriyan et al., 2014). Currently, there are no effective treatments for SCI to promote regeneration and restore function in humans despite numerous attempts involving physical rehabilitation, anti-inflammatory and anti-apoptotic drugs, stem cell transplants, and the use of bio-scaffolds (Badhiwala et al., 2018; Silva et al., 2014; Varma et al., 2013). The lack of successful translation from pre-clinical to patient interventions can be partly attributed to the limited understanding of biological differences between human and animal model systems, which is due to the scarcity of studies conducted with human tissue (Chhabra &

Sarda, 2017a; Ramer et al., 2014; Silva et al., 2014; Varma et al., 2013). Understandably, acquiring human spinal cord tissue to study is difficult for ethical and technical reasons. We report a technique for obtaining viable spinal cord tissue from neurologically deceased organ donors to enable the study of live human tissue and cell physiology. Importantly, this will also allow the direct comparison with the small and large animal models that have been advocated for translation of animal therapies to humans (Kwon et al., 2011).

One promising strategy to repair the spinal cord that has proven helpful in animal studies involves the utilization of spinal cord neural stem and progenitor cells (NSPCs) (Kadoya et al., 2016; Kumamaru, Kadoya et al., 2018; Moreno-Manzano et al., 2009; Ohori et al., 2006; Panayiotou & Malas, 2013; Yousefifard et al., 2016). Spinal cord NSPCs are predominately located surrounding the central canal in the ependymal layer and possess the inherent ability to self-renew and differentiate into the different cell types of the central nervous system (Sabelström, Stenudd, & Frisén, 2014; Weiss et al., 1996). Therefore, given the right conditions, NSPCs may be capable of regenerating the neurons, oligodendrocytes, and astrocytes that have undergone cellular death following SCI. NSPCs may also beneficially modulate their surroundings by secreting trophic factors and providing anatomical support for cellular regeneration (Goldshmit et al., 2012; Hawryluk et al., 2012; Sabelström et al., 2013). As such, understanding the factors controlling NSPC proliferation and their differentiation is pivotal for their application in regenerative strategies. However, most research into NSPC behavior has been conducted in rodent cells with little comparison to primary human NSPCs, thereby limiting clinical translatability (Dromard et al., 2008; A. J. Mothe et al., 2011; Varghese et al., 2009). Consequently, a method to allow direct comparisons between human and animal NSPC differentiation and proliferation would enhance the clinical translation of regenerative interventions.

Rodent NSPCs have been well characterized for their differentiation and proliferation profiles using the Neurosphere assay, which involves the selective culture and study of NSPCs in controlled environments (Grégoire et al., 2015; Hamilton et al., 2009; Iris Kulbatski & Tator, 2009; Meletis et al., 2008). Self-renewing NSPCs give rise to neurospheres which can be treated under defined conditions to assess the influence of exogenous signaling. NSPCs from adult human organ donors with a neurological determination of death (NDD) can be cultured similarly for characterizing differentiation and self-renewal properties (Dromard et al., 2008; A. J. Mothe et al., 2011; Varghese et al., 2009). However, primary human NSPCs require an adherent basement membrane matrix such as Matrigel to expand, while primary rodent NSPCs have historically been cultured as neurospheres in suspension (A. J. Mothe et al., 2011; Weiss et al., 1996). Different *in vitro* models (adherent vs. suspension) impact NSPC phenotype; thus, a direct comparison between human and rat NSPC studies cannot be made (Walker & Kempermann, 2014). Therefore, it is not clear if human and animal NSPCs differ in their differentiation and proliferation profiles.

In this chapter, we developed an in vitro protocol to assess the differentiation and proliferation of adult spinal cord NSPCs and directly compare human, pig, and rat NSPCs under identical *in vitro* conditions. This direct comparison of human and animal NSPC behavior would improve our understanding of the regenerative potential of human NSPCs. It could also inform us how to optimize the translation of treatments by comparing the effect of pre-clinical drugs on human and animal NSPCs.

Human spinal cords were obtained from NDD organ donors and were processed immediately for cell culture using the Neurosphere assay. NDD organ donors were identified as detailed in the Trillium Gift of Life Donor Resource Manual (Trillium Gift of Life Network, 2015). We selected pigs and rats as our comparative species due to their predominance in previous preclinical and

basic science research animal models (Cheriyan et al., 2014; K. T. Kim et al., 2018). Here, we processed primary NSPCs from humans, pigs, and rats identically as an adherent layer to eliminate potential confounding cell culture differences and allow a direct comparison. Our culture protocol involves an expansion of primary NSPCs and enables an assessment of the proliferation and differentiation responses of human, pig, and rat NSPCs to extrinsic factors in parallel.

2.3 Materials

All procedures and experiments are performed using a sterile technique. The quantities mentioned represent the minimum requirements for the extraction and culture of one human, pig, or rat spinal cord.

2.3.1 Spinal cord extraction

1. Dissection buffer: Hank's balanced salt solution (HBSS, $Ca2^{+,}$ and Mg^{2+} free) + 2% Penicillin-Streptomycin (PS) + 0.6% D-glucose
2. Tiletamine/zolazepam (Telazol®)
3. Sodium pentobarbital (Fatal-Plus®)
4. 50 mL falcon tube (x1; Falcon™)
5. Surgical tools for humans: Sternal saw (System 7 Sternum Saw – Stryker™7207-000-000), bone osteotome, 32 mm, 9 ½" (Blacksmith Surgical, BS-13-34329), mallet (Blacksmith Surgical, BS-13-34011), Deaver Retractor #3 (Sklar Surgical Instruments, 60-3212), Debakey tissue forceps (Sklar Surgical Instruments, 52-5307), Mayo scissors, straight (Sklar Surgical Instruments, 15-1555), Metzenbaum scissors (Sklar Surgical Instruments, 22-1057), Harrington-Mixter clamp (Sklar Surgical Instruments, 55-3012), scalpel handle #3 (BS-01-10001), surgical Scalpel Blade No. 10 (Bard-Parker® Cat. No. 37110).

6. Surgical tools for pigs: Autopsy saw (Stryker^{TM}Model #810 – Mopec, BD001), spinal column blade (Mopec, BD112), large section blade (Mopec, BD101), bone osteotome, 15 mm, 8”(Blacksmith Surgical, BS-13-34270), mallet (Blacksmith Surgical, BS-13-34011), scalpel handle #4 (BS-01-10003), surgical Scalpel Blade No. 23 (Swann-Morton® No. 0310), scalpel handle #3 (BS-01-10001), surgical Scalpel Blade No. 10(Bard-Parker® Cat. No. 37110), Adson needle holder (Blacksmith Surgical, BS-09-26025), Adson tissue forceps (Blacksmith Surgical, BS-9024), microscissors (McPherson-Vannas Micro Scissors, straight, 8cm long, 0.1mm tips, 5mm blades; Kent Scientific Corporation, INS600124), paddle retractors (Kelly Retractors 64X76mm, 10.5"; Medline Industries, Inc., MDS1815630), finger retractors (Finger Volkmann Retractors 6 prong, 4 1/2"; Medline Industries, Inc., MDS1838106)
7. Surgical tools for rats: Curved standard operating scissors (Medline Industries, Inc., MDS0812115), tissue forceps with teeth (Medline Industries, Inc., TRI66190H), fine operating with scissors straight blades (Medline Industries, Inc., MDS0800411), hemostat forceps (Medline Industries, Inc., MDS1222310), fine forceps (Medline Industries, Inc., DYND04046H), micro-dissection scissors (Medline Industries, Inc., MDG3860761).

2.3.2 Central canal dissection

1. 100 mm Petri dishes (x3) with 15mL HBSS in each
2. 1.5 mL microcentrifuge tube (x1)
3. Dissection microscope
4. Tray with ice
5. Surgical tools for humans and pigs: fine forceps (x3) (Medline Industries, Inc., DYND04046H), a scalpel handle (Medline Industries, Inc., MDS10801), scalpel blade No. 13 (Swann-Morton® No. 0239), Iris scissors with straight edges (Medline Industries, Inc.,

MDS0859411), Wescott micro-scissors with curved blades (Medline Industries, Inc., MDS0910311)

6. Surgical tools for rats: fine forceps (x3) (Medline Industries, Inc., DYND04046H), a scalpel handle (Medline Industries, Inc., MDS10801), scalpel blade No. 13 (Swann-Morton® No. 0239), micro-Iris scissors with straight edges (Medline Industries, Inc., MDS0729836), McPherson-Vannas micro Iris scissors with curved blades (Medline Industries, Inc., MDS0707764)

2.3.3 Tissue dissociation, purification, and primary cell seeding

1. Papain Dissociation kit (Worthington biochemical Inc., LK003150)
2. Rotary Shaker
3. Centrifuge
4. 15 mL and 50 mL canonical tubes (Falcon™)
5. Serological pipettes (5 mL, 10 mL, and 25 mL, Corning™)
6. 40 µm nylon cell strainer (VWR, 10054-462)
7. Hemocytometer
8. Matrigel (Growth factor reduced; Corning™, 354230) coated six-well plates (see note 1)
9. Neurobasal-A medium (ThermoFisher Scientific, 10888022)
10. L-glutamine, 200 mM (Gibco, A2916801)
11. Penicillin-Streptomycin (PS), 10,000 U/mL (Gibco, 15140122)
12. B27™ minus vitamin A (B27), 50X (Gibco, 12587010)
13. Human recombinant epidermal growth factor (EGF, Sigma, E9644)
14. Human recombinant basic fibroblast growth factor (bFGF2, Sigma, F3685)
15. Heparin (Sigma, H3149)

16. 1:1DMEM/F12 (Sigma, D8900)
17. Hormone mix: 1:1 DMEM/F12, 0.6% glucose, 3 mM $NaHCO_3$, 5 mM HEPES, 25 µg/mL insulin, 100 µg/mL apo-transferrin, 10 µM putrescine, 30 nM selenium, and 20 nM progesterone in distilled water
18. Serum-free media (SFM): Neurobasal-A medium, 2mM L-glutamine, 100 U/mL PS, 1% B27, and 10% hormone mix
19. Proliferation media (EFH): SFM + 20 ng/mL EGF + 20 ng/mL bFGF2 + 2 µg/mL heparin

2.3.4 NSPC culture and passaging

1. Proliferation media (EFH)
2. Ultra-low attachment six-well plates (Corning™, C3516)
3. StemProAccutase (Gibco, A1110501)
4. Hemocytometer
5. 15 mL canonical tubes

2.3.5 NSPC treatment assay

1. Proliferation media (EFH)
2. Fetal bovine serum (FBS) (Corning™, 35015CV)
3. 96-well plate with black wells (ThermoFisher Scientific, 137101) coated with Matrigel-growth factor reduced
4. 1X Phosphate buffer saline (PBS): [NaCl]=137 mM, [KCl]=2.7 mM, [Na_2HPO_4] =10 mM, [KH_2PO_4] =1.8 mM, pH 7.4
5. Bromodeoxyuridine (BrdU, Sigma, B5002)
6. StemProAccutase

7. Hemocytometer
8. 15 mL canonical tubes.

2.3.6 Immunocytochemistry and immunohistochemistry

1. 4% paraformaldehyde (Sigma, P6148) in 1X PBS, pH 7.4
2. 1X PBS
3. Normal goat serum (NGS, ThermoFisher Scientific, P131873)
4. 0.3% Triton-X (Sigma, X100) in 1X PBS
5. 2 M hydrochloric acid
6. Borax buffer, pH 9.2
7. Cryomold (10mm x 10mm x 5mm) (Adwin Scientific, 25608-922)
8. Tissue-Tek® O.C.T. Compound (Andwin Scientific, 4583)
9. Liquid nitrogen
10. Cryostat
11. Gelatin-coated microscope slides (Fisher Scientific, NC0785009)
12. Microscope slide box (Heathrow Scientific, WWG52RX89)
13. Anti-fluorescent quenching agent (Elabscience, E-IR-R119)
14. Hydrophobic barrier pen (Vector Laboratories, H4000)
15. StainTray™ (EBioscience, 44-0404-10)
16. Coverslip sealant (Biotium, 23005)
17. Hoechst 33342, trihydrochloride, trihydrate (Invitrogen, H3570)
18. Primary antibodies: See Table 1 for a list of all primary antibodies used

19. Secondary antibodies: Goat anti-mouse IgG AlexaFlour®488 and 594 (Abcam, ab150113 and ab150116), Goat anti-Rabbit IgG AlexaFlour488 and 594 (Abcam, ab150077 and ab150080) (see note 2)

2.4 Methodology

This protocol, summarized in Figure 2.1, describes the extraction of human, pig, and rat spinal cord tissue using an anterior approach for humans and a posterior approach for pigs and rats. It also describes how to culture NSPCs from all species using identical methods to allow the direct comparison of NSPC behavior.

All animals were treated strictly with the Canadian Council on Animal Cares guidelines for the Care and Use of Experimental Animals. The Animal Care Committee of the Ottawa Hospital Research Institute approved all protocols. For the extraction of human spinal cord tissue, ethics approval was obtained from the Ottawa Health Science Network Research Ethics Board. The consent form and process complied with the template the University of Ottawa provided and followed the Tri-Council Policy Statement Guidelines (Canadian Institutes of Health Research, 2018). Informed written consent was obtained from the next of kin of the deceased organ donor.

2.4.1 Spinal cord extraction for humans (20-40 min), pigs (20-40 min), and rats (10-20 min)

Human spinal cord is extracted from adult (≥18 years old) NDD following aortic cross-clamping and removal of other transplant organs approximately 2 hours after cessation of circulation. The rostral thoracic spinal cord is more easily attained if the heart and lungs are retrieved for transplant. The spinal cord tissue is extracted using the same anterior exposure for transplant organ removal (simulated in pig, Figure 2.2 A-C).

1. Contain the remaining tissues and organs with a green towel and use a Deaver retractor to retract and expose the spinal column.

2. Identify the sacral promontory and count the lumbar vertebrae to determine the L2 level.

3. Using an osteotome and the mallet, perform a transverse wedged-shaped osteotomy through the L2 vertebral body to expose the spinal canal and allow the footplate of the sternal saw to be placed under the posterior aspect of the vertebral body.

4. Using the sternal saw angled 45° medially (Figure 2.2 A), cut through the vertebral bodies in a caudal to rostral direction, holding the sternal saw's footplate up against the posterior aspect of the vertebral body to ensure the cord and thecal sac are not damaged. Take care not to change the angle of the sternal saw, as this could result in difficulty retrieving the sternal saw. Then, mobilize the tissues and organs to the contralateral side and perform the same maneuvers on the contralateral side.

5. After performing the transverse cuts bilaterally with the sternal saw, remove the vertebral bodies using an osteotome to detach the rostral attachment (Figure 2.2 C).

6. Using a closed Harrington-Mixter clamp to dissect the thecal sac circumferentially, starting at the second lumbar vertebral level. Using the Harrington-Mixter clamp, gently retract the thecal sac ventrally. Use the Metzenbaum scissors to transect the thecal sac at the L2 level. Then, retract the dura ventrally with forceps and use the Metzenbaum or Mayo scissors to cut the nerve roots bilaterally in a caudal to cranial direction. This allows the thecal sac containing the spinal cord to be mobilized and minimizes trauma to the spinal cord tissue. Once the thecal sac has been dissected to the rostral end of the vertebral exposure, transect the rostral end of the thecal sac with the spinal cord using Metzenbaum scissors or a number 10 blade.

7. Incise the dura with Metzenbaum scissors and place the extracted spinal cord tissue in the sterile cold (4°C) dissection media in a 50 mL conical tube on ice for transport to the tissue culture room. Typically, the spinal cord is sectioned into 20-25 cm long sections. If the thoracic organs were removed, the spinal cord could be more easily extracted to the higher thoracic levels.

While an anterior approach was used in humans because of the organ donation positioning and exposure, extracting the pig spinal cord described here utilizes a posterior approach given the ease of this approach and that the pigs did not undergo organ tissue retrieval and exposure.

1. First, sedate pigs with 4 mg/kg of intramuscular tiletamine/zolazepam (Telazol®) and anesthetize with 2% isoflurane in 100% oxygen. Then, euthanize pigs by administrating sodium pentobarbital (Fatal-Plus®) intravenously at ≥100 mg/kg according to institution-approved animal protocol.

2. Orient the pig in the prone position. Using a No.4 scalpel handle with a No. 23 blade, make a longitudinal incision over the spinous processes starting from the T1 thoracic vertebrae and ending at the L2 lumbar vertebrae (See note 3). Make two transverse incisions perpendicular to the longitudinal incisions at the first thoracic and last lumbar vertebrae (Figure 2.2 D).

3. Make deep incisions running adjacent to the spinous processes, lamina, and transverse processes to expose the spinous processes of the vertebrae (Figure 2.2 E). For this cut, ensure that the incisions are deep to uncover the ribs and that all the paraspinal muscles are severed from their insertions.

4. Expose the posterior spinal column by retracting the paraspinal muscles with a paddle or sharp prong finger retractors. If retraction is not possible, excise the para-spinal muscles and

overlying skin by dissecting the fascia of the muscles using a scalpel with a No. 23 blade. After the para-spinal muscles have been separated from the underlying fascia, make a longitudinal incision lateral to the muscle to remove the muscle.

5. Cut through the lamina using an autopsy saw mounted with a large section or spinal column blade. Cut through the lamina by angling the saw orthogonal to the lamina and stopping before the spinal canal (Figure 2.2 A). Cut the vertebral column with the desired spinal cord length to be extracted.

6. Sever the rostral and caudal ends of the spinous processes using an osteotome and mallet, being cautious not to sever the spinal cord. Remove the spinous processes and lamina using an osteotome and mallet to avoid damaging the cord (Figure 2.2 F). Then, lift the dura-covered spinal cord using tooth forceps and carefully dissect it rostrally. Sharply cut the spinal cord at the exposed rostral end with a No.3 scalpel handle with a No. 10 blade. Use Metzenbaum or Mayo scissors and forceps to cut the nerve roots bilaterally in a caudal to cranial direction.

7. Place the extracted spinal cord tissue in the sterile cold (4°C) dissection media in a 50 mL conical tube on ice for transport to the tissue culture room. A 25-30 cm spinal cord section from the upper thoracic to the lower lumbar region can be obtained under usual conditions. The time elapsed between euthanasia and extraction of the spinal cord is 30-40 minutes.

The extraction of rat spinal cord tissue also uses a posterior approach.

1. Anaesthetize rats with 4% isoflurane in 100% oxygen and euthanize them by decapitation according to institution-approved animal protocol.

2. Place rats on their ventral surface and sterilize skin on the dorsal surface with 70% ethanol.

3. Excise the skin on the dorsal surface around and along the vertebral column using scissors.

4. Make a bilateral incision around the vertebral column at the caudal end of the lumbar spinal cord using operating scissors and then cut the vertebral column transversely.

5. Perform a bilateral laminectomy from the point of transection towards the rostral direction. Use dissection scissors to cleave the lamina and retract the dorsal vertebral column until the entire spinal cord length is exposed.

6. Gently lift the spinal cord from the caudal end using fine forceps and cleave the spinal nerves in the rostral direction. Place the extracted spinal cord tissue in the sterile cold (4°C) dissection media in a petri dish on ice.

2.4.2 Dissection of human, pig, and rat spinal cord (20-40 min)

The procedure outlined here describes the excision of the ependymal cell containing the region of the central canal of the spinal cord. This technique is novel compared to previous methods (Dromard et al., 2008; A. Mothe & Tator, 2015) and may be advantageous given the considerable reduction of contaminating white and grey matter. Briefly, the spinal cord is cleansed of its meninges, sectioned into thin slices (~1-2 mm) using a scalpel blade, then micro-dissected to excise a cuboidal tissue sample containing the central canal (Figure 2.3). Consistency in the dissection technique is necessary to obtain a similar primary cell population between biological replicates and to minimize contamination from progenitor cells in the surrounding grey and white matter tissue.

1. Transfer the spinal cord segment using tissue forceps into the first sterile petri dish containing cold dissection buffer.

2. Clean the spinal cord of the dura using straight-edge dissection scissors. Proceed to remove the underlying arachnoid under a dissection microscope by holding the tissue in place with fine forceps and cutting away the meninges using curved edge microscissors. Start from either end of the whole spinal cord tissue, pull away the meninges with forceps, then place one edge of microscissors between the meninges and the underlying tissue and cut all the way down to the opposite end (Figure 2.3 B, see note 4).
3. Once cleaning is complete (Figure 2.3 C), wash the spinal cord in cold dissection buffer and place it in a new petri dish with cold dissection buffer for sectioning.
4. Section the tissue into thin ~1-2 mm sections using a scalpel blade and forceps. Start at either end of the tissue and orient the forceps downwards to hold the tissue on its lateral ends. Using the perpendicular edge of the forceps to guide the blade, proceed to section the tissue transversely. Sectioning is facilitated by the removal of meninges in the previous steps.
5. Transfer the thin sections to a new petri dish with cold dissection for central canal dissection (Figure 2.3 D). Initiate dissection from the ventral sulcus and cut towards the central canal using curved-edge microscissors; use forceps to hold tissue sections in place during dissection. Stop cutting just before reaching the central canal and start cutting towards either lateral direction. Complete the dissection by cutting around the central canal region to excise a cuboidal piece (Figure 2.3 E). It is crucial to use curved edge micro-scissors in this step to avoid excision of the central canal region from the underside of the section.
6. Ensure enough spinal cord is sectioned to yield enough primary cells for culture. Typically, 5-7 sections yield 1-5x10^6 cells. Alternatively, one gram of dissected central canal tissue yields 5x10^7 cells.

7. Transfer the dissected central canal tissue into sterile 1.5 mL microcentrifuge tubes and mechanically dissociate the tissue using scissors until completely minced. Keep the microcentrifuge tubes on ice while preparing the tissue dissociation kit.

2.4.3 Tissue dissociation, purification, and NSPC seeding (2-3 hours)

1. The minced central canal tissue is dissociated into single cells using a papain / DNase treatment from Worthington Biochemicals, according to the manufacturer's instructions. Transfer the minced tissue into a 15 mL conical tube containing the papain solution and place it on a rocker platform at 37 degrees. Use 0.2-0.4 g of tissue per vial provided in the kit and incubate for 1-2 hours. This should yield 1-2x10^7 cells per vial.
2. Following digestion, triturate using a 10mL pipette until the tissue fragments are disintegrated to form a cloudy solution.
3. Centrifuge at 500 x g for 5 minutes, discard the supernatant and resuspend the cells in an ovomucoid/albumin solution from the dissociation kit to inhibit papain activity.
4. Set up a discontinuous gradient centrifugation to purify NSPCs of contaminant (post-mitotic and glial) cells and debris. Using a 10 mL pipette, gently lay the resuspended cells in step 3 onto 5 mL of albumin-ovomucoid solution from the dissociation kit.
5. Centrifuge at 70 x g for 6 minutes, discard the supernatant and resuspend the cells in 10 mL of warm EFH.
6. Filter the cells through a 40 μm sterile filter using 100-1000 μL tips, add 30 mL of warm EFH, and then centrifuge at 300 x g for 5 minutes.
7. Resuspend the cells in 1 mL of warm EFH and count the cell density using a hemocytometer.
8. Seed the primary cells in 6-well plates pre-coated with Matrigel at a density of 20 cells/μL in a total of 4 mL EFH, then incubate at 37˚C, 5% CO_2, 20% O_2 for one week undisturbed.

2.4.4 Feeding (15-30 min) and passaging (30-45 min) primary NSPC cultures

The protocol described in this section is based on Mothe and Tator (2015), who have optimized *in vitro* culture conditions and techniques to propagate adult human spinal cord NSPCs through multiple passages successfully. They also demonstrated that primary human NSPCs require an adherent substrate to be successfully passaged, which can then be assessed as neurospheres. Although rat NSPC cultures do not need an adherent substrate to grow, we cultured NSPCs from all species as an adherent layer in this protocol to mitigate the confounding effects of the culture conditions.

1. After one week, replace 50% of the medium with warm EFH containing double the concentration of mitogens (40 ng/mL EGF and FGF2). NSPCs are fed this way every two or three days for the next one-three weeks until adherent cultures are visibly expanding (see note 5).
2. Once proliferating NSPCs are visible (Figure 2.4), remove 100% of the media, wash with warm PBS, and replace media with 2 mL of fresh warm EFH. Cultures are fed by replacing 100% of the media every 2-3 days while monitoring their growth (see note 6).
3. Passage the cells before they reach confluence using Accutase (see note 7). Add enough Accutase to cover the surface (1 mL per well of a 6-well plate). Incubate at room temperature for 5-10 minutes while regularly observing to see if cells have lifted. Knock the plate on the side to detach cells.
4. Transfer the lifted cells into a sterile conical tube, wash each well with warm PBS, and transfer washes into the tube.
5. Centrifuge at 300 x g for 5 minutes, discard the supernatant, and resuspend in 1 mL of warm EFH.

6. Count the cell density to seed NSPCs for secondary expansion or conditioned treatment.

2.4.5 Generating neurospheres (30-45 min)

Primary cultures can be passaged and seeded in suspension to further select for self-renewing NSPCs and eradicate progenitors. Under these conditions, self-renewing stem cells will form neurospheres that can be separated from non-stem cells by mass centrifugation. The steps below can be used to culture secondary (and beyond) neurospheres of human, pig, and rat NSPCs (Figure 2.4).

1. Seed secondary NSPCs in 6 well plates at a density of 10 cells/µL in a total of 2 mL EFH, then incubate at 37˚C, 5% CO_2, 20% O_2.
2. Allow NSPCs to grow for one week unperturbed to prevent neurosphere aggregation (see note 8).
3. After one week, transfer the media containing neurospheres into a 15 mL conical flask. Wash the wells with warm PBS and transfer washes into the 15 mL conical flask.
4. Centrifuge at 300 rpm for 5 minutes, discard the supernatant containing dead/single cells, and resuspend in 1-2 mL Accutase. Triturate using a 1000 µL pipette tip and incubate for 5-10 minutes at room temperature.
5. Centrifuge the cell suspension at 1500 rpm for 5 minutes, discard the supernatant, and resuspend in 1 mL warm EFH.
6. Count the cell density and seed NSPCs for tertiary expansion (10 cells/µL) or conditioned treatment.

2.4.6 Treatment and direct comparison of species NSPC (up to 3 weeks)

Here, we demonstrate a functional assay to characterize the differentiation and proliferation of human, pig, and rat NSPCs under identical conditions. The parameters of this assay (cell density, culture conditions, and time spent in culture) were all optimized for treating NSPCs for up to two weeks without becoming over-confluent. Importantly, this assay is versatile in assessing various exogenous factors.

1. Seed primary derived NSPCs onto Matrigel-coated 96-well plates in 150 uL EFH. The cell density (1-5 cells/μL) will depend on the treatment (see note 9). Leave cultures incubated at 37˚C, 5% CO_2, and 20% O_2 for three days undisturbed. This step is to further select for NSPCs and allows enough time for NSPCs to adhere to the basement surface.
2. Aspirate the media and wash with warm PBS (50 uL). Ensure that conditioned media/treatments are prepared and warmed at 37˚C.
3. To induce differentiation, replace the PBS wash with 1% FBS in 150 uL SFM. To induce proliferation, replace the PBS wash with 150 uL EFH. Incubate at 37˚C, 5% CO_2, 20% O_2, and replace media with fresh media every two to three days. NSPCs can be treated for up to two weeks in 1% FBS or EFH without reaching confluency.
4. To assess proliferation, a DNA analog (e.g., BrdU, EdU) can be used as a marker for the S-phase of the cell cycle. In our experiments, BrdU (10 μM) is added 24 hours before fixing.
5. Fix NSPC cultures at desired time points (up to two weeks) using 4% PFA. Incubate cultures with PFA for 20 minutes at room temperature, followed by three PBS (50 uL) washes. Cultures need not be characterized immediately; add 100 μL PBS into each well and store the plate at 4 degrees.

2.4.7 Immunocytochemistry of cultured NSPCs (2 days)

A method of NSPC characterization by immunocytochemistry is proposed here. This involves the fluorescent labeling specific cellular phenotypes according to their molecular signatures (see table 1). A working volume of 50 µL/well is used for a 96-well plate.

1. Remove PBS from each well to be stained and add 50 µL of PBS for 10 minutes at room temperature to equilibrate.
2. Pre-treat with 10% NGS to prevent non-specific antibody binding and with 0.3% Triton-X to permeabilize cells for 30 minutes at room temperature. If staining for membrane receptors, such as O4, skip the permeabilization step. Wash each well three times with PBS for 5 minutes at room temperature.
3. For BrdU staining, DNA denaturation is required by incubating cultures with 2 M HCl at 37 degrees for 30 minutes. Wash twice with borax for 5 minutes each, followed by three washes with PBS for 5 minutes each.
4. Dilute the primary antibody in 10% NGS in PBS according to the optimized dilution (see table 1) and incubate at 4 degrees overnight.
5. The next day, wash each well three times with PBS for 5 minutes at room temperature.
6. Dilute the secondary antibody (1:500) in PBS and incubate for 2 hours at room temperature (see note 10). Wash three times with PBS.
7. Counterstain nuclei with Hoechst (1:2000 dilution in PBS) for 5 minutes at room temperature. Wash twice with PBS and add 100 µL PBS into each well for storage. NSPCs are now ready to be visualized by immunofluorescence.

2.4.8 Cryosectioning (>2 days)

1. Fix spinal cord tissue sections (3-5 mm thick) in PFA for 36-48 hours at 4 °C
2. Decant or aspirate PFA and wash the sections with PBS three times for 5 minutes each wash.
3. Prepare spinal cord tissue for cryosectioning by placing a single spinal cord section into a cryomold containing tissue-tek, ensuring the tissue is submerged in tissue-tek.
4. Using long forceps to grip the cryomold, gently place the cryomold above liquid nitrogen such that the cryomold makes contact with liquid nitrogen without being fully submerged. The tissue-tek containing spinal cord tissue will freeze in a matter of seconds.
5. Immediately place the frozen embedded block into a cryostat with an internal temperature of -20 °C and allow the sample to equilibrate.
6. Mount the embedded block onto a metal chuck using tissue-tek as an adhesive.
7. Proceed to section the embedded block at 20 µm (or less) according to standard cryosectioning practices. Following each section, adhere the tissue onto a gelatin-coated microscope slide (see note 11).

2.4.9 Immunohistochemistry of spinal cord sections (2 days)

We performed immunohistochemistry on cryo-sectioned slices from fixed human spinal cord to characterize the ependymal layer of the human spinal cord and validate antibodies used in immunocytochemistry.

1. Place microscope slides to be immunostained into a humidified StainTray™.
2. Create a barrier using a hydrophobic pen around tissue slices to be stained with a single antibody.

3. Add enough PBS within the hydrophobic barrier to submerge the tissue and allow the tissue to equilibrate at room temperature.
4. Remove PBS using a pipette and add enough volume of blocking (10% NGS) and permeabilizing (0.3% Triton-X) buffer for 30 minutes at room temperature. If staining for membrane receptors, such as O4, skip the permeabilization step. Wash each well three times with PBS for 5 minutes at room temperature.
5. Dilute the primary antibody in 10% NGS in PBS according to the optimized dilution (see table 1) and add it to the tissue. Incubate at 4 °C overnight.
6. The next day, wash the tissue three times with PBS for 5 minutes at room temperature.
7. Dilute the secondary antibody (1:500) in PBS and incubate the tissue for 2 hours at room temperature (see note 10). Wash three times with PBS for 5 minutes at room temperature.
8. Counterstain nuclei with Hoechst (1:2000 dilution in PBS) for 5 minutes at room temperature. Wash twice with PBS for 5 minutes at room temperature, then aspirate PBS from the slide.
9. Use Kimwipes to remove as much PBS from the slides without damaging the tissue.
10. Place a small amount of anti-fluorescence quenching agent onto the slide and mount a coverslip ensuring no air bubbles are formed.
11. Use a coverslip sealant to affix the coverslip to the microscope slide. The tissue is now ready to be visualized by immunofluorescence.

2.5 Results and Discussion

We have successfully cultured primary spinal cord NSPCs from three species using comparable dissection techniques and identical culture conditions. Here, we describe a model to treat NSPCs with exogenous factors using the same parameters for all species, allowing for a direct comparison

of species NSPC proliferation and differentiation. We also describe a means to characterize NSPC proliferation and differentiation using immunocytochemistry (Table 1), permitting visualization and quantification of cellular phenotypes. We confirmed that human, pig, and rat NSPCs are self-renewing (Figure 2.4) and express the neural stem cell marker Sox2 (Figure 2.5). Unlike NSPCs in the brain that co-express Sox2 and GFAP, NSPCs in the spinal cord express Sox2 but not GFAP (Figure 2.8). This permits the characterization of spinal cord NSPCs using Sox2 alone (Lim & Alvarez-Buylla, 2016; Martínez-Cerdeño & Noctor, 2018; Becker, Becker, & Hugnot, 2018; Dromard et al., 2008; Meletis et al., 2008). We've shown that human and rat NSPCs can differentiate into β-iii tubulin+ neurons, GFAP+ astrocytes, and O4+ oligodendrocytes (Figure 2.5, Table 2). We also found that pig NSPCs differed in not forming identifiable O4+ oligodendrocytes under the conditions tested. Therefore, our model, for the first time, can allow direct comparisons of human and animal NSPC proliferation and differentiation utilizing identical culture conditions to identify intrinsic differences between the human and animal cells.

Initially, primary NSPCs from all species were stimulated to proliferate with mitogen treatment (EGF, FGF2) and grown on Matrigel, a necessity for humans and pigs but not rat NSPCs (A. Mothe & Tator, 2015). We have cultured NSPCs from all species on Matrigel as an adherent mono-layer since the culture system (adherent vs. suspension) may affect the proportion of stem, progenitor, and mature cells in the final population (Walker & Kempermann, 2014). Also, the adherent layout results in a uniform distribution of primary-derived NSPCs with minimal cell-to-cell contact allowing the direct assessment of exogenous factors. The advantage of this setting is that the causal mechanisms can be easily examined by modifying the chemical composition of the media. This model, however, presents a limitation in the interpretation of data and inference to in vivo behavior where cell-to-cell contact is present.

Using the mono-layer method, primary NSPCs were passaged upon reaching confluence and counted to determine the yield of NSPCs per ten thousand primary cells seeded. When comparing species, the yield of human NSPCs was less than porcine NSPCs, and the yield of both human and porcine NSPCs was significantly less than rodent NSPCs (Table 2). This suggests that animal models may have more NSPCs or that their NSPCs can proliferate more than humans. Expectedly, it took less time for NSPCs to attain confluence from rodents (2-3 weeks) and porcine (2.5-6 weeks) compared to humans (4-10 weeks). This is reflected in the doubling rate, which was greatest for humans and least for rodents (Table 2).

The Neurosphere assay has been used over the past three decades to culture NSPCs, yet the conditions of this assay have been optimized for rodent NSPCs (Gil-Perotín et al., 2013; A. Mothe & Tator, 2015; Walker & Kempermann, 2014). Previous attempts to culture adult human spinal cord NSPCs have been challenging due to inadequate culture conditions or intrinsic variability among donor NSPCs (Arvidsson et al., 2011; Jha, Liu, Chrenek, Madsen, & Cardozo, 2013; A. J. Mothe et al., 2011). As such, the greatest self-renewal capacity of human NSPCs may be unattainable using the Neurosphere assay (Dromard et al., 2008). This may explain the significant difference in yield between human and rodent NSPC cultures. Also, the yield varied greatly between humans (Figure 2.6) but not rats, suggesting the methods used are reproducible and that the organ donor profile (e.g., age, sex, medical background, cause of death, and time elapsed from cross-clamp to spinal cord harvest) will likely influence the yield to some extent. Finally, the yield of porcine NSPCs varied, given the low viability of spinal cord tissue during the initial harvest attempts. Unlike humans, porcine was not perfused. Also, the initial spinal cord harvest attempts required more time with porcine than with rodents, indicating that the time elapsed between spinal cord harvest and cell culture may be a crucial variable for primary NSPC yield.

To further select for self-renewing NSPCs, primary NSPCs can be passaged and seeded at low cell density (≤ 10 cells/μL) to form neurospheres. These neurospheres grow from the self-renewal activity of stem cells and thus may better portray the NSPC lineage profile (Narayanan et al., 2016). Secondary (and beyond) neurospheres can be dissociated into single cells and assessed similarly to primary-derived NSPCs using our model. It is important to note, however, that NSPC behavior is expected to change with increased time in culture and with an increased passage. Therefore, assessing primary NSPCs portrays in vivo behavior best since they spend minimal time outside their natural niche (Gil-Perotín et al., 2013).

The proposed model can evaluate and compare human, pig, and rat NSPC responses concerning many physiological and disease processes. Importantly, this model could depict causal mechanisms that would be impossible to obtain otherwise from living patients or post-mortem samples. For example, response to physiologically and clinically relevant exogenous factors can be assessed. This model can also optimize a combination of growth factors to promote human NSPC survival and differentiation following transplant. Growth factors are commonly used with rodent and human NSPC transplants, but potential differences in signaling mechanisms between species may hinder the translation of such treatments (Kadoya et al., 2016; S. Karimi-Abdolrezaee et al., 2010; Kumamaru, Kadoya, et al., 2018; Lu et al., 2012; A. J. Mothe et al., 2011). As such, it is important to consider how human NSPCs would respond to exogenous factor treatments, which can be assessed *in vitro* using our proposed model. Ultimately, the evaluation of human NSPCs and comparison with animal model NSPCs can clarify how human NSPCs respond to SCI and advance the translation of regenerative strategies.

According to our knowledge, adult pig spinal cord NSPCs have not been previously characterized for differentiation. In this study, we did not observe oligodendrocyte differentiation from our pig

cultures using the O4 antibody and under the conditions tested. While O4 has been reported to label oligodendrocytes obtained from the brains of adult pigs, their protocol differed in that they obtained NSPCs from the brain rather than the spinal cord, cultured their NSPCs as neurospheres rather than in a monolayer, and utilized a different O4 antibody (Liard et al., 2009). Furthermore, a separate study that also cultured pig brain NSPCs could not obtain $O4^+$ oligodendrocytes upon differentiation, demonstrating the difficulty in generating mature oligodendrocytes in culture (E. Kim et al., 2018). In our study, it is unlikely that the O4 antibody did not recognize the pig epitope since immunohistochemical staining was observed in pig spinal cord sections (Figure 2.7 B). Besides, we have used NG2 and Olig2 for rodent cell labeling. However, we did not pursue further assessment in humans and pigs because these are markers for early oligodendrocyte progenitors and do not exclusively label the oligodendrocyte lineage. We also tried CNPase and PDGFR; however, while we could get labeling in rats, we could not get labeling in humans. This finding highlights a challenge for conducting cross-species comparisons in which reagents that cross-react with all species being tested are needed to understand the translational assessment of animal studies to humans. Thus, in the end, since we wanted to identify terminally differentiated oligodendrocytes, and because more preclinical studies are done with rodents rather than pigs, we used O4 for labeling of oligodendrocytes.

Another cross-species difference was delineated during the immunohistochemical validation of antibodies in spinal cord sections (Figures 2.7 and 2.8). A study by Garcia-ovejero and colleagues (2015) reported that the adult human spinal cord differs from rodents and primates concerning the morphology and cellular composition of the central canal. Unlike rodents and primates with a patent central canal lumen, the human spinal cord central canal has been described as occluded, resembling a perivascular pseudorosette. This observation in humans was prevalent in individuals

above 18 years old and in spinal cord regions below the cervical level. The observed perivascular pseudorosettes in humans were described by three characteristic features that differ from the central canal of animal models. First, a dense area of $GFAP^+$ astrocytic cells surround and occasionally infiltrates ependymal cells. Second, groups or chains of variable-sized protoplasmic cells surrounded by lax extracellular matrix expressing beta-catenin and CD15. Lastly, vimentin+ and βiii tubulin+ cells surround VWF^+ and $fibronectin^+$ blood vessels. Interestingly, Garcia-ovejero and colleagues (2015) did not detect any $Sox2^+$ ependymal cells, which is in stark contrast to previously characterized NSPCs from the human and animal spinal cord (Cawsey et al., 2015; Dromard et al., 2008; Hamilton et al., 2009; Marichal et al., 2012; Meletis et al., 2008; Sabourin et al., 2009a).

We found contrasting evidence to the study by Garcia-ovejero and colleagues (2015) using immunohistochemical staining of spinal cord sections (Figure 2.8 A-G). Most prominently, we observed a patent central canal lumen in the thoracic spinal cord of humans, including a 67-year-old donor and porcine spinal cord (Figure 2.7 A). Lining the human central canal were tightly packed cells that express Sox2, CD15, vimentin, Jagged1, and S100β (Figure 2.8 A-E), which have been previously shown to be expressed in ependymal cells (Dromard et al., 2008; Hamilton et al., 2009; Marichal et al., 2012; Sabourin et al., 2009b). While Sox2, Vimentin, Jagged1, and S100β labelled all ependymal cells, CD15 labelling was absent in the ventral central canal, as previously shown in the human and rodent spinal cord central canal (Dromard et al., 2008; Sabourin et al., 2009a). Furthermore, unlike Garcia-ovejero and colleagues (2015), there was a lack of βiii tubulin and GFAP labelling in ependymal cells. However, positive labelling in the surrounding grey matter was profuse (Figure 2.8 F, G).

In rodents, although rare, GFAP has been observed in the dorsal ependymal layer. At the same time, βiii tubulin is absent, with the occasional exception of cerebrospinal fluid-contacting neurons (Sabourin et al., 2009b). However, in the human spinal cord central canal, it has been reported by other groups that GFAP is absent or present exclusively in the lateral and dorsal ependymal cells, thus requiring further characterization of GFAP in humans (Cawsey et al., 2015). To our knowledge, cerebrospinal fluid-contacting neurons are yet to be discovered in humans, although there is evidence in non-human primates (Alfaro-Cervello et al., 2014; Djenoune et al., 2014). Ultimately, our observations contradict the notion that the human spinal central canal is occluded and replaced by perivascular pseudorosettes. Moreover, this study's molecular characterization of human central canal ependymal cells agrees with previous rodent studies (Hamilton et al., 2009; Marichal et al., 2012; Sabourin et al., 2009b).

A possible reason for these discrepancies could be that Garcia-ovejero and colleagues (2015) utilized spinal cord tissue with post-mortem delays ranging from 3 to 15 hours (some patients had unknown values for post-mortem delay). Meanwhile, organ donors in our study were kept on life-support and perfused with cold storage solution (e.g., Belzer UW cold storage solution) during the organ harvest. Also, donors in this study had their spinal cord tissue harvested within 3 hours of cross-clamping and fixed immediately. A separate study by Hugnot and colleagues (2008) also reported a patent central canal in the spinal cords of organ donors. Their method involved lowering the body temperature and maintaining blood circulation, which likely preserved tissue integrity. These differences in post-mortem delays and tissue preservation may have influenced tissue viability and affected the morphology of central canals.

Further evidence suggesting the perivascular pseudorosettes may be a post-mortem artifact stems from their RNA characterization. Garcia-ovejero and colleagues (2015) report that perivascular

pseudorosettes are more enriched for genes related to ependymoma than a neurogenic niche. However, the incidence of ependymomas is predicted to be below 3 per million people, which is in stark contrast to the prevalence of perivascular pseudorosettes (<90% above the age of 18) observed in the study by Garcia-ovejero and colleagues (2015) (Louis et al., 2007). Therefore, observing perivascular pseudorosettes replacing a patent central canal in adult humans may be an artifact due to prolonged post-mortem delays and tissue preservation methods.

In conclusion, the model described here is the first to directly compare the differentiation and proliferation behaviour of primary adult human and animal spinal cord NSPCs. This assay uses the same parameters for all species, is reproducible, and allows for high-throughput testing. This model can help identify species-dependent cell-intrinsic mechanisms, which would be necessary to translate regenerative strategies targeting human spinal cord NSPCs.

2.6 Notes

1. Matrigel plates should be prepared in advance and kept at 4°C until ~1 hour before use. Use a dilution of 1:25 in SFM to coat a thin Matrigel basement layer. We recommend warming the Matrigel plates at room temperature immediately after papain digestion is initiated. Matrigel polymerizes slowly at room temperature to form a basement membrane and is required for the expansion of primary human primary NSPCs. Matrigel can be replaced by other surface coatings such as laminin, poly-D-Lysine, and collagen (A. J. Mothe et al. 2011).
2. Optimization of antibody dilutions (primary and secondary) is necessary before immunostaining, especially if antibodies are purchased from a different manufacturer or lot number.

3. Generally, the first thoracic vertebrae are the first palpable spinous process at the rostral end, and the last lumbar vertebrae are the last palpable spinous process at the caudal end. There are 14 thoracic and six lumbar vertebrae in pigs.
4. The spinal cord must be removed from its meninges (dura and arachnoid) to facilitate sectioning the spinal cord into thin segments. The dura is relatively easy to remove and does not require a dissection microscope, while removal of the arachnoid requires closer attention and should be performed under a dissection microscope. The spinal cord with the dura and arachnoid removed will also minimize endothelial contamination.
5. Observing cultures regularly and tracking any areas with cell growth is important. Human NSPCs start to proliferate in small patches and grow radially outwards. However, cell growth is not uniformly distributed throughout the wells and is inconsistent between human cultures. Therefore, each primary human culture must be frequently observed and treated uniquely.
6. Do not allow cells to reach confluence (over-crowding), as lifting NSPCs during the passage becomes difficult. At this stage (near confluence), we recommend preparing your NSPC treatment protocol and reagents.
7. Accutase is a milder dissociation enzyme than trypsin and is preferred for the delicate treatment of NSPCs.
8. Seeding NSPCs at a low cell density and expanding for one week is recommended to minimize sphere aggregation. This would render results more variable and reduce cell viability.
9. The cell density used depends on the conditions. For example, EFH will stimulate NSPC self-renewal, while FBS will induce differentiation. The latter process involves rapid division of progenitor cells, and thus NSPCs will attain confluence quicker in FBS than

NSPCs stimulated to self-renewal. For this reason, it is recommended to seed NSPCs at a lower cell density (1 cell/µL) when stimulating differentiation compared to when promoting self-renewal (5 cells/µL).

10. Co-staining using several antibodies is possible if all primary antibodies are generated in different animals, and all secondary antibodies bear different fluorophores.
11. If tissue sections are to be stained immediately, place slides in a humidified StainTray™ until immunohistochemistry is performed. Otherwise, store the slide in a microscope slide box.

2.7 Acknowledgements

We thank the families that have consented to our study and permitted the donation of spinal cord tissue from their beloved ones to advance medical science research. We want to acknowledge the Ottawa Hospital Department of Neurosurgery and TGLN for permitting spinal cord extractions from organ donors and the University of Ottawa Heart Institute Animal Care and Veterinary Service for providing pigs. We also thank Isaac Kim, Ellen McDoney, Hesham Ismail, Annemarie Dedek, and Tongda Li for assisting during the porcine spinal cord harvests.

2.8 Figures and Tables

Figure 2.1 Experimental workflow depicting spinal cord harvest (20-40 min), spinal cord sectioning and central canal dissection (20-40 min), tissue dissociation and purification (2-3 hours), NSPC culture (up to 10 weeks), treatment (up to 3 weeks), and characterization (2 days)

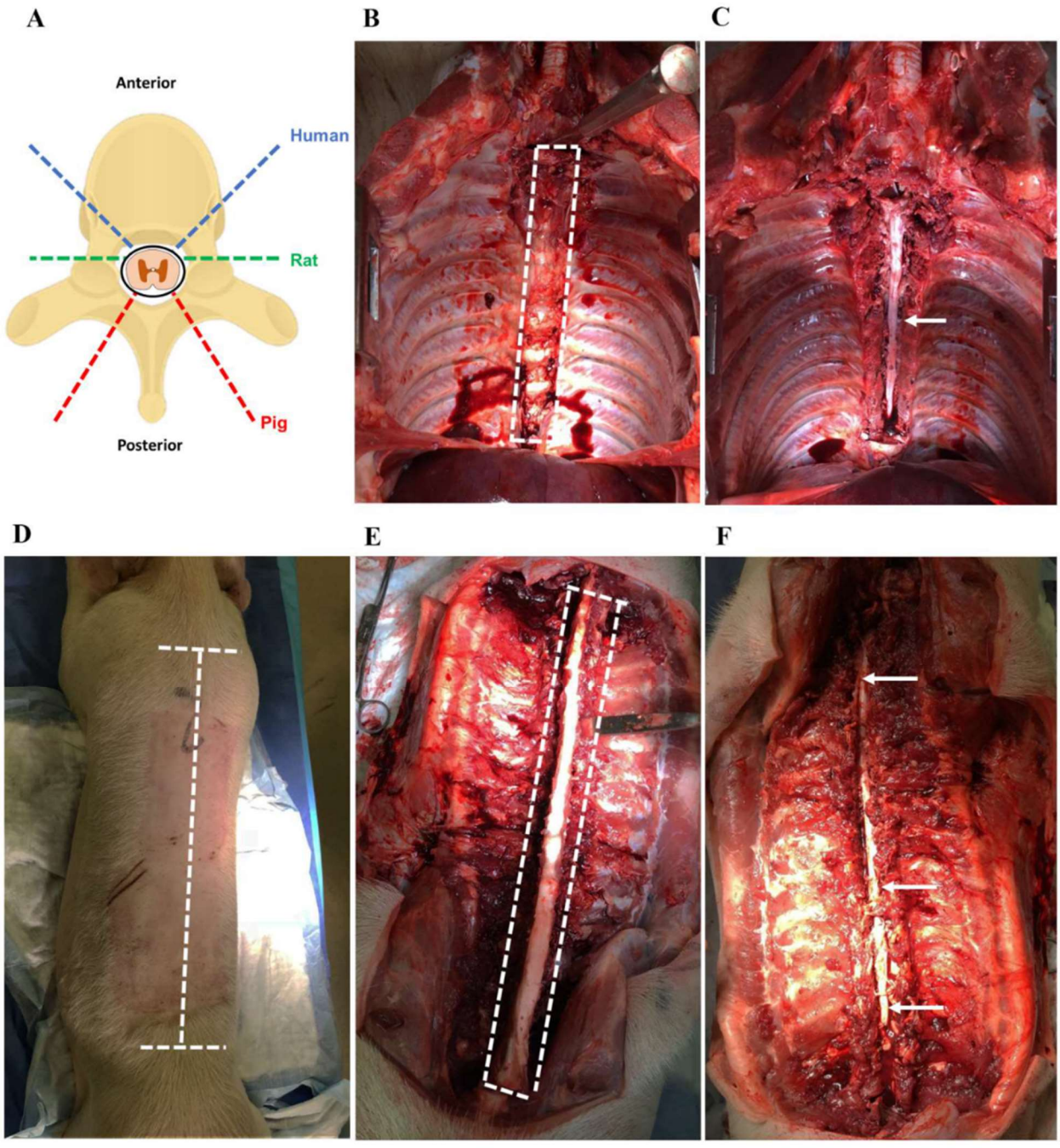

Figure 2.2 Spinal cord harvest simulation in porcine via an anterior approach

(A) Angles of approach for laminectomy in humans, rats, and pigs to extract the spinal cord. The dashed blue line indicates humans, green indicates rats, and red indicates pigs. (B) Laminectomy of the human spinal cord using anterior approach simulated in a pig (T2-T12). The heart, lungs, esophagus, and major vessels have been removed for improved visibility. The dashed white line indicates the spinal cord region to be cut. (C) Exposed spinal cord post-laminectomy using the anterior approach from T2-T12. The arrow indicates the thecal sac containing the spinal cord tissue. (D) Laminectomy of the pig spinal cord using a posterior approach with incision lines marked. The dashed white line indicates incisions required to expose the vertebral column. (E) Laminectomy of the pig spinal cord using the posterior approach with the vertebral column exposed and paraspinal muscles removed for clarity. The dashed white line indicates cuts required to expose the spinal cord. (F) Exposed spinal cord post-laminectomy using the posterior approach from T1 to L2. The arrows indicate the thecal sac containing the spinal cord tissue.

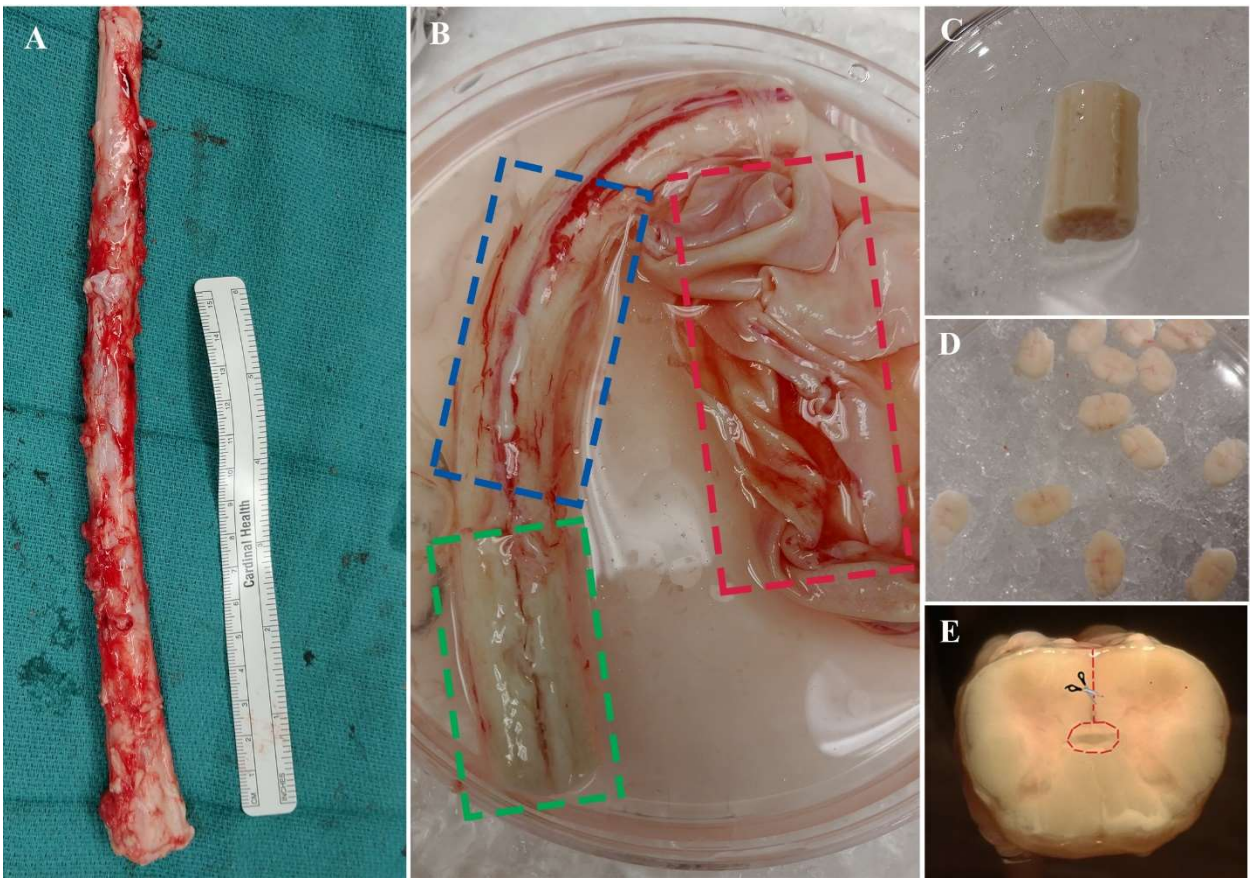

Figure 2.3 Procedure for spinal cord cleaning, sectioning, and micro-dissection

(A) Spinal cord is extracted from NDD adult human organ donors. (B) Dashed boxes indicate the three layers of meninges; dura in red, arachnoid in blue, and pia in green. (C) Spinal cord segment after removal of meninges and ready for sectioning. (D) ~1-3 mm thick sections to be dissected. (E) A cross-sectional view of the spinal cord; the dashed line in red indicates the direction of central canal dissection.

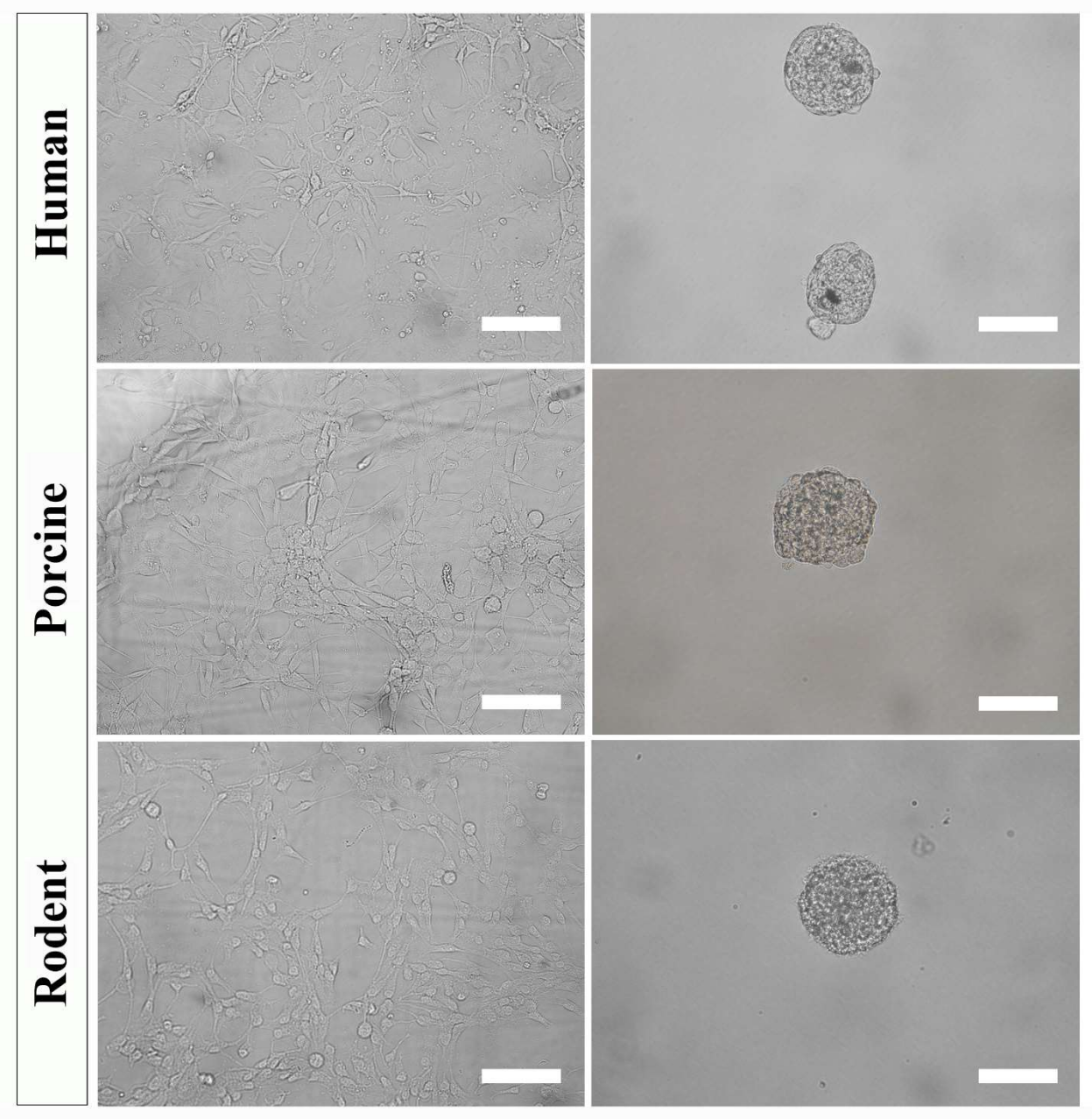

Figure 2.4 Adherent and suspension cultures of spinal cord NSPCS

Primary NSPC cultures from adult human, pig, and rat spinal cords are cultured under identical conditions as an adherent layer (column 1). NSPCs can be passaged and cultured in suspension at low cell density to form neurospheres (column 2). Images were taken at 20x magnification. Scale bar = 100 μm

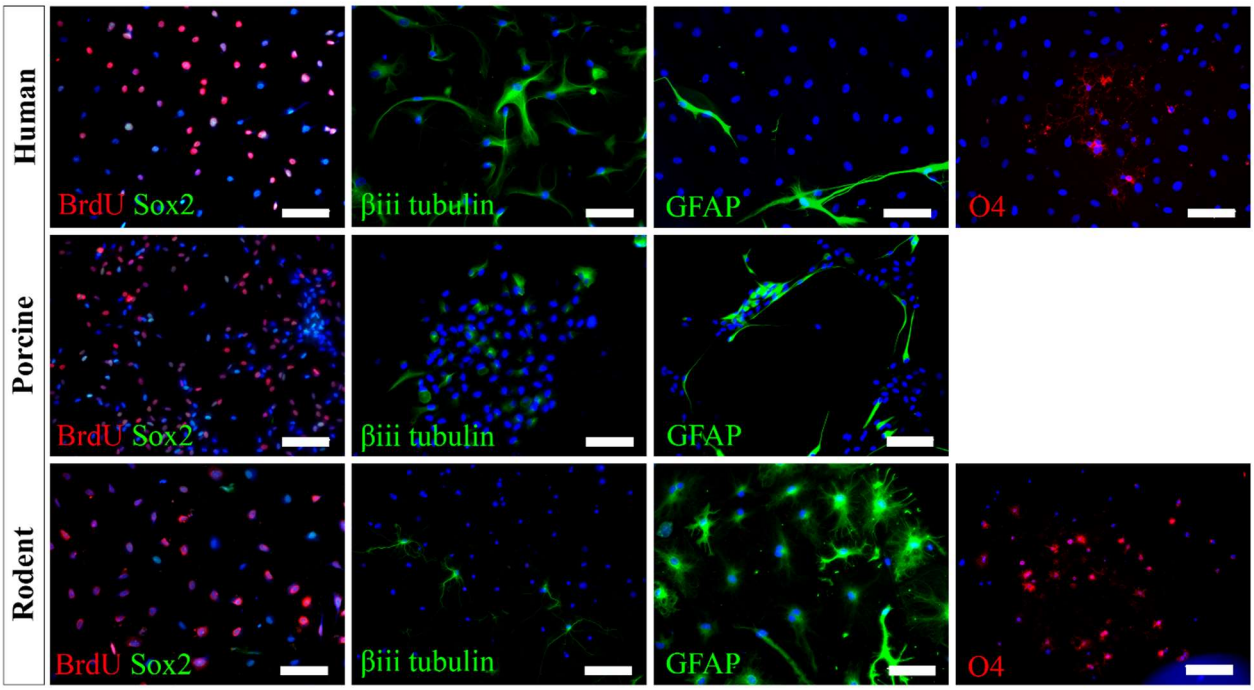

Figure 2.5 Human, pig, and rat NSPCs are proliferative and exhibit multi-lineage differentiation

Human, pig, and rat primary NSPCs express the neural stem cell marker Sox2 and proliferate ($BrdU^+$) in the presence of mitogens. Upon differentiation, NSPCs generate β-iii $tubulin^+$ neural precursors, $GFAP^+$ astrocytes, and $O4^+$ oligodendrocytes. No $O4^+$ staining was observed from pig NSPCs. Scale bar = 100 μm.

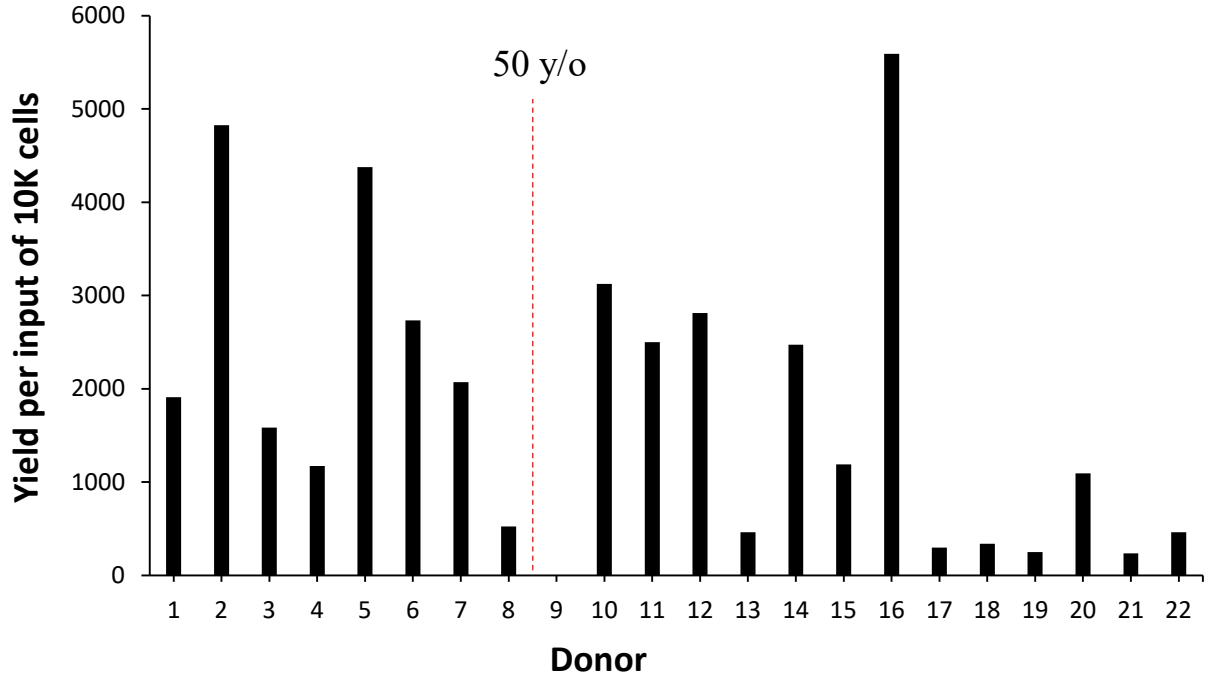

Figure 2.6 Yield of primary human NSPCs varies by donor

Adult human (n=22) spinal cords from the thoracic region were processed similarly for primary culture and expansion of NSPCs. Cultures were passaged upon attaining confluence, or cessation of growth, and quantified. Yield per input was calculated by dividing the total number of cells obtained upon passaging per 10,000 cells initially seeded. Donors ranged from 18 to 71 years old, with the youngest to oldest arranged from left to right. Donors "1-8" were younger than 50 years old.

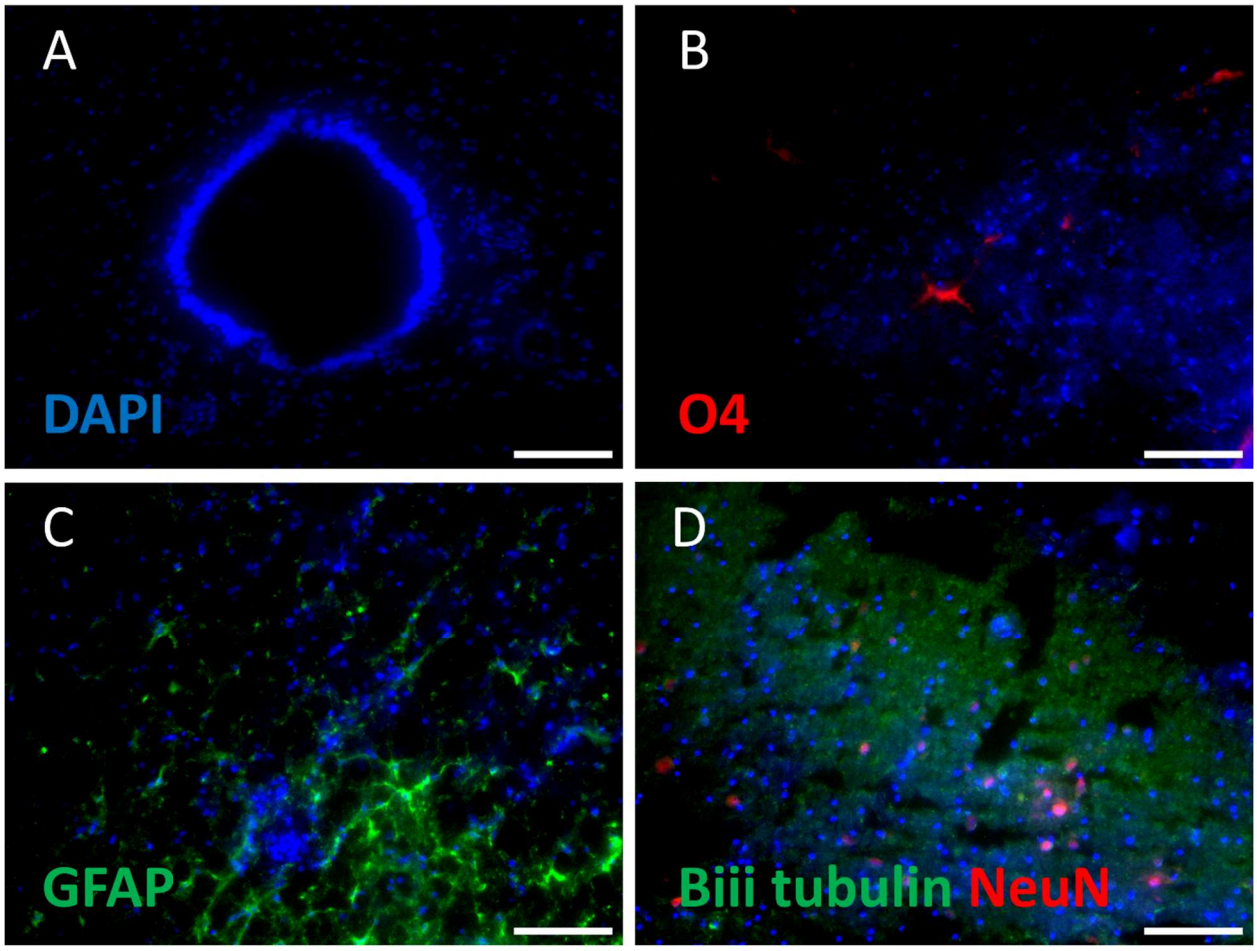

Figure 2.7 Immunohistochemical validation of antibodies in porcine spinal cord

(A) nuclear DNA staining with DAPI demonstrating a patent central canal. (B) Positive oligodendrocyte labelling using the O4 marker. (C) Positive astrocyte labelling using the GFAP marker. (D) positive neuronal labelling using the βiii tubulin and NeuN markers.

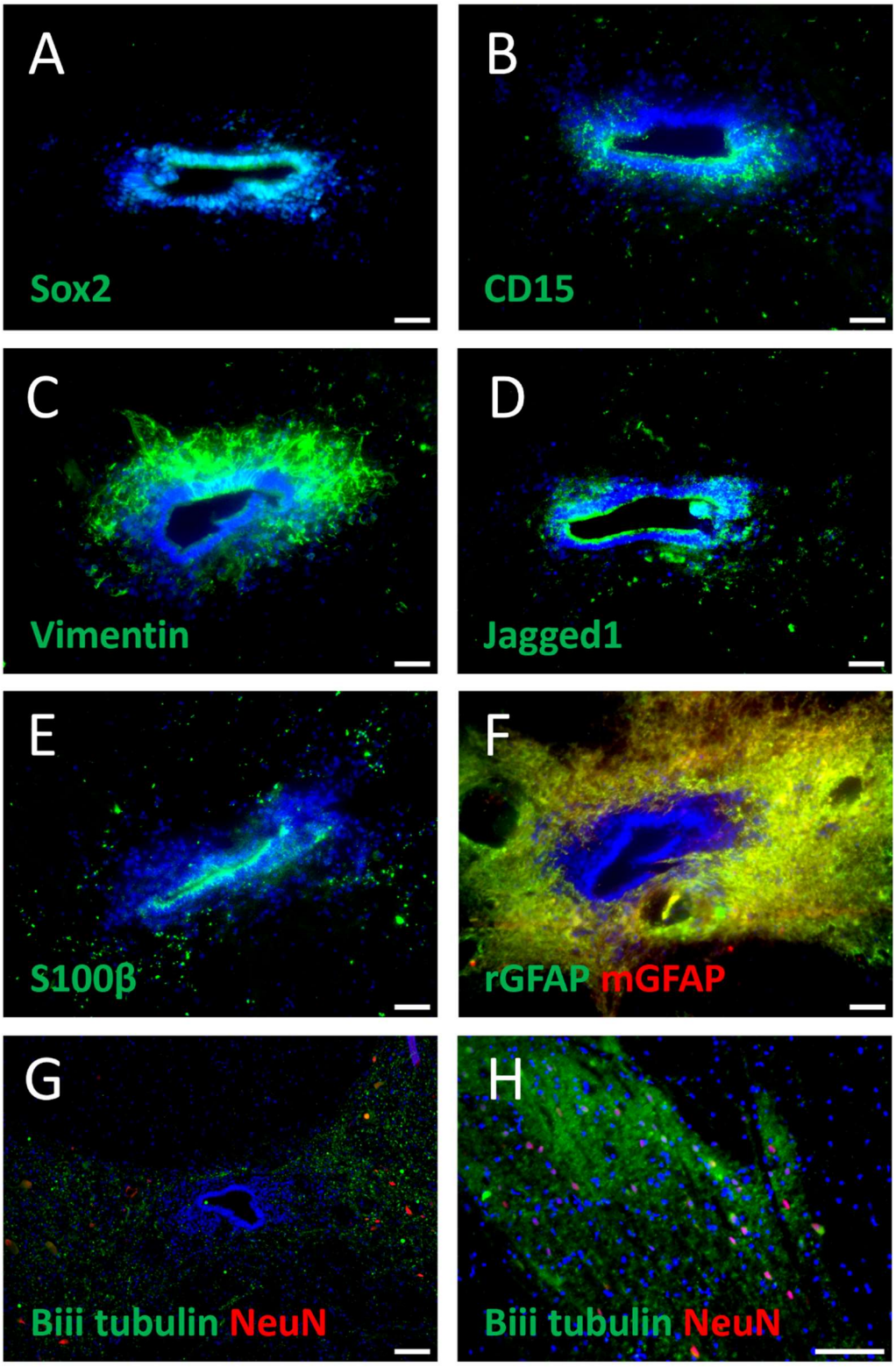
A
Sox2
B
CD15
C
Vimentin
D
Jagged1
E
S100β
F
rGFAP mGFAP
G
Biii tubulin NeuN
H
Biii tubulin NeuN

Figure 2.8 Characterization of the human spinal cord central canal and immunohistochemical validation of antibodies

(A) Sox2 staining was present in all ependymal cells and localized to the nucleus. (B) CD15 staining was present in ependymal cells within the dorsal and lateral domains of the central canal but absent in the ventral domain. (C) Vimentin staining labelled all ependymal cells with long filamentous processes extending into the sub-ependymal zone. (D) Jagged1 staining was visible on the apical surface of most ependymal cells. (E) S100β staining was visible throughout the cytoplasm of all ependymal cells. (F) GFAP staining using mouse and rabbit monoclonal antibodies labelled astrocytes in the sub-ependymal zone and surrounding grey matter. (G) βiii tubulin and NeuN staining revealing neuronal processes and nuclei in the grey matter surrounding the central canal. (H) βiii tubulin and NeuN staining in the dorsal horn.

Table 2.1 Descriptions of the antibodies, including antibody specificity, dilution used, and source. GFAP, glial fibrillary acidic protein; BrdU, bromodeoxyuridine; Sox2, Sex Determining Region Y-box Transcription Factor 2

Marker	Specificity	Dilution	Antibody Manufacturer
β-iii tubulin	Cytoskeletal protein abundant in neural precursors	1:500	STEMCELL Technologies
GFAP	Intermediate filament cytoskeletal protein	1:1000	EMD Millipore

	expressed in astrocytes and brain stem cells		
O4	Membrane receptor in mature oligodendrocytes	1:500	R&D Systems
BrdU	cell cycle (S-phase) checkpoint used as a proliferation marker	1:2000	EMD Millipore
Sox2	Transcription factor necessary for the self-renewal of neural stem cells	1:1000	Abcam
Vimentin	Intermediate filament protein expressed in CNS astrocyte and ependymal cells	1:1000	SantaCruz
CD15	Carbohydrate adhesion molecule expressed on the apical surface of dorsal and lateral ependymal cells	1:500	SantaCruz

NeuN	Nuclear protein expressed in postmitotic neurons	1:2000	Abcam
Jagged-1	Cell surface ligand that interacts with notch receptors found in ependymal cells	1:500	SantaCruz
S100β	Calcium binding protein expressed in ependymal cells of the brain and spinal cord	1:300	SantaCruz

Table 2.2 Expected differentiation profile of primary-derived spinal cord NSPCs that have been treated with 1% FBS for seven days

	Human	**Pig**	**Rat**
Neurons	≈45%	≈20%	≈10%
Astrocytes	≈5%	≈35%	≈40%
oligodendrocytes	<1%	*	≈5%

* Oligodendrocytes were not detected with the O4 antibody and under the conditions tested

Table 2.3 Average yield of primary NSPCs grown as neurospheres or mono-layer and the average doubling time for primary NSPCs grown as a mono-layer. Values are shown as mean ± standard deviation

Species	Replicates	Yield of primary NSPCs per 10K cells (neurosphere method)	Yield of primary NSPCs per 10K cells (mono-layer method)	Primary NSPC doubling rate (days)
Human	13	NS[a]	$2.5x10^3 \pm 0.2x10^3$ [b]	5.8 ± 1.8
Porcine	6	NS[a]	$4.1x10^4 \pm 3.6x10^4$ [c]	4.3 ± 2.5
Rodent	15	17.2 ± 6.8[d]	$1.2x10^5 \pm 2.0x10^4$	1.3 ± 0.2

[a]Not sufficient; the conditions used to culture neurospheres were not adequate for human and porcine NSPCs

[b]A significant difference relative to rodent NSPCs ($p<0.01$)

[c]A significant difference relative to rodent NSPCs ($p<0.0001$)

[d]Weiss et al. (1996)

Chapter 3: Primary Human, Pig, and Rat Spinal Cord NSPCs are Transcriptionally Unique and Exhibit Distinct Responses to Inflammatory and Regenerative cues

3.1 Abstract

Treatment of spinal cord injury (SCI) using neural stem/progenitor cells (NSPCs) has yet to be successfully translated from animal model testing to human therapy, likely due to species differences in NSPC function. To address cell-intrinsic differences among humans and animal models, we compared human, pig, and rat spinal cord NSPCs for their proliferation, differentiation, and transcriptome profiles using identical *in vitro* conditions. We demonstrate that the proliferation rate of NSPCs from humans and pigs is less than of rats. Human NSPCs generate more neurons and fewer glia than pig and rat NSPCs. The distinct differentiation trends among human, pig, and rat NSPCs are reflected in their transcriptomic profiles at the level of individual genes and collective gene sets. Upon exposure to inflammatory factors, human NSPCs do not undergo reactive astrogliosis but rather increase neurogenesis. On the contrary, pig and rat NSPCs exhibit glial scarring mechanisms. When stimulated with regeneration factors, we found that human NSPCs cannot be directed to differentiate using the same conditions for rat NSPCs. These findings suggest cell-intrinsic differences in NSPCs among species that may influence the pathogenesis of SCI and affect the translation of regenerative strategies that target human NSPCs.

3.2 Introduction

Trauma to the spinal cord can result in widespread cellular damage and death, leading to persistent impairment of sensory and motor functions. Despite the inadequacy of the spinal cord to repair itself, there exists a pool of regenerative NSPCs that possess the potential to replenish the cells lost due to injury (Becker et al., 2018). NSPCs are located within the ependymal layer of the central

canal and along the entire rostral-caudal axis of the spinal cord (Meletis et al., 2008; Weiss et al., 1996). In rodent models of SCI, NSPCs become activated and upregulate their proliferation in response to inflammatory signals, but they do not regenerate effectively. Instead, NSPCs contribute to glial scarring, providing neurotrophic support and restoring tissue homeostasis (Barnabé-Heider et al., 2010; Cusimano et al., 2018; Hawryluk et al., 2012; Sabelström et al., 2013). The glial scar, characterized by reactive astrocytes, has been well-studied in rats and is a major therapeutic target for SCI interventions (Cregg et al., 2014; Sofroniew, 2009).

Interestingly, in some lower amphibians and fish, NSPCs are directly involved in regenerating a fully transected spinal cord (Becker & Becker, 2015). This effect is first mediated by an increase in NSPC proliferation followed by differentiation into a "glial bridge" that permits axon growth across the lesion (Goldshmit et al., 2012; Hui et al., 2015). Such stark differences in NSPC response amongst lower and higher vertebrates highlight the cell-intrinsic and environmental factors at play, and determination of which may allow mammalian NSPCs to recapitulate NSPCs of regeneration-competent species (Becker et al., 2018). As such, it is postulated that NSPCs may be an endogenous target to promote the regeneration and repair of the spinal cord. To achieve this feat in humans, understanding the mechanisms regulating human NSPC proliferation and differentiation into all three neural lineages is required to direct NSPC-mediated regeneration.

Due to technical and ethical restraints in studying human NSPCs, small and large animal models, including rats and pigs, have been used to study the pathophysiology of SCI and develop therapeutic strategies (Alizadeh et al., 2019; Cheriyan et al., 2014). Although animal models are valuable tools and have provided much insight into the matter, very little is known about spinal cord NSPCs from the clinical target (Cawsey et al., 2015; Dromard et al., 2008; A. J. Mothe et al., 2011; A. Mothe & Tator, 2015; Paniagua-Torija et al., 2018; Varghese et al., 2009). Specifically,

the role of human spinal cord NSPCs after injury and whether they are inducible to regenerate is unknown. We sought to address these questions by characterizing adult human spinal cord NSPCs *in vitro* in various environments that mimic inflammatory signals after injury or induce regeneration.

Our study obtained viable spinal cord tissue from neurologically deceased adult organ donors (Table 1). We immediately processed the spinal cord tissue for cell culture using the Neurosphere assay (A. Mothe & Tator, 2015). Using this system, NSPCs were treated with a variety of inflammatory molecules that have known implications in rat glial scarring to predict mechanisms of human NSPC pathophysiology (Ruxandra Covacu & Brundin, 2015; Grégoire et al., 2015; Kandasamy, Reilmann, Winkler, Bogdahn, & Aigner, 2011; M. K. Kang & Kang, 2008; S. Okada et al., 2004; Yu et al., 2012). Similarly, human NSPCs were induced to proliferate with mitogens (Weiss et al., 1996) and directed to differentiate with signaling molecules for drug screening and optimization of growth factor cocktails. Notably, we characterized adult human, rat, and in some cases, pig spinal cord NSPCs using identical culture parameters, thus controlling for all cell-extrinsic factors. This study provides the first direct comparison of adult human spinal cord NSPCs with animal counterparts of basic science and pre-clinical importance.

3.3 Methods

3.3.1 Ethics statement

Animals

All animal use was performed in strict compliance with the Guide to the Care and Use of Experimental Animals prepared by the Canadian Council of Animal Care and protocols approved

by the Animal Care Committee of the University of Ottawa. A total of 6 female pigs (12-14 weeks) and ten female rats (Sprague Dawley, eight weeks old, Charles River) were used.

Human subjects

For the harvesting of human spinal cord tissue, ethics approval for the study was obtained from the Ottawa Health Science Network Research Ethics Board and from the Trillium-Gift of Life Network (TGLN), which oversees organ donation in Ontario. Patients were identified to study personnel after neurologic determination of death (NDD) was assessed by TGLN. Informed written consent was obtained from the family of the deceased organ donor for tissue collection. More information related to the subjects can be found in Table 1

3.3.2 Spinal cord harvest and primary NSPC culture

All the spinal cord samples used in this study were from the thoracic region. Human spinal cords were harvested using an anterior approach, according to Galuta and colleagues (2020). Briefly, the spinal cord was exposed from the surrounding tissues and organs, and then transverse cuts were made at the L2 level of the spinal cord and at the most rostral level. Using a sternal saw angled 45° medially, transverse cuts were made in a caudal to rostral direction on both lateral sides of the spinal cord to remove the vertebral bodies.

The harvested spinal cord was placed in cold, sterile dissection media: 1X Hank' Balanced Salt Solution (HBSS)+ 0.6% D-glucose + 2% penicillin-streptomycin (PS) (Gibco, 15140122) and processed immediately for micro-dissection. The central canal region was excised under a dissection microscope, leaving out contaminant surrounding grey and white matter, then dissociated using a papain dissociation kit (Worthington Biochemical Inc., LK003150) according to the manufacturer's instructions.

Following purification, cells were re-suspended in a serum-free media (SFM), which consisted of: Neurobasal-A medium (ThermoFisher Scientific, 10888022), 2 mM L-glutamine (Gibco, A2916801), 100 U/mL PS, 1% B27-vitamin A (Gibco, 12587010), and 10% hormone mix (1:1 DMEM/F12 (Sigma, D8900), 0.6% glucose, 3 mM $NaHCO_3$, 5 mM HEPES, 25 µg/mL insulin, 100 µg/mL apo-transferrin, 10 µM putrescine, 30 nM selenium, and 20 nM progesterone in distilled water). Cells were seeded at 20 cells/µL onto matrigel (Corning™, 354230) coated six-well plates in a total of 4 mL of proliferation media (1X EFH): SFM + 20 ng/mL human epidermal growth factor (EGF) (Sigma, E9644) + 20 ng/mL human basic fibroblast growth factor (FGF2) (Sigma, F3685) + 2 µg/mL heparin (Sigma, H3149) and incubated at 37˚C, 5% CO_2, 20% O_2 for one week undisturbed. Cultures were fed every 2-3 days for 1-2 weeks by replacing half the culture medium with an equivalent amount of 2X EFH. Once adherent cultures were visibly expanding, cultures were fed by replacing the full media with 2 mL of 1X EFH. Cultures were fed this way before reaching confluence, at which point NSPCs were passaged and assessed.

Pig spinal cord tissue was harvested using a posterior approach, according to Galuta and colleagues (2020), and was processed similarly to the human spinal cord for the culture of primary NSPCs. Rat spinal cord tissue was harvested by performing a laminectomy, according to Galuta and colleagues (2020), and processed similarly to human and pig spinal cord.

3.3.3 Assessment of exogenous factors on NSPC differentiation and proliferation

Primary NSPC cultures were passaged using Accutase (Gibco, A1110501) and incubated at 37ºC for 5 minutes. Lifted NSPCs were centrifuged at 300xg for 5 minutes and resuspended in 1X EFH to calculate cell density. NSPCs were seeded at a cell density depending on the treatment and onto Matrigel-coated 96 well plates (150µL/well) in 1X FH for two days before exogenous factor treatment. To assess the intrinsic NSPC differentiation potential, NSPCs were seeded at 1 cell/µL,

and differentiation was induced with 1% fetal bovine serum (FBS) (Corning™, 35015CV) treatment in SFM. For assessment of inflammatory factors, NSPCs were seeded at either 5 cells/µL and treated with 20 ng/mL Il-6 (Invivogen, rcyec-hil6) or 20 ng/mL TNF-α (PeproTech, 300-01A), or NSPCs were seeded at 2 cells/µL and treated with 20 ng/mL TGF-β1 (PeproTech, 100-21). All inflammatory factor treatments were assessed in SFM. For assessment of regenerative factors, NSPCs were seeded at 5 cells/µL and directed to differentiate with 50, 100, and 500 ng/mL RA (Sigma, R2625), 20 ng/mL BDNF (PeproTech, 450-02), 20 ng/mL GDNF (PeproTech, 450-10), 40 and 100 ng/mL PDGFα (PeproTech, 100-13A), or 40 and 100 ng/mL BMP4 (PeproTech, 120-05ET) treatment in SFM. To induce self-renewal, NSPCs were treated with 1X EFH. Control included SFM treatment alone. NSPCs were treated for one and two weeks, fixed with 4% paraformaldehyde (PFA) (Sigma, P6148), and characterized by immunocytochemistry. Cultures for which proliferation was assessed had bromodeoxyuridine (BrdU) (Sigma, B5002) administered 24 hours before being fixed at one and two weeks.

3.3.4 Primary glial culture and inflammatory treatment

Primary human and pig spinal cord glia were cultured according to a modified protocol from De Vellis & Cole (2012). Spinal cord tissues were cleaned and sectioned according to the methods in Chapter 2. The parenchymal white matter was dissected under a microscope, and the tissue was dissociated into single cells using a papain dissociation kit (Worthington Biochemical Inc., LK003150) according to the manufacturer's instructions. The cells were resuspended in DMEM/F12 (ThermoFisher Scientific, 11320033) supplemented with 10% FBS and 1% PS and seeded at 50 cells/µL. Cultures were fed every other day with 10% FBS in DMEM/F12 and passaged every 6-8 days. On passage 3, glial cells were seeded at 20 cells/µL in a 96-well plate and fed with 10% FBS in DMEM/F12 for the next two days to allow cells to adhere and proliferate.

On day 3, wells were washed three times with PBS, then media was replaced with 20 ng/mL Il-6, 20 ng/mL TNF-α, or 20 ng/mL TGF-β1. Inflammatory factor treatments were assessed in SFM, 0.1% FBS, or 1% FBS. Control includes SFM, 0.1% FBS, or 1% FBS treatment alone. Glial cultures were treated for four days, fixed with 4% paraformaldehyde (PFA), and characterized by immunocytochemistry. Cultures for which proliferation was assessed had BrdU administered 24 hours before being fixed.

3.3.5 Immunocytochemistry

Fixed cultures were blocked with 10% normal goat serum (NGS) (ThermoFisher Scientific, P131873) and permeabilized with 0.3% Triton-X in PBS for 30 minutes at room temperature. However, wells stained for O4 were only blocked and not permeabilized. Cultures were washed three times with PBS, then incubated with respective primary antibodies with 10% NGS in PBS overnight at 4 ºC.

The following antibodies were used: mouse anti-O4 IgM (1:500) (Novus Biologicals, MAB1326) to label oligodendrocytes, mouse anti-β-iii tubulin IgG (1:500) (STEMCELL Technologies, 01409) (SantaCruz, 80005) to label immature neurons, rabbit anti-GFAP (1:1000) IgG (EMD Millipore, Ab5804) to label astrocytes, mouse anti-Nestin (10C2) IgG (1:500) (SantaCruz, 23927) and mouse anti-Nestin IgG (1:1000) (SantaCruz, 33677) to label human and rat progenitor cells, respectively, and rabbit anti-Sox2 IgG (1:1000)(Abcam, ab97959) to label neural stem cells, and mouse anti-BrdU IgG (1:2000) (EMD Millipore, MAB4072) as a marker of proliferation.

The following day, cultures were washed three times with PBS and incubated with respective species-matched secondary conjugated antibodies in PBS for 2 hours at room temperature. The following secondary antibodies were used: goat anti-mouse IgG Alexa Fluor 488 (1:300) (Abcam,

Ab150113), goat anti-rabbit IgG Alexa Fluor 488 (1:500) (Abcam, Ab150077), goat anti-mouse IgG Alexa Fluor 594 (1:300) (Abcam, ab150116), goat anti-rabbit IgG Alexa Fluor 594 (1:500) (Abcam, ab150080), and goat anti-mouse IgM Alexa Fluor 594 (1:300) (ThermoFisher, A-21044). Cultures were washed three times with PBS, counterstained with Hoeschst (1:2000) (ThermoFisher, 62249), and processed for immunofluorescent visualization.

3.3.6 NSPC characterization and statistical analysis

Immuno-stained cultures were visualized using a Nikon Ti Eclipse Epifluorescence. Ten images were taken of each well for each treatment (n=3 wells). Images were analyzed using Image J software. The total number of immuno-positive cells was counted as a percentage of Hoechst-labeled nuclei to calculate the mean percent differentiation and proliferation. The fold change in immuno-positive cells was calculated relative to control (SFM) for regenerative and inflammatory factor treatments. Data are presented as a mean percent or fold change ± standard error. Statistical analyses were carried out using GraphPad Prism. When analyzing the mean percent differentiation and proliferation between species, significance was determined using an ordinary one-way analysis of variance (ANOVA) followed by a Tukey's Test. When analyzing the fold change data in treatment relative to the control within species, significance was determined using a two-tailed paired t-test.

3.3.7 RNA sequencing and data analysis

Primary human (n=3), pig (n=3), and rat (n=3) NSPCs were cultured according to the protocol outlined in section 3.3.2. A description of the samples is summarized in Table 2. Once primary NSPCs reached confluency, cultures were passaged, and 50,000 cells were transferred to a 15 mL conical tube containing SFM. The cells were centrifuged at 300xg for 5 minutes, and the

supernatant was aspirated. Cell pellets were lysed, and RNA was extracted using the RNeasy Micro Kit (Qiagen, 74004). A total of 20 µL of RNA was extracted in RNase-free water and stored at -20 °C until further use. A 1 µL sample was used to quantify the RNA concentration using NanoDrop™. To confirm RNA sample quality, 1000-5000 pg/µL of RNA from each sample were assessed using a Fragment Analyzer, and only samples with RQN values greater than seven were used for downstream RNA sequencing. 50 ng of RNA per sample was shipped to StemCore Laboratories (Ottawa, Canada) for RNA library preparation, and samples were sequenced using the NextSeq platform.

Quality control on the samples was performed using FastQC to assess the quality of the raw sequences. A summary report of quality control metrics and mapping statistics can be retrieved here: http://www.ogic.ca/projects/ahmad_galuta/spinal_cord_SC_hs_rn_ss/reports/multiqc_report.html. Picard RNA-seq metrics were used to assess the mapped reads (mapped to the appropriate species' transcriptome using hisat2). Reads were assigned to transcript sequences using Salmon (https://combine-lab.github.io/salmon/); human transcript sequences were retrieved from GENCODE v35, and rat and pig sequences were from Ensembl release 104. Human orthologs of pig and rat genes were identified using the Ensembl BioMart service; 15,241 human gene IDs were found in all three (human, pig, and rat) datasets. Transcript abundances were imported for each species using the tximport library and combined to provide gene-level counts and abundances. Each dataset was filtered to retain only genes for which a common human gene ID was identified and combined into a single DESeq dataset.

Differential gene expression between species was assessed using DESeq2. The rlog-transformed normalized counts were calculated for principal component analysis (PCA) and hierarchical

clustering. PCA was applied to the matrix of gene expression values using the 500 most variable genes in the dataset. Hierarchical clustering was calculated using Euclidian distance between rlog-transformed normalized count values for all transcripts. DESeq2 was used to calculate fold change in gene expression and a p-value between species. Multiple testing correction was done using the Benjamini-Hochberg method to calculate a q-value or false discovery rate (FDR). Volcano plots and heat maps of differentially expressed (DE) genes were generated using the fold change results. Fold change scatter plots were generated for all genes and protein-coding genes only. A 5% FDR cut-off was used for these analyses to determine whether a gene is significantly DE between conditions. UCell-like scores were calculated for gene sets comprising markers for CNS cell types according to Andreatta & Carmona (2021) based on the Mann-Whitney U statistic. Scores calculated for each sample rank how highly the genes comprising a cell type signature are expressed within that sample relative to the expression of all genes.

To identify functional changes in gene expression between species, gene set enrichment analysis (GSEA) was performed. Genes were ranked for the comparisons between humans and rats and between humans and pigs using the metric $\log_2$FoldChange. GSEA was run against gene sets from the MSigDB collections H (hallmark gene sets), C2 (curated gene sets), CP (canonical pathways), C5 (Gene Ontology annotations), and C8 (cell type signatures).

Functional enrichment analysis for DE genes was also performed using gProfiler to identify annotations that are enriched in sets of DE genes. DE genes were filtered to include only genes with an FDR of <0.01 and a $\log_2$(fold change) greater than +2 or less than –2. gProfiler was run twice with the "ordered query" for the pig and rat data, once each for the genes that are upregulated and downregulated. This analysis used the list of genes commonly identified in all three species as a background gene set for running the hypergeometric probability function.

3.3.8 Electrophysiology

Individual coverslips were removed from culture well plates and placed under a Zeiss examiner A1 microscope at room temperature. The recording bath solution was an artificial cerebrospinal fluid (ACSF) consisting of 125 mM NaCl; 3 mM KCl; 26 mM $NaHCO_3$; 11.25 mM NaH_2PO_4; 2 mM $CaCl_2$; 1 mM $MgCl_2$; and 20 mM glucose. Cultures were examined for cells visually identified as putative neurons using a DAGE MTI camera. Micropipettes were prepared from 4-inch-long thin wall glass pipettes from World Precision Instruments using a Sutter Instruments flaming micropipette puller. Heat and velocity settings were set to achieve a pipette resistance of 6-14 megaOhms (MΩ). Following pulling, micropipette tips were fire polished using a Narishige Scientific Instrument fire polisher. Once an isolated cell of interest was identified, micropipettes were filled with internal recording solution consisting of 140 mM K-gluconate; 10 mM NaCl; 10 mM HEPES; 1 mM EGTA; 4 mM Mg-ATP; and 0.2 mM Na_2-GTP at a pH of ~7.3 and an osmolarity between 290-295 mOSM. Electrophysiological patch-clamp recordings were acquired using Axon Digidata 1550 and Multiclamp 700B from Molecular Devices Axon Instruments, controlled through associated Clampex (pClamp 10) software.

Once whole-cell configuration was achieved, current clamp protocols were run at specific current injection steps, depending on the resting membrane potential. Standard starting steps were -20 by 5 picoAmperes (pA) but altered up to -100 by 20 pA for low input resistance cells. The magnitude of current injection steps was adjusted so that each step represented a membrane potential change of approximately 10 mV. Following this, the same protocols were run while holding the resting membrane potential at -50 or -60 mV through tonic injection of negative current. Following current clamp recordings, voltage-clamp recordings of spontaneous currents were performed at -60 mV for 1-5 minutes, depending on the presence or absence of spontaneous events. Membrane

potential was then incrementally increased to +40 mV, where another recording was performed for 5-10 minutes to test voltage-dependent rectification of synaptic events. The potential was further increased to +60 mV, and a third voltage-clamp recording was acquired for 10 minutes.

Trace analyses were completed in Clampfit 10.7 software. Capacitance was taken from initial whole-cell statistics generated by Clampex software during 5 mV test voltage steps. Resting membrane potential, input resistance, and decay constant were calculated from current clamp recordings. Resting membrane potential was measured and averaged during the rest period before the initial hyperpolarizing current injection steps and adjusted for a calculated liquid junction potential of 14.6 mV based on the above external and internal solutions. Input resistance was calculated from the average difference between baseline and steady state potential for hyperpolarizing and depolarizing current steps in the linear range. This was then divided by the corresponding current injection step size to give input resistance. Average spontaneous excitatory postsynaptic current amplitude and decay constant were calculated for voltage clamp recordings. Selected events possessed a stable baseline, with no other major event occurring within 200 ms of the acquisition period. Detected events were aligned in pClamp software and averaged. Shapiro-Wilk statistical tests were performed on all data sets to determine normal distribution. ANOVA and student's t-test statistical analyses were performed on normally distributed datasets, with posthoc Tukey HSD. Data are presented as mean ± standard error.

3.4 Results

3.4.1 Human NSPCs are functionally distinct compared to pig and rat NSPCs under differentiation conditions

The spontaneous differentiation of NSPCs *in vitro* is commonly induced by serum which contains many factors that promote the differentiation, survival, and adherence of NSPCs (Gil-Perotín et al., 2013; Narayanan et al., 2016). Following treatment with 1% fetal bovine serum (FBS), the resulting progeny of human (n=15), pig (n=5), and rat (n=10) NSPCs were positive for markers of differentiated neural lineage cells, including β-iii tubulin$^+$ neurons, O4$^+$ oligodendrocytes, and GFAP$^+$ astrocytes (Figure 3.1). However, we did not observe any O4$^+$ oligodendrocytes from pig NSPCs under the conditions tested.

There was a stark difference in the percentage of differentiated progeny generated from human NSPCs compared to pig and rat NSPCs (Figure 3.1 B, D-F). Human NSPCs have a strong potency for producing the neuronal lineage as identified with β-iii tubulin labeling (54.8±1.6% and 52.1±1.3% β-iii tubulin$^+$ after one and two weeks, respectively) (Figure 3.1 F) but weakly generate glia (0.47±0.08% and 0.23±0.06% GFAP$^+$ after one and two weeks, respectively; 0.013±0.01% and 0.029±0.01% O4$^+$ after one and two weeks, respectively) (Figure 3.1 D, E). On the contrary, rat NSPCs differentiated predominately into astrocytes (38.0±2.3% and 38.9±1.7% GFAP$^+$ after one and two weeks, respectively) and to a lesser extent into neurons (7.0±1.6% and 8.7±1.7% β-iii tubulin$^+$ after one and two weeks, respectively) and oligodendrocytes (4.9±0.4% and 6.3±0.6% O4$^+$ after one and two weeks, respectively) (Figure 3.1 D-E). Pig NSPCs mainly differentiated into astrocytes (36.7±2.0% and 52.9±2.4% GFAP$^+$ after one and two weeks, respectively) and, to a lesser extent, neurons (15.1±1.4% and 23.0±2.4% β-iii tubulin$^+$ after one and two weeks, respectively) (Figure 3.1 D-F), thus mirroring the differentiation profile of rats.

Human NSPCs formed significantly more neurons and fewer astrocytes compared to pig ($p<0.0001$) and rat ($p<0.0001$) NSPCs (Figure 3.1 E, F). However, pig NSPCs generated significantly more astrocytes ($p<0.01$) and neurons ($p<0.05$) than rat NSPCs after two weeks of differentiation (Figure 3.1 E, F). Rat NSPCs generated significantly more oligodendrocytes than human and pig NSPCs ($p<0.0001$) (Figure 3.1 D).

In addition, the proliferation rate of NSPCs under these conditions, which primarily reflects progenitor cell activity, was measured using BrdU labeling strategy to identify dividing cells within the last 24 hours of differentiation (Figure 3.1 A, C). The proliferation rate of rat NSPCs at one week was significantly greater compared to human ($p<0.05$) and pig ($p<0.01$) NSPCs. At two weeks, the proliferation rate was reduced for all species, indicating that NSPCs are approaching terminal differentiation, and this was significantly the lowest for pig NSPCs ($p<0.0001$). Nestin immuno-reactivity revealed proliferating progenitor cells throughout the two-week differentiation period (Figure S3.1 B, F).

To obtain a greater percentage of NSPCs in culture, human cultures (n=5) were passaged twice and assessed similarly to primary-derived NSPCs. The proliferation rate of secondary-derived NSPCs (68.8±6.8% $BrdU^+$) was greater than primary-derived NSPCs (35.1 ±5.1% $BrdU^+$) at one week, reflecting a population with a more significant proportion of proliferating NSPCs (Figures 3.1 B and S3.2 A). Furthermore, the differentiation profile of human secondary-derived NSPCs (Figure S3.2 B) followed the same trend as primary-derived NSPCs (Figure 3.1 A, C), as mostly neurons and only a few glial cells were generated (61.3±5.8% neurons, 0.85±0.39% astrocytes, 0.44±0.22% oligodendrocytes after one week), indicating that the primary culture is sufficient to study NSPC behavior.

3.4.2 The overall transcriptomes of primary NSPCs are distinct among species

Primary human (n=3), pig (n=3), and rat (n=3) NSPCs had their RNA extracted and processed using bulk RNA sequencing. The total number of annotated genes from pig and rat NSPCs was slightly more than 50% of the annotated genes from human NSPCs (Table 3). From the total annotated genes, approximately 55% of rats and 59% of pigs were found to have human orthologs (Table 3). When assigning a high-confidence score to rat and pig genes, the percentage of human orthologs dropped to 43% for rats and 51% for pigs (Table 3). It must be noted that some annotated genes from rats and pigs did not have a human ortholog, while other genes had multiple human orthologs (Figure S3.3 A-D). A total of 15,241 genes were common among all three species and 12,496 genes when accounting for high-confidence human orthologs (Figure S3.3 E, F).

From the genes found in common between species, we determined the percentage of differentially expressed (DE) genes (Table 4). More DE genes exist between humans and rats (59.9% of total orthologs) compared to humans and pigs (56.6% of total orthologs). Also, rats and pigs have more DE genes (59.4% of total orthologs) than humans and pigs. A visual summary of the DE genes, including the top 50 most upregulated and downregulated genes in rats or pigs compared to humans, is represented in Figures 3.2 and 3.3. Of all the genes in common among species (15,241 genes), 6,350 genes were significantly DE in rats and pigs compared to humans (Figure 3.4 A). A list of the top 30 most upregulated and downregulated genes that are DE in both rats and pigs compared to humans is shown in Figure 3.4 B. These genes were most DE between rats and humans, but also DE in pigs in the same direction as rats.

When comparing the 500 most variable genes in common among all species, a PCA plot, which accounts for 96% of the variance, grouped the samples by species along the PC1 and PC2 axes. Interestingly, pigs and rats were closely located along the PC2 axis and separately from humans

(Figure 3.4 C). Similarly, a PCA plot using the first and third components, which accounts for 51% of the variance, grouped the samples by species along PC1 but not for the human samples along PC3 (Figure 3.4 C). A hierarchical clustering analysis reveals that the overall gene expression between NSPCs of the same species was similar but distinct between species (Figure 3.4 D). These results suggest that human, pig, and rat NSPCs bear different transcriptomes, which may underlie the differences in their differentiation and proliferation profiles.

3.4.3 The transcriptomes of NSPCs closely reflect their functional behaviour

To investigate DE genes associated with the functional profiles of human (n=3), pig (n=3), and rat (n=3) NSPCs, we analyzed the relative expression of specific genes that are markers for neural stem cells, oligodendrogenesis, neurogenesis, astrogenesis, and proliferation (Figure 3.5). Out of the six neural stem cell markers evaluated, rat NSPCs had the highest expression of *NES*, *PROM1*, and *CD24* compared to human and pig NSPCs. Meanwhile, human NSPCs expressed *EGFR* at a higher level and *MSI1* and *MSI2* at a lower level compared to pig and rat NSPCs (Figure 3.5 A).

The expression of oligodendrocyte markers mirrored the differentiation profiles of NSPCs. Rat NSPCs expressed the highest levels of *OLIG1*, *OLIG2*, *SOX10*, and *CNP*, which were relatively low in both human and pig NSPCs. Moreover, human NSPCs expressed a higher level of *SOX10* and *CNP* but a lower level of *OLIG2* compared to pig NSPCs (Figure 3.5 B).

Human, pig, and rat NSPCs preferentially expressed different subsets of neurogenesis markers. Human NSPCs were enriched in *NRXN3*, *HEY2*, *COL6A2*, *SEMA5A*, and *PNMA2*. Rat NSPCs were enriched in *CPNE6*, *SLC17A6*, *DLL3*, *CXCR4*, *GAD1*, *GAP43*, *DCC*, *DCX*, and *OLFM1*. Meanwhile, pigs were enriched in *MNX1*, *PAX3*, *SLIT2*, and *GBX2* (Figure 3.5 C).

The relative gene expression of astrogenesis markers in NSPCs also reflects their differentiation profiles, with an overall higher expression of these markers in rat and pig NSPCs. Specifically, rat NSPCs expressed a higher level of *SLC1A3*, *FGFR3*, *FABP7*, *NFIA*, and *NFIB* compared to human NSPCs, although *SOX9* and *GFAP* were expressed at a lower level. Meanwhile, pig NSPCs expressed *NFIA*, *NFIB*, and *GFAP* at a higher level than human NSPCs, but *SLC1A3* was expressed at a lower level (Figure 3.5 D).

Concerning proliferation markers, human NSPCs express *HOXC10*, *IGF2*, *COL18A1*, *ENPEP*, and *EGFR* at a significantly higher level than both pig and rat NSPCs. Meanwhile, rat NSPCs expressed *BCAT1*, *DCC*, *EGR4*, *CDKN1A*, *CCNG1*, and *MGMT* at a significantly higher level and *CDK6*, *TEP1*, and *TGFBR2* at a significantly lower level compared to human NSPCs. Pig NSPCs expressed *CDKN1A*, *BCAR3*, *CCNG1*, *MGMT*, *TEP1*, and *BCAT1* at a significantly higher level and *DCC*, *PMP22*, *LYN*, and *RARRES1* at a significantly lower level compared to human NSPCs (Figure 3.5 E). Using the UCell scoring method for the markers mentioned above, it was determined that rat NSPCs had the highest score for neural stem cell and oligodendrogenesis markers (Figure 3.5 F).

To investigate sets of DE genes with standard biological functions, we performed a gene set enrichment analysis (GSEA) (Figure 3.6). When focusing on hallmark gene sets, most gene sets significantly different in pig and rat NSPCs or in either species were downregulated compared to human NSPCs. Interestingly, the gene set most significantly downregulated in pig and rat NSPCs was “epithelial to mesenchymal transition.” Also, human NSPCs were more enriched in genes associated with inflammation and immune response regulation (Figure 3.6 A). Concerning canonical functions in the CNS, human and pig NSPCs were mostly similar except for “dopaminergic neurogenesis,” which was enriched in pig NSPCs. On the other hand, rat NSPCs

were enriched in most of these canonical functions with a notable increase in “oligodendrocyte specification and differentiation” (Figure 3.6 B). When comparing gene ontology (GO) molecular functions in the CNS, human and pig NSPCs were similar except for “chemokine activity,” which was enriched in human NSPCs. Meanwhile, rat NSPCs were enriched in gene sets associated with ion channel activity and neurotransmitter binding and activity (Figure 3.6 C).

Concerning GO biological processes in the CNS, rat NSPCs demonstrated a consistent enrichment in gene sets associated with synaptic and neurotransmitter biology. Interestingly, rat NSPCs were enriched in “oligodendrocyte development” and “negative regulation of neuron differentiation,” mirroring the differentiation trends of rat and human NSPCs. Meanwhile, pig NSPCs were enriched in “neuron fate commitment,” “ventral spinal cord development,” and cilium-related genes (Figure 3.6 D). When comparing cell type signatures, oligodendrocyte and astrocyte gene sets were enriched in rats compared to human NSPCs. Rat NSPCs were also enriched in many “midbrain neurotypes” gene sets that were determined by other studies, while these same gene sets were downregulated in pig NSPCs relative to human NSPCs (Figure 3.6 E).

We also analyzed the functional enrichment of DE genes between human, pig, and rat NSPCs using gProfiler (Figure S3.4, Table S1 and S2). Only terms related to the CNS were selected for analysis. Similar to the results of the GSEA, rat NSPCs were enriched in gene sets that pertain to synaptic biology, ion channels, and oligodendrocyte biology (Figure S3.4 A). On the contrary, few gene sets related to the CNS were downregulated in rat NSPCs, including axon guidance, pluripotent stem cell differentiation pathway, and growth factor binding (Figure S3.4 B). Interestingly, pig NSPCs were enriched in only a few gene sets related to cilia and microtubules (Figure S3.4 C). More gene sets were downregulated in pig NSPCs, including terms related to synaptic biology, dendrites, axonal development, and ion channels (Figure S3.4 D).

3.4.4 Differentiating human NSPCs exhibit a subset of functional properties of neurons

Given the neuronal fate preference of human NSPCs, we sought to determine the functional properties of these cells over ten weeks in serum differentiation conditions. Whole-cell patch-clamp recordings were performed on visually-identified putative neurons possessing: fusiform or non-circular, three-dimensional cell bodies; minimal contact with other cells to limit potential gap junction interference; no membrane blebbing or dark stained vacuoles; and at least one process thinner than the cell body itself (Figure 3.7 A). In current clamp recordings on cells cultured for 2 to 10 weeks in 1% FBS, depolarizing current injections steps failed to induce action potentials at either resting membrane potentials (Figure 3.7 B) or membrane potentials held between -50mV or -60mV (Figure 3.7 C) (n=27 cells). Most differentiating NSPCs had membrane capacitances under 10 pF, with no cells above 30 pF (Figure 3.7 D), consistent with cells with relatively limited dendritic and/or axonal processes. The resting membrane potential (RMP) of recorded cells (-34.7 ± 3.4 mV, n=27) was more depolarized than that for mature spinal neurons (Hildebrand et al., 2011) and did not significantly vary across time in culture (-39.8 ± 6.0 mV at weeks 2-4, -33.8 ± 10.1 mV at weeks 5-6, and -32.6 ± 4.6 mV at weeks 7-10; Figure 3.7 E). Similarly, there was no significant change in input resistance between 2 and 10 weeks in culture, with an average Rn value of 1.04 ± 0.17 GΩ, n=22 (Figure 3.7 F). The lack of action potentials, relatively depolarized membrane potentials, low capacitance, and high input resistance suggest that human NSPCs lack many functional attributes of fully mature neurons (Hildebrand et al., 2011) under baseline *in vitro* differentiation conditions.

Although human NSPCs did not exhibit action potentials, we were surprised to observe numerous small amplitude (< 5 mV), exponentially decaying deflections in membrane potential in many of our current clamp recording traces, which resembled excitatory postsynaptic potentials (data not

shown). To investigate the possibility of spontaneously occurring excitatory synaptic responses in differentiating human NSPCs, voltage-clamp recordings were performed at holding potentials of -60mV, +40mV, and +60mV. Most recorded cells (n=17 cells, 82.35%) exhibited spontaneous transient inward currents at negative holding potentials and outward currents at positive potentials, with a higher frequency of events at positive potentials (Figure 3.7 G). The exponential decay constant of aligned events was 11.1 ± 2.0 ms (n=10) for inward currents at -60 mV and 21.1 ± 2.4 ms (n=12) for outward currents at +60 mV (Figure 3.7 H), which is similar to deactivation rates for ionotropic glutamate receptors (Traynelis et al., 2010). The absolute amplitude of spontaneous events was also greater at positive potentials compared to negative holding membrane potentials (Figure 3.7 I). Taken together, the outward rectification, the increased frequency at depolarized potentials, and the moderate decays rates of the spontaneous currents we observed are consistent with excitatory postsynaptic responses mediated by ionotropic NMDA receptors (Paoletti, Bellone, & Zhou, 2013). In support of glutamate-mediated synaptic responses, we found that a large percentage of human NSPCs expressed the neuronal glutamate-synthesis enzyme glutaminase (GLS1, Figure 3.7 J).

3.4.5 Inflammation induces glial scarring mechanisms from pig and rat NSPCs but not from human NSPCs

We treated human (n=8), pig (n=5), and rat (n=6) NSPCs with inflammatory factors that are upregulated after SCI in all three species and are implicated with glial scarring in rats (Ruxandra Covacu & Brundin, 2015; Grégoire et al., 2015; Kandasamy et al., 2011; M. K. Kang & Kang, 2008; S. Okada et al., 2004; Yu et al., 2012). Rat NSPCs had significantly increased astrogliosis after treatment with either Il-6 (3.9±0.6 fold, $p<0.0001$), TNFα (5.0±0.9 fold, $p<0.0001$), or TGFβ (4.0±0.6 fold, $p<0.0001$) for one week (Figure 3.8). However, after two weeks of treatment, the

fold change in astrogliosis was reduced under all treatments and no longer significant with TGFβ treatment. Pig NSPCs had significantly increased astrogliosis after one week of treatment with TGFβ (1.47±0.04 fold, $p<0.0001$) (Figure 3.8 D). Moreover, treatment of pig NSPCs for two weeks with any factor significantly increased astrogliosis (Il-6: 1.38±0.04 fold, $p<0.0001$; TNFα: 1.26±0.05 fold, $p<0.0.1$; TGFβ: 1.45±0.04 fold, $p<0.0001$) (Figure 3.8 B-D), mimicking the response of rat NSPCs but at a later time point. On the contrary, human NSPCs did not increase astrogliosis after treatment with any factor for two weeks (Figure 3.8 B-D). Even when all the inflammatory factors were tested in combination, there was no increase in astrogliosis (Figure S3.5 A; n=3 humans); this effect was consistent across the three donors tested, except in one donor ("H25") where Il-6 treatment for two weeks had increased astrogliosis (Figure S3.5 C, $p<0.01$). In a preliminary assay (n=2 humans), inflammatory factors were applied at double the concentration, yet there was no increase in astrogliosis (Figure S3.5 B). Instead, TGFβ treatment had reduced astrogliosis after one (0.12±0.7 fold, $p<0.01$) and two weeks (0.15±0.11 fold, $p<0.01$), and Il-6 and TNFα treatment had reduced astrogliosis after one (0.14±0.07 fold, $P<0.01$) and two (0.13±0.10 fold, $p<0.01$) weeks, respectively.

Besides assessing primary NSPCs, we sought to determine the effect of the inflammatory factors on human (n=3) and pig (n=3) spinal cord astrocytes since these cells are significant contributors to the glial scar in rat models of SCI (Figure S3.6). The treatment of pig glia with any inflammatory factor in SFM had induced astrogliosis (Il-6: 1.81±0.05 fold, $p<0.0001$; TNFα: 1.92±0.06 fold, $p<0.0001$; TGFβ: 1.90±0.08 fold, $p<0.0001$). However, in the presence of FBS, the increase in astrogliosis was subdued in an FBS dose-dependent manner. Still, TNFα and Il-6 induced astrogliosis in the presence of FBS, while the effect of TGFβ was masked. On the other hand, human glia significantly increased astrogliosis when treated with Il-6 (3.1±1.0, $p<0.05$), TNFα

(9.04±2.3 fold, $p<0.01$), and TGFβ (15.6±4.4 fold, $p<0.0001$) but only when the inflammatory factors were applied in 1% FBS (Figure S3.6 A).

Next, we assessed neurogenesis which is strongly inhibited by inflammation in rat models of SCI (Ruxandra Covacu & Brundin, 2015). Rat NSPCs that were treated with Il-6, TNFα, or TGFβ had reduced neurogenesis over two weeks (one week: 0.07±0.07 fold, 0.04±0.03 fold, and 0.03±0.02 fold; two weeks: 0-fold, 0.02±0.02 fold, and 0.12±0.09 fold for Il-6, TNFα, and TGFβ, respectively) (Figure 3.9). Pig NSPCs treated with TNFα experienced reduced neurogenesis over two weeks (one week: 0.81±0.04,$p<0.0001$; two weeks: 0.62±0.05, $p<0.0001$) (Figure 3.9 C). However, TGFβ had increased neurogenesis after two weeks of treatment (1.5±0.1, $p<0.0001$) (Figure 3.9 D). Surprisingly, human NSPCs responded oppositely to rat NSPCs. Il-6 had increased neurogenesis after one (1.7±0.1 fold, $p<0.0001$) and two weeks (1.2±0.1 fold, $p<0.001$) (Figure 3.9 B). Similarly, TGFβ treatment had increased neurogenesis after one (1.24±0.09 fold, $p<0.05$) and two weeks (1.34±0.04 fold, $p<0.0001$) (Figure 3.9 D).

To simulate physiological conditions more accurately, we replicated the above inflammation conditions but in 1% FBS (n= 6 humans, 3 rats; Figure S3.7). Under these conditions, human NSPCs did not upregulate astrogliosis, similar to the observations made using serum-free conditions. Il-6 applied for one week, or TNFα and TGFβ applied for one and two weeks had significantly reduced astrogliosis. Meanwhile, rat NSPCs treated for one week with TGFβ had increased astrogliosis, but the effects of Il-6 and TNFα were subdued in the presence of FBS. Treatment of rat NSPCs for two weeks had reduced astrogliosis similar to serum-free conditions, suggesting that 1% FBS was insufficient to enhance cell survival of NSPCs after prolonged inflammatory treatment (Figure S3.7 A). When assessing neurogenesis, the presence of FBS masked the inductive effect of inflammatory factors on human NSPCs, and only Il-6 or TGFβ

applied for one week was able to increase neurogenesis significantly. Meanwhile, the inhibitory effect of inflammatory factors on rat NSPCs was maintained in FBS, although neurogenesis was rescued to some extent (Figure S3.7 B).

To model post-injury induction of proliferation, we measured the proliferation rate of NSPCs within the last 24 hours of inflammatory treatment (Figure 3.10). Rat NSPCs treated with TNFα for one week had reduced proliferation (0.77±0.10 fold, $p<0.05$) (Figure 3.10 C). However, there were no significant changes otherwise. Pig NSPCs were induced to proliferate with Il-6 and TGFβ treatment for one week (7.3±1.4 fold, $p<0.0001$ and 5.5±0.6, $p<0.0001$, respectively) (Figure 3.10 B, D). However, two weeks of treatment with TGFβ had reduced the proliferation rate of pig NSPCs (0.35±0.11 fold, $p<0.0001$), likely due to cultures attaining confluence (Figure 3.10 D). For validation, we compared the average number of cells per field view in the images used for cell counting. Indeed, pig NSPCs treated with TGFβ for one week had the most significant average number of cells per field view compared to human and rat NSPCs suggesting that the pig NSPC population had expanded the fastest and reached confluency under this condition (Figure S3.8). Human NSPCs had increased their proliferation after treatment with any inflammatory factors over the two weeks (Figure 3.10 B-D). Also, it was found that TGFβ was the most potent proliferation agent for human NSPCs (one week: 5.5±0.6 fold, $p<0.001$; two weeks: 2.9±0.8 fold, $p<0.01$) (Figure 3.10 D).

3.4.6 Human NSPCs require a unique molecular intervention to predictably direct cell fate

To utilize human NSPCs effectively for regenerative purposes, it is crucial to understand the forces controlling their differentiation and proliferation. To direct the differentiation of NSPCs into neurons, oligodendrocytes, or astrocytes, human (n=3-5) and rat (n=5) NSPCs were treated with a single exogenous factor over two weeks (Figure 3.11).

Retinoic acid was shown to increase neuronal differentiation of human (n=3) and rat (n=5) NSPCs, but there were different effects of treatment duration (Figure 3.11 A (i-iii), B (i-iii), G). At a high concentration [500 ng/mL], neuronal differentiation of rat NSPCs had significantly increased progressively with time (1.9±0.2 fold, $p<0.01$ and 3.0±0.2 fold, $p<0.0001$ after one and two weeks, respectively). However, human NSPCs did not significantly increase neuronal differentiation with time (Figure 3.11 G). At a lower concentration [50 ng/mL], neuronal differentiation of rat NSPCs significantly increased but only after two weeks of treatment (1.6±0.4 fold, $p<0.05$). Meanwhile, neuronal differentiation of human NSPCs was significantly increased at one (1.4±0.1 fold, $p<0.0001$) and two weeks (1.4±0.1 fold, $p<0.0001$). Ultimately, a high concentration of RA was most effective for human and rat NSPCs at one and two weeks, respectively.

The PDGFα receptor is expressed in spinal cord NSPCs, and its ligand, PDGFα, can induce oligodendrocyte differentiation of rat NSPCs (Iris Kulbatski & Tator, 2009; Meletis et al., 2008; Moreno-Manzano et al., 2009; Sevc, Matiasova, Kutna, & Daxnerova, 2014). In our assay, PDGFα at a low [40 ng/mL] and high concentration [100 ng/mL] had significantly increased oligodendrocyte differentiation of rat (n=5) NSPCs at any time of treatment (Figure 3.11 C (i-iii), H). This effect was most significant when PDGFα was applied at a low concentration for one week (40 ng/mL: 8.5±1.4 fold, $p<0.0001$; 100 ng/mL: 3.7±0.3 fold, $p<0.0001$). On the contrary, human (n=3) NSPCs did not increase oligodendrocyte differentiation under any of the conditions tested (Figure 3.11 H) despite expressing the gene for the receptor of this ligand (data not shown). Therefore, PDGFα [40-100 ng/mL] treatment for up to two weeks could induce oligodendrocyte differentiation in rat but not human NSPCs.

BMP4 acts as a morphogen and differentiation factor during spinal cord development and can stimulate astrocyte differentiation of adult rat NSPCs (Cole et al., 2016; Q. Xiao et al., 2010). In

our assay, BMP4 applied at a high concentration [100 ng/mL] was most effective on rat (n=5) NSPCs and had significantly increased astrocyte differentiation after two weeks of treatment (1.8±0.1 fold, $p<0.0001$) (Figure 3.11 E (i, ii), I). On the contrary, only a low concentration of BMP4 [40 ng/mL] had significantly increased astrocyte differentiation of human (n=5) NSPCs when applied for one (1.9±0.3, $p<0.01$) and two (2.1±0.4, $p<0.01$) weeks (Figure 3.11 D (i, ii), I). To examine a potential gradient effect of BMP4 on human NSPCs, we tested a very low concentration [4 ng/mL] in a separate assay (n=5 humans). Here, it was determined that astrocyte differentiation was inversely proportional to the concentration of BMP4 (Figure S3.9). Therefore, BMP4 could increase astrocyte differentiation of human and rat NSPCs, albeit most effective at low and high concentrations, respectively.

To induce self-renewal, human (n=8), pig (n=6), and rat (n=10) NSPCs were treated with EGF and FGF2 for one or two weeks (Figure 3.11 F (i-iii), J). The proliferation rate was similar between human (43.0±1.9% and 29.0±1.5% after one and two weeks, respectively) and pig (46.0±3.5% and 22.9±2.9% after one and two weeks, respectively) NSPCs. Meanwhile, the proliferation rate was significantly lower from human ($p<0.0001$) and pig ($p<0.01$) NSPCs compared to rat NSPCs (62.0±2.5% and 46.8±1.5% after one and two weeks). The proliferation rate of NSPCs from all species was reduced after two weeks of mitogen treatment relative to one week.

3.5 Discussion

In this study, we compared the differentiation, proliferation, and transcriptome profiles of primary spinal cord NSPCs from adult humans with a small and large animal model of SCI. It was determined that pig and rat NSPCs are astrocyte-dominant and exhibit glial scarring mechanisms, whereas human NSPCs portray a neuron-dominant phenotype and anti-glial scarring mechanisms.

Differences between small and large mammals were also observed as rat NSPCs displayed the most significant proliferation rate and differentiation into oligodendrocytes. Such differences between human, pig, and rat NSPCs were also reflected in their expression of genes associated with specific functional behaviours. In particular, pig and rat NSPCs expressed a higher level of transcription factors for astrocyte specification compared to human NSPCs, and rat NSPCs expressed a higher level of transcription factors for oligodendrocyte specification compared to both human and pig NSPCs. We also determined that stimulating human NSPCs to regenerate may require a unique intervention that incorporates the type of growth factor, its concentration, and duration of application. For instance, human and rat NSPCs could be induced to differentiate into neurons or astrocytes using growth factors, albeit most effective at different concentrations and durations of application. Also, inducing oligodendrocyte differentiation from human NSPCs using PFGFα was unsuccessful despite being effective on rat NSPCs. Our findings support the notion that cell-intrinsic differences exist among primary spinal cord NSPCs from humans, pigs, and rats, which is reflected in their functional and transcriptional profiles.

The characterization of spinal cord NSPCs from adult humans has seldom been performed (Dromard et al., 2008; A. J. Mothe et al., 2011). A study by Mothe and colleagues (2011) demonstrated that human thoracic NSPCs bear little potential for spontaneous differentiation into the neuronal or glial lineages. However, neuronal differentiation could be enhanced 19-fold with dibutyrl cyclic AMP treatment suggesting a high propensity of human NSPCs for neurogenesis. Other groups have similarly studied human NSPCs from the filum terminale and reported a high potential for neurogenesis (Arvidsson et al., 2011; Jha et al., 2013; Varghese et al., 2009). In our study, we report robust spontaneous differentiation of adult human spinal cord NSPCs into neurons, significantly greater than pig and rat NSPCs. Our transcriptome analysis of human, pig,

and rat NSPCs revealed a differential expression of neurogenic markers between species that may underlie their neurogenic capacities. While each species preferentially expressed a different subset of neurogenic markers, human NSPCs were enriched specifically in *NRXN3*, *HEY2*, *COL6A2*, *SEMA5A*, and *PNMA2*, suggesting that these genes may be important for neurogenesis. There may also be genes inhibiting neurogenesis that are upregulated in pig and rat NSPCs. This is reflected in our GSEA report, in which rat NSPCs are enriched in genes associated with negative regulation of neuron differentiation. Unexpectedly, we could not obtain electrophysiological data representative of mature neurons from differentiated human NSPCs despite the protein expression of glutaminase. This may be because the culture conditions, consisting of 1% FBS, are inadequate for the long-term culture and maturation of human NSPC-derived neurons. In line with this assumption, rat NSPCs were enriched in gene sets associated with ion channel, synapse, and neurotransmitter processes. This suggests that human NSPCs in this study were not genetically primed for neuronal maturation.

The differentiation potential of rat NSPCs has been characterized by many *in vivo* and *in vitro* studies making rats a valuable model for comparison (Iris Kulbatski & Tator, 2009; Namiki & Tator, 1999; Weiss et al., 1996). Our work and others have consistently shown that rat NSPCs tend to favor glial lineages over neuronal differentiation, which contrasts with the *in vitro* differentiation potential of human NSPCs (Cusimano et al., 2018; Iris Kulbatski & Tator, 2009; Meletis et al., 2008). The differentiation profile of pig spinal cord NSPCs has not been characterized before. Yet, the pig model has been emphasized as a crucial pre-clinical animal model for SCI (K. T. Kim et al., 2018). To our knowledge, we have characterized pig spinal cord NSPC differentiation for the first time and observed that pig NSPCs behave more similarly to a rat than human NSPCs under the conditions tested. However, it is unknown whether pig spinal cord

NSPCs are astrocytic in vivo, similar to their rat counterparts (K. T. Kim et al., 2018; J. H. T. Lee et al., 2013a).

Expectedly, the astrogenic tendencies of pig and rat NSPCs were reflected in the expression of genes that are markers for astrocytes, including *SLC1A3*, *FGFR3*, *FABP7*, *SOX9*, and *GFAP*. However, some of these genes were only enriched in either pig or rat NSPCs suggesting that pig and rat NSPCs may differentiate into different forms of astrocytes. For instance, pig NSPCs expressed a higher level of *GFAP*, which is more prevalent in white matter fibrous astrocytes, while rat NSPCs expressed a higher level of *SLC1A3* which is more prevalent in grey matter protoplasmic astrocytes (Köhler, Winkler, & Hirrlinger, 2021; Oberheim, Goldman, & Nedergaard, 2012). Both pig and rat NSPCs were enriched in the transcription factors *NFIA* and *NFIB*, which are responsible for inducing gliogenesis in the developing human and rodent spinal cord (Deneen et al., 2006; Matuzelski et al., 2017; Q. Zhang et al., 2021). *NFIA* has also been shown to inhibit neurogenesis by upregulating *HES5*, which may explain the reduced neurogenic capacity of pig and rat NSPCs compared to human NSPCs (Deneen et al., 2006). As such, it would be interesting to evaluate the influence of *NFIA* and *NFIB* in driving astrocyte differentiation from human, pig, and rat NSPCs.

The differentiation potential for oligodendrocytes was low for all species, which may result from the culture conditions used, the maturity of NSPCs, and their transcriptional profiles. Myelinating $O4^+$ oligodendrocytes are generated over multiple stages of differentiation and development (Nagoshi et al., 2018; Waly, Macchi, Cayre, & Durbec, 2014). Moreover, endogenous oligodendrogenesis ensues neurogenesis and astrogenesis (Le Dréau & Martí, 2013). In support of this, rat NSPCs were passaged eight times to induce maturity and differentiated mainly into oligodendrocytes (Figure S3.2 G). However, pig NSPCs have also been passaged nine times to

induce maturity and differentiated with 1% FBS or PDGFα; no oligodendrocytes were observed. Therefore, the conditions employed in this study may not have been sufficient to generate $O4^+$ oligodendrocytes from matured human and pig NSPCs.

Moreover, the distinct transcriptional profile of rat NSPCs may be an essential driver of oligodendrogenesis. Relative to human and pig NSPCs, we have observed a significant enrichment of genes in rat NSPCs that mark the oligodendrocyte lineage, including *OLIG1*, *OLIG2*, *SOX10*, and *CNP* (Kuhn, Gritti, Crooks, & Dombrowski, 2019). Also, our GSEA and gProfiler reports have consistently indicated an enrichment of gene sets in rat NSPCs associated with oligodendrocyte specification, differentiation, and development. Therefore, rat NSPCs may be intrinsically primed at the transcriptional level to generate oligodendrocytes. The lack of such genes in human and pig NSPCs may underlie their resistance to differentiate into oligodendrocytes (Llorens-Bobadilla et al., 2020). This information may be used to induce a gene expression profile in human NSPCs using signalling molecules or genetic manipulations to promote oligodendrocyte differentiation.

Besides the differentiation profile, the division rate was observed to differ among species suggesting that differentiation kinetics are species-specific. Interestingly, rat NSPCs displayed an increased proliferation capacity throughout the two weeks compared to human and pig NSPCs. This information implies that rat progenitors maintain their degree of stemness for longer and may underlie an improved ability to repopulate cells after SCI. Concomitantly, rat NSPCs had the highest UCell score for "neural stem cells" based on their transcriptional profile of NSPC markers suggesting rat NSPCs portray more of a neural stem cell phenotype.

Despite easily forming neurons, it is still unclear whether human spinal cord NSPCs are neurogenic in vivo (Cawsey et al., 2015; Paniagua-Torija et al., 2018). This is complicated, given that NSPCs

in a healthy spinal cord are quiescent and only get activated when exposed to inflammatory factors present in an SCI (Lacroix et al., 2014). In rat models of SCI, NSPCs migrate to the lesion and differentiate predominately into astrocytes, thus contributing to the glial scar (Barnabé-Heider et al., 2010; Cusimano et al., 2018). The glial scar has been a significant proponent of therapeutic interventions for SCI. Several inflammatory molecules, including Il-6, TNFα, and members of the TGFβ superfamily of cytokines, have been directly implicated in driving rat NSPCs to adopt astrocytic fates (M. K. Kang & Kang, 2008; Ma et al., 2019; S. Okada et al., 2004; Pfeffer, Donner, Guo, Dunbar, & Yang, 1998; Q. Xiao et al., 2010). However, whether inflammation induces a similar pathophysiological process in larger mammals, including humans, is unclear (K. T. Kim et al., 2018).

Two studies in humans served to address this question by observing the central canal area of post-mortem spinal cord tissue from patients with SCIs and non-injured control patients (Cawsey et al., 2015; Paniagua-Torija et al., 2018). Cawsey and colleagues (2015) report a correlation between the amount of $Nestin^{+}$ activated progenitor cells with the severity of injury and time from injury, an outcome similarly observed in rat SCI (Lacroix et al., 2014; McDonough & Martínez-Cerdeño, 2012). Meanwhile, Paniagua-Torija and colleagues (2018) describe a lack of proliferation within the ependymal layer of injured patients regardless of injury severity or time after injury. Yet, neither study observed a prominent glial scar like that commonly observed in rat SCI.

For the first time, we have conducted a functional assay on human spinal cord NSPCs to predict the pathophysiological response to inflammation. We found that the mechanisms that drive glial scarring in animal models do not apply to human NSPCs within the assessed time frame. We also observed a time-dependent response in rat and pig NSPCs that may reflect differences in animal size, whereby pathophysiological processes occur at a longer time scale in larger animals (J. H. T.

Lee et al., 2013a). Therefore, the NSPC response to inflammation may be inherently different in humans than in animal models following SCI. Ultimately, this information cautions against the translation of experimental treatments that target NSPCs to modify the glial scar considering the lack of evidence, from our study and others, that NSPCs contribute to glial scarring in humans (Cawsey et al., 2015; Paniagua-Torija et al., 2018).

Still, this does not rule out the possibility of glial scarring from occurring in human SCI, considering that glial cells have also been shown to contribute to glial scarring in rodent models of SCI (Barnabé-Heider et al., 2010; Van Der Laan, De Groot, Elices, & Dijkstra, 1997). Astrocytes, in particular, undergo reactive astrogliosis whereby they exhibit a hypertrophic morphology, upregulate the expression of intermediate filament protein GFAP, and production of inhibitory CSPG molecules (Liddelow & Barres, 2016; Seiji Okada, Hara, Kobayakawa, Matsumoto, & Nakashima, 2018; Yu et al., 2012).

Therefore, to further investigate the formation of a glial scar in human SCI, we assessed whether primary human and pig glia undergo reactive astrogliosis following inflammatory treatment with Il-6, TNFα, or TGFβ1. After inflammatory treatment, we observed that human and pig glial cultures exhibited increased GFAP expression. Specifically, pig glia underwent astrogliosis in the absence of serum and the degree of astrogliosis was subdued with increasing concentrations of serum. This may be due to serum masking the effect of the inflammatory factors. On the contrary, human glia only underwent astrogliosis in the presence of 1% FBS. The lack of astrogliosis from human glia in SFM may be due to the very low baseline levels of $GFAP^+$ astrocytes (<5%, data not shown) and the requirement for FBS to promote cell survival. Meanwhile, pig glial cultures had a baseline level of at least 38% $GFAP^+$ astrocytes in SFM and FBS (data not shown). Since

astrocytes require FBS for survival and expansion, it would be worth replicating the human glia treatments in SFM starting off with a higher baseline level of astrocytes.

Despite the observation that pig glia undergo astrogliosis following inflammatory treatment, it is not known whether glial scarring is prominent in pig SCI, possibly due to the novelty of the animal model (K. T. Kim et al., 2018). As such, we are unable to make a cross-reference of human glia with pig glia *in vivo*. Still, this information may inform us of the pathophysiological mechanisms mediated by glial cells after SCI in humans, although it must be taken lightly since the *in vivo* inflammatory environment is more complex than our *in vitro* assays. Ultimately, unlike primary NSPCs, primary human glia appear to undergo reactive astrogliosis following inflammatory treatment in FBS.

It is proposed that the injured spinal cord can be regenerated by targeting endogenous NSPCs by stimulating their proliferation and differentiation. In our study, we stimulated NSPCs to proliferate and demonstrated that humans and pigs possess a smaller percentage of NSPCs that undergo proliferation compared to rat NSPCs. This may reflect an inherent limitation of NSPCs from larger animals that spend more time in the cell cycle (Björklund, 2019).

In line with this assumption, we determined a different subset of proliferation and cell cycle-related genes that were upregulated in either rat NSPCs or human and pig NSPCs. For instance, *BCAT1* was significantly enriched in rat NSPCs relative to human and pig NSPCs. *BCAT1* codes for an enzyme that metabolizes branched-chain amino acids and plays an important role in promoting the proliferation of multiple cancer cell lines, embryonic stem cells, and neural stem cells (Bible, 2013; Karsten et al., 2003; Tönjes et al., 2013; P. Wang et al., 2018). Similarly, *EGR4* was upregulated in rat NSPCs, which has been shown to inhibit tumor suppressors (e.g., *PTEN*, *CDKN1B*, and

TP53) and induce the expression of cell cycle regulators (e.g., cyclins D1, D2, and D3) (Baron, Adamson, Calogero, Ragona, & Mercola, 2006; Cera et al., 2018; Poiana et al., 2020).

On the other hand, human and pig NSPCs were enriched in *HOXC10*, *CDK6*, *TEP1*, and *TGFβR2*, which have roles implicated with cell cycle progression. *HOXC10* levels fluctuate during the cell cycle, and a high level has been shown to arrest the cell cycle during metaphase (Gabellini et al., 2003; Rogulja-Ortmann & Technau, 2008). *CDK6* is activated early during the G1-phase and promotes progression to the S-phase, so higher levels of *CDK6* may indicate a greater proportion of cells in the G1-phase. *TEP1* (also known as *PTEN*) acts as a tumor suppressor gene and inhibits progression through the cell cycle by regulating G0 to G1 entry (M. Groszer et al., 2001; Matthias Groszer et al., 2006). *TGFβR2* has been shown to reduce proliferation by increasing the cell cycle length, causing cell cycle exit, and NSPC quiescence (Falk et al., 2008; Kandasamy et al., 2014). Therefore, the higher expression of genes promoting cell cycle progression and lower expression of genes suppressing cell cycle progression in rat NSPCs may underlie their enhanced proliferative capacity.

Of equal importance to stimulating proliferation is to direct the differentiation of human NSPCs. Growth and trophic factors have been used to accomplish this feat in rats, but the same growth factors may not apply to human NSPCs. We've shown that the same conditions used to direct a response from rat NSPCs do not bring about the same reaction from human NSPCs. For instance, PDGFα treatment did not induce oligodendrocyte differentiation of human NSPCs, although it was effective for rat NSPCs at low and high concentrations. This is despite human NSPCs expressing the gene for the receptor of PDGFα at a higher level than rat NSPCs. Therefore, the generation of human oligodendrocytes may require another intervention that considers the cell-intrinsic characteristics of human NSPCs. Besides the type of growth factor used, we demonstrated that the

concentration of growth factors and their duration of application might need to be optimized to produce the desired effect from human NSPCs.

Further investigations are needed to determine the optimal growth factors and durations of growth factor application to induce regeneration from human NSPCs. The development of such regenerative strategies should be reproducible and effective across donors. Also, it is crucial to determine the conditions required to promote the successful differentiation of oligodendrocytes from human NSPCs, which has been historically challenging (Goldman & Kuypers, 2015). Such investigations could be carried out similarly to the one presented in this study, whereby animal models of pre-clinical importance are used in direct comparison to human NSPCs.

A limitation of using *in vitro* assays is that the physiological nature of NSPCs is expected to change based on the culture conditions used. For instance, a previous study performed single-cell RNA sequencing of rodent NSPCs, revealing cell clusters of "activated NSPCs" and "quiescent NSPCs." Both cell clusters exhibited ependymal cell properties, which were more enriched in the quiescent NSPCs (Shu et al., 2021). In our study, human NSPCs were enriched in epithelial to mesenchymal transition genes, indicating a phenotype transformation from their epithelial nature *in vivo*. Interestingly, pig NSPCs were enriched in cilium and microtubule biology genes but had downregulation of genes related to neuronal development, suggesting that pig NSPCs may resemble ependymal cells *in vivo* more than human NSPCs.

Therefore, to minimize the deviations in NSPC biology and induction of artificial phenotypes, we analyzed secondary NSPCs in all of our functional assays. Secondary NSPCs are expected to portray the physiological nature of NSPCs *in vivo* more accurately than NSPCs that have been serially passaged (Gil-Perotín et al., 2013). However, the analysis of secondary NSPCs may pose another limitation since these cultures represent a heterogeneous population of cells that includes

NSPCs but also progenitors and terminally differentiated cells (Gil-Perotín et al., 2013; Reynolds & Rietze, 2005).

For this reason, primary NSPCs were seeded at a low cell density and cultured in conditions that select for self-renewing NSPCs, which is expected to yield a primary population consisting primarily of NSPCs (H. Azari, Louis, Sharififar, Vedam-Mai, & Reynolds, 2011; Narayanan et al., 2016). Furthermore, upon passaging primary NSPCs, progenitors and terminally differentiated cells are strongly reduced since the culture conditions do not select for these contaminant cells (Reynolds & Rietze, 2005). Therefore, the analysis of secondary NSPCs in our assays is expected to portray mostly NSPC behaviour and not contaminant cells.

To validate that secondary NSPCs are not significantly contaminated by terminally differentiated cells, we passaged secondary NSPCs to further select for NSPCs and assayed the resulting tertiary NSPCs. We observed that tertiary NSPCs possessed a greater proliferation rate than secondary NSPCs, indicative of a population more enriched in stem cells. Notably, the differentiation profiles of tertiary and secondary NSPCs were similar in that mostly neurons and a few glia were generated. These experiments demonstrate that secondary NSPC cultures could accurately portray NSPC behaviour despite the possibility of some contaminant cells.

Considering the differences in NSPC behaviour and transcriptome between species newly discovered in this study, we can speculate on the role of human NSPCs during SCI and the potential of stimulating human NSPCs to regenerate. Interestingly, a significant amount of spontaneous recovery occurs in rodents after an SCI that plateaus following the first month (Kakuta et al., 2019; Ung, Lapointe, Tremblay, Larouche, & Guertin, 2007). This is in contrast to human SCI, during which most spontaneous recovery occurs within nine months but can last up to 18 months post-SCI (Drazin & Boakye, 2014). Therefore, could differences in the regenerative capacity between

rodents and human NSPCs account to some degree for the enhanced spontaneous recovery in rodents? In rats, NSPCs increase their proliferation following an SCI, but the same observation has not been made in humans (Lacroix et al., 2014; Paniagua-Torija et al., 2018). In support of this information, our functional and molecular characterizations of human NSPCs *in vitro* suggest that human NSPCs possess a reduced proliferation capacity relative to rat NSPCs. Therefore, SCI in humans may not induce as significant of a proliferative response from NSPCs compared to rodents.

In a rodent SCI, NSPCs offer neuroprotection and mitigate chronic inflammation by secreting trophic and immunomodulatory factors associated with improved functional outcomes (Cusimano et al., 2018; Hawryluk et al., 2012; Kokaia et al., 2012; Sabelström et al., 2013). Interestingly, our RNA sequencing data indicates that human NSPCs are enriched in gene sets associated with inflammation and immunomodulation. However, these genes may code for pro-inflammatory proteins and enhance secondary injury. It is also important to note that the NSPCs characterized in this study were isolated from healthy spinal cord tissue, which may not reflect their pathophysiological state (Moreno-Manzano et al., 2009; Shu et al., 2021). Therefore, it would be interesting to characterize human NSPCs isolated from injured spinal cord tissue or NSPCs that are treated with inflammatory factors produced in SCI.

As part of the neuroprotective effect, rodent NSPCs have been shown to differentiate into astrocytes contributing to the glial scar. The tendency of rat NSPCs to differentiate into astrocytes may be due to their transcriptional profile and factors present in the injured spinal cord (M. K. Kang & Kang, 2008; Shihabuddin et al., 2000b; Shu et al., 2021). We have shown that human NSPCs differ significantly in this aspect. They do not express astrocyte-lineage transcription factors and do not undergo astrogliosis when treated with inflammatory factors. In support of our data, other studies investigating the injured human spinal cord failed to observe any glial scarring

(Cawsey et al., 2015; Paniagua-Torija et al., 2018). Interestingly, human NSPCs in our study were demonstrated to be highly neurogenic. Therefore, determining a means of activating endogenous NSPCs after SCI in humans may enhance neurogenesis, given their intrinsic tendency to form neurons *in vitro*.

Another mechanism that can contribute to spontaneous recovery, particularly in incomplete SCIs, is remyelination by oligodendrocytes. Rodent NSPCs have been shown to differentiate into oligodendrocytes post-SCI and contribute to remyelination (Barnabé-Heider et al., 2010; Meletis et al., 2008; Moreno-Manzano et al., 2009). Furthermore, the differentiation of rodent NSPCs into oligodendrocytes can be further enhanced to significantly improve axonal transmission and functional recovery post-SCI (Llorens-Bobadilla et al., 2020). Our functional and molecular characterization demonstrates that rat NSPCs have a superior capacity to generate oligodendrocytes compared to human and pig NSPCs, likely due to the high expression of oligodendrocyte-specifying transcription factors. Therefore, the reduced potential of human NSPCs to differentiate into oligodendrocytes may impair remyelination and spontaneous recovery post-SCI. As such, it will be essential to determine effective differentiation factors to induce oligodendrocytes from human NSPCs, which can be conducted using an assay similar to the one presented in this study.

In summary, we have demonstrated that spinal cord NSPCs from humans, pigs, and rats vary regarding their fundamental properties, including proliferation, differentiation, and transcriptome profiles. We found that human NSPCs are neurogenic, while animal model NSPCs are astrogenic. Moreover, human and animal model NSPCs do not exhibit the same pathophysiological mechanisms and responses to regenerative factors *in vitro*. Ultimately, comparing NSPCs from humans and animal models in an environment-controlled setting may allow for the determination

of species-specific molecular mechanisms that can be exploited for promoting regeneration in humans.

3.6 Acknowledgements

We thank the families that have consented to our study and permitted the donation of spinal cord tissue from their beloved ones to advance medical science research. We want to thank Mahmoud Bedawy, Hussam Jabri, Mohammad Alshardan, Michael Taccone, Carolyn Lai, Jessica Rabski, Hesham Ismail, Tongda Li, and Annemarie Dedek for their help with spinal cord harvests. We also thank Stem Core Laboratories and Chris Porter for assisting in RNA sequencing and data analysis. We acknowledge the Ottawa Hospital Department of Surgery, Division of Neurosurgery, and TGLN for permitting spinal cord extractions from organ donors and the University of Ottawa Heart Institute Animal Care and Veterinary Service for providing pigs. This study was funded by the Ottawa Hospital Department of Surgery Research Program Award and the Ontario Graduate Scholarship.

3.7 Figures and Tables

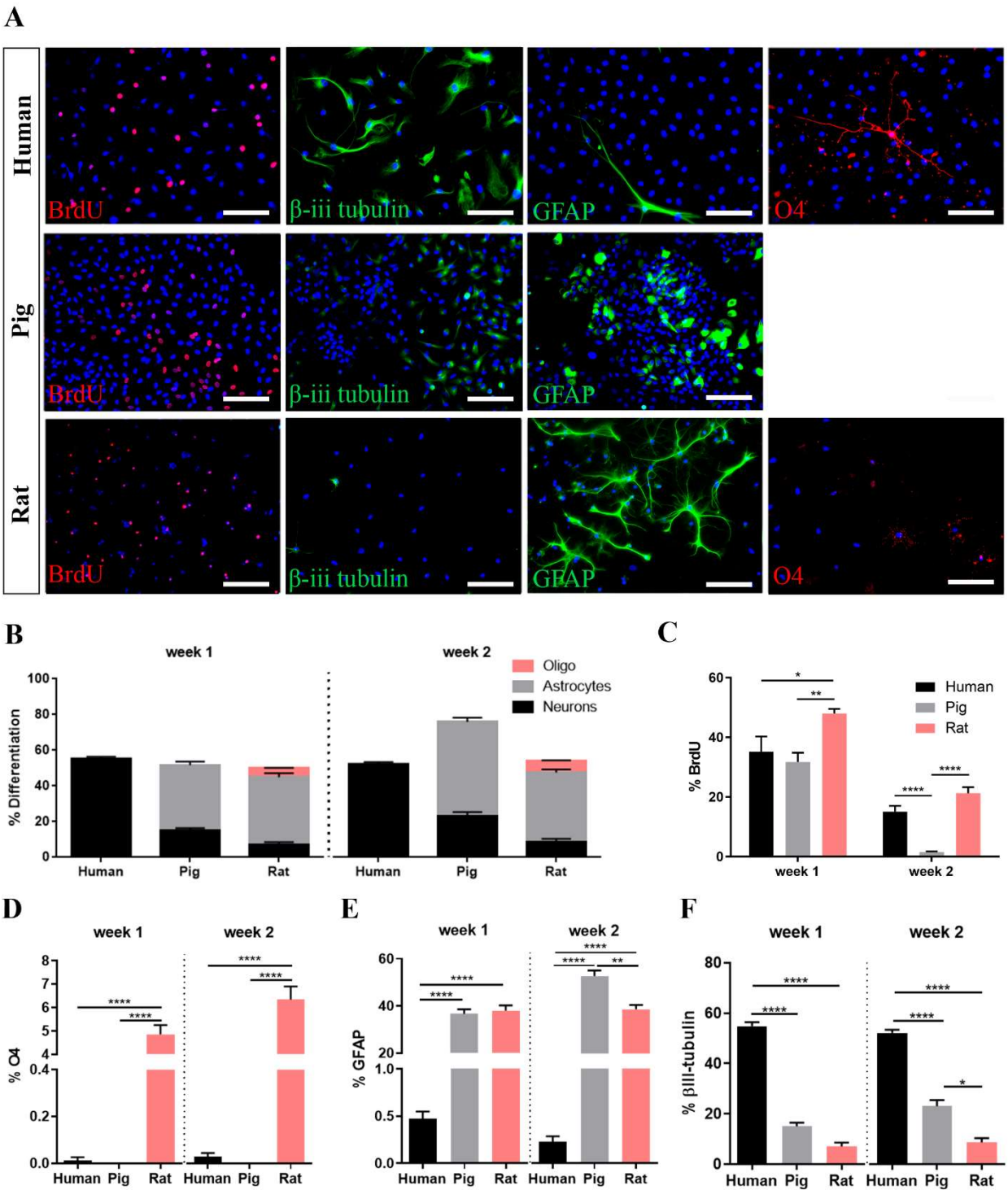

Figure 3.1 Human, pig, and rat NSPCs vary in their intrinsic differentiation and proliferation profiles

Primary-derived NSPCs were differentiated in 1% FBS for one or two weeks, then immuno-stained for differentiation and proliferation markers. (A) Representative images of human, pig, and rat NSPCs immuno-stained for BrdU, O4, GFAP, and β-iii tubulin. (B, D-F) The percentage of $O4^+$ oligodendrocytes, $GFAP^+$ astrocytes, and β-iii $tubulin^+$ neurons grouped (B) or individually (D-F). (B) The percentage of $BrdU^+$ NSPCs reflecting progenitor cell proliferation; BrdU was administered within the last 24 hours of culture. n=15 humans, 5 pigs, 10 rats. Mean ± s.e.m; *p<0.05, **p<0.01, ***p<0.001, ****p<0.0001. Scale bar = 100 μm.

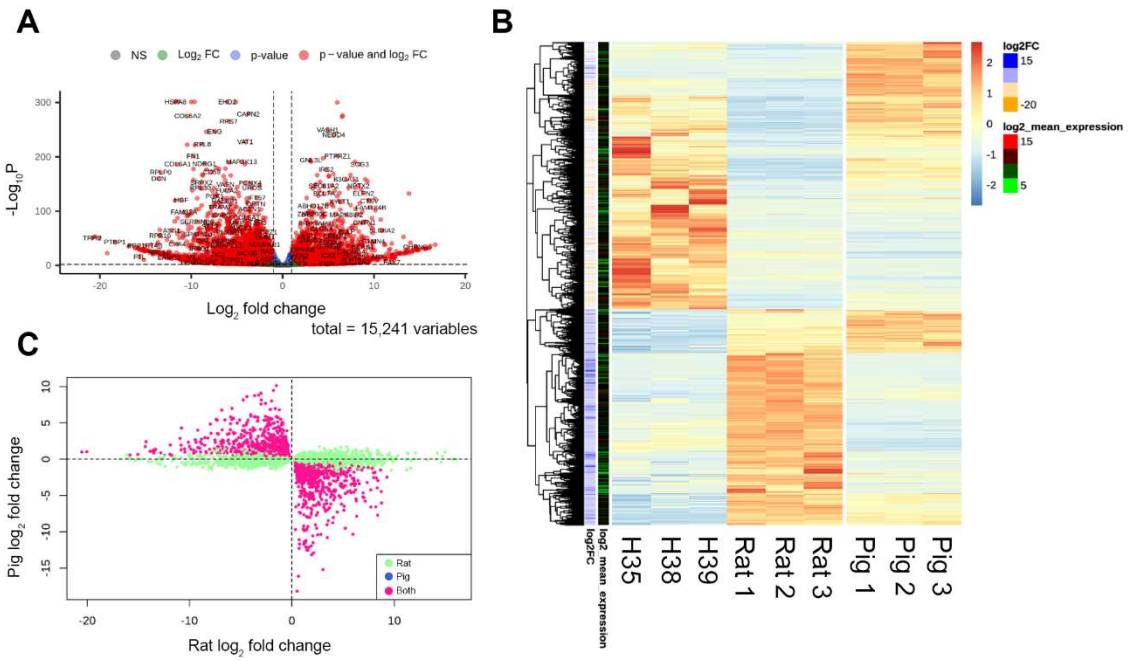

D

Upregulated		Downregulated	
GMCL2	PPP1R2B	TFPI2	TWF1
PPM1B-SLC3A1	A0A2R8Y471	ACTG1	PSMB3
GABRG1	E9PCH4	TUBA1B	COL13A1
CR1	COMMD3-BMI1	PRG4	ELOB
NCBP2L	B4DLN1	PTBP1	SIGIRR
SERPINB7	A0A0B4J269	ATN1	TES
ADAMTS20	B3GALT5	NME2	F10
A0A3B3ITX8	A0A494C116	CAPZA1	MIF
BOD1L2	H0YC42	GORASP2	LY6K
C1QL2	CUX2	EIF1	NDUFB11
H3BMM5	ATP5MGL	PHB	FAIM
ARHGAP19-SLIT1	KCNA3	ASPN	TSPAN8
TAS1R2	ANKRD62	RBPJ	C11orf1
J3KR12	PTPN5	FTL	CDCP1
HS2ST	SLC25A52	GALNT5	CALCOCO2
ANP32D	A0A2R8YF50	A1BG	MPZ
CHRNG	M0QZ92	MORC2	RPL27A
TSNAX-DISC1	ACTR3C	CBR1	GLE1
E7EQ34	V9GYY5	AGTR1	ITGA11
RESP18	PCDH8	SECTM1	JPT2
M0QXG9	DBX2	CHCHD10	SLC16A4
GSX1	MINAR2	GLT8D2	RPL31
HNRNPCL2	A0A2R8Y4E6	PPP1R14B	TBX18
A0A3B3IS95	HEPHL1	PHETA2	DCN
TTC9B	B8ZZF3	CD46	RPS12

Figure 3.2 Human and rat NSPCs differentially express 7,755 genes

(A) Volcano plot of genes that are enriched in rat (>0) and human (<0) NSPCs. Red dots indicate single DE genes with a fold change ≥2 and a p-value <0.05. A total of 15,241 genes found in

common between human, pig, and rat NSPCs were analyzed. (B) Heatmap and hierarchical clustering of DE genes between human and rat NSPCs from (A). The color scale indicates the relative gene expression: red represents an upregulation, and blue represents a downregulation. Human samples are labelled as “H35”, “H38”, and “H39”. (C) Scatter plot of genes significantly DE in rat NSPCs relative to human NSPCs. 4,418 genes with a fold change≥2 and a p-value <0.05 are shown. Pink dots indicate DE genes in pig and rat NSPCs, while green dots indicate DE genes only in rat NSPCs. (D) The top 50 DE genes upregulated or downregulated in rat NSPCs relative to human NSPCs. n=3 humans, n=3 rats.

A

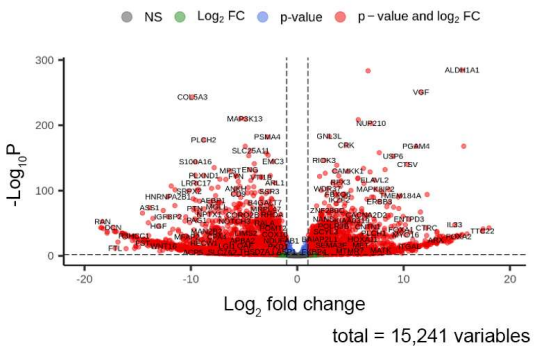

B

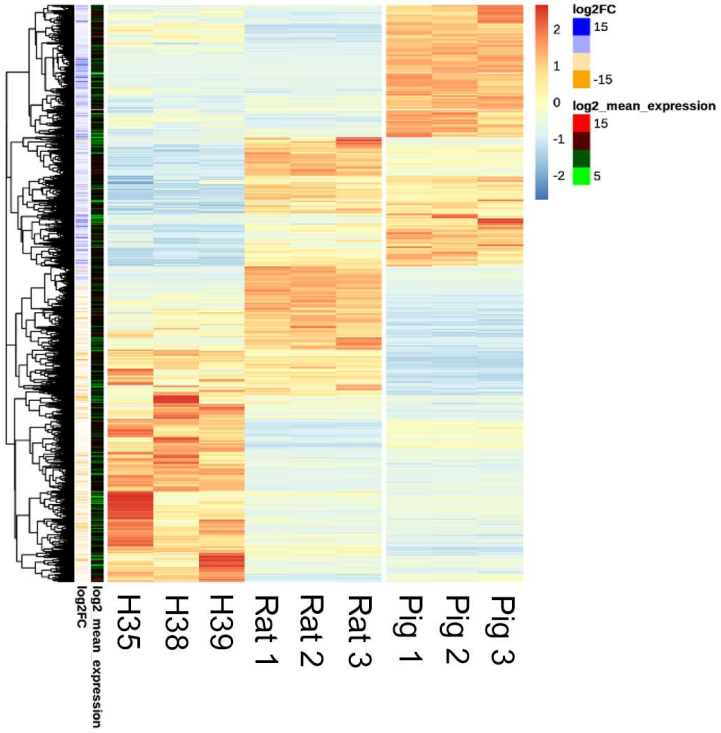

C

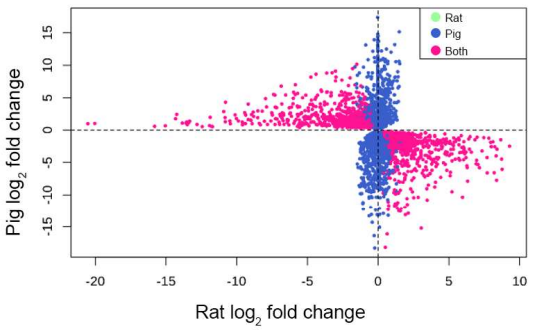

D

Upregulated	
A0A0B4J269	B4DLN1
ANKRD62	HOXB13
TTC22	C16orf54
H0YC42	GMCL2
A0A3B3IS95	TLR7
BOD1L2	NPFFR2
ALDH1A1	PPP1R2B
A0A2R8Y471	TSNAX-DISC1
FOXA2	SLC25A52
ANP32D	FOLR2
A0A3B3IS24	TTLL13P
E9PCH4	HNRNPCL2
BARX1	PLET1
IL33	CCDC60
FAM237B	MYL1
H3BMM5	V9GYY5
E7EQ34	H1-3
KRT5	COMMD3-BMI1
FGF19	ARX
GK3P	ATXN3L
M0QXG9	HEMGN
ENPP6	H3BQ15
TRH	UGT2A3
TMPRSS11D	TLX3
DMP1	ACTR3C

Downregulated	
PFDN5	EPHB6
RPL13	R3HCC1
RAN	STRA6
SELENOK	FAM111A
LAMA2	RPL9
ITGBL1	CRABP1
DCN	RPL27A
OLFML1	NME2
RPS17	ATP5PD
FTL	CMKLR1
RPL23	TRPC6
TMEM119	A2M
TMEM120A	IGFBP1
DMAC1	ADGRL4
NIPSNAP1	CYP1B1
TSPAN8	FST
PFN1	CD46
MGP	SUSD5
RPS15	C16orf89
AGTR1	RNF112
EGFLAM	SLC14A1
AK5	SHROOM2
COLEC12	CALHM2
ASPN	SLCO1C1
EEF1B2	SECTM1

Figure 3.3 Human and pig NSPCs differentially express 7,347 genes

(A) Volcano plot of genes that are enriched in pig (>0) and human (<0) NSPCs. Red dots indicate single DE genes with a fold change ≥2 and a p-value <0.05. A total of 15,241 genes found in common between human, pig, and rat NSPCs were analyzed. (B) Heatmap and hierarchical clustering of DE genes between human and pig NSPCs from (A). The color scale indicates the relative expression: red represents an upregulation, and blue represents a downregulation. Human samples are labelled as "H35", "H38", and "H39". (C) Scatter plot of genes significantly DE in pig NSPCs relative to human NSPCs. 3,920 genes with a fold change≥2 and a p-value <0.05 are shown. Pink dots indicate DE genes in pig and rat NSPCs, while blue dots indicate DE genes only in pig NSPCs. (D) The top 50 DE genes that are upregulated or downregulated in pig NSPCs relative to human NSPCs. n=3 humans, n=3 pigs.

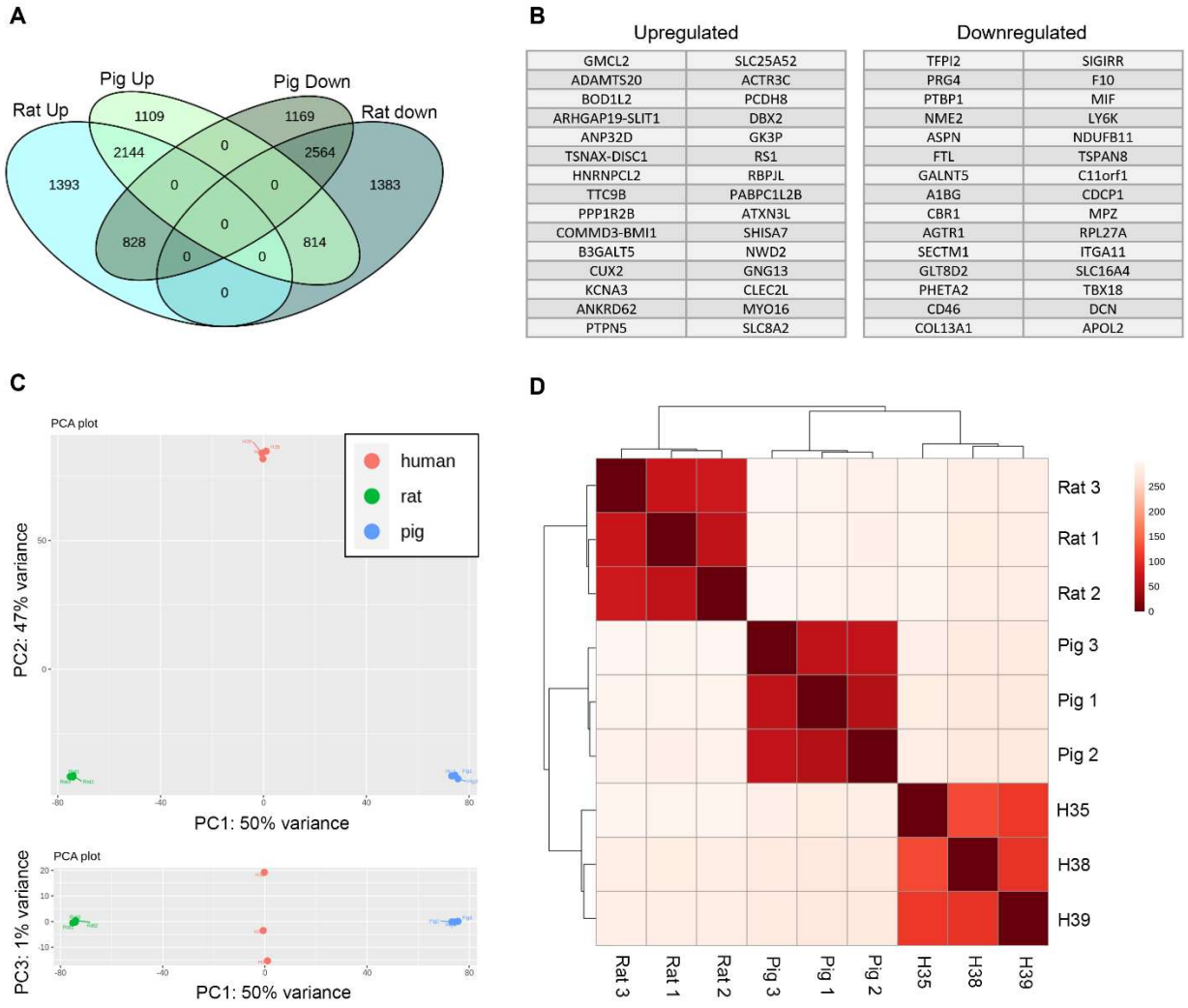

B

Upregulated		Downregulated	
GMCL2	SLC25A52	TFPI2	SIGIRR
ADAMTS20	ACTR3C	PRG4	F10
BOD1L2	PCDH8	PTBP1	MIF
ARHGAP19-SLIT1	DBX2	NME2	LY6K
ANP32D	GK3P	ASPN	NDUFB11
TSNAX-DISC1	RS1	FTL	TSPAN8
HNRNPCL2	RBPJL	GALNT5	C11orf1
TTC9B	PABPC1L2B	A1BG	CDCP1
PPP1R2B	ATXN3L	CBR1	MPZ
COMMD3-BMI1	SHISA7	AGTR1	RPL27A
B3GALT5	NWD2	SECTM1	ITGA11
CUX2	GNG13	GLT8D2	SLC16A4
KCNA3	CLEC2L	PHETA2	TBX18
ANKRD62	MYO16	CD46	DCN
PTPN5	SLC8A2	COL13A1	APOL2

Figure 3.4 The overall transcriptomes of human, pig, and rat NSPCs are distinct

(A) Venn diagram of DE genes in pig and rat NSPCs relative to human NSPCs, including directionality (upregulation or downregulation). 6,350 genes with a fold change≥2 and q-value<0.05 are shown. (B) The top 30 genes DE in the same direction (upregulation or downregulation) in both rat and pig NSPCs relative to human NSPCs. (C) Principal component analysis (PCA) using the 500 most variable genes between human, pig, and rat NSPCs. The PCA on top includes PC1 vs. PC2, which accounts for 97% variance, and the PCA on the bottom includes PC1 vs. PC3, which accounts for 51% variance. The red, blue, and green dots indicate

biological replicates of human, pig, and rat NSPCs. (D) Hierarchical clustering analysis for all transcripts (15,241 genes) found in common among human, pig, and rat NSPCs. Human samples are labelled as “H35”, “H38”, and “H39”. n=3 humans, n=3 pigs, n=3 rats.

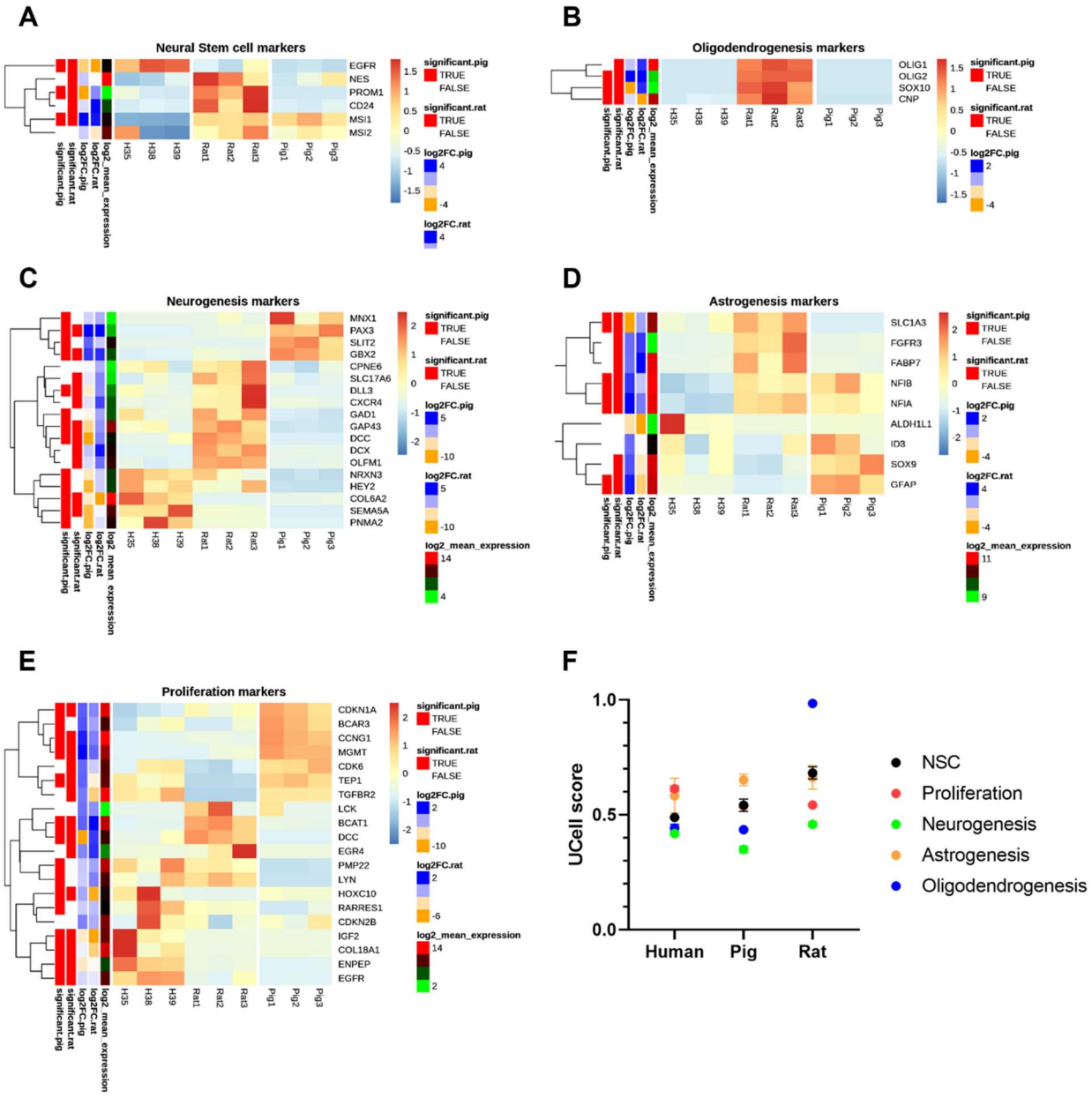

Figure 3.5 Genetic markers for NSPCs and their functional behaviour are differentially expressed between human, pig, and rat NSPCs

Heatmap and hierarchical clustering of markers that are characteristic of (A) neural stem cells (NSCs), (B) oligodendrogenesis, (C) neurogenesis, (D) astrogenesis, and (E) proliferation. The color scale indicates the relative expression: red represents an upregulation, and blue represents a downregulation. The red columns on the left-hand side indicate that a gene is significantly DE between pig and human NSPCs or rat and human NSPCs. Human samples are labelled as "H35", "H38", and "H39". (F) UCell-like scoring system that ranks the genes in (A-F) according to their expression level across biological replicates of the same species. n=3 humans, n=3 pigs, n=3 rats.

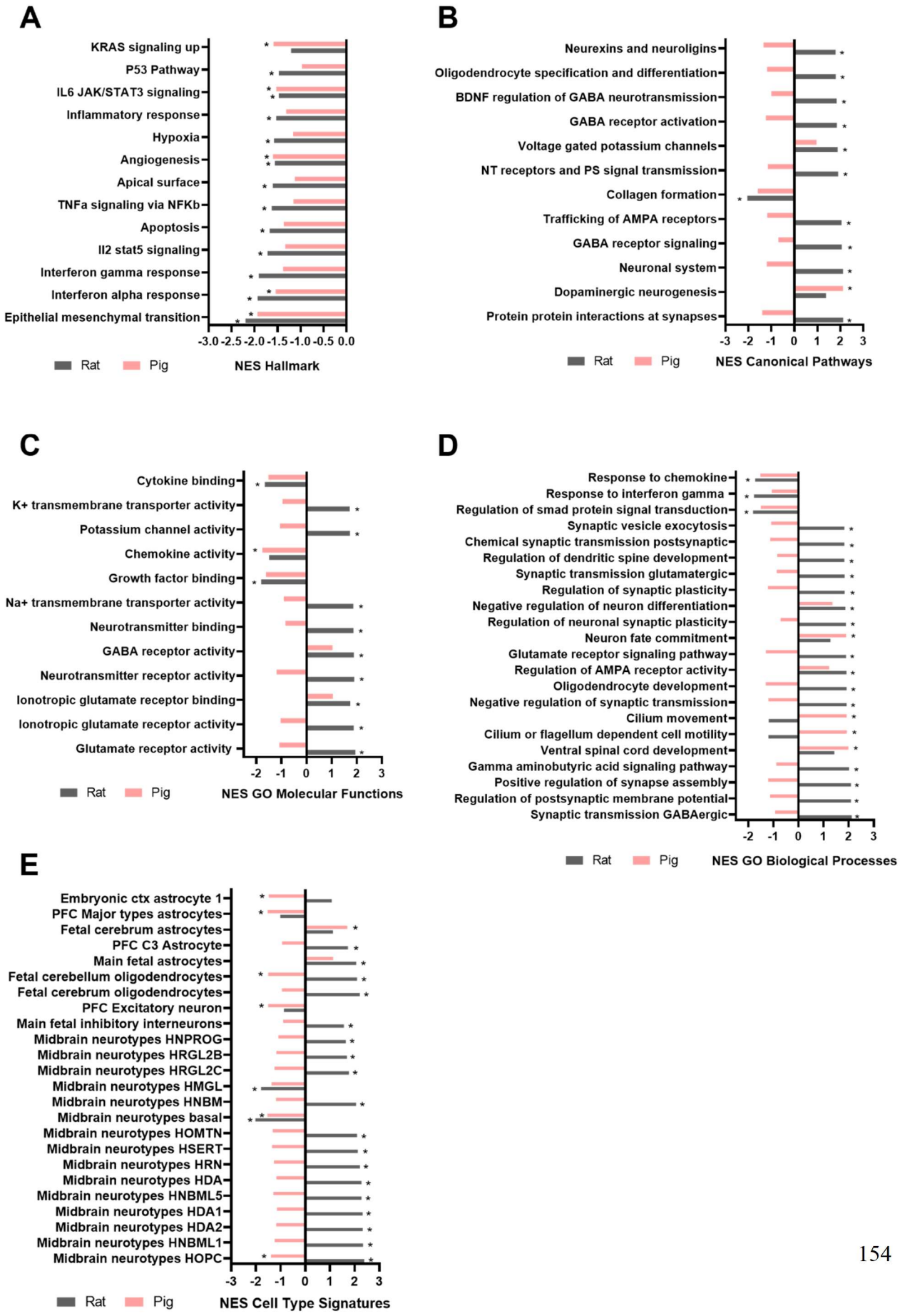
A
KRAS signaling up
P53 Pathway
IL6 JAK/STAT3 signaling
Inflammatory response
Hypoxia
Angiogenesis
Apical surface
TNFa signaling via NFKb
Apoptosis
Il2 stat5 signaling
Interferon gamma response
Interferon alpha response
Epithelial mesenchymal transition
-3.0 -2.5 -2.0 -1.5 -1.0 -0.5 0.0
Rat
Pig
NES Hallmark
B
Neurexins and neuroligins
Oligodendrocyte specification and differentiation
BDNF regulation of GABA neurotransmission
GABA receptor activation
Voltage gated potassium channels
NT receptors and PS signal transmission
Collagen formation
Trafficking of AMPA receptors
GABA receptor signaling
Neuronal system
Dopaminergic neurogenesis
Protein protein interactions at synapses
-3 -2 -1 0 1 2 3
Rat
Pig
NES Canonical Pathways
C
Cytokine binding
K+ transmembrane transporter activity
Potassium channel activity
Chemokine activity
Growth factor binding
Na+ transmembrane transporter activity
Neurotransmitter binding
GABA receptor activity
Neurotransmitter receptor activity
Ionotropic glutamate receptor binding
Ionotropic glutamate receptor activity
Glutamate receptor activity
-2 -1 0 1 2
Rat
Pig
NES GO Molecular Functions
D
Response to chemokine
Response to interferon gamma
Regulation of smad protein signal transduction
Synaptic vesicle exocytosis
Chemical synaptic transmission postsynaptic
Regulation of dendritic spine development
Synaptic transmission glutamatergic
Regulation of synaptic plasticity
Negative regulation of neuron differentiation
Regulation of neuronal synaptic plasticity
Neuron fate commitment
Glutamate receptor signaling pathway
Regulation of AMPA receptor activity
Oligodendrocyte development
Negative regulation of synaptic transmission
Cilium movement
Cilium or flagellum dependent cell motility
Ventral spinal cord development
Gamma aminobutyric acid signaling pathway
Positive regulation of synapse assembly
Regulation of postsynaptic membrane potential
Synaptic transmission GABAergic
-2 -1 0 1 2 3
Rat
Pig
NES GO Biological Processes
E
Embryonic ctx astrocyte 1
PFC Major types astrocytes
Fetal cerebrum astrocytes
PFC C3 Astrocyte
Main fetal astrocytes
Fetal cerebellum oligodendrocytes
Fetal cerebrum oligodendrocytes
PFC Excitatory neuron
Main fetal inhibitory interneurons
Midbrain neurotypes HNPROG
Midbrain neurotypes HRGL2B
Midbrain neurotypes HRGL2C
Midbrain neurotypes HMGL
Midbrain neurotypes HNBM
Midbrain neurotypes basal
Midbrain neurotypes HOMTN
Midbrain neurotypes HSERT
Midbrain neurotypes HRN
Midbrain neurotypes HDA
Midbrain neurotypes HNBML5
Midbrain neurotypes HDA1
Midbrain neurotypes HDA2
Midbrain neurotypes HNBML1
Midbrain neurotypes HOPC
-3 -2 -1 0 1 2 3
Rat
Pig
NES Cell Type Signatures

Figure 3.6 Gene set enrichment analysis (GSEA) of primary human, pig, and rat NSPCs

Gene set enrichment was analyzed using the GSEA preranked algorithm and ran against a subset of available gene sets from MSigDB. A normalized enrichment score (NES) was calculated for pig and rat NSPCs relative to human NSPCs. The NES was used to compare gene sets for the categories (A) hallmark gene sets, (B) canonical pathways, (C) GO molecular functions, (D) GO biological processes and (E) cell-type signatures. Gene sets with a significant positive or negative NES are indicated by *, representing a q-value<0.05. Pigs (n=3) and rats (n=3) are indicated by pink and grey bars, respectively. The full report can be accessed here.

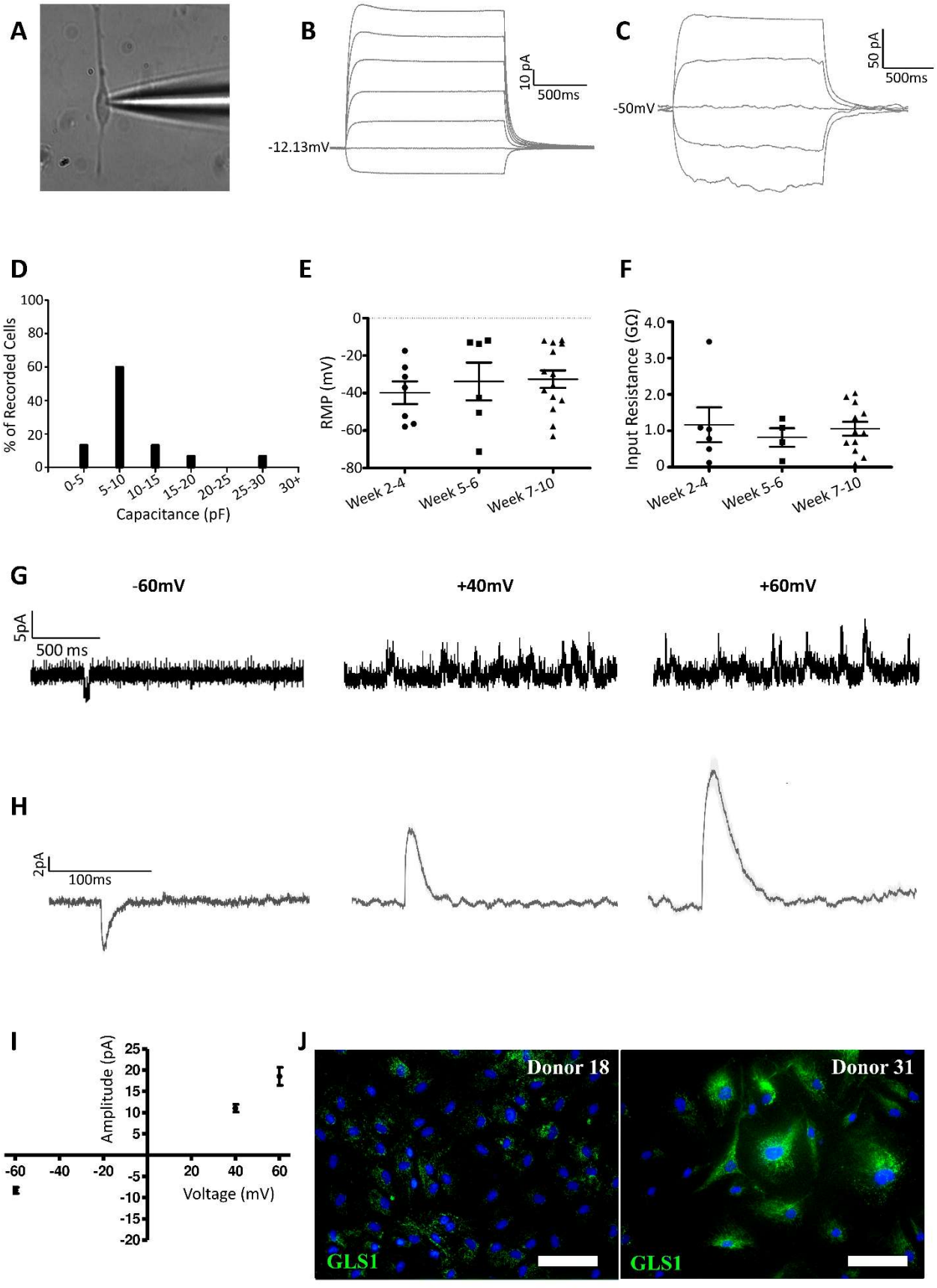
A
B
10 pA
500ms
-12.13mV
C
50 pA
500ms
-50mV
D
% of Recorded Cells
100
80
60
40
20
0
0-5
5-10
10-15
15-20
20-25
25-30
30+
Capacitance (pF)
E
RMP (mV)
0
-20
-40
-60
-80
Week 2-4
Week 5-6
Week 7-10
F
Input Resistance (GΩ)
4.0
3.0
2.0
1.0
0
Week 2-4
Week 5-6
Week 7-10
G
-60mV
+40mV
+60mV
5pA
500 ms
H
2pA
100ms
I
Amplitude (pA)
25
20
15
10
5
-5
-10
-15
-20
-60
-40
-20
20
40
60
Voltage (mV)
J
Donor 18
GLS1
Donor 31
GLS1

Figure 3.7 NSPCs expressing neuronal markers do not reach electrophysiological maturity over ten weeks *in vitro*

(A) Representative image of neuron-like cells produced from human NSPCs. (B) No action potentials were observed in any recorded cell, even when membrane potential was held at -50mV (C). Current steps at -20 by 5pA (B) or -100 by 20pA (C). (D) The majority of recorded cells showed capacitance values under 10 pF. (E) Resting membrane potential and (F) input resistance did not significantly change over time in culture, with few cells reaching mature neuron membrane potential levels. (G) Representative voltage clamp recordings and (H) average event traces at -60mV (left), +40mV (middle), and +60mV (right) holding potentials. (I) When event amplitudes at each holding voltage are plotted, an intercept above zero is observed. This is consistent with outward rectification and suggests glutamate signaling. (J) Staining for glutaminase (GLS1) in two human donor NSPC cultures under differentiation conditions suggests high glutamate production.

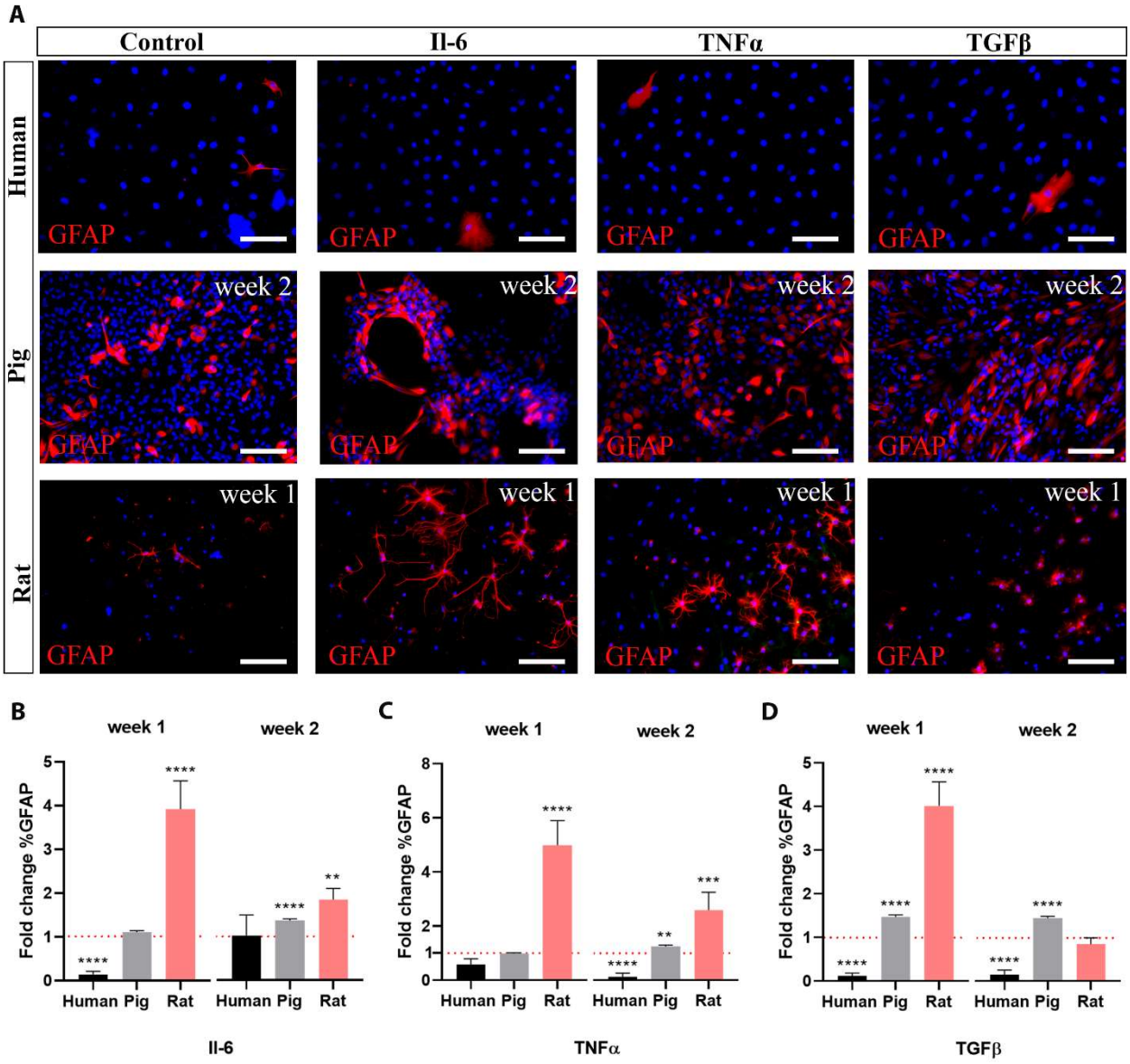

Figure 3.8 Inflammatory factors increase reactive astrocyte differentiation of pig and rat but not human NSPCs

(A) representative images of human, pig, and rat NSPCs treated with Il-6, TNF-α, and TGF-β. (B-D) Quantification of the fold change in $GFAP^+$ astrocytes after one or two weeks of treatment with (B) Il-6, (C) TNF-α, or (D) TGF-β in serum-free media. n=8 humans, 5 pigs, 6 rats. mean ± s.e.m; *p<0.05, ***p<0.001, ****p<0.0001 relative to control (SFM). Scale bar = 100 μm.

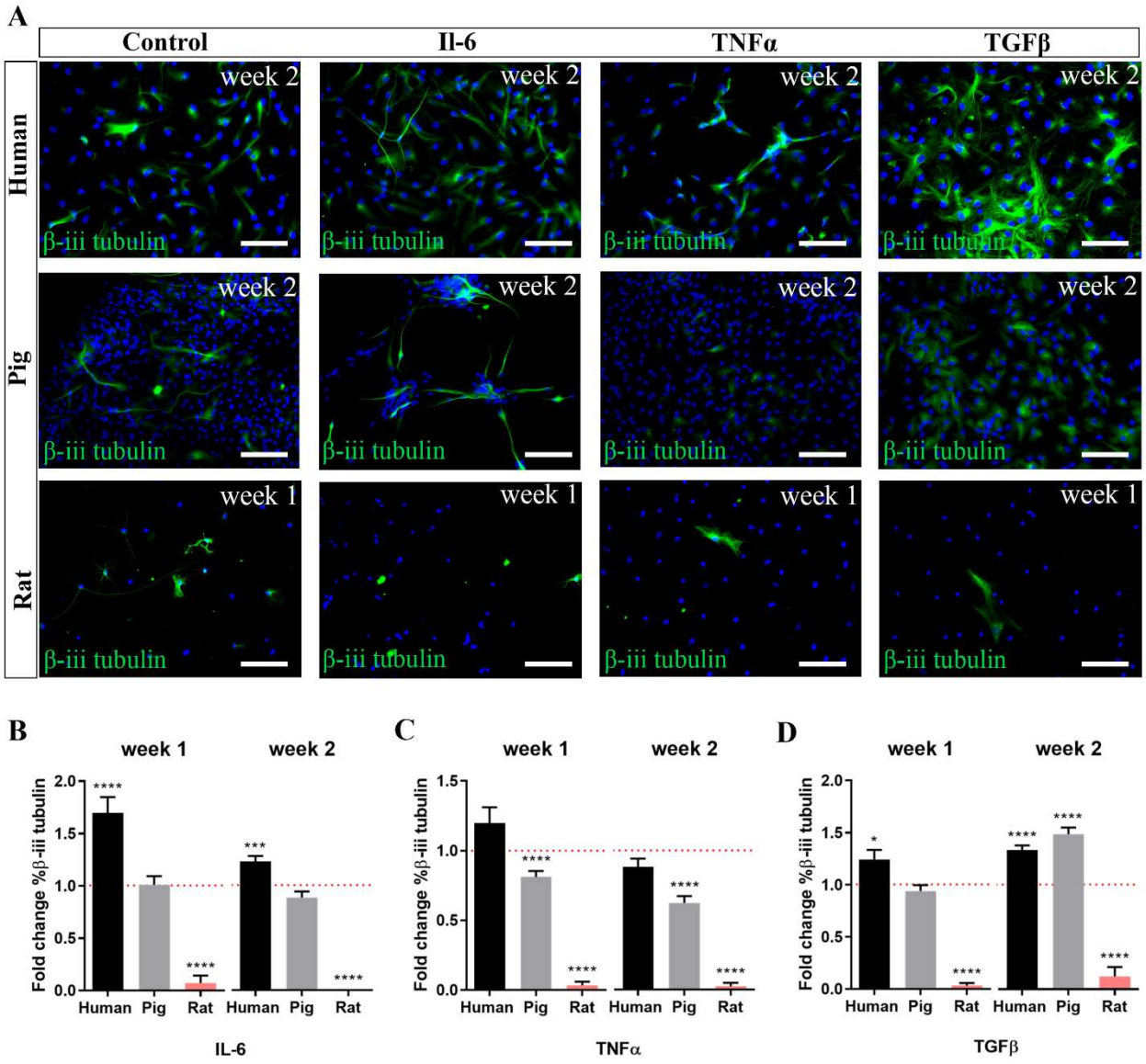

Figure 3.9 Increased human and reduced rat NSPC neuronal differentiation in response to inflammatory factors

(A) representative images of human, pig, and rat NSPCs treated with Il-6, TNF-α, and TGF-β. (B-D) Quantification of the fold change in β-iii tubulin^{+} neurons after one or two weeks of treatment

with (B) Il-6, (C) TNF-α, or (D) TGF-β in serum-free media. n=8 humans, 5 pigs, 6 rats. mean ± s.e.m; ***p<0.001, ****p<0.0001 relative to control (SFM). Scale bar = 100 μm.

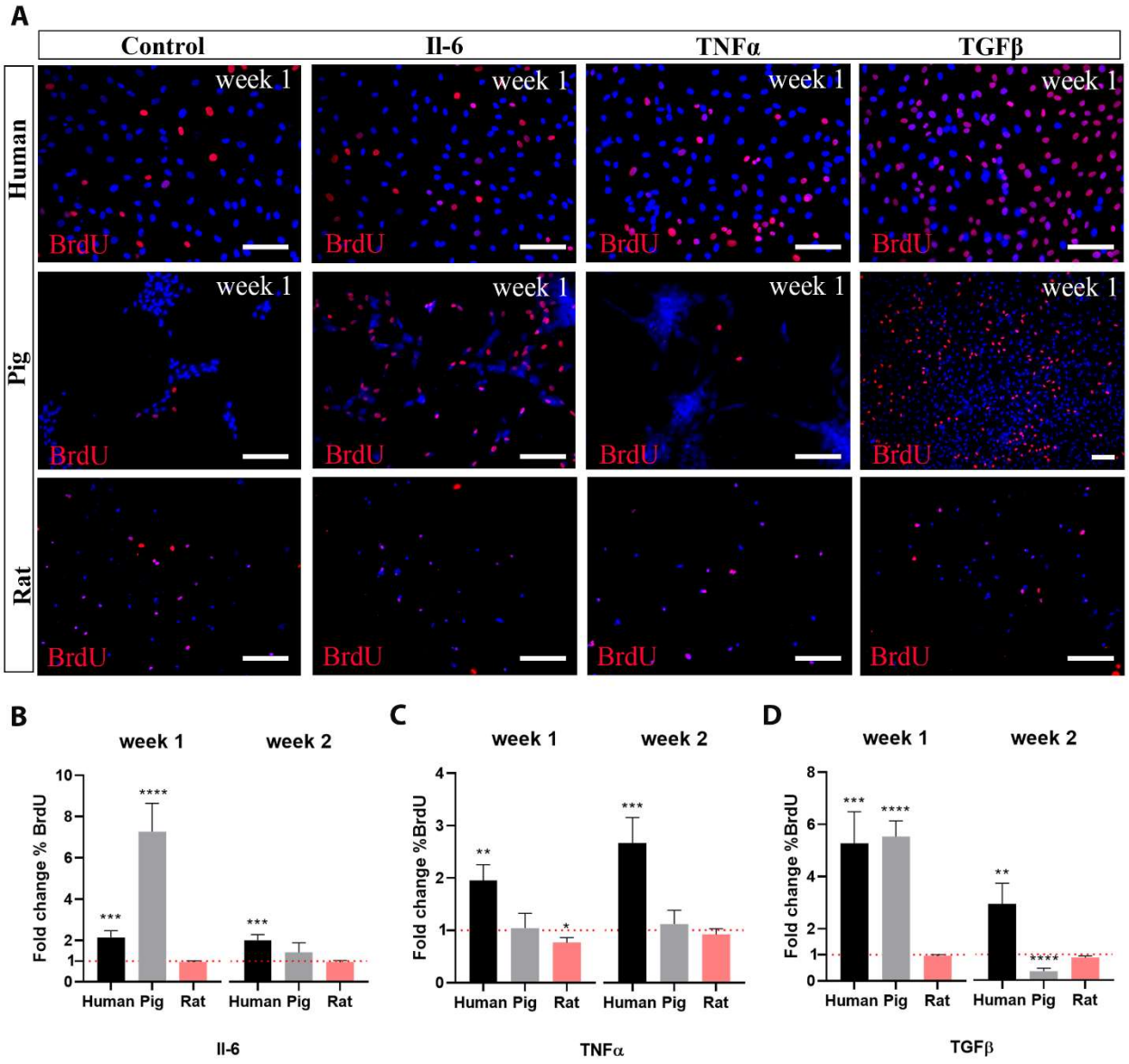

Figure 3.10 Inflammatory factors induce proliferation of human and pig but not rat NSPCs

(A) representative images of human, pig, and rat NSPCs treated with Il-6, TNF-α, and TGF-β. (B-D) Quantification of the fold change in Brdu^{+} proliferating NSPCs after one or two weeks of

treatment with (B) Il-6, (C) TNF-α, or (D) TGF-β in serum-free media. n=8 humans, 5 pigs, 6 rats. mean ± s.e.m; **p<0.01, ****p<0.0001 relative to control (SFM). Scale bar = 100 μm.

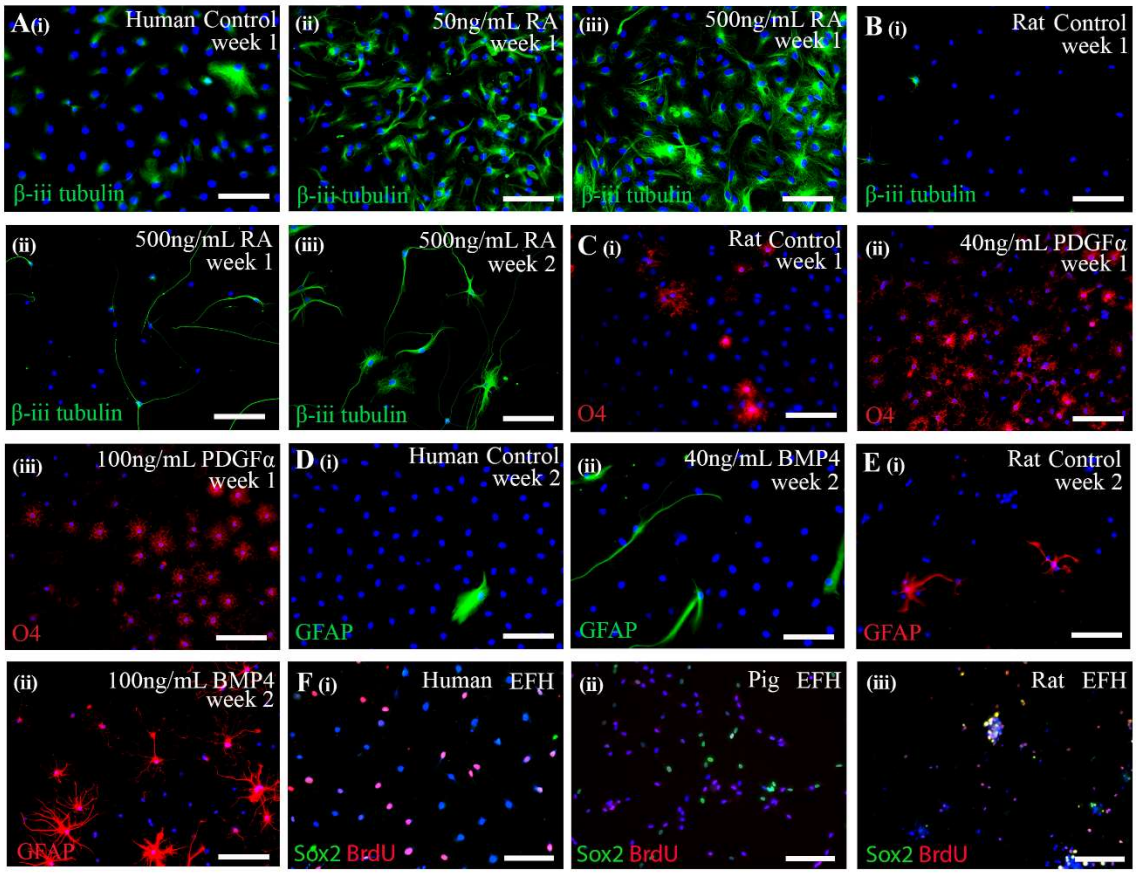
A(i) Human Control week 1
β-iii tubulin
(ii) 50ng/mL RA week 1
β-iii tubulin
(iii) 500ng/mL RA week 1
β-iii tubulin
B (i) Rat Control week 1
β-iii tubulin
(ii) 500ng/mL RA week 1
β-iii tubulin
(iii) 500ng/mL RA week 2
β-iii tubulin
C (i) Rat Control week 1
O4
(ii) 40ng/mL PDGFα week 1
O4
(iii) 100ng/mL PDGFα week 1
O4
D (i) Human Control week 2
GFAP
(ii) 40ng/mL BMP4 week 2
GFAP
E (i) Rat Control week 2
GFAP
(ii) 100ng/mL BMP4 week 2
GFAP
F (i) Human EFH
Sox2 BrdU
(ii) Pig EFH
Sox2 BrdU
(iii) Rat EFH
Sox2 BrdU

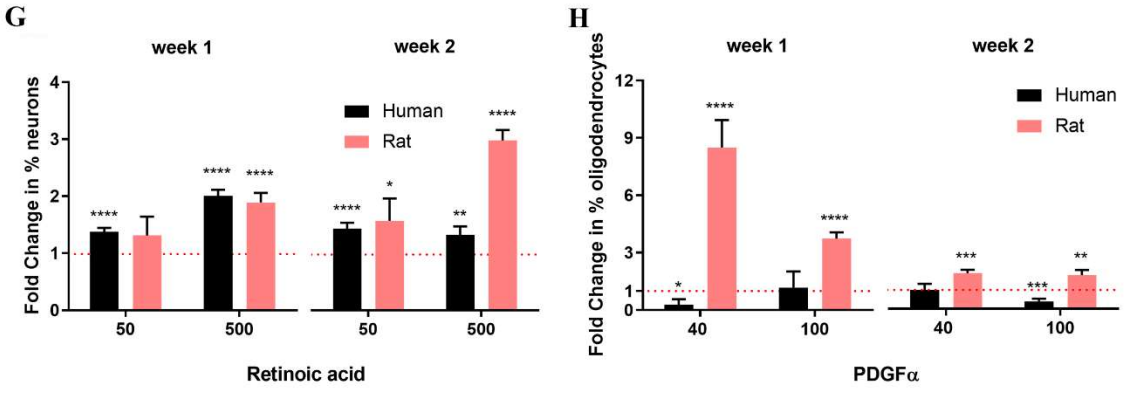
G
week 1
week 2
Human
Rat
Fold Change in % neurons
Retinoic acid
50
500
H
week 1
week 2
Human
Rat
Fold Change in % oligodendrocytes
PDGFα
40
100

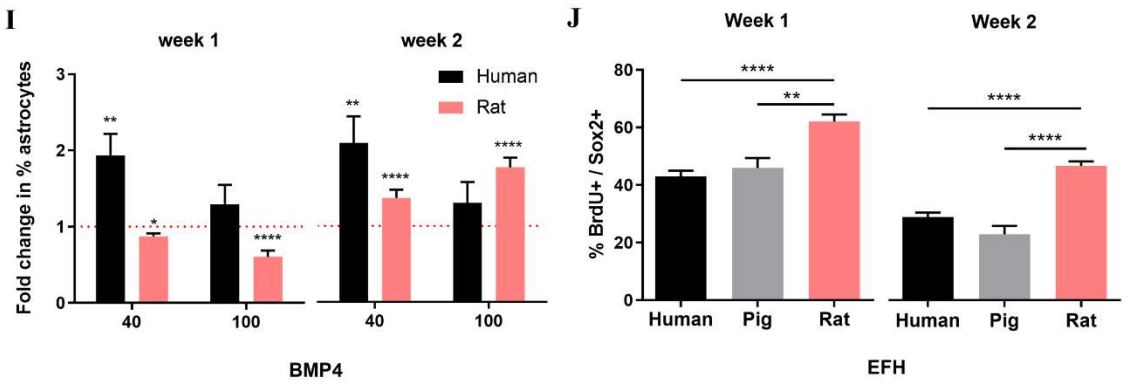
I
week 1
week 2
Human
Rat
Fold change in % astrocytes
BMP4
40
100
J
Week 1
Week 2
% BrdU+ / Sox2+
Human
Pig
Rat
EFH

Figure 3.11 Human and rat NSPCs exhibit distinct differentiation and proliferation responses to exogenous factors

(A) Human NSPCs treated with (ii) 50 ng/mL and (iii) 500 ng/mL of retinoic acid for one week significantly increased the percentage of neurons in a dose-dependent manner relative to (i) control. (B) Rat NSPCs treated with 500 ng/mL of retinoic acid significantly increased the percentage of neurons after (ii) one and (iii) two weeks relative to (i) control. (C) Rat NSPCs treated with (ii) 40 ng/mL and (iii) 100 ng/mL PDGF-α significantly increased the percentage of oligodendrocytes relative to (i) control. (D) Human NSPCs treated with (ii) 40 ng/mL BMP-4 significantly increased the percentage of astrocytes relative to (i) control. (E) Rat NSPCs treated with (ii) 100 ng/mL BMP-4 significantly increased the percentage of astrocytes relative to (i) control. (F) Treatment with mitogens induced proliferation of NSPCs, which was significantly less for (i) human and (ii) pig NSPCs relative to (iii) rat NSPCs. (G) Human and rat NSPCs treated with retinoic acid [50 ng/mL and 500 ng/mL] had an increased fold change in neuron differentiation. (H) Rat but not human NSPCs treated with platelet-derived growth factor-α [40 ng/mL and 100 ng/mL] had an increased fold change in oligodendrocyte differentiation. (I) An increased fold change in astrocyte differentiation was induced from human and rat NSPCs when treated with 40 ng/mL and 100 ng/mL of bone morphogenic protein-4, respectively. (J) Human and pig NSPCs exhibited a lower rate of self-renewal relative to rat NSPCs when treated with mitogens (20 ng/mL of EGF and FGF2). Control consists of treatment with SFM alone. $n \geq 3$, mean ± s.e.m; *$p<0.05$, **$p<0.01$, ***$p<0.001$, ****$p<0.0001$. Scale bar = 100 μm

Table 3.1 Organ donor demographic information including age, sex, cause of death, time from brain death to organ donation, and time from cardiac arrest to spinal cord harvest. M: male, F: female, CA: cardiac arrest, BD: brain death, SD: standard deviation

Age (mean ± SD, range)	Sex	Cause of death	Time from BD declaration to organ donation (mean ± SD, range)	Time from CA to spinal cord harvest (mean ± SD, range)
45.6 ± 15.7, 22-67 years old	11M 2F	Traumatic brain injury Hemorrhage (intracerebral, subarachnoid) Anoxic brain injury Hematoma (subdural) Hypoxic Asphyxiation Hypertension/stroke	48.5 ± 37.4, 17-151 hours	100.8 ± 31.8, 62-155 minutes

Table 3.2 Description of the human, pig, and rat NSPC samples used for RNA sequencing. All NSPC samples were derived from the thoracic spinal cord. M: male, F: female, DIV: days *in vitro*

Species	Age	Sex	DIV
Human	64	F	44
Human	31	M	65
Human	51	F	63
Pig	8-10 weeks	F	40
Pig	8-10 weeks	F	18

Pig	8-10 weeks	F	18
Rat	7-8 weeks	F	22
Rat	7-8 weeks	F	22
Rat	7-8 weeks	F	22

Table 3.3 The total number of annotated genes determined by bulk RNA sequencing, including human orthologs of pig and rat NSPCs and high-confidence human orthologs

Species	Number of annotated genes	Number of genes with human orthologs	Percentage of human orthologs	Number of genes with high-confidence human orthologs	Percentage of high-confidence human orthologs
Human	60,237	60,237	100%	60,237	100%
Rat	31,992	17,550	54.9%	13,694	42.8%
Pig	31,781	18,732	58.9%	16,135	50.8%

Table 3.4 The number and percentage of differentially expressed (DE) orthologs between human, pig, and rat NSPCs at a false discovery rate of 5%. A total of 15,241 human orthologs were found in common among all three species, and 12,496 genes were determined to be "high-confidence" orthologs

Species comparison	DE orthologs	% DE orthologs	DE high-confidence orthologs	% DE high-confidence orthologs
Rat vs. Human	9,126	59.9%	7,755	62.1%
Pig vs. Human	8,628	56.6%	7,347	58.8%
Pig vs. Rat	9,046	59.4%	7,767	62.2%

3.8 Supplementary Figures and Tables

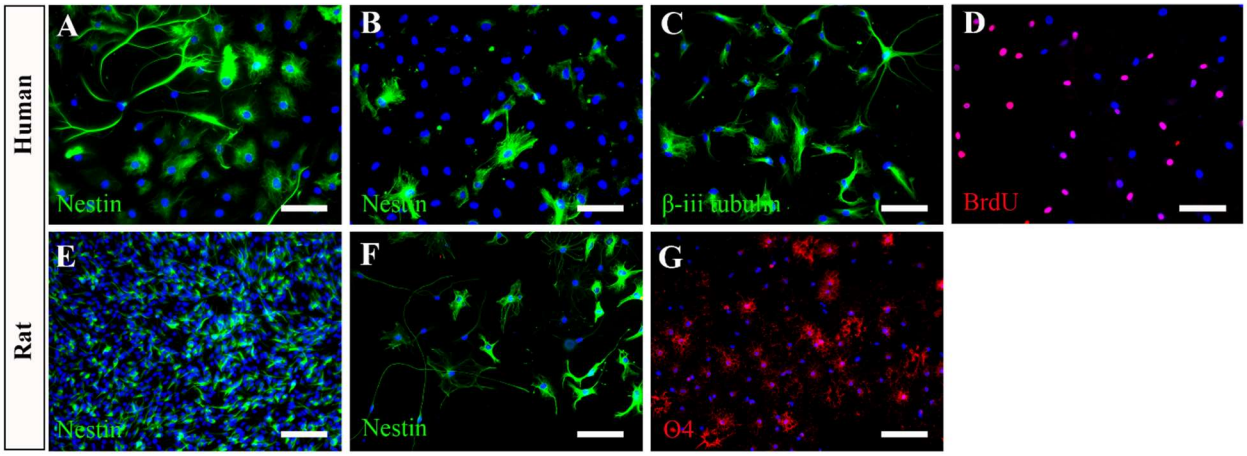

Figure S3.1 Immuno-cytochemistry for human and rat neural progenitors, secondary-derived human NSPC differentiation and proliferation, and rat NSPC oligodendrocyte differentiation

(A, E) Nestin$^+$ immuno-staining of proliferating human and rat NSPCs treated with EFH. (B, F) Nestin$^+$ immuno-staining of differentiating human and rat NSPCs treated with 1% FBS. (C, D) β-iii tubulin$^+$ and BrdU immuno-staining of differentiating secondary-derived human NSPCs treated with 1% FBS. (G) Passage 9 Rat NSPCs treated with 1% FBS differentiated mostly into O4$^+$ oligodendrocytes. Scale bar = 100 µm

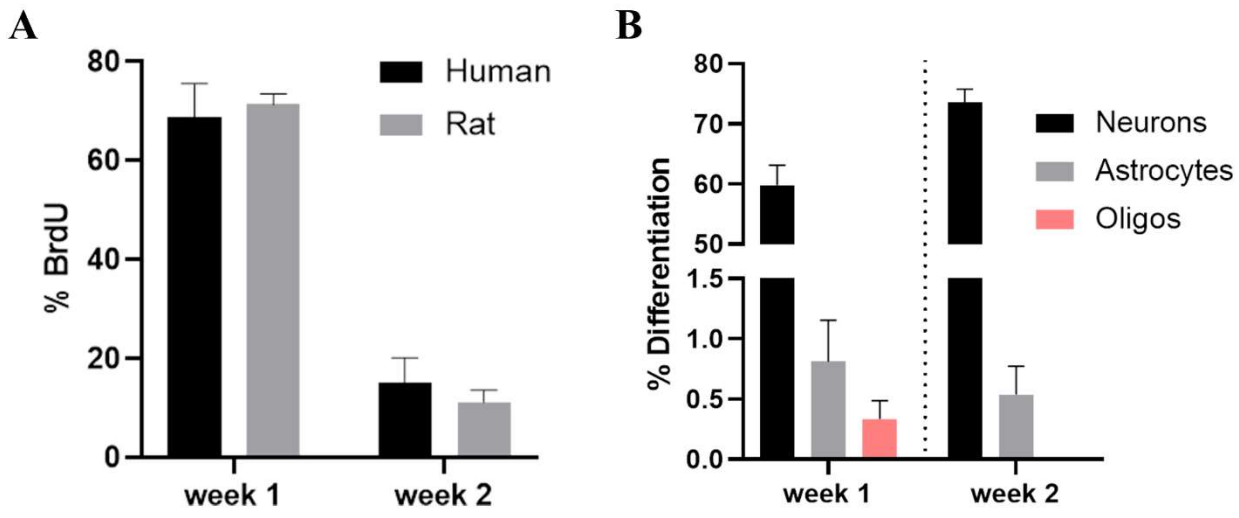

Figure S3.2 Human secondary-derived NSPCs have increased proliferation and a similar differentiation profile as primary-derived NSPCs

(A) Quantification of the percentage of $BrdU^+$ proliferating secondary-derived NSPCs in 1% FBS for one or two weeks. BrdU was administered within the last 24 hours of culture. (B) The percentage of β-iii $tubulin^+$ neurons, $GFAP^+$ astrocytes, and $O4^+$ oligodendrocytes from human secondary-derived NSPCs differentiated in 1% FBS for one or two weeks. n= 6 humans, 5 rats. Mean ± s.e.m.

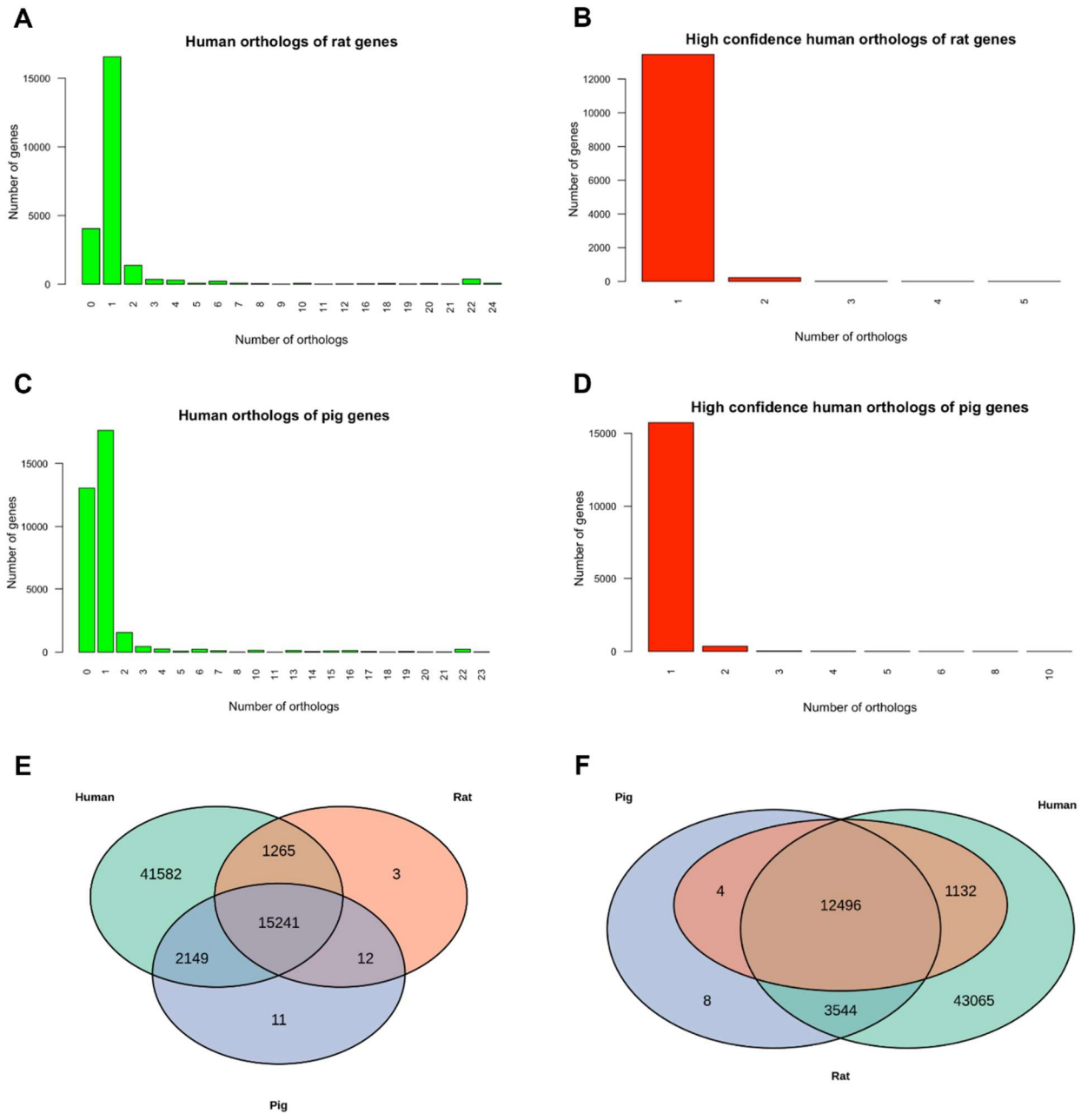

Figure S3.3 Number of total human orthologs and high-confidence human orthologs in pig and rat NSPCs

The IDs of human orthologs of the pig and rat NSPC genes were determined using the Ensembl database and assigned a confidence score of zero or one (high-confidence). (A) the total number of genes in rat NSPCs with the corresponding number of human orthologs. (B) the number of

genes in rat NSPCs with the corresponding number of high-confidence human orthologs. (C) the total number of genes in pig NSPCs with the corresponding number of human orthologs. (D) the number of genes in pig NSPCs with the corresponding number of high-confidence human orthologs. (E) Venn diagram showing the total number of orthologs and the orthologs in common between species. (F) Venn diagram showing the number of high-confidence orthologs and the high-confidence orthologs in common between species. n = 3 humans, pigs, rats.

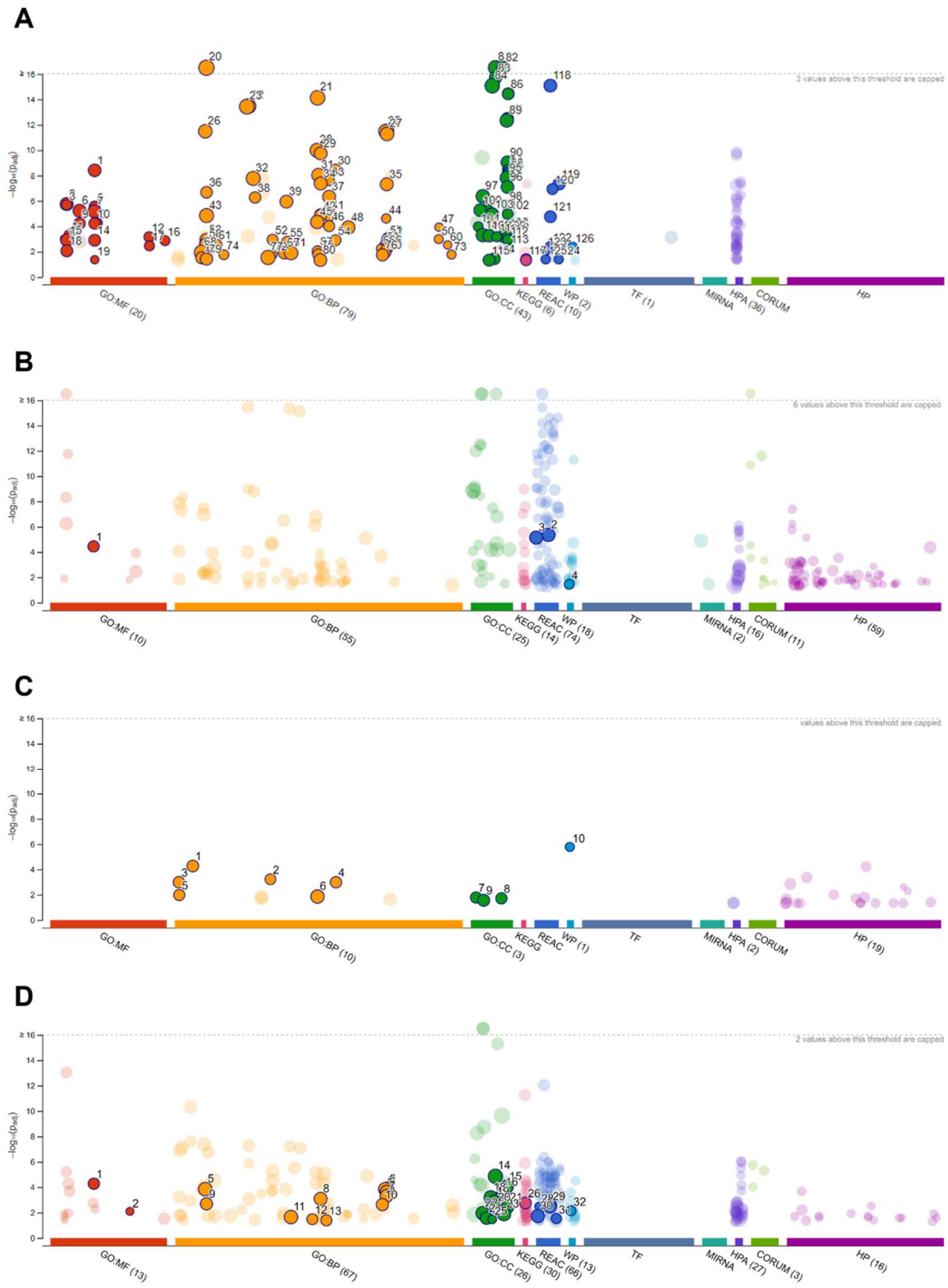

Figure S3.4 Functional enrichment analysis of DE genes between human, pig, and rat NSPCs

Gene set enrichment was analyzed using gProfiler for only the orthologs (15,241 genes) found in common among all species. Gene sets related to the CNS are shown to be (A) upregulated in rat NSPCs, (B) downregulated in rat NSPCs, (C) upregulated in pig NSPCs, and (D) downregulated in pig NSPCs. Bold numbered circles are gene sets that are DE with a $\log_2$FC greater than or less than two and a false discovery rate q-value<0.01. More information for each gene set can be seen in Table S1 and S2 in the order they are listed. n=3 humans, pigs, rats.

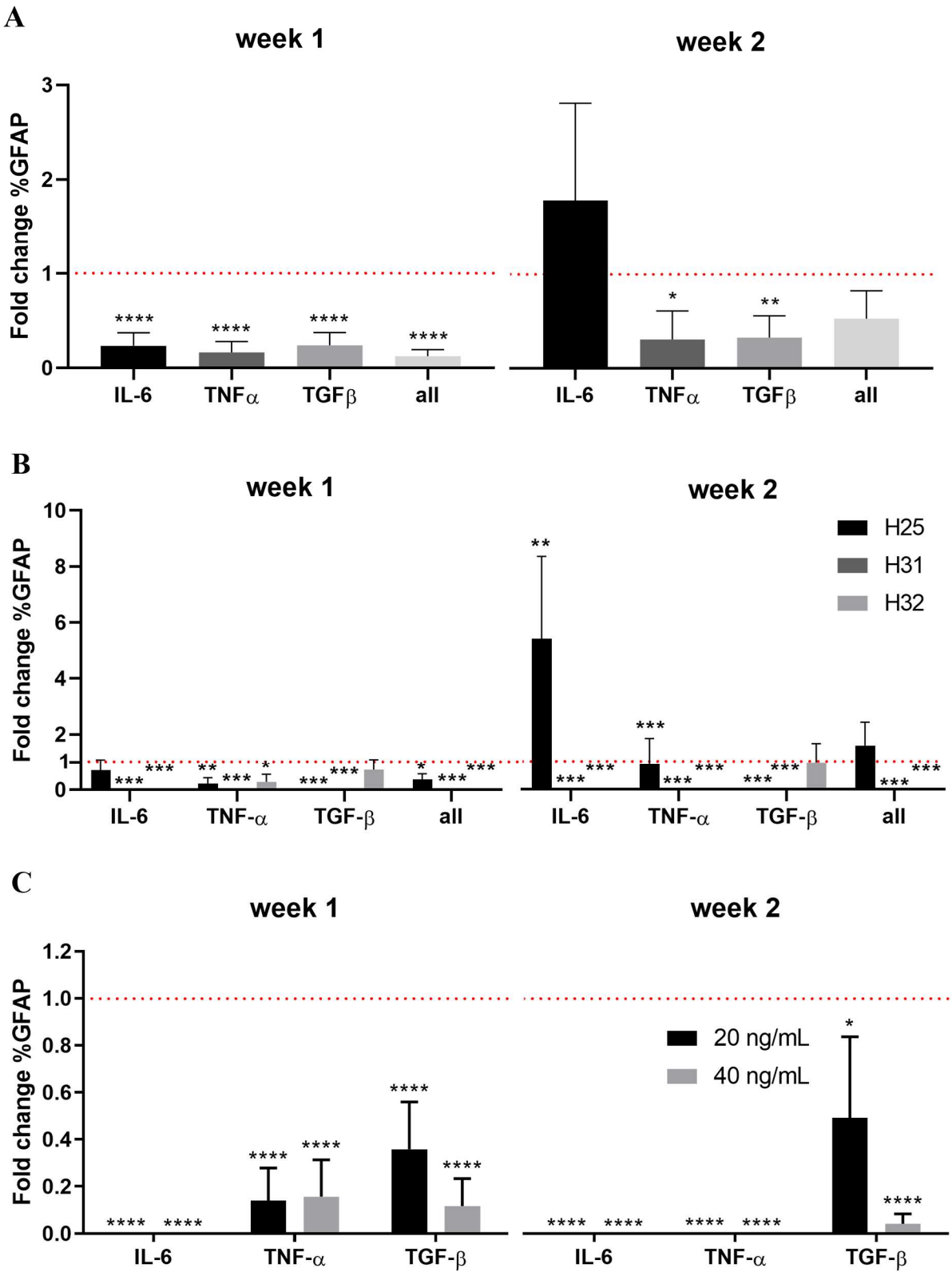
A
week 1
week 2
Fold change %GFAP
IL-6
TNFα
TGFβ
all
B
week 1
week 2
Fold change %GFAP
H25
H31
H32
IL-6
TNF-α
TGF-β
all
C
week 1
week 2
Fold change %GFAP
20 ng/mL
40 ng/mL
IL-6
TNF-α
TGF-β

Figure S3.5 Human NSPCs treated with inflammatory factors in combination or at higher concentrations does not induce astrocyte differentiation

(A) Quantification of the fold change in $GFAP^+$ astrocytes after one or two weeks of treatment with Il-6, TNFα, TGFβ, or all factors in combination (n=3). (B) The effect of inflammatory factor treatment for each donor (n=3 humans). (C) The fold change in $GFAP^+$ astrocytes after one or two weeks of treatment with Il-6, TNFα, and TGFβ at 20 ng/mL and 40 ng/mL each (n=2 humans). Mean ± s.e.m; *p<0.05, **p<0.01, ***p<0.001, ****p<0.0001 relative to control (SFM).

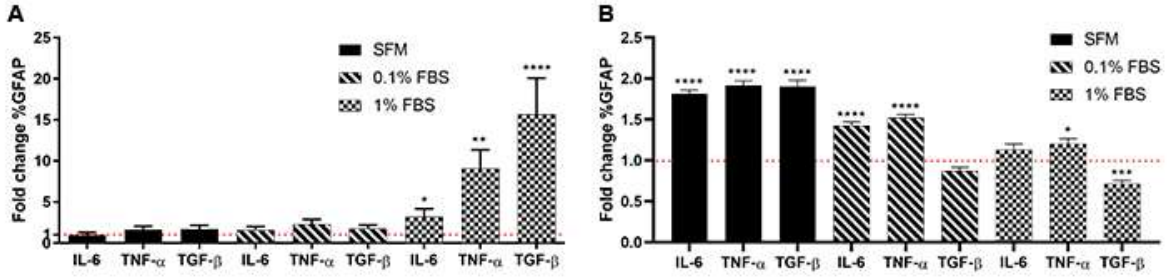

Figure S3.6 Reactive astrogliosis is induced in human and pig glia when treated with inflammatory factors in FBS and FBS-free media, respectively

Passage 3 glia were treated with Il-6, TNFα, or TGFβ in serum-free, 0.1% FBS, or 1% FBS media for four days. The fold change in $\%GFAP^+$ astrocytes was quantified for (A) Human glia (n=3 humans) and (B) pig glia (n=3 pigs). Mean ± s.e.m; *p<0.05, **p<0.01, ***p<0.001, ****p<0.0001 relative to the respective control (SFM, 0.1% FBS, or 1% FBS).

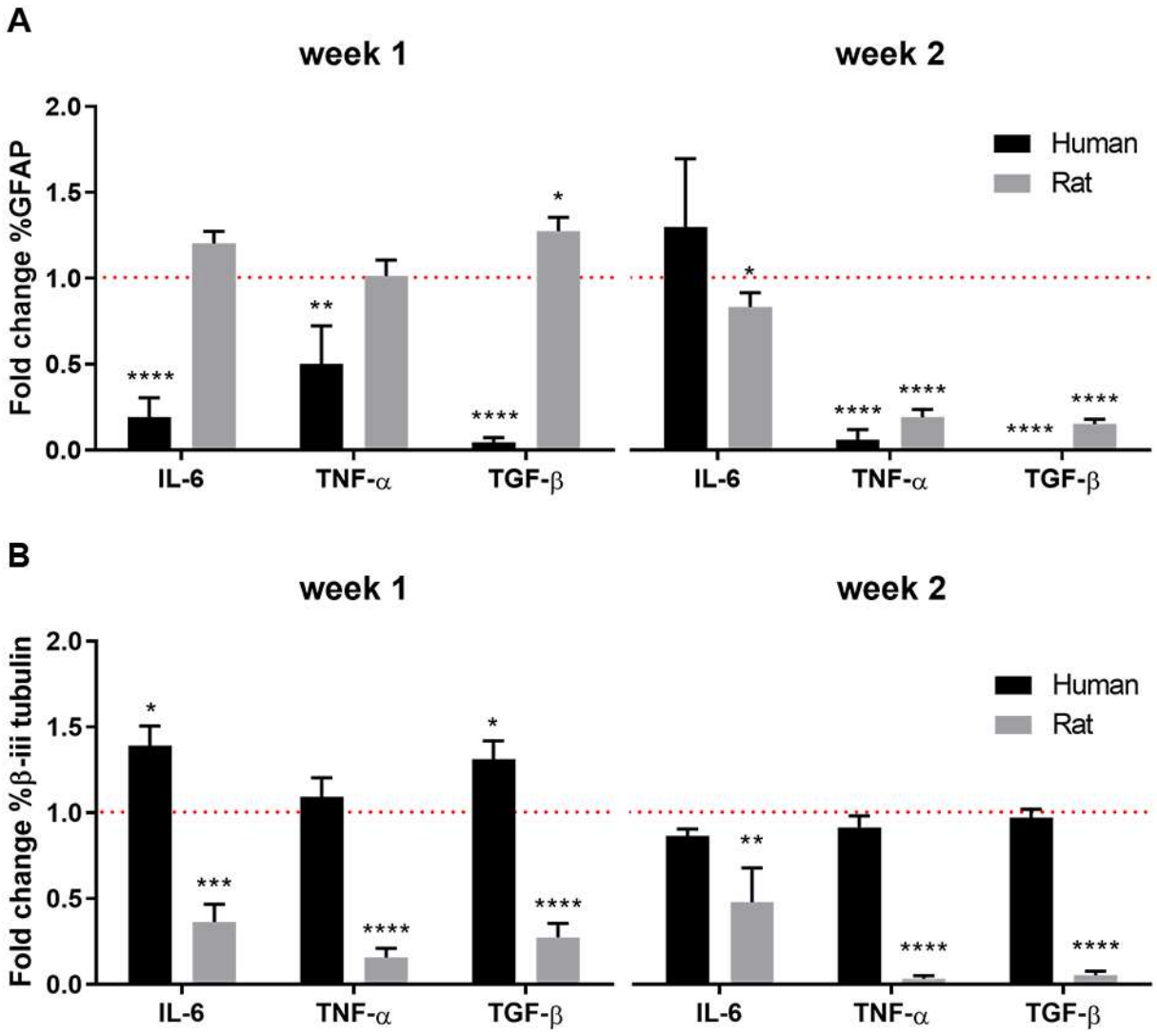

Figure S3.7 Human and rat NSPCs treated with inflammatory factors in 1% FBS mirror the responses in serum-free media

(A) Quantification of the fold change in $GFAP^+$ astrocytes of human and rat NSPCs after one or two weeks of treatment with Il-6, TNFα, and TGFβ in 1% FBS. (B) The fold change in $\beta iii\ tubulin^+$ neurons of human and rat NSPCs after one or two weeks of treatment with Il-6, TNFα, TGFβ in 1% FBS. n= 6 humans, 3 rats. Mean ± s.e.m; *p<0.05, **p<0.01, ***p<0.001, ****p<0.0001 relative to control (1% FBS).

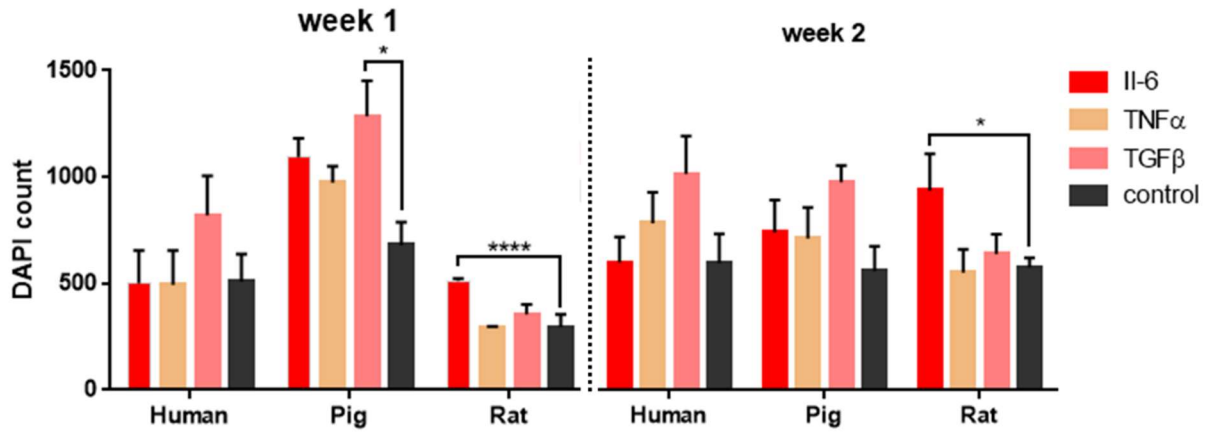

Figure S3.8 Pig NSPCs had the highest average cell count per picture at one week of inflammatory treatment

Ten non-biased images were captured for each well, and the total number of $DAPI^+$ cells was counted to determine the average cell count per picture, depicted on the Y-axis. n=8 humans, 5 pigs, 6 rats. Mean ± s.e.m; *p<0.05, ****p<0.0001

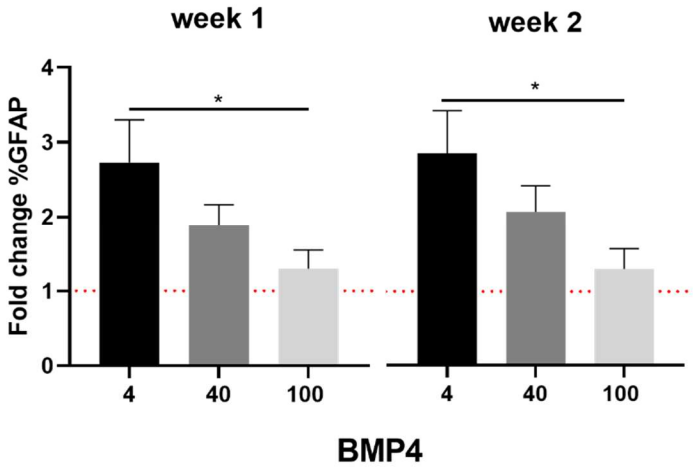

Figure S3.9 BMP4 promotes astrocyte differentiation of human NSPCs inversely proportional to its concentration

Primary-derived human NSPCs were treated with 4, 40, or 100 ng/mL of BMP4 for one or two weeks. The fold change in $GFAP^+$ astrocytes was quantified. n=5 humans. Mean ± s.e.m; *p<0.01 relative to control (SFM).

Table S3.1 Complete list of gene sets for terms related to the CNS that are upregulated or downregulated in pig NSPCs analyzed using gProfiler. The complete report can be accessed here for upregulated and downregulated gene sets. GO = gene ontology, MF = molecular function, BP = biological pathway, CC = cellular component, KEGG = Kyoto Encyclopedia of Genes and Genomes, REAC = Reactome, TF = transcription factor, WikiPathways

Upregulated in pig vs. human			Downregulated in pig vs. human		
Database	**Term**	**Adjusted p-value**	**Database**	**Term**	**Adjusted p-value**

GO:BP	cilium movement	5.37069E-05	GO:MF	growth factor binding	5.24E-05
GO:BP	axoneme assembly	0.000599789	GO:MF	platelet-derived growth factor binding	0.007967
GO:BP	cilium or flagellum-dependent cell motility	0.001032004	GO:BP	trans-synaptic signaling	0.000131
GO:BP	cilium-dependent cell motility	0.001032004	GO:BP	chemical synaptic transmission	0.000143
GO:BP	microtubule bundle formation	0.010431143	GO:BP	anterograde trans-synaptic signaling	0.000143
GO:BP	neuron projection morphogenesis	0.01380052	GO:BP	synaptic signaling	0.000241
GO:CC	axoneme	0.016438147	GO:BP	regulation of trans-synaptic signaling	0.000483
GO:CC	ciliary plasm	0.01941026	GO:BP	modulation of chemical synaptic transmission	0.000813
GO:CC	motile cilium	0.027496001	GO:BP	axon guidance	0.002029
WP	Dopaminergic neurogenesis	1.65837E-06	GO:BP	neuron projection guidance	0.002323

			GO:BP	regulation of ion transport	0.022406
			GO:BP	regulation of synapse organization	0.027311
			GO:BP	regulation of neurotransmitter secretion	0.03299
			GO:BP	cell morphogenesis involved in neuron differentiation	0.037167
			GO:BP	regulation of neurotransmitter transport	0.040952
			GO:BP	trans-synaptic signaling	0.000131
			GO:BP	chemical synaptic transmission	0.000143
			GO:BP	anterograde trans-synaptic signaling	0.000143
			GO:BP	synaptic signaling	0.000241
			GO:BP	regulation of trans-synaptic signaling	0.000483
			GO:BP	modulation of chemical synaptic transmission	0.000813

			GO:BP	regulation of synapse assembly	0.001809
			GO:BP	axon guidance	0.002029
			GO:BP	neuron projection guidance	0.002323
			GO:BP	regulation of synapse organization	0.027311
			GO:BP	regulation of neurotransmitter secretion	0.03299
			GO:BP	cell morphogenesis involved in neuron differentiation	0.037167
			GO:BP	regulation of neurotransmitter transport	0.040952
			GO:CC	synapse	1.37E-05
			GO:CC	postsynapse	9.23E-05
			GO:CC	synaptic membrane	0.000241
			GO:CC	dendritic spine	0.000621
			GO:CC	somatodendritic compartment	0.000657
			GO:CC	neuron spine	0.001169

			GO:CC	postsynaptic membrane	0.003682
			GO:CC	neuron to neuron synapse	0.003741
			GO:CC	dendrite	0.011114
			GO:CC	dendritic tree	0.013079
			GO:CC	synaptic cleft	0.033614
			GO:CC	synapse	1.37E-05
			REAC	Nervous system development	0.003011
			REAC	Ca2+ activated K+ channels	0.003144
			REAC	Neuronal System	0.003333
			REAC	Axon guidance	0.018557
			REAC	Signaling by PDGF	0.02913
			WP	Pluripotent stem cell differentiation pathway	7.077×10 -3

Table S3.2 Complete list of gene sets for terms related to the CNS that are upregulated or downregulated in rat NSPCs analyzed using gProfiler. The complete report can be accessed here for upregulated and downregulated gene sets. GO = gene ontology, MF = molecular function, BP = biological pathway, CC = cellular component, KEGG = Kyoto Encyclopedia of Genes and Genomes, REAC = Reactome, TF = transcription factor, WikiPathways

Upregulated in rat vs. human			Downregulated in rat vs. human		
Database	**Term**	**Adjusted p-value**	**Database**	**Term**	**Adjusted p-value**
GO:MF	gated channel activity	3.86E-09	GO:MF	growth factor binding	3.60E-05
GO:MF	ion channel activity	1.73E-06	GO:MF	platelet-derived growth factor binding	0.014958
GO:MF	extracellular ligand-gated ion channel activity	2.04E-06	REAC	Nervous system development	4.49E-06
GO:MF	transmitter-gated ion channel activity	2.64E-06	REAC	Axon guidance	7.19E-06
GO:MF	transmitter-gated channel activity	2.64E-06	REAC	Developmental Biology	0.004299
GO:MF	channel activity	5.87E-06	WP	Pluripotent stem cell differentiation pathway	0.035574
GO:MF	passive transmembrane transporter activity	6.49E-06			
GO:MF	neurotransmitter receptor activity	5.6E-05			
GO:MF	ligand-gated ion channel activity	5.91E-05			

GO:MF	ligand-gated channel activity	5.91E-05			
GO:MF	glutamate receptor activity	0.000441			
GO:MF	postsynaptic neurotransmitter receptor activity	0.000679			
GO:MF	ionotropic glutamate receptor activity	0.001017			
GO:MF	voltage-gated channel activity	0.001236			
GO:MF	cation channel activity	0.001237			
GO:MF	transmitter-gated ion channel activity involved in the regulation of postsynaptic membrane potential	0.001328			
GO:MF	neurotransmitter receptor activity involved in the regulation of	0.003385			

	postsynaptic membrane potential				
GO:MF	voltage-gated ion channel activity	0.008547			
GO:MF	GABA-gated chloride ion channel activity	0.042021			
GO:BP	nervous system development	6.74E-17			
GO:BP	generation of neurons	7.40E-15			
GO:BP	neuron differentiation	3.33E-14			
GO:BP	neurogenesis	3.67E-14			
GO:BP	trans-synaptic signaling	2.95E-12			
GO:BP	anterograde trans-synaptic signaling	3.22E-12			
GO:BP	chemical synaptic transmission	3.22E-12			
GO:BP	synaptic signaling	5.23E-12			
GO:BP	neuron development	1.02E-10			

GO:BP	synapse organization	1.79E-10			
GO:BP	regulation of postsynaptic membrane potential	3.45E-09			
GO:BP	neuron projection morphogenesis	9.06E-09			
GO:BP	neuron projection development	1.67E-08			
GO:BP	positive regulation of synapse assembly	2.44E-08			
GO:BP	modulation of chemical synaptic transmission	4.17E-08			
GO:BP	regulation of trans-synaptic signaling	4.82E-08			
GO:BP	synapse assembly	2.04E-07			
GO:BP	regulation of nervous system development	4.63E-07			
GO:BP	regulation of nervous system process	5.29E-07			

GO:BP	regulation of membrane potential	1.12E-06			
GO:BP	regulation of synapse structure or activity	1.22E-05			
GO:BP	positive regulation of nervous system development	1.3E-05			
GO:BP	regulation of synapse organization	1.34E-05			
GO:BP	central nervous system development	1.41E-05			
GO:BP	postsynapse assembly	2.38E-05			
GO:BP	cell morphogenesis involved in neuron differentiation	4.47E-05			
GO:BP	regulation of synapse assembly	9.65E-05			
GO:BP	regulation of excitatory synapse assembly	0.000116			

GO:BP	axon development	0.000121			
GO:BP	synaptic membrane adhesion	0.000764			
GO:BP	excitatory synapse assembly	0.001008			
GO:BP	chemical synaptic transmission, postsynaptic	0.001034			
GO:BP	synaptic transmission, glutamatergic	0.001117			
GO:BP	axonogenesis	0.001146			
GO:BP	excitatory postsynaptic potential	0.001246			
GO:BP	myelination	0.001678			
GO:BP	ensheathment of neurons	0.002377			
GO:BP	axon ensheathment	0.002377			
GO:BP	brain development	0.002679			
GO:BP	postsynaptic specialization assembly	0.002802			

GO:BP	regulation of postsynaptic density organization	0.002891			
GO:BP	glial cell differentiation	0.002935			
GO:BP	modulation of excitatory postsynaptic potential	0.004499			
GO:BP	regulation of postsynaptic density assembly	0.005107			
GO:BP	regulation of neurotransmitter receptor activity	0.005179			
GO:BP	postsynaptic density assembly	0.005506			
GO:BP	regulation of postsynapse organization	0.00601			
GO:BP	oligodendrocyte differentiation	0.009129			
GO:BP	ion transport	0.011383			

GO:BP	gliogenesis	0.011892			
GO:BP	regulation of postsynaptic specialization assembly	0.012535			
GO:BP	regulation of ion transport	0.012568			
GO:BP	ionotropic glutamate receptor signaling pathway	0.016611			
GO:BP	ligand-gated ion channel signaling pathway	0.016611			
GO:BP	dendrite morphogenesis	0.016794			
GO:BP	oligodendrocyte development	0.017213			
GO:BP	neuron projection guidance	0.017798			
GO:BP	ion transmembrane transport	0.027951			
GO:BP	neurotransmitter transport	0.029845			

GO:BP	axon guidance	0.037122			
GO:BP	regulation of neurogenesis	0.045373			
GO:CC	synapse	5.18E-20			
GO:CC	synaptic membrane	4.84E-17			
GO:CC	postsynaptic membrane	1.94E-16			
GO:CC	neuron projection	8.37E-16			
GO:CC	integral component of synaptic membrane	3.55E-15			
GO:CC	intrinsic component of synaptic membrane	3.61E-15			
GO:CC	intrinsic component of postsynaptic membrane	3.02E-13			
GO:CC	integral component of postsynaptic membrane	3.19E-13			
GO:CC	postsynapse	4.50E-13			
GO:CC	glutamatergic synapse	8.93E-10			

GO:CC	integral component of postsynaptic specialization membrane	3.64E-09			
GO:CC	postsynaptic specialization membrane	5.60E-09			
GO:CC	postsynaptic specialization	9.18E-09			
GO:CC	presynapse	1.47E-08			
GO:CC	intrinsic component of postsynaptic specialization membrane	1.72E-08			
GO:CC	neuron to neuron synapse	7.96E-08			
GO:CC	axon	4.20E-07			
GO:CC	intrinsic component of presynaptic membrane	2.26E-06			
GO:CC	asymmetric synapse	5.21E-06			
GO:CC	postsynaptic density	5.31E-06			

GO:CC	presynaptic membrane	9.99E-06			
GO:CC	integral component of presynaptic membrane	1.06E-05			
GO:CC	neuronal cell body	1.18E-05			
GO:CC	ionotropic glutamate receptor complex	0.000105			
GO:CC	postsynaptic density membrane	0.000234			
GO:CC	GABA-ergic synapse	0.000304			
GO:CC	dendrite	0.000488			
GO:CC	ion channel complex	0.000551			
GO:CC	dendritic tree	0.000581			
GO:CC	excitatory synapse	0.000659			
GO:CC	neurotransmitter receptor complex	0.000689			
GO:CC	integral component of postsynaptic density membrane	0.001124			

GO:CC	intrinsic component of postsynaptic density membrane	0.005381			
GO:CC	neuron spine	0.035484			
GO:CC	cation channel complex	0.045738			
KEGG	GABAergic synapse	0.038416			
KEGG	Glutamatergic synapse	0.04643			
REAC	Neuronal System	8.10E-16			
REAC	Transmission across Chemical Synapses	4.48E-08			
REAC	Protein-protein interactions at synapses	1.15E-07			
REAC	Neurotransmitter receptors and postsynaptic signal transmission	1.74E-05			
REAC	Neurexins and neuroligins	0.003949			
REAC	GABA receptor activation	0.007908			

REAC	Trafficking of AMPA receptors	0.039697			
REAC	Glutamate binding, activation of AMPA receptors, and synaptic plasticity	0.039697			
WP	GABA receptor signaling	0.004077			

Chapter 4: Isogenic NSPCs Derived from the Adult Human Spinal Cord and Pluripotent Stem Cells Exhibit Distinct Functional and Transcriptional Signatures

4.1 Abstract

Induced pluripotent stem cells (iPSCs) have enabled the unprecedented genesis and use of neural stem/progenitor cells (NSPCs) for treating spinal cord injury (SCI). However, the molecular and functional homology between iPSC-derived NSPCs and bona fide spinal cord NSPCs is unknown. We now report the first characterization of bona fide spinal cord NSPCs compared to isogenic iPSC-derived NSPCs that have been regionalized to the spinal cord (iPSC-SC) and brain (iPSC-Br). We used RNA-Seq and *in vitro* assays to demonstrate that bona fide NSPCs exhibit distinct functional and transcriptional phenotypes relative to iPSC-SC and -Br NSPCs. Bona fide and iPSC-SC NSPCs portrayed a spinal cord regionalization, while iPSC-Br NSPCs portrayed a dorsal forebrain regionalization. Relative to bona fide NSPCs, both iPSC-derived NSPCs exhibited functional and transcriptional properties of early developmental stages, including embryonic patterning genes and greater proliferation rates. The differentiation profiles were most alike between bona fide and iPSC-Br NSPCs and dissimilar between bona fide and iPSC-SC NSPCs, possibly due to the prolonged development of iPSC-SC NSPCs that involves neuromesodermal progenitors. Thus, we demonstrate distinct regional, developmental, and functional phenotypes between bona fide spinal cord NSPCs and iPSC-derived NSPCs. If these differences are reconciled, the clinical success of iPSC-derived NSPC therapies for SCI may be improved.

4.2 Introduction

The transplant of NSPCs into the injured spinal cord has been a highly pursued strategy to promote regeneration and repair (Assinck et al., 2017; Gazdic et al., 2018; Yousefifard et al., 2016). Transplanted NSPCs can differentiate into neurons, oligodendrocytes, and astrocytes, with each

cell type capable of mediating regeneration in the forms of neuronal relays, remyelination, and secretion of trophic factors (de Freria et al., 2021; Mortazavi et al., 2015; Yamazaki et al., 2020; Yuan et al., 2016). However, the translation of this strategy has been hampered due to ethical and technical concerns with the acquisition of human NSPCs for transplant (Chhabra & Sarda, 2017b; Trounson & McDonald, 2015). Fortunately, advances in cellular reprogramming have enabled researchers to create human NSPCs that are devoid of the previous ethical and technical challenges associated with using embryonic and patient-derived tissue (Galiakberova & Dashinimaev, 2020; Xie, Tang, Li, & Ding, 2017). Through genetic, epigenetic, and/or proteomic interventions, somatic cells such as fibroblasts can be reprogrammed and undergo phenotypic changes to resemble NSPCs (G. Chen et al., 2011; Seo et al., 2017; Steinle et al., 2019). Furthermore, reprogrammed NSPCs can be generated in a patient-autologous manner to reduce the chance of graft rejection.

A standard method of generating reprogrammed human NSPCs first involves creating induced pluripotent stem cells (iPSCs) (Bordoni, Fantini, Pansarasa, & Cereda, 2018; K. Takahashi & Yamanaka, 2006a). iPSCs are embryonic-like stem cells with the potential to self-renew indefinitely and form all three germ layers, thus providing a scalable method of generating human NSPCs (Bordoni et al., 2018). The transplant of iPSC-derived NSPCs for SCI repair has gathered tremendous pre-clinical evidence that has led to the implementation of clinical trials for the first time since iPSC-technology was developed (Nagoshi et al., 2019; Sugai et al., 2021). However, several vital considerations are yet to be determined for the optimal use of iPSC-derived NSPCs in a clinical setting (Iida et al., 2018). One such consideration is the nature of the iPSC-derived NSPCs being used (Kadoya et al., 2016). This is because various differentiation protocols exist for generating iPSC-derived NSPCs, with each population possessing unique functional and

molecular attributes (Galiakberova & Dashinimaev, 2020). Furthermore, the differentiation of iPSC-derived NSPCs can suffer from reproducibility issues due to inherited genetic variation among humans (S. M. Kim et al., 2016; Strano, Tuck, Stubbs, & Livesey, 2020b). As such, there is debate about which differentiation protocol can reproducibly generate iPSC-derived NSPCs that would be most effective for SCI repair.

To answer this question, studies in animal models have transplanted different regionalized NSPCs, including the spinal cord and brain (Kadoya et al., 2016; Kajikawa et al., 2020; S. Karimi-Abdolrezaee et al., 2010; Soheila Karimi-Abdolrezaee et al., 2006; Kumamaru, Kadoya, et al., 2018). In a side-by-side comparison, NSPCs obtained from the spinal cord have consistently out-performed NSPCs from the brain in promoting neurological and functional improvement following SCI (Kadoya et al., 2016; Kumamaru, Kadoya et al., 2018). Similarly, iPSCs or embryonic stem cells differentiated into NSPCs with a spinal cord phenotype have produced better outcomes than NSPCs with a brain phenotype (Kadoya et al., 2016; Kajikawa et al., 2020; Kumamaru, Kadoya et al., 2018). This is likely due to the ability of spinal cord NSPCs to differentiate into phenotypically appropriate neurons of the spinal cord and integrate with the local neuroanatomy (Ceto et al., 2020; Kumamaru, Lu, Rosenzweig, Kadoya, & Tuszynski, 2019). This suggests that iPSC differentiation protocols should produce NSPCs resembling bona fide spinal cord NSPCs for effective SCI repair. Yet, no reports in the literature indicate that iPSC-SC NSPCs phenocopy bona fide spinal cord NSPCs from adult humans at the molecular or functional level.

We address this gap in our study by differentiating patient-derived iPSCs into NSPCs bearing either a spinal cord (iPSC-SC) or dorsal forebrain identity (iPSC-Br) (Chambers et al., 2009; Kumamaru, Kadoya, et al., 2018). Moreover, we characterized primary bona fide spinal cord NSPCs from the same patient, thus establishing an isogeneic comparison between the three NSPC

types. Using RNA-sequencing and *in vitro* functional assays, we characterized the transcriptome, proliferation, and differentiation profiles of NSPCs. By comparing the three NSPC types, we could distinguish NSPCs based on their regional, developmental, and functional signatures. By comparing the same NSPC type across patients, we were able to evaluate the reproducibility of the iPSC-differentiation protocols and correlate the transcriptome profile to specific differentiation trends. In doing so, this is the first study to establish a direct comparison of isogeneic NSPCs derived from the adult human spinal cord and iPSCs.

4.3 Methods

4.3.1 Ethics statement

For harvesting human spinal cord and skin tissue, ethics approval for the study was obtained from the Ottawa Health Science Network Research Ethics Board and the Trillium-Gift of Life Network (TGLN), which oversees organ donation in Ontario. Patients were identified to study personnel after neurologic determination of death (NDD) was assessed by TGLN. Informed written consent was obtained from the family of the deceased organ donor for tissue collection. More information related to the subjects can be found in Table 4.1.

4.3.2 Spinal cord harvest and primary NSPC culture

Human spinal cords were harvested using an anterior approach, according to Galuta et al. (2020). Briefly, the spinal cord was exposed from the surrounding tissues and organs, and then transverse cuts were made at the L2 level of the spinal cord and at the most rostral level. Using a sternal saw angled 45° medially, transverse cuts were made in a caudal to rostral direction on both lateral sides of the spinal cord to remove the vertebral bodies.

The harvested spinal cord was placed in cold, sterile dissection media: 1X Hank' Balanced Salt Solution (HBSS)+ 0.6% D-glucose + 2% penicillin-streptomycin (PS) and processed immediately for micro-dissection. The central canal region was excised under a dissection microscope, leaving out contaminant surrounding grey and white matter, then dissociated using a papain dissociation kit according to the manufacturer's instructions.

Following purification, cells were re-suspended in a serum-free media (SFM), which consisted of: Neurobasal-A medium, 2 mM L-glutamine, 1% PS, 1% B27-vitamin A, and 10% hormone mix (1:1 DMEM/F12, 0.6% glucose, 3 mM $NaHCO_3$, 5 mM HEPES, 25 µg/mL insulin, 100 µg/mL apo-transferrin, 10 µM putrescine, 30 nM selenium, and 20 nM progesterone in distilled water). Cells were seeded at 20 cells/µL onto Matrigel-coated six-well plates in a total of 4 mL of proliferation media (1X EFH): SFM + 20 ng/mL human epidermal growth factor (EGF) + 20 ng/mL human basic fibroblast growth factor (FGF2) + 2 µg/mL heparin and incubated at 37˚C, 5% CO_2, 20% O_2 for one week undisturbed. Cultures were fed every 2-3 days for 1-2 weeks by replacing half the culture medium with an equivalent amount of 2X EFH. Once adherent cultures were visibly expanding, cultures were fed by replacing the full media with 2 mL of 1X EFH. Cultures were fed this way until confluency was attained.

4.3.3 Skin harvest and primary fibroblast culture

Human skin tissue samples were harvested in the operating room under sterile conditions. A 2 cm x 2 cm full thickness elliptical sample from the periumbilical region was excised, placed in a cold, sterile HBSS solution on ice, and transported to the lab. The skin tissue was transferred to a petri dish in a biohood for dissection. Using forceps to grip the tissue, any subcutaneous fat was removed using scissors. A 0.5 cm x 0.5 cm piece of the dermis layer was excised using scissors or a scalpel. The excised dermal chunks were transferred to a 1.5 mL microcentrifuge tube and cut into smaller

pieces using micro-scissors. The minced tissue was transferred into a sterile 30 mL beaker containing a magnetic stirrer and DMEM/F12 media (Gibco^{TM}, 11320033) with 0.14 Wunsch units/mL of Liberase Blendzyme 3 (Millipore Sigma, #5401020001) and 1% PS. The beaker was covered in foil, placed on a magnetic hot plate, and heated at 37°C for 60 minutes.

Following enzymatic digestion, the media containing dermal tissue was transferred to a 50 mL conical tube, and 25 mL of fibroblast media (FM): 10% FBS and 1% P-S in DMEM/F12 was added. The solution was triturated forcefully using a 10 mL serological pipette and then centrifuged at 300 xg for 5 minutes. The supernatant was removed, and cells were resuspended in 10 mL of FM. The resuspended solution was then filtered through a 40 μm mesh and plated in a tissue culture-treated T75 flask (VWR, 10062-862). Primary fibroblasts were allowed to adhere and expand for one week, and then the complete media was aspirated and replaced with 10 mL of fresh FM. Cultures were fed every 2-3 days until ~80% confluency was attained. At this point, cultures were passaged by aspirating the media, and 3.5 mL of TrypLE^{TM} Express (Gibco^{TM}, 12604013) was added. Cultures were incubated for 5 minutes at 37 °C, and 10 mL of FM was added to the flask to inactivate TrypLE. The cell suspension was transferred to a 15 mL tube and centrifuged at 300 xg for 5 minutes. The supernatant was aspirated, and cells were resuspended in 1 mL of FM for cell counting. Cells were seeded at 10 cells/μL in T75 flasks and fed with FM every 2-3 days. Once cells attained ~80% confluency, they were passaged and used for electroporation, and the remaining cells were frozen.

4.3.4 iPSC reprogramming from dermal fibroblasts

Fibroblasts were reprogrammed into iPSCs by episomal transfection. Specifically, secondary fibroblasts were pre-treated with 0.167 mg/mL valproic acid (Millipore Sigma, P4543) for 2 hours and then passaged. $5x10^5$ cells were transferred to a 15 mL conical tube and centrifuged at 300 xg

for 5 minutes. The cells were resuspended in 0.5 mL of DMEM/F12 and transferred to an electroporation cuvette (Bio-Rad, 1652088). The following plasmids were added to the cell suspension at a concentration of 20 µg/mL per plasmid: pCXLE-Oct3/4 (Addgene, 27077), pCXLE-hsk (Addgene, 27078), pCXLE-hµl (Addgene, 27080). To optimize plasmid concentration, a pCE-GFP plasmid (Addgene, 41858) was used to express GFP in transfected cells. The cell suspension was electroporated (Bio-Rad Gene Pulser Xcell Total Electroporation System, 1652660) with two pulses lasting 20 ms each at 200V. The cells were diluted to 6 mL in 10% FBS in DMEM/F12 and distributed into three wells of a 6-well plate coated with Matrigel. The media was replaced with fresh 10% FBS in DMEM/F12 without antibiotics for the next two days. Starting day three of post-electroporation, the media was replaced with TeSR™-E7™ (STEMCELL Technologies, 05914) and fed every day for 21-28 days. iPSC colonies started to emerge within 3-4 weeks of feeding with TeSR™-E7™ and passaged according to the steps outlined in section 4.3.5

4.3.5 iPSC primary culture, propagation, and freezing

Primary iPSCs were manually passaged into a new 6-well plate coated with Matrigel. Using a yellow (20-200 µL) pipette tip, fibroblasts surrounding iPSC colonies were scraped away, ensuring that iPSC colonies remained intact. The media was aspirated and replaced with warm TeSR™-E8™ media (STEMCELL Technologies, 05990). Using a sterile 22-gauge needle, horizontal and vertical cuts were made into iPSC colonies. The iPSC aggregates from one colony were transferred using a yellow pipette tip to a single well of a 6-well plate containing 2 mL of TeSR™-E8™ media. This process was repeated for each primary iPSC colony, placing cells from different colonies into separate wells. Once all iPSC colonies were manually passaged, the 6-well plate was rocked back and forth to disperse the colonies and then incubated at 37 °C.

Secondary iPSC cultures were fed daily with fresh, warm TeSRTM-E8TM media for 5-7 days. Once iPSCs reached confluency, they were passaged into new wells using ReLeSR™ (STEMCELL Technologies, 05872) according to the manufacturer's instructions. Briefly, media from the well was aspirated, and 1 mL of ReLeSR™ was added. Following a 1-minute incubation, 75% of the ReLeSR™ was removed, and the cultures were incubated at 37 °C for 6-8 minutes. 1 mL of TeSR™-E8™ media was added to each well, and plates were knocked on the side for 30 seconds to lift iPSC colonies. The media containing the lifted colonies were transferred using a 2 mL serological pipette to a 15 mL conical tube. iPSCs were diluted 1:10-1:50 in TeSR™-E8™ media and transferred to a new well of a 6-well plate. The plate was rocked back and forth to disperse the colonies and then incubated at 37 °C. The remaining excess iPSCs were centrifuged and resuspended in mFreSR™ (STEMCELL Technologies, 05855). 1 mL of mFreSR™ was added for each well of a 6-well plate. The iPSCs were transferred to cryovials and frozen overnight at -80 °C in a Mr. Frosty™ Freezing Container (Fisher Scientific™, 5100-0001) and then transferred to liquid nitrogen for long-term storage.

Tertiary iPSCs were fed with TeSR™-E8™ media daily for 5-7 days. However, only high-quality iPSC colonies were passaged onwards. High-quality iPSC colonies were morphologically determined by size, clearly defined boundaries, minimal spontaneous differentiation, and tightly bound iPSCs with large nuclei (Figure 4.1). The top 3 iPSC colonies were passaged five times and then differentiated into regionalized spinal cord or brain NSPCs.

4.3.6 Generation and differentiation of iPSC-derived brain NSPCs

Passage five iPSCs derived from a single colony were differentiated into dorsal forebrain-regionalized NSPCs using the dual-SMAD inhibition protocol (Chambers et al., 2009). First, iPSC colonies to be passaged had surrounding differentiated cells scraped away using a yellow pipette

tip. The wells were aspirated and washed with PBS. iPSCs were then passaged into single cells using Accutase for 5 minutes. The wells were washed with knockout™ DMEM/F12 (Gibco™, 12660012), and the cell suspension was transferred to a 15 mL conical tube and centrifuged at 300 xg for 5 minutes. The iPSCs were resuspended in 1 mL of TeSR™-E8™ media for cell counting. iPSCs were transferred to an appropriate volume of STEMdiff™ Neural Induction Media (STEMCELL Technologies, 08581) containing 10 μM of Y-27632 (STEMCELL Technologies, 73802) at a concentration of 1000 cells/μL and seeded onto Matrigel-coated 6-well plates with 2 mL per well. The plates were rocked back and forth and incubated at 37 °C.

iPSC-derived Brain (iPSC-Br) NSPCs were fed daily with fresh STEMdiff™ Neural Induction Media for seven days. On day seven, iPSC-Br NSPCs were passaged using Accutase and seeded in Matrigel-coated 6-well plates at 100 cells/μL in STEMdiff™ Neural Induction Media containing 10 μM of Y-27632. Secondary iPSC-Br NSPCs were fed daily with fresh STEMdiff™ Neural Induction Media for seven days and then passaged similarly to primary iPSC-Br NSPCs. Tertiary iPSC-Br NSPCs were fed daily with fresh STEMdiff™ Neural Induction Media for seven days and then passaged similarly to primary iPSC-Br NSPCs. During the passage of tertiary iPSC-Br NSPCs, cells were seeded into a Matrigel-coated 6-well plate at 20 cells/μL in STEMdiff™ Neural Progenitor Medium (STEMCELL Technologies, 05833) containing 10 μM of Y-27632. At this stage, iPSC-Br NSPCs are expected to fully develop into a dorsal forebrain phenotype. iPSC-Br NSPCs were fed daily with STEMdiff™ Neural Progenitor Medium for seven days and then passaged for assessment of differentiation and proliferation (section 4.3.8) or RNA sequencing (section 4.3.11). During each passage of iPSC-Br NSPCs, excess cells were centrifuged and resuspended in STEMdiff™ Neural Progenitor Freezing Medium (STEMCELL Technologies, 05838) at a concentration of $1x10^6$ cells/mL. Resuspended cells were transferred to cryovials and

frozen overnight at -80 °C in a Mr. Frosty™ Freezing Container, then moved to liquid nitrogen for long-term storage.

4.3.7 Generation and differentiation of iPSC-derived spinal cord NSPCs

The same iPSC line that was used to differentiate into iPSC-Br NSPCs was also used for differentiation into iPSC-derived spinal cord (iPSC-SC) NSPCs using a protocol developed by Kumamaru et al. (2018). Passage five iPSCs were dissociated into single cells using Accutase and resuspended in 1 mL of Neural Induction Media (NIM), which consists of: N2B27 media (47.5% knockout™ DMEM/F12, 47.5% Neurobasal-A medium, 1% P-S, 1% L-glutamine, 1% N2 (Gibco™, 17502001), 2% B27-vitamin A) supplemented with 100 nM LDN-193189 (BioGems, 1066208), 10 µM SB-431542 (BioGems, 3014193), 4 µM CHIR-99021 (BioGems, 2520691), 10 µM DAPT (BioGems, 2088055), 100 ng/mL FGF2 (PeproTech, 100-18B), 100 ng/mL FGF8b (PeproTech, 100-25), and 0.36 U/mL heparin (Millipore Sigma, H3149). iPSCs were counted and diluted in an appropriate volume of NIM containing 10 µM of Y-27632 at a cell density of 100 cells/µL, then seeded into a Matrigel-coated 6-well plate. Cells were fed daily with fresh NIM for five days and then passaged into another Matrigel-coated 6-well plate at a cell density of 100 cells/µL in NIM containing 10 µM of Y-27632. Cells were fed daily with fresh NIM for another five days.

After ten days of feeding with NIM, iPSC-SC NSPCs were passaged and resuspended in 1 mL of Neural Maintenance Media (NMM), consisting of N2B27 media supplemented with 2 µM SB-431542, 3 µM CHIR-99021, and 200 nM Hh-Ag1.5 (BioVision, B2160). iPSC-SC NSPCs were counted and diluted in an appropriate volume of NMM containing 10 µM of Y-27632 at a cell density of 20 cells/µL, then seeded into a Matrigel-coated 6-well plate. iPSC-SC NSPCs were fed daily with fresh NMM for 18 days and passaged whenever confluency was attained. On day 28,

iPSC-SC NSPCs were passaged and used for assessment of differentiation and proliferation (section 4.3.8) or RNA sequencing (section 4.3.11). During each passage of iPSC-SC NSPCs, excess cells were centrifuged and resuspended in STEMdiff™ Neural Progenitor Freezing Medium at a concentration of $1x10^6$ cells/mL. Resuspended cells were transferred to cryovials and frozen overnight at -80 °C in a Mr. Frosty™ Freezing Container, then moved to liquid nitrogen for long-term storage.

4.3.8 Assessment of NSPC differentiation and proliferation

iPSC-SC and -Br NSPCs cultured for 28 days were used for differentiation and proliferation assessments. On day 28, iPSC-derived NSPCs were passaged using Accutase and resuspended in 1 mL of their respective proliferation media (STEMdiff™ Neural Progenitor Medium for iPSC-Br NSPCs and NMM for iPSC-SC NSPCs) for cell counting. iPSC-derived NSPCs were seeded into 96-well plates at a cell density of 5 cells/µL in their respective proliferation media containing 10 µM of Y-27632. For the next two days, iPSC-derived NSPCs were fed daily with their respective proliferation media to allow cells to adhere and proliferate. On day three, iPSC-derived NSPCs had their media replaced with the appropriate conditions to induce proliferation or differentiation.

For proliferation assessment, iPSC-derived NSPCs were fed daily with EFH. For differentiation assessment, iPSC-derived NSPCs were treated with two different media compositions. iPSC-Br NSPCs were fed with either (1) BrainPhys™ Neuronal Media (STEMCELL Technologies, 05790) supplemented with 2% SM1 (STEMCELL Technologies, 05792), 1% N2, 20 ng/mL BDNF (PeproTech, 450-02), 20 ng/mL GDNF (PeproTech, 450-10), 200 nM Ascorbic acid (STEMCELL Technologies, 72132), and 1 mM dibutyryl-cAMP (STEMCELL Technologies, 73882) or (2) SFM supplemented with 1% FBS. iPSC-SC NSPCs were fed with either (1) N2B27 media supplemented

with 200 nM Ascorbic acid and 1 mM dibutyryl-cAMP or (2) SFM supplemented with 1% FBS. Condition (1) was used as a positive control for differentiation, while condition (2) was used to directly compare the differentiation of iPSC-derived NSPCs with primary bona fide NSPCs. iPSC-derived NSPCs fed with differentiation media had their media replaced with fresh media every 2-3 days. The proliferation and differentiation assessment lasted for either one or two weeks, then fixed with 4% paraformaldehyde (PFA) and characterized by immunocytochemistry (section 4.3.9). Cultures had 10 μM BrdU added 24 hours before being fixed.

4.3.9 Immunocytochemistry

Fixed cultures were blocked with 10% normal goat serum (NGS) and permeabilized with 0.3% Triton-X in PBS for 30 minutes at room temperature. Wells that were stained for O4 were only blocked and not permeabilized. Cultures were washed three times with PBS, then incubated with respective primary antibodies with 10% NGS in PBS overnight at 4 ºC.

The following antibodies were used: mouse anti-O4 IgM (1:500) (Novus Biologicals, MAB1326) to label oligodendrocytes, mouse anti-β-iii tubulin IgG (1:500) (STEMCELL Technologies, 01409) (SantaCruz, 80005) to label immature neurons, rabbit anti-GFAP (1:1000) IgG (EMD Millipore, Ab5804) to label astrocytes, mouse anti-Nestin (10C2) IgG (1:500) (SantaCruz, 23927) to label progenitor cells, mouse anti-Pax6 IgG (1:500) (SantaCruz, 53108) and rabbit anti-Sox2 IgG (1:1000) (Abcam, ab97959) to label neural stem cells, mouse anti-BrdU IgG (1:2000) (EMD Millipore, MAB4072) as a marker of proliferation, and rabbit anti-Nanog IgG (1:200) (Cell Signalling Technology, 4903) and mouse anti-Oct3/4 IgG (1:400) (BD Biosciences, 611203) to label iPSCs.

The following day, cultures were washed three times with PBS and incubated with respective species-matched secondary conjugated antibodies in PBS for 2 hours at room temperature. The following secondary antibodies were used: goat anti-mouse IgG Alexa Fluor 488 (1:300) (Abcam, Ab150113), goat anti-rabbit IgG Alexa Fluor 488 (1:500) (Abcam, Ab150077), goat anti-mouse IgG Alexa Fluor 594 (1:300) (Abcam, ab150116), goat anti-rabbit IgG Alexa Fluor 594 (1:500) (Abcam, ab150080), and goat anti-mouse IgM Alexa Fluor 594 (1:300) (ThermoFisher, A-21044). Cultures were washed three times with PBS, counterstained with Hoeschst (1:2000) (ThermoFisher, 62249), and processed for immunofluorescent visualization.

4.3.10 Functional characterization of NSPCs and statistical analysis

Immuno-stained cultures were visualized using a Nikon Ti Eclipse Epifluorescence. Ten images were taken for each treatment (n=3 wells per marker). Images were analyzed using Image J software. The total number of immuno-positive cells was counted as a percentage of Hoechst-labeled nuclei to calculate the mean percent differentiation and proliferation. Data are presented as a mean percent ± standard error. Statistical analyses were carried out using GraphPad Prism. When analyzing the mean percent differentiation and proliferation between NSPC types, significance was determined using an ordinary one-way analysis of variance (ANOVA) followed by a Tukey's Test. When analyzing the mean percent differentiation and proliferation between two related groups (Figures S4.7), significance was determined using a two-tailed paired t-test.

4.3.11 RNA sequencing and data analysis

Primary bona fide NSPCs, iPSC-Br NSPCs, and iPSC-SC NSPCs were cultured according to the protocol outlined in sections 4.3.2, 4.3.6, and 4.3.7, respectively. Once bona fide and iPSC-derived NSPCs reached confluency, cultures were passaged, and 50,000 cells were transferred to a 15 mL

conical tube containing SFM. The cells were centrifuged at 300 xg for 5 minutes, and the supernatant was aspirated. Cell pellets were lysed, and RNA was extracted using the RNeasy Micro Kit (Qiagen, 74004). A total of 20 µL of RNA was extracted in RNase-free water and stored at -20 °C until further use. A 1 µL sample was used to quantify the RNA concentration using NanoDrop™. To confirm RNA sample quality, 1000-5000 pg/µL of RNA from each sample were assessed using a Fragment Analyzer, and only samples with RQN values greater than seven were used for downstream RNA sequencing. 50 ng of RNA per sample was shipped to StemCore Laboratories (Ottawa, Canada) for RNA library preparation and sequenced using the NextSeq platform.

Quality control on the samples was performed using FastQC to assess the quality of the raw sequences. A summary report of quality control metrics and mapping statistics can be retrieved here: http://www.ogic.ca/projects/ahmad_galuta/human_spinal_cord_SC_iPSC/reports/multiqc_report.html. Reads were mapped to the human genome/transcriptome with HISAT2, and the Picard 'CollectRnaSeqMetrics' tool was run to assess the fraction of reads mapping to coding and non-coding sequences. Reads were assigned to transcripts using Salmon; human transcript sequences were retrieved from GENCODE v35. Quantification for 60,237 genes was imported from salmon using the tximport library. The data were filtered to retain data for 24,006 genes with five or more counts in two or more NSPC types and combined into a single DESeq dataset.

Differential gene expression between NSPC types was assessed using DESeq2. The rlog-transformed normalized counts were calculated for principal component analysis (PCA) and hierarchical clustering. PCA was applied to the matrix of gene expression values using the 500 most variable genes in the dataset. Hierarchical clustering was calculated using Euclidian distance

between rlog-transformed normalized count values for all transcripts. DESeq2 was used to calculate fold change in gene expression and a p-value between NSPC types. Multiple testing correction was done using the Benjamini-Hochberg method to calculate a q-value or false discovery rate (FDR). Volcano plots and heatmaps of differentially expressed (DE) genes were generated using the fold change results. Fold change scatter plots were generated for all genes and protein-coding genes only. A 5% FDR cut-off was used for these analyses to indicate whether a gene is significantly DE between conditions.

To identify functional changes in gene expression between NSPC types, gene set enrichment analysis (GSEA) was performed. Genes were ranked for the comparisons between bona fide and iPSC-SC NSPCs and bona fide and iPSC-Br NSPCs using the metric $\log_2$FoldChange. GSEA was run against a subset of gene sets from MSigDB, including H (hallmark gene sets), C2 (curated gene sets), CP (canonical pathways), C5 (Gene Ontology annotations), and C8 (cell type signatures).

Functional enrichment analysis for DE genes was also performed using gProfiler to identify annotations that are enriched in sets of DE genes. DE genes were filtered to include only genes with an FDR of <0.01 and a $\log_2$(fold change) greater than +2 or less than –2. gProfiler was run twice with the "ordered query" option for the iPSC-SC and iPSC-Br data, once each for the genes that are upregulated and downregulated. For this analysis, the list of 24,006 genes retained after the filtering step of DESeq2 analysis was used as a background gene set for running the hypergeometric probability function.

4.4 Results

4.4.1 Generation and molecular characterization of iPSCs

Dermal fibroblasts were reprogrammed into iPSCs from three organ donors who also had their spinal cords harvested for the culture of primary NSPCs. Reprogramming was achieved by electroporating fibroblasts in the presence of episomal vectors. The electroporation parameters were optimized by testing different media (DMEM/F12 vs. Opti-MeM), plasmid concentrations (10, 20, and 40 μg/mL), and electroporation voltages (200-300 V). Qualitatively, it was observed that transfection efficiency was similar when using DMEM/F12 and Opti-MeM as electroporation buffers, but the post-electroporation survival in Opti-MeM was lower. The fluorescence intensity was similar between 20 μg/mL and 40 μg/mL of pCE-GFP but significantly lower using 10 μg/mL. A high electroporation voltage of 300 V resulted in significant cell death and poor transfection efficiency, while 200 V produced the greatest viability and transfection efficiency (Figure S4.1). Ultimately, the optimized conditions used for all reprogramming experiments include DMEM/F12 as an electroporation buffer, 20 μg/mL of episomal vectors, and a voltage of 200V.

At least three primary iPSC colonies from each donor were manually passaged to create iPSC lines. At passage 5, iPSC colonies showed typical morphology, including a defined colony boundary containing small, circular, tightly bound cells with large nuclei (Figure 4.1). iPSC colonies expressed markers for pluripotent stem cells, including Oct3/4, Oct4a, Nanog, and Sox2 (Figure 4.1), while they were negative for the fibroblast markers Vimentin and PDGFα (data not shown). On the other hand, fibroblasts were labeled positive for Vimentin and PDGFα, while they were negative for Oct3/4 and Nanog. Surprisingly, fibroblasts were positive for Sox2, whose expression was densely localized in small pockets in the nucleus (Figure S4.2). Therefore, we successfully genetically reprogrammed dermal fibroblasts into iPSCs from three donors.

4.4.2 Generation of iPSC-SC and -Br NSPCs

A single iPSC line from each donor was dissociated into single cells and differentiated into NSPCs bearing either a dorsal forebrain (iPSC-Br) or spinal cord (iPSC-SC) phenotype. The iPSC-Br NSPCs were generated using a well-established protocol that involves dual inhibition of the SMAD pathways (Chambers et al., 2009). These cultures were uniform in morphology consisting of multi-polar, spindle-like cells (Figure 4.2). The iPSC-SC NSPCs were generated via a differentiation route distinct from iPSC-Br NSPCs involving a neuromesodermal progenitor intermediate (Kumamaru, Kadoya et al., 2018). iPSC-SC NSPCs contained two types of colony growth: (1) flat colonies without defined shapes or boundaries and (2) adherent neurosphere-like colonies (Figure 4.2).

Concerning molecular characterization, iPSC-SC, and iPSC-Br NSPCs were positive for the neural stem cell marker Sox2 (Figure 4.2) and negative for pluripotency markers (data not shown). Furthermore, iPSC-Br NSPCs expressed Pax6, a marker for dorsal forebrain NSPCs, and iPSC-SC expressed Nestin, a marker for neural progenitor cells (Figure 4.2). Concerning functional characterization, both iPSC-SC and iPSC-Br NSPCs could be passaged at least ten times, reflecting their prolonged self-renewal ability. Under differentiation conditions, both iPSC-SC and iPSC-Br NSPCs generated β-iii tubulin^{+}/Map2^{+} neurons, but only iPSC-Br NSPCs generated GFAP^{+} astrocytes (Figure 4.2).

4.4.3 The transcriptional profiles of iPSC-SC and -Br NSPCs diverge and are distinct from bona fide NSPCs

Bona fide (n=3), iPSC-SC (n=3), and iPSC-Br (n=3) NSPCs had their RNA extracted and processed for bulk RNA sequencing. Importantly, all NSPC types were derived from the same

donor, and iPSC-derived NSPCs were generated from the same iPSC line to minimize genetic variation between cell types of the same donor. A description of the samples processed for RNA sequencing is depicted in Table 2. An additional three samples of bona fide NSPCs, previously characterized in Chapter 3, were included in this analysis. A total of 24,006 genes were analyzed and compared among the three NSPC types.

There were fewer DE genes between iPSC-SC and iPSC-Br NSPCs (2,015 genes, 8% of total genes) compared to either iPSC-derived NSPCs and bona fide NSPCs (Table 3). Unexpectedly, there were more DE genes between bona fide and iPSC-SC NSPCs (8,737 genes, 36% of total genes; Figure 4.3 A) compared to bona fide and iPSC-Br NSPCs (5,555 genes, 23% of total genes; Figure 4.4 A). 4,600 genes (19% of total genes) were considered DE in both iPSC-SC and -Br NSPCs compared to bona fide NSPCs (Figure 4.5 A). As such, most of the DE genes between iPSC-Br and bona fide NSPCs (83%) were also DE between iPSC-SC and bona fide NSPCs (Figure 4.4 B), and only 955 genes were uniquely DE in iPSC-Br (Figure 4.4 C). On the other hand, iPSC-SC NSPCs had 4,137 genes that were uniquely DE (Figure 4.3 C). Of the 4,600 DE genes in both iPSC-SC and -Br NSPCs relative to bona fide NSPCs, 2,496 genes were upregulated, 2,090 genes were downregulated, and only 14 genes were DE in opposite directions (Figure 4.5 A). A list of the most upregulated and downregulated protein-coding genes in either iPSC-SC, iPSC-Br, or both are depicted in Figures 4.3 D, 4.4 D, and 4.5 B.

When comparing the 500 most variables genes, a PCA plot separates cell type along the PC1 (69% variance) but not the PC2 axis (7% variance) (Figure 4.5 C, upper panel). Furthermore, along the PC1 axis, iPSC-SC and iPSC-Br NSPCs are closer than either iPSC-derived NSPCs are to bona fide NSPCs. Unexpectedly, iPSC-Br NSPCs were closer to bona fide NSPCs than iPSC-SC NSPCs. Interestingly, along the PC2 axis, there appears to be some association between NSPC

types derived from the same donor; “H17” NSPCs had the highest score while “H25” NSPCs had the lowest score, except for bona fide NSPCs from “H17” and “H18” whose orders were switched. In another PCA plot with PC1 (69% variance) vs. PC3 (6% variance) axes, iPSC-SC and iPSC-Br NSPCs are now separated, but associations between cell types of the same donor are lost (Figure 4.5 C, lower panel).

Hierarchical clustering analysis of the overall transcriptome further demonstrates that bona fide NSPCs cluster separately from iPSC-derived NSPCs (Figure 4.5 D). Interestingly, the iPSC-SC NSPCs cluster together more closely than bona fide NSPCs cluster with one another. On the other hand, iPSC-Br NSPCs appear more dissimilar, especially the sample “H18,” which shows more similarity to bona fide NSPCs than samples “H17” and H25”. Overall, the transcriptome profiles of iPSC-derived NSPCs are more similar to each other than to bona fide NSPCs, and surprisingly, iPSC-Br and bona fide NSPCs are more similar compared to iPSC-SC and bona fide NSPCs.

4.4.4 Bona fide and iPSC-derived NSPCs portray segregated regional, developmental, and cellular phenotypes

To further characterize NSPCs, we compared DE genes and gene sets that are markers for different CNS regions, developmental processes, and cell types. We used several genes to depict regional specificity to the spinal cord and brain, and dorsal and ventral regionalization (Figures 4.6 and S4.3). In addition, we conducted a GSEA and gProfiler analysis of DE genes (Figures 4.7 and S4.4).

Concerning spinal cord regionalization, we determined the enrichment of most *HOX* genes in bona fide and iPSC-SC NSPCs compared to iPSC-Br NSPCs (Figures 4.6 A and S4.3 A). Moreover, iPSC-SC NSPCs expressed a higher level of *HOXB1* and *HOXB9* but a lower level of *HOXA4*,

HOXA10, *HOXC9*, and *HOXD8* relative to bona fide NSPCs. Interestingly, iPSC-Br NSPCs from "H18" expressed a high level of *HOXB5*, *HOXD13*, and *HOXB2* (Figure S4.3). Our GSEA and gProfiler analysis suggest that iPSC-SC NSPCs are enriched in gene sets associated with "spinal cord development" and "spinal cord cell differentiation" compared to bona fide NSPCs. These gene sets were not enriched in iPSC-Br NSPCs (Figures 4.7 D and S4.4 A). Instead, iPSC-Br NSPCs were downregulated in genes associated with "spinal cord injury" (Figure S4.4 D).

Concerning brain regionalization, we determined that iPSC-Br NSPCs were enriched in genes that are markers for the dorsal forebrain (*EMX1*, *TBR1*, *TBR2*, *FOXG1*, *PAX6*), midbrain (*EN1*, *EN2*, *PAX5*, *SIM1*) and other brain markers (*OTX1*, *OTX2*, *LHX2*, *ZIC3*) compared to bona fide NSPCs (Figures 4.6 B and S4.3 B). Interestingly, these markers were not DE between iPSC-Br and -SC NSPCs. A GSEA report indicates that both iPSC-derived NSPCs are enriched in gene sets associated with brain development, including the forebrain, hindbrain, and diencephalon development (Figure 4.7 D). Further analysis using gProfiler indicates that iPSC-Br NSPCs are particularly enriched in gene sets associated with "forebrain generation of neurons" and "neuron fate commitment." In contrast, iPSC-SC NSPCs are enriched in "hindbrain morphogenesis" and "cell differentiation" (Figure S4.4 A, C).

In addition to the regional spinal cord and brain markers, we assessed genes that pattern the dorsal-ventral axis (Figures 4.6 C, D and S4.3 C, D). For ventral markers, both iPSC-SC and -Br NSPCs expressed a higher level of *NKX6.2*, *FOXA1*, *SULF1* and a lower level of *DCN*, *FGL2*, and *PRSS23* relative to bona fide NSPCs. Also, iPSC-Br NSPCs expressed a higher level of *SHH* (Figures 4.6 C and S4.3 C). For dorsal markers, both iPSC-SC and -Br NSPCs expressed a higher level of *GDF10*, *EFNB3*, and *DCLK1* and a lower level of *HEXB* relative to bona fide NSPCs. Also, iPSC-SC NSPCs expressed a higher level of *PAX3* and a lower level of *A2M* (Figures 4.6 D and S4.3

D). Our GSEA and gProfiler analysis indicate that both iPSC-SC and -Br NSPCs are enriched in genes associated with dorsal-ventral pattern formation (Figure S4.4 A, C). Furthermore, iPSC-SC NSPCs were enriched in "dorsal and ventral spinal cord development" as well as an "anterior-posterior specification" (Figures 4.7 D and S4.4 A).

Considering the pluripotent and adult origins of iPSC-derived NSPCs and bona fide NSPCs, we assessed DE genes associated with developmental programs. Interestingly, the pluripotent markers *LIN28A* and *LIN28B* were two of the most enriched genes in iPSC-derived NSPCs (Figures 4.3 D and 4.4 D). Also, the neural crest stem cell marker *POU4F1* was more enriched in iPSC-SC than -Br NSPCs relative to bona fide NSPCs (Log_2FC = 13.5 and 7.3 for iPSC-SC and -Br NSPCs) (Figure 4.3 D). Concomitant with the expression of early developmental markers, both iPSC-derived NSPCs were enriched in gene sets associated with "embryo development" and "transcriptional regulation of pluripotent stem cells." However, we detected a downregulation of genes related to "pluripotent stem cell differentiation pathway" (Figure S4.4). Furthermore, iPSC-SC NSPCs were exclusively enriched in "embryonic pattern specification," "embryonic stem cell pluripotent pathways," and "neural crest differentiation," which is indicative of an earlier developmental stage than iPSC-Br NSPCs (Figures 4.7 C, D and S4.4 A).

Unexpectedly, both iPSC-derived NSPCs were enriched in "endoderm differentiation" (Figure 4.7 C). However, only iPSC-SC NSPCs were enriched in "mesodermal commitment pathway," "somite development," and "somitogenesis," reflecting the distinct developmental path of iPSC-SC NSPCs involving a neuromesodermal progenitor (NMP) intermediate (Figures 4.7 C and S4.4 A). Within the context of CNS development, both iPSC-derived NSPCs were enriched in "ectoderm differentiation," "neural tube development," "CNS development," "neuron development," and "axogenesis" (Figures 4.7 D and S4.4 A, C). Lastly, in line with the

differentiation protocol used to induce iPSC-SC NSPCs, there was an enrichment of Wnt beta-catenin and FGFR signaling and downregulation of TGFβ signaling (Figure 4.7 A, D).

Concerning cell phenotypes, iPSC-derived NSPCs were enriched in gene sets associated with NSPCs and neurons, including "embryonic cortex NSCs" and "prefrontal cortex major type NPCs" (Figures 4.7 E and S4.4). They were also enriched in "fetal cerebrum astrocytes," "main fetal astrocytes," and "prefrontal cortex astrocytes," which have genes in common with NSPCs in the developing brain (D. A. Lim & Alvarez-Buylla, 2016; J. Zhang & Jiao, 2015). iPSC-derived NSPCs were also enriched in multiple neuron-related gene sets, including "neuron differentiation," "neuron development," "forebrain neuron differentiation," "neuron projection development," "midbrain neurotypes," and "neuronal system." Concurrent with an earlier developmental stage, only iPSC-SC NSPCs were enriched in "embryonic cortex excitatory neurons," "fetal cerebrum inhibitory neurons," and "main fetal inhibitory interneurons" (Figure 4.7 E). Concerning glial development, iPSC-Br NSPCs were consistently downregulated in gene sets associated with "gliogenesis," while iPSC-SC NSPCs were enriched in "gliogenesis" and "glial cell differentiation" (Figure S4.4 A, D).

In addition to CNS cell phenotypes, we also compared the transcriptomes of NSPCs with single nuclei RNA sequencing data of ependymal cells from the adult human spinal cord (n=7, Figure 4.8). Neither bona fide nor iPSC-derived NSPCs completely recapitulated the transcriptome of spinal cord ependymal cells (Figure 4.8 A). iPSC-SC and -Br NSPCs were enriched in a similar subset of ependymal genes that did not overlap with those enriched in bona fide NSPCs (Figure 4.8 B). Relative to bona fide NSPCs, iPSC-derived NSPCs were most enriched in *CD24*, *PROM1*, *ZBBX*, *MSI1*, *PAX6*, and *BMP7*, while *FMO3*, *HEY2*, *PRSS23*, and *HEXB* were most downregulated (Figure 4.8 C). Also, iPSC-Br NSPCs were exclusively enriched in *FOXJ1* and

CTNNB1, while *EGFR* and *NKX6.1* were downregulated. Meanwhile, iPSC-SC were exclusively enriched in *NOTCH1* and *PAX3*, while *A2M*, *EFHB*, *NFIA*, and *VWA3B* were downregulated (Figure 4.8 C).

These results indicate that iPSC-SC and -Br NSPCs portray regionalized populations that mimic endogenous spinal cord and brain NSPCs. Both iPSC-derived NSPCs exhibit an early developmental stage indicative of their embryonic-like origin, while iPSC-SC NSPCs also portray features of NMPs. Furthermore, iPSC-derived NSPCs are enriched in genes that program the development of the CNS and neurons. Lastly, neither bona fide nor iPSC-derived NSPCs mimic the transcriptional profile of endogenous spinal cord ependymal cells. However, bona fide and iPSC-derived NSPCs expressed a different subset of genes that were DE relative to ependymal cells. An enrichment map depicting some enriched gene sets of interest in iPSC-SC relative to bona fide NSPCs is shown in Figure S4.8.

4.4.5 iPSC-derived NSPCs express a higher level of NSPC and neurogenic-related genes

To evaluate the functionality of NSPCs at the transcriptome level, we assessed for markers of NSPCs, neurogenesis, astrogenesis, oligodendrogenesis, and proliferation (Figures 4.9 and S4.5). iPSC-derived NSPCs were enriched in most NSPC markers including *CD24*, *MSI1*, *SOX2*, *NES*, and *PROM1* while there was no significant difference in the expression of *FUT4* and *MSI2* relative to bona fide NSPCs (Figures 4.9 A and S4.5 A). iPSC-SC NSPCs were exclusively enriched in *BMI1*, while iPSC-Br NSPCs had *EGFR* downregulated compared to bona fide NSPCs (Figures 4.9 A and S4.5 A). iPSC-derived NSPCs were also enriched in the gene sets “embryonic cortex NSCs” and “prefrontal cortex major types NPCs,” while iPSC-SC NSPCs were significantly enriched in “NSC population maintenance” (Figure 4.7 D, E).

Concerning proliferation markers, a different subset of genes was preferentially enriched in bona fide and iPSC-derived NSPCs (Figures 4.9 B and S4.5 B). iPSC-derived NSPCs were enriched in *TENM2*, *BCAT1*, *DCC*, *BCAR3*, and *CDK6* while bona fide NSPCs were enriched in *RARRES1*, *TGFBR2*, *JUNB*, *CDKN2B*, and *PMP22*. Furthermore, bona fide NSPCs were enriched in *COL18A1* and *MGMT* relative to iPSC-SC NSPCs and *ENPEP*, *EGFR*, and *HOXC10* relative to iPSC-Br NSPCs (Figures 4.9 B and S4.5 B). The GSEA report indicates that iPSC-derived NSPCs were significantly enriched in "positive regulation of NPC proliferation," while iPSC-SC NSPCs were significantly enriched in "NPC proliferation" (Figure 4.7 D).

Concerning neurogenesis markers, iPSC-derived NSPCs were enriched in most of the selected genes, including *DCX*, *GBX2*, *ASCL1*, *CXCR4*, *DLL3*, *SLIT3*, *FGF13*, *DCC*, *OLFM1*, and *SLC17A5* while the genes *SEMA5A*, *HEY2*, and *COL6A2* were downregulated (Figures 4.9 C and S4.5 C). Also, iPSC-SC NSPCs were exclusively enriched in *PAX3*, while iPSC-Br NSPCs had *CPNE6* downregulated relative to bona fide NSPCs (Figures 4.9 C and S4.5 C). The GSEA report for iPSC-SC NSPCs indicates a significant enrichment of "dopaminergic neurogenesis," "forebrain neuron differentiation," "neuron fate commitment," "postsynaptic neurotransmitter receptor activity," "neurexins," "neuroligins," and "synaptic vesicle pathway" (Figure 4.7 B-D). Interestingly, iPSC-SC NSPCs were also enriched in "negative regulation of neuron differentiation," which contrasts with the enrichment of multiple neurogenesis-related gene sets (Figure 4.7 D). Only "voltage-gated calcium channel activity" was enriched in both iPSC-SC and -Br NSPCs (Figure 4.7 B).

Concerning markers of gliogenesis, iPSC-derived NSPCs were enriched in astrocyte markers *FGFR3* and *FABP7*, while bona fide NSPCs were enriched in *GFAP* (Figures 4.9 D and S4.5 D). Also, iPSC-SC NSPCs were enriched in *SLC1A3*, but *NFIA* was downregulated relative to bona

fide NSPCs (Figures 4.9 D and S4.5 D). The oligodendrocyte marker *NCAM1* was enriched in iPSC-derived NSPCs, but bona fide NSPCs were enriched in *PDGFRA* and *CSPG4* (Figures 4.9 E and S4.5 E). Also, bona fide NSPCs were enriched in *OLIG1* relative to iPSC-Br NSPCs and *GAPDH* relative to iPSC-SC NSPCs (Figures 4.9 E and S4.5 E). The GSEA and gProfiler report indicated that iPSC-derived NSPCs were enriched in "early developmental stage astrocytes," but oligodendrocyte development was not enriched (Figures 4.7 E and S4.4).

4.4.6 Bona fide and iPSC-Br NSPCs are highly neurogenic, but bona fide NSPCs proliferate less than both iPSC-derived NSPCs

To correlate the transcriptional profile with functional behavior, we assessed the differentiation and proliferation profiles of NSPCs (n=3 bona fide, iPSC-SC, iPSC-Br). Importantly, NSPCs were functionally evaluated at the same time that their RNA was extracted for sequencing. Furthermore, bona fide and iPSC-derived NSPCs were cultured under identical conditions to eliminate the possible influence of culture media.

We have previously demonstrated in Chapter 3 that primary bona fide NSPCs are neurogenic and differentiate primarily into β-iii tubulin$^+$ neurons. Under identical differentiation conditions consisting of 1% FBS, iPSC-Br NSPCs generated a significantly greater percentage of β-iii tubulin$^+$ neurons after one week of differentiation than both bona fide ($p<0.001$) and iPSC-SC ($p<0.0001$) NSPCs (bona fide: 38.3±3.2%, iPSC-SC: 5.8±0.5%, iPSC-Br: 55.7±3.5% βiii-tubulin$^+$) (Figure 4.10 A, D). However, after two weeks of differentiation, the percentage of β-iii tubulin$^+$ neurons was similar between bona fide and iPSC-Br NSPCs but significantly less ($p<0.0001$) from iPSC-SC NSPCs (bona fide: 42.2±2.1%, iPSC-SC: 9.6±0.6%, iPSC-Br: 40.3±3.4% βiii-tubulin$^+$) (Figure 4.10 A, D).

We compared neuronal differentiation among NSPCs from individual donors (n=3) to evaluate whether the observed neuronal differentiation trend was consistent across donors (Figure S4.6). iPSC-Br NSPCs from "H17" and "H25" differentiated significantly more into β-iii tubulin^{+} neurons compared to bona fide NSPCs after one and two weeks of differentiation (Figure S4.6 A, I). iPSC-Br NSPCs from "H18" also produced more neurons than bona fide NSPCs after one week of differentiation. However, after two weeks of differentiation, iPSC-Br NSPCs from "H18" made significantly fewer neurons than bona fide NSPCs (Figure S4.6 E). In all three donors, iPSC-SC NSPCs differentiated the least into neurons (Figure S4.6 A, E, I).

To evaluate the effect of the differentiation media on neuron differentiation, we treated iPSC-SC (n=3) and iPSC-Br (n=3) NSPCs with 1% FBS in Neurobasal-A medium or the manufacturer's recommended differentiation media (i.e., positive control). Here, iPSC-Br NSPCs differentiated into β-iii tubulin^{+} neurons to a similar extent in either 1% FBS or positive control (Figure S4.7 A). However, iPSC-SC NSPCs differentiated into neurons significantly less in 1% FBS after two weeks compared to the positive control (FBS: 9.6±0.6%, positive control: 13.5±0.7% βiii-tubulin^{+}, $p<0.05$) (Figure S4.7 A).

We've also previously demonstrated in Chapter 3 that bona fide NSPCs differentiate little into GFAP^{+} astrocytes. Here, we show that iPSC-Br (n=3) NSPCs differentiated into astrocytes slightly more than bona fide NSPCs after two weeks of differentiation (bona fide: 0.05±0.03%, iPSC-Br: 1.6±0.5% GFAP^{+}, $p<0.01$) (Figure 4.10 B, D). This was observed in samples "H18" and "H25" but not "H17," which did not differentiate into astrocytes (Figure S4.6 B, F, J). However, iPSC-Br NSPCs differentiated into astrocytes only after two weeks of differentiation, indicating that one week of differentiation is insufficient to generate astrocytes. This observation was consistent using either 1% FBS or positive control as differentiation media, although fewer astrocytes were

produced in 1% FBS (FBS: 1.6±0.5%, positive control: 5.6±0.9% $GFAP^+$, $p<0.05$) (Figure S4.7 B). Finally, we did not detect any O4+ oligodendrocytes in any of the cultures under the conditions tested (data not shown).

In addition to neuronal and glial differentiation, we measured the proliferation rate in differentiation conditions, which reflects progenitor cell proliferation. After one week of differentiation, iPSC-SC (n=3) and iPSC-Br (n=3) NSPCs exhibited similarly high rates of proliferation that were significantly greater than that of bona fide (n=3) NSPCs (bona fide: 66.4±2.5%, iPSC-SC: 82.5±1.8%, iPSC-Br: 80.8±2.9% $BrdU^+$, $p<0.0001$) (Figure 4.10 C). Following two weeks of differentiation, the proliferation rate of all NSPCs was reduced compared to one week, indicating that some NSPCs have reached terminal differentiation (bona fide: 20.0±2.3%, iPSC-SC: 65.8±2.5%, iPSC-Br: 66.2±3.8% $BrdU^+$) (Figure 4.10 C). Over two weeks, the proliferation rates of iPSC-SC and -Br NSPCs were significantly greater than that of bona fide NSPCs ($p<0.0001$). These observations were consistent among individual donors, except for "H18," in which all three NSPC types had a similar proliferation rate at one week (Figure S4.6 G). The differentiation media used (1% FBS vs. positive control) did not significantly alter the proliferation rate of iPSC-derived NSPCs (Figure S4.7 C).

In a separate assay, we treated NSPCs (n=3 bona fide, iPSC-SC, iPSC-Br) with mitogens and measured the proliferation rate, which reflects self-renewing NSPCs. Following one week of treatment, iPSC-SC and -Br NSPCs exhibited high rates of proliferation, which were significantly greater than that of bona fide NSPCs (bona fide: 48.0±2.1%, iPSC-SC: 82.9±1.6%, iPSC-Br: 77.7±1.8% $BrdU^+/Sox2^+$, $p<0.0001$) (Figure 4.10 E). After two weeks of treatment, iPSC-SC and -Br NSPCs maintained a high proliferation rate while that of bona fide NSPCs was reduced (bona fide: 28.8±2.3%, iPSC-SC: 83.2±1.5%, iPSC-Br: 86.2±0.8% $BrdU^+/Sox2^+$) (Figure 4.10 E). These

trends were consistent among individual donors, except for "H25," in which all three NSPC types had a similar proliferation rate at one week (Figure S4.6 L).

4.5 Discussion

We found that iPSCs differentiated into regionalized spinal cord and brain NSPCs do not fully recapitulate the transcriptional nor functional nature of *in vitro* and *in situ* bona fide spinal cord NSPCs. Notably, we characterized bona fide and iPSC-derived NSPCs acquired from the same donor to mitigate the influence of genetic variation between humans. We observed that iPSC-SC and -Br NSPCs exhibited regional specificity to the spinal cord and brain, respectively. However, despite a regional homology between iPSC-SC and bona fide NSPCs, there was a more significant homology in the overall gene expression between iPSC-Br and bona fide NSPCs. Interestingly, bona fide and iPSC-derived NSPCs were neurogenic but displayed varying neurogenic potentials at the transcriptome and functional levels. Indeed, given their pluripotent origins, both iPSC-SC and -Br NSPCs were enriched in genes related to the transcriptional regulation of pluripotency and embryo development. In addition, iPSC-SC NSPCs were enriched in genes related to mesodermal differentiation and somitogenesis, reflecting their distinct developmental pathway involving NMPs. Concurrent with an early developmental stage, both iPSC-derived NSPCs had a greater proliferation rate than bona fide NSPCs. These results indicate the distinct regional, developmental, and functional phenotypes of genetically reprogrammed NSPCs relative to endogenous human spinal cord NSPCs, which may impact the success of their clinical applications for SCI.

iPSC-derived NSPCs have been touted as promising regenerative tools for spinal cord repair. Still, it is unclear whether they bear any homology to endogenous spinal cord NSPCs in adult humans.

For the first time, we address this gap by comparing bona fide spinal cord NSPCs with iPSC-derived NSPCs. The iPSC-derived NSPCs in our study were generated to portray a spinal cord or dorsal forebrain phenotype with the expectation that iPSC-SC NSPCs would bear a greater functional and transcriptional resemblance to bona fide NSPCs. Moreover, bona fide and iPSC-derived NSPCs were generated from the same donors to establish an isogenic comparison of cell types. Isogeneity is a crucial factor since iPSCs and iPSC-derived NSPCs will be influenced to a certain degree by the donor's genetic makeup (Strano et al., 2020b).

First, we confirmed that iPSC-SC and iPSC-Br NSPCs expressed markers characteristic of NSPCs at the protein and transcriptional level, including Sox2, Nestin, Pax6, CD24, MSI1, and PROM1. Sox2 is a transcription factor necessary for the self-renewal of NSPCs and was found to be expressed in all NSPC types (Pagin et al., 2021). Our GSEA report also indicated that iPSC-derived NSPCs portray cellular phenotypes of embryonic cortex NSPCs and prefrontal cortex NSPCs, further validating their NSPC nature.

Next, we discerned the regional specificity of iPSC-derived NSPCs by evaluating the expression of spinal cord and brain gene markers. During embryonic development, the posterior and anterior CNS develop via distinct routes, acquiring unique gene expression profiles related to their regional position (Chambers et al., 2009; Henrique et al., 2015; Kumamaru, Kadoya, et al., 2018). NSPCs that form the spinal cord emerge from a bipotent NMP cell that also contributes to the paraxial mesoderm (Henrique et al., 2015). In accordance, our GSEA report indicates that iPSC-SC but not iPSC-Br NSPCs are enriched in genes associated with mesodermal differentiation and somitogenesis, suggesting that iPSC-SC cultures may contain NMPs or NMP-derived mesoderm.

NMPs that specialize into NSPCs go on to express *HOX* genes that predictably pattern the rostral-caudal axis of the spinal cord (Kumamaru, Kadoya et al., 2018). *HOX* genes are expressed in a

sequential and contiguous manner within NSPCs of the hindbrain (*HOX1-5*), spinal cord cervical (*HOX5-8*), thoracic (*HOX8-9*), and lumbosacral (*HOX10-13*) segments (Lippmann et al., 2015). Therefore, the expression of specific *HOX* genes in NSPCs will determine, to an extent, the regional identity and development of distinct neural subtypes along the rostral-caudal axis of the spinal cord (Philippidou & Dasen, 2013).

Our study confirmed that bona fide and iPSC-SC NSPCs express most *HOX* genes significantly more than iPSC-Br NSPCs. Furthermore, bona fide NSPCs were most enriched in *HOX7-11*, corresponding with the spinal cord regions (thoracic-lumbar) from where they were obtained. Relative to bona fide NSPCs, iPSC-SC NSPCs were enriched in *HOXB1* but expressed a lower level of *HOX7-10* genes suggesting that iPSC-SC NSPCs portray a more rostral phenotype. Our GSEA report further validates the enrichment of spinal cord development genes in iPSC-SC but not iPSC-Br NSPCs.

On the other hand, iPSC-Br NSPCs were generated by dual-SMAD inhibition, which is expected to yield NSPCs with a dorsal forebrain phenotype (Chambers et al., 2009). Indeed, iPSC-Br NSPCs were found to be enriched in multiple forebrain and midbrain brain markers relative to bona fide NSPCs. Unexpectedly, iPSC-SC NSPCs were also enriched in many of these brain-specific genes. Further analysis using a GSEA indicated that both iPSC-Br and -SC NSPCs were enriched in forebrain and hindbrain development as well as multiple "midbrain neurotypes". Therefore, while iPSC-Br NSPCs may be regionalized to the brain, iPSC-SC NSPCs express regional markers of both the spinal cord and the brain suggesting that iPSC-SC NSPCs require further regional specification.

An essential feature of NSPCs to mediate regeneration is their ability to proliferate (Gazdic et al., 2018). We observed that both iPSC-SC and -Br NSPCs exhibited significantly greater proliferation

rates than bona fide NSPCs under differentiation and proliferation conditions. This was not unexpected given the pluripotent and adult origins of iPSC-derived NSPCs and bona fide NSPCs, respectively. During embryonic development, NSPCs exhibit a shorter cell cycle length as they are tasked with populating the nervous system. On the other hand, adult NSPCs acquire temporary states of quiescence and divide only when needed to avoid exhausting the stem cell pool (Morales & Mira, 2019). Concurrent with this understanding, our GSEA report indicates that iPSC-derived NSPCs are enriched in gene sets associated with NSPC population maintenance, NSPC proliferation, cell cycle checkpoints, DNA replication, and G2/M checkpoint. Additional indicators of quiescence in adult NSPCs include a metabolic switch from glycolysis to oxidative phosphorylation and the expression of cell adhesion proteins (Morante-Redolat & Porlan, 2019; Morizur et al., 2018). Indeed, bona fide NSPCs were enriched in gene sets associated with oxidative phosphorylation and extracellular matrix organization and regulators. Therefore, the highly proliferative behaviour of iPSC-derived NSPCs relative to bona fide NSPCs may reflect their respective developmental stages as embryonic and adult stem cells.

Achieving high rates of neurogenesis from NSPCs may be essential to improve neurological outcomes after an SCI since secondary damage can induce the death of neurons and loss of connections in the spinal cord (Alizadeh et al., 2019; Ceto et al., 2020; de Freria et al., 2021). Surprisingly, we found that bona fide NSPCs were functionally more similar to iPSC-Br NSPCs than iPSC-SC NSPCs. While bona fide and iPSC-Br NSPCs mainly differentiated into neurons, iPSC-SC NSPCs produced significantly fewer neurons. This was unexpected since iPSC-SC NSPCs were designed to portray a similar functional profile as bona fide NSPCs and were previously shown to differentiate into various spinal interneurons and motor neurons (Kumamaru, Kadoya, et al., 2018). However, Kumamaru and colleagues' (2018) study did not report the

percentage of differentiated neurons. Following correspondence with the authors, it was indicated that iPSC-SC NSPCs were differentiated at least 40 days after neural induction and that neuronal differentiation proceeded for ten weeks. This contrasts with our study in which iPSC-SC NSPCs were differentiated 28 days following neural induction and only allowed to differentiate for two weeks. Therefore, the iPSC-SC NSPCs in our study may reflect a more primitive stem cell state, and further maturation *in vitro* is required to enhance their neurogenic potential.

Several observations from our study support the assumption that iPSC-SC NSPCs exist in an early developmental state. First, we detected the expression of genes that pertain to NMPs or NMP-derived mesoderm in iPSC-SC cultures. This would represent a developmental stage not fully specialized into NSPCs from the bipotent NMP state (Verrier, Davidson, Gierliński, Dady, & Storey, 2018). Second, it is known that during embryonic and post-natal development, NSPCs differentiation proceeds sequentially via neurogenesis, astrogenesis, and finally, oligodendrogenesis (Temple, 2001). Given the low neurogenic potential of iPSC-SC NSPCs in this study, they may be at a developmental stage that is still early in the neurogenesis phase. Third, iPSC-SC NSPCs in this study did not differentiate into astrocytes or oligodendrocytes, suggesting that they are in the neurogenesis phase and have not undergone a "gliogenic switch" (Tiwari & Berninger, 2017).

Meanwhile, both bona fide and iPSC-Br NSPCs differentiated into astrocytes. Concomitantly, iPSC-SC NSPCs expressed a significantly lower level of *NFIA* than bona fide and iPSC-Br NSPCs; *NFIA* is a transcription factor responsible for initiating the gliogenic switch in NSPCs (Deneen et al., 2006). Finally, Kumamaru and colleagues (2018) reported the differentiation of iPSC-SC NSPCs into mature astrocytes and oligodendrocytes only after 3 and 6 months, respectively, of post-grafting into the spinal cord, suggesting that a long period of developmental

maturation is required to form glial cells. Therefore, it would be of great interest to mature iPSC-SC NSPCs over time *in vitro* and track the changes in their differentiation profile as they become more developmentally mature.

The use of iPSC-derived NSPCs for SCI repair can be conducted through an autologous or allogenic transplant (Nagoshi et al., 2019). The autologous transplant requires that iPSC-derived NSPCs are generated from the patient, while an allogeneic transplant can be achieved using a cell bank (Khazaei et al., 2017). Although autologous transplant minimizes graft rejection and the use of immunosuppressants, it may not be as reproducible as using a cell bank. For instance, iPSCs from independent donors differentiated into dorsal forebrain NSPC exhibit varying dorsoventral and rostrocaudal phenotypes and neuronal progeny due to differences in endogenous Wnt signaling activity (Strano et al., 2020b). Therefore, to use iPSC-derived NSPCs in an autologous manner, it is important to ensure that the differentiation of iPSCs reproducibly generates NSPCs with similar regenerative attributes.

Our study generated two developmentally distinct NSPCs populations from three donors and failed to observe reproducibility in the functional or transcriptional phenotypes of iPSC-derived NSPCs. For instance, concerning spinal cord regionalization, iPSC-SC NSPCs from "H25" expressed *HOX* genes at a higher level than "H17" and "H18". Also, iPSC-Br NSPCs from "H18" surprisingly expressed a high level of spinal cord markers *HOXB5*, *HOXD13*, and *HOXB2*, but the same was not observed with "H17" and "H25". With respect to brain regionalization, iPSC-Br NSPCs from "H25" expressed a higher level of brain markers (*LXH2*, *EN1*, *EN2*, *BMP7*, *IRX3*, *OTX1*) compared to "H17" and "H18". Meanwhile, donor "H18" had iPSC-SC NSPCs expressing a higher level of brain markers than iPSC-Br NSPCs.

There was also a lack of reproducibility among iPSC-Br NSPCs from different donors concerning neuronal differentiation and expression of neurogenic genes. Specifically, iPSC-Br NSPCs from "H18" had the lowest expression of neurogenesis-related genes concomitant with the least neuronal differentiation rate compared to "H17" and "H25". Also, iPSC-Br NSPCs from "H18" and "H25" differentiated into astrocytes, but those from "H17" did not. Therefore, iPSC-derived NSPCs with the same regional identity from different donors exhibit variations in their transcriptional and functional profiles. This implies that the autologous transplant of iPSC-derived NSPCs requires NSPCs to be screened for markers, such as a high neurogenic potential, that will ensure more consistent outcomes across patients. Despite these findings, further biological replicates are needed to effectively evaluate the reproducibility of iPSC differentiation protocols.

Accumulating evidence in animal models suggests that primary spinal cord NSPCs or iPSC-SC NSPCs yield the most significant benefits for SCI repair (Kadoya et al., 2016; Kajikawa et al., 2020; Kumamaru, Kadoya et al., 2018). This is likely due to the cellular homology between NSPC grafts and the spinal cord cells (Kadoya et al., 2016). However, how likely are iPSC-SC NSPCs effective in treating human SCI? One way of answering this question could involve comparing the homology between human iPSC-SC NSPCs and bona fide spinal cord NSPCs.

Our study applied a differentiation protocol described by Kumamaru and colleagues (2018) to generate iPSC-SC NSPCs. We determined a discrepancy in the transcriptional and functional attributes of iPSC-SC NSPCs compared to bona fide spinal cord NSPCs. Although both NSPC populations expressed regional markers of the spinal cord, we detected significant differences in their developmental and functional profiles. iPSC-SC NSPCs portrayed features of an early developmental stage, such as enhanced proliferation and genes regulating embryonic development.

On the other hand, bona fide NSPCs exhibited transcriptional signatures of quiescence and differentiated more into neurons and astrocytes.

It would be worthwhile to mature iPSC-SC NSPCs to evaluate if they attain a more significant homology to bona fide NSPCs. Furthermore, the characterization of bona fide NSPCs in this study could serve as a target for future iPSC differentiation protocols to recapitulate. It would also be interesting to characterize iPSC-SC NSPCs generated using alternative iPSC differentiation protocols than the one used in this study (Bianchi et al., 2018b; Kajikawa et al., 2020; Olmsted et al., 2020). Comparing different iPSC-SC NSPCs with bona fide NSPCs could help determine which NSPC populations would best suit SCI repair. However, their transplant in a pre-clinical animal model is needed to properly evaluate whether iPSC-SC or bona fide NSPCs are better suited for SCI repair.

In summary, we generated and characterized iPSC-SC and -Br NSPCs from three organ donors whose spinal cord NSPCs were also evaluated. Importantly, this study is the first to directly compare isogeneic primary and iPSC-derived NSPCs. Using transcriptional and functional analyses, we found that bona fide spinal cord NSPCs and iPSC-derived NSPCs exhibited distinct regional, developmental, and functional phenotypes. Further biological replicates are needed to support these findings. This information may allow for the genetic reprogramming of patient-derived NSPCs that resemble endogenous spinal cord NSPCs, consequently improving cell transplantation's effectiveness for SCI repair.

4.6 Acknowledgements

We are grateful for the families that have consented to our study and permitted the donation of spinal cord tissue from their beloved ones to advance medical science research. We want to thank

Mahmoud Bedawy, Hussam Jabri, Mohammad Alshardan, Michael Taccone, Carolyn Lai, Jessica Rabski, Hesham Ismail, Tongda Li, and Annemarie Dedek for their help with spinal cord harvests. We also thank Stem Core Laboratories and Chris Porter for assisting in RNA sequencing and data analysis. We want to acknowledge the Ottawa Hospital Department of Surgery, Division of Neurosurgery, and TGLN for permitting spinal cord extractions from organ donors. This study was funded by the Ottawa Hospital Department of Surgery Research Program Award. Also, we would like to thank the generous donors to The Ottawa Hospital Foundation.

4.7 Figures and Tables

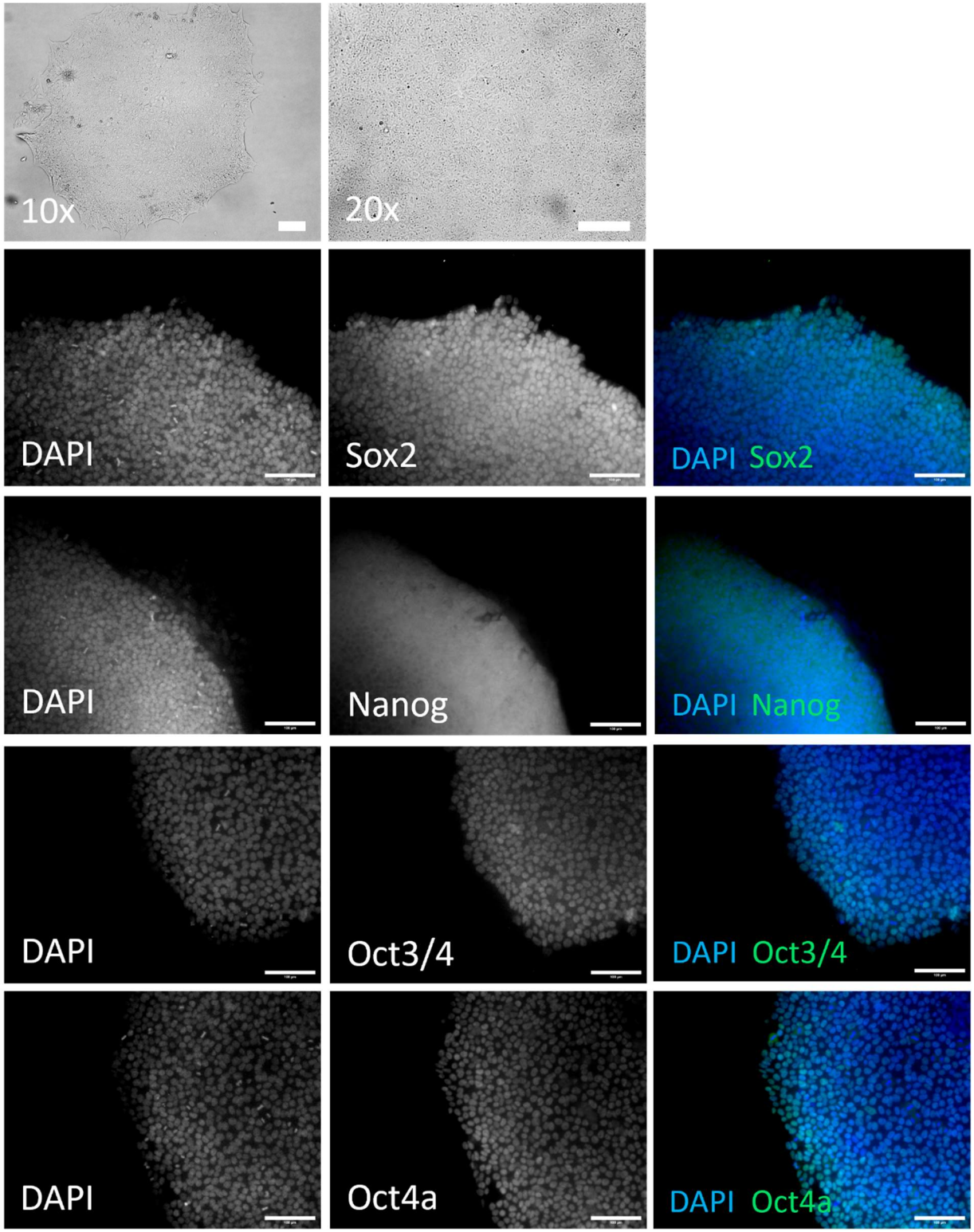

Figure 4.1 Morphological and molecular characterization of iPSCs

iPSC colonies were morphology identified by a defined colony boundary and individual, tightly packed cells with large nuclei using bright field microscopy (upper panels). iPSC colonies were immunopositive for Sox2, Nanog, Oct3/4, and Oct4a (panels in rows two-five). The left panels indicate nuclei (DAPI), the middle panels indicate a particular marker and the right panels are the merged images. Scale bar = 100 µm

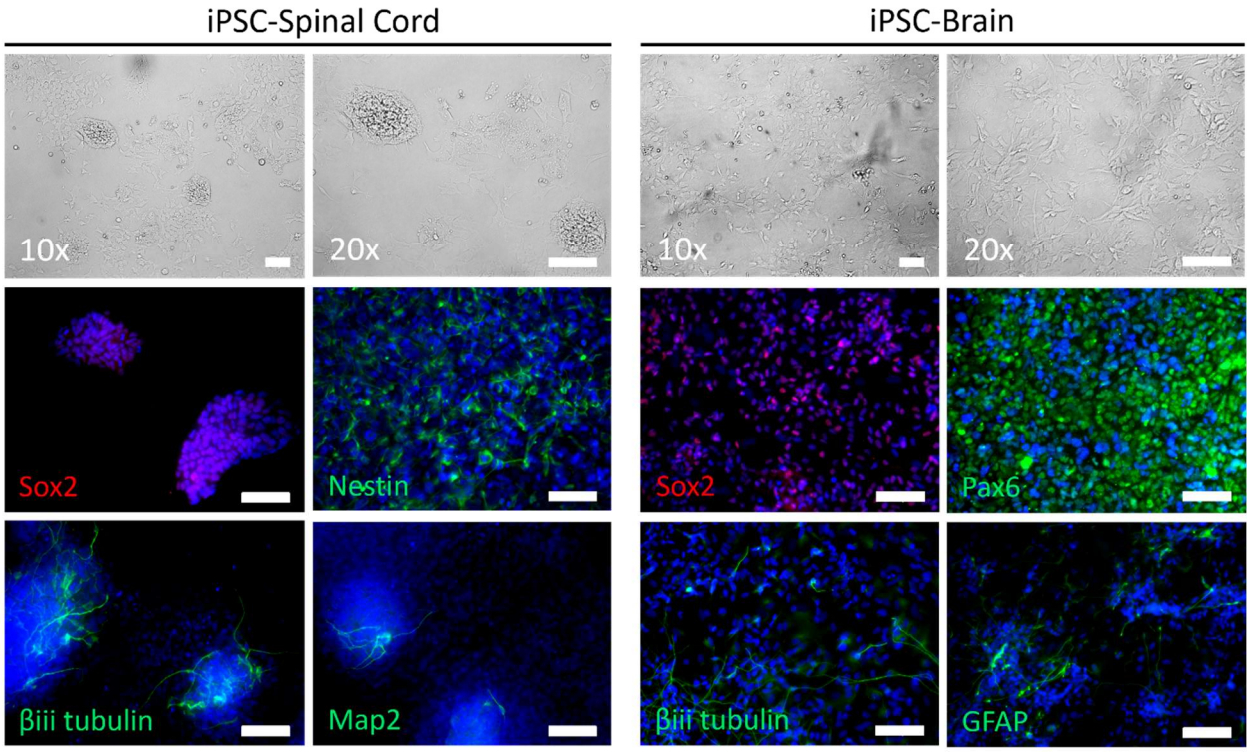

Figure 4.2 Morphological and molecular characterization of iPSC-SC and Br NSPCs

Left panel: iPSC-SC NSPCs were generated via a neuromesodermal progenitor intermediate. Bright-field images (magnified at 10x and 20x) show two types of colonies growth, including flat colonies with no boundaries and adherent neurosphere-like colonies. iPSC-SC NSPCs were

immunostained and labeled positive for neural stem cell markers Sox2 and Nestin. Upon differentiation, iPSC-SC NSPCs expressed the neuronal markers β-iii tubulin and Map2. Right panel: iPSC-Br NSPCs were generated by dual-SMAD inhibition. Bright-field images (magnified at 10x and 20x) show uniformly spread multi-polar cells with spindle-like projections. iPSC-Br NSPCs were immunostained and labeled positive for the neural stem cell marker Sox2 and dorsal marker Pax6. Upon differentiation, iPSC-Br NSPCs expressed the neuronal marker β-iii tubulin and the astrocyte marker GFAP.

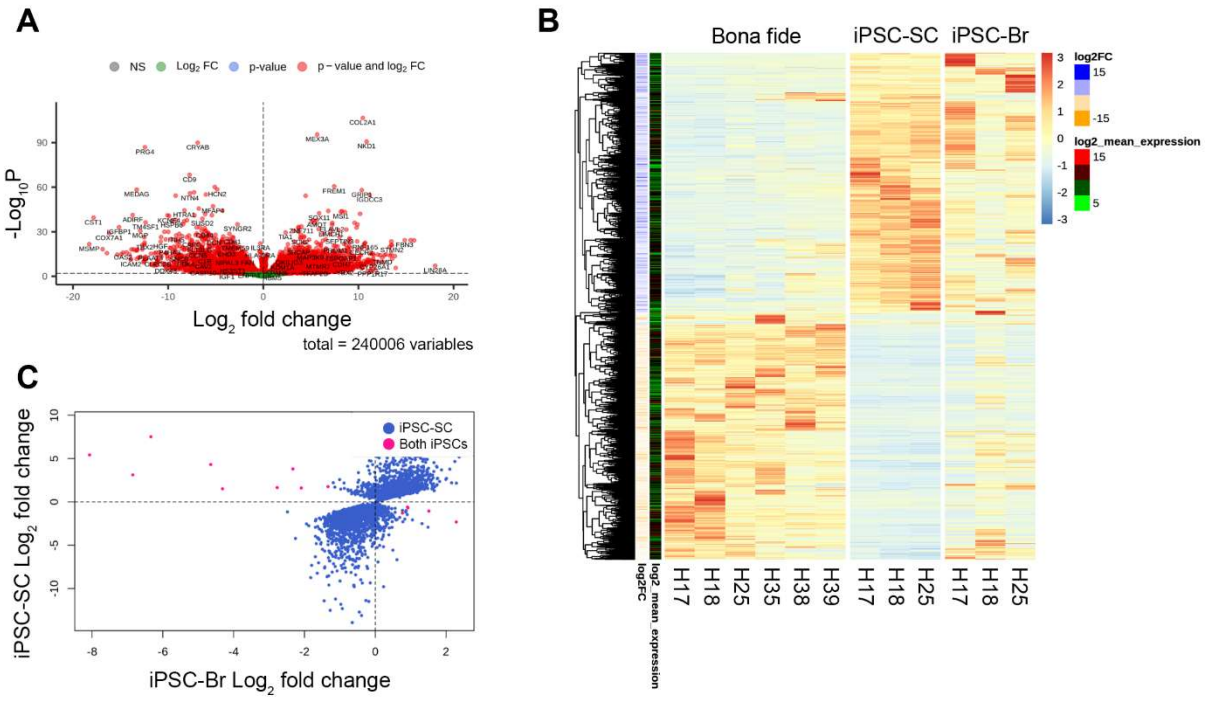

D

Upregulated

LIN28A	FGF3
LIN28B	SP8
NELL2	KIRREL2
FBN3	BEND4
PCDH8	HRH3
DCX	CLVS2
POU4F1	GDAP1L1
STMN2	IGDCC3
CAMKV	CUX2
SFRP2	OLIG3
SLC7A3	SLC16A10
RAB3C	FOXB1
ST8SIA3	NKD1
LIX1	CACNA1E
TNMD	KCNK5
FGF9	SYT2
FAM181A	RNF165
VRTN	NEUROD4
CYP26A1	SALL4
TERT	C2CD4C
DSC3	RFX4
SYT4	ADGRG2
DSC2	NPY
PPP1R17	COL2A1
SYN3	GRIP1

Downregulated

CST1	PLAAT4
APOL3	MMP1
COX7A1	NKAPL
XAF1	GSTM5
IGFBP1	RTP4
ESM1	BTC
OAS2	CLEC2B
BHMT2	ACKR4
ICAM2	HGF
SLC14A1	OAS1
ADIRF	CST4
MEDAG	S100A6
OR51E2	RXFP1
ANGPTL5	OASL
MGP	VSIR
RNF128	DDX43
CST2	TRPV2
C2CD6	CMKLR1
CYTIP	TSLP
TBX2	S100A4
CCDC68	KCNE4
PRG4	P4HA3
TM4SF1	HHEX
IL1RL1	FPR1
SERPINA3	SRGN

Figure 4.3 iPSC-SC and bona fide NSPCs differentially express 8,737 genes

(A) Volcano plot of genes that are enriched in iPSC-SC (>0) and bona fide (<0) NSPCs. Red dots indicate single DE genes with a fold change ≥2 and a p-value <0.05. A total of 24,006 genes were analyzed. (B) Heatmap and hierarchical clustering of DE genes between iPSC-SC and bona fide NSPCs from (A). The color scale indicates the relative expression: red represents an upregulation, and blue represents a downregulation in iPSC-SC NSPCs. (C) Scatter plot of DE genes exclusively in iPSC-SC NSPCs relative to bona fide NSPCs. A total of 4,137 genes with a fold change≥2 and a p-value <0.05 are shown. Blue dots indicate DE genes only in iPSC-SC NSPCs. (D) The top 50 DE genes upregulated or downregulated in iPSC-SC NSPCs relative to bona fide NSPCs. n=6 bona fide, n=3 iPSC-SC.

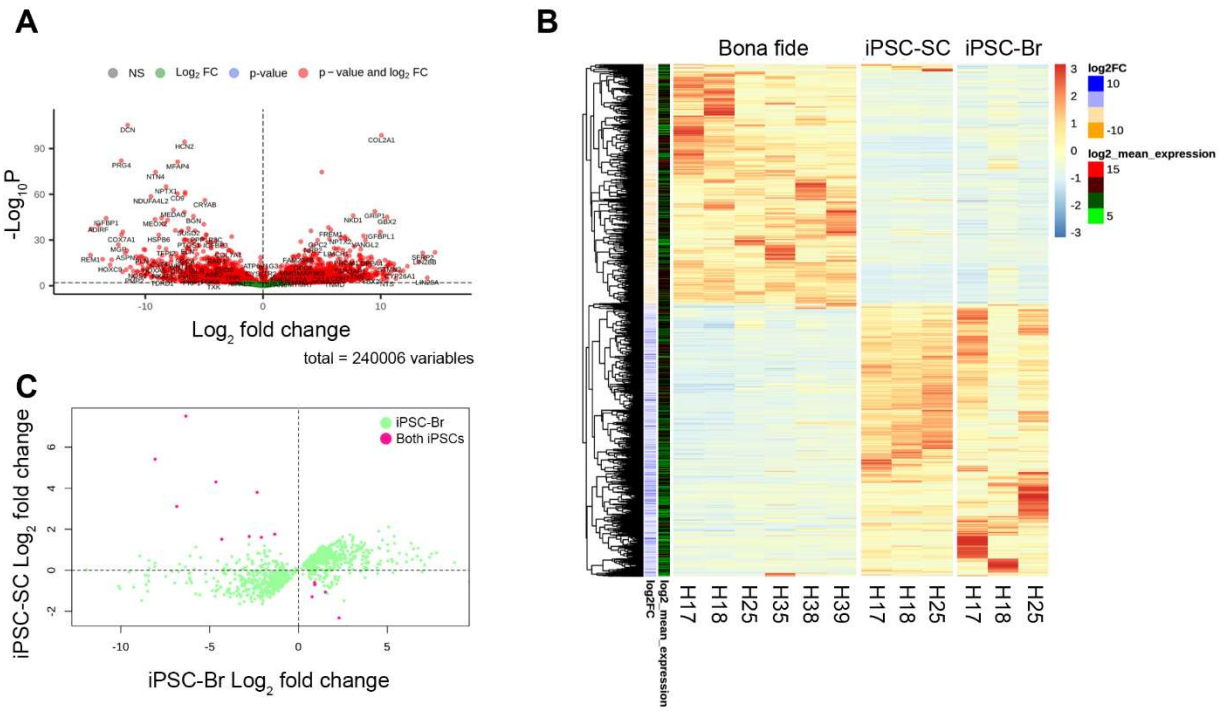

D

Upregulated

NELL2	SYN3
LIN28A	RPRML
LIN28B	UBXN10
SFRP2	TNFRSF8
SLC7A3	CUX2
SYT2	COL2A1
CYP26A1	VRTN
PCDH8	IGFBPL1
RAB3C	FOXB1
KCNK5	TNNT2
TRIM71	RASSF10
BTBD17	FAM181A
MMP9	RHOH
STMN2	AMER2
CAMKV	GRIP1
DSC2	DCX
GDAP1L1	BLACAT1
RNF43	INSM1
GBX2	IL2RB
NTS	ST8SIA3
FBN3	DPPA4
SLC18A3	DCAF12L1
APLNR	ZMAT4
C2CD4C	YBX2
PPP1R17	COL9A1

Downregulated

REM1	C1QTNF7
CST1	CST2
ADIRF	HOXA10
ITIH2	KRBOX1
IGFBP1	CHRM2
HOXC9	ITGBL1
ANGPTL5	NUPR1
MGP	RXFP1
PRG4	SDR42E1
COX7A1	PRELP
HOXB8	OMD
ASPN	CYTIP
FOXD2	OSR2
DCN	NDUFA4L2
FHL5	HOXC6
HTR2A	TDRD9
PMP2	HOXB7
TBX2	DPT
NOS1	ACKR4
EMX2	HOXA5
TSPAN8	MSMP
VSIR	MEOX2
FABP4	IQSEC3
OR51E2	NTN4
PLN	HOXA3

Figure 4.4 iPSC-Br and bona fide NSPCs differentially express 5,555 genes

(A) Volcano plot of genes that are enriched in iPSC-Br (>0) and bona fide (<0) NSPCs. Red dots indicate single DE genes with a fold change ≥2 and a p-value <0.05. A total of 24,006 genes were analyzed. (B) Heatmap and hierarchical clustering of DE genes between iPSC-Br and bona fide NSPCs from (A). The color scale indicates the relative expression: red represents an upregulation, and blue represents a downregulation in iPSC-Br NSPCs. (C) Scatter plot of DE genes exclusively in iPSC-Br NSPCs relative to bona fide NSPCs. 955 genes with a fold change≥2 and a p-value <0.05 are shown. Green dots indicate DE genes only in iPSC-Br NSPCs. (D) The top 50 DE genes upregulated or downregulated in iPSC-Br NSPCs relative to bona fide NSPCs. n=6 bona fide, n=3 iPSC-Br.

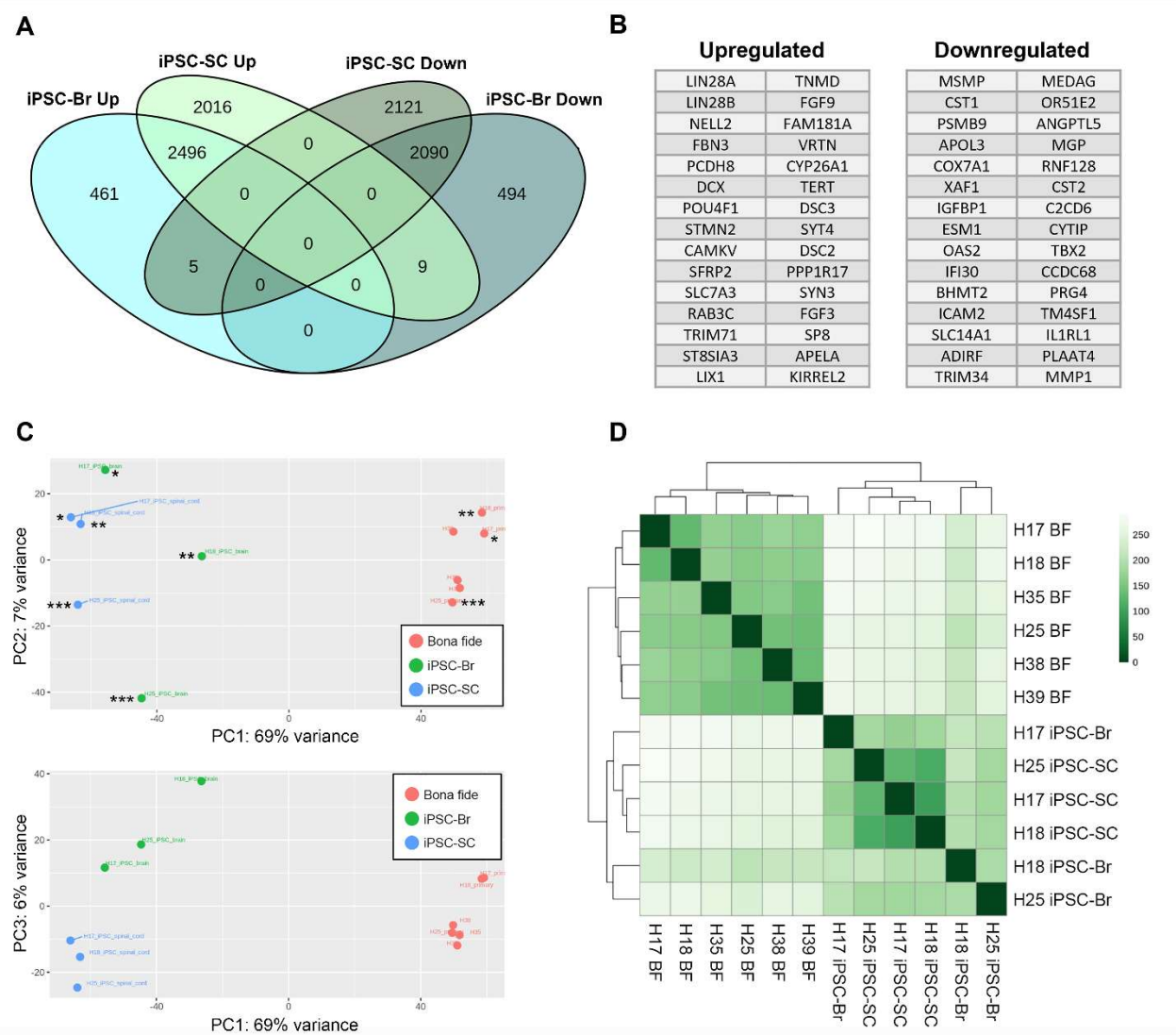

Upregulated	
LIN28A	TNMD
LIN28B	FGF9
NELL2	FAM181A
FBN3	VRTN
PCDH8	CYP26A1
DCX	TERT
POU4F1	DSC3
STMN2	SYT4
CAMKV	DSC2
SFRP2	PPP1R17
SLC7A3	SYN3
RAB3C	FGF3
TRIM71	SP8
ST8SIA3	APELA
LIX1	KIRREL2

Downregulated	
MSMP	MEDAG
CST1	OR51E2
PSMB9	ANGPTL5
APOL3	MGP
COX7A1	RNF128
XAF1	CST2
IGFBP1	C2CD6
ESM1	CYTIP
OAS2	TBX2
IFI30	CCDC68
BHMT2	PRG4
ICAM2	TM4SF1
SLC14A1	IL1RL1
ADIRF	PLAAT4
TRIM34	MMP1

Figure 4.5 The transcriptomes of iPSC-Br and bona fide NSPCs are more similar than iPSC-SC and bona fide NSPCs

(A) Venn diagram of DE genes in both iPSC-SC and -Br NSPCs relative to bona fide NSPCs, including directionality (upregulation or downregulation). 4,600 genes were DE in both iPSC-SC and -Br NSPCs with a fold change≥2 and q-value<0.05. (B) The top 30 genes DE in the same direction (upregulation or downregulation) in both iPSC-SC and -Br NSPCs relative to bona fide NSPCs. (C) Principal component analysis (PCA) using the 500 most variable genes between bona

fide, iPSC-SC, and -Br NSPCs. The PCA on top includes PC1 vs. PC2, which accounts for 76% variance, and the PCA on the bottom includes PC1 vs. PC3, which accounts for 75% variance. The red, blue, and green dots indicate biological replicates of bona fide, iPSC-SC, and iPSC-Br NSPCs. In the top panel, *, **, and *** represent H17, H18, and H25, respectively. (D) Hierarchical clustering analysis for all transcripts (24,006 genes) found in common among bona fide, iPSC-SC, and -Br NSPCs. n=6 bona fide, n=3 iPSC-SC, n=3 iPSC-Br.

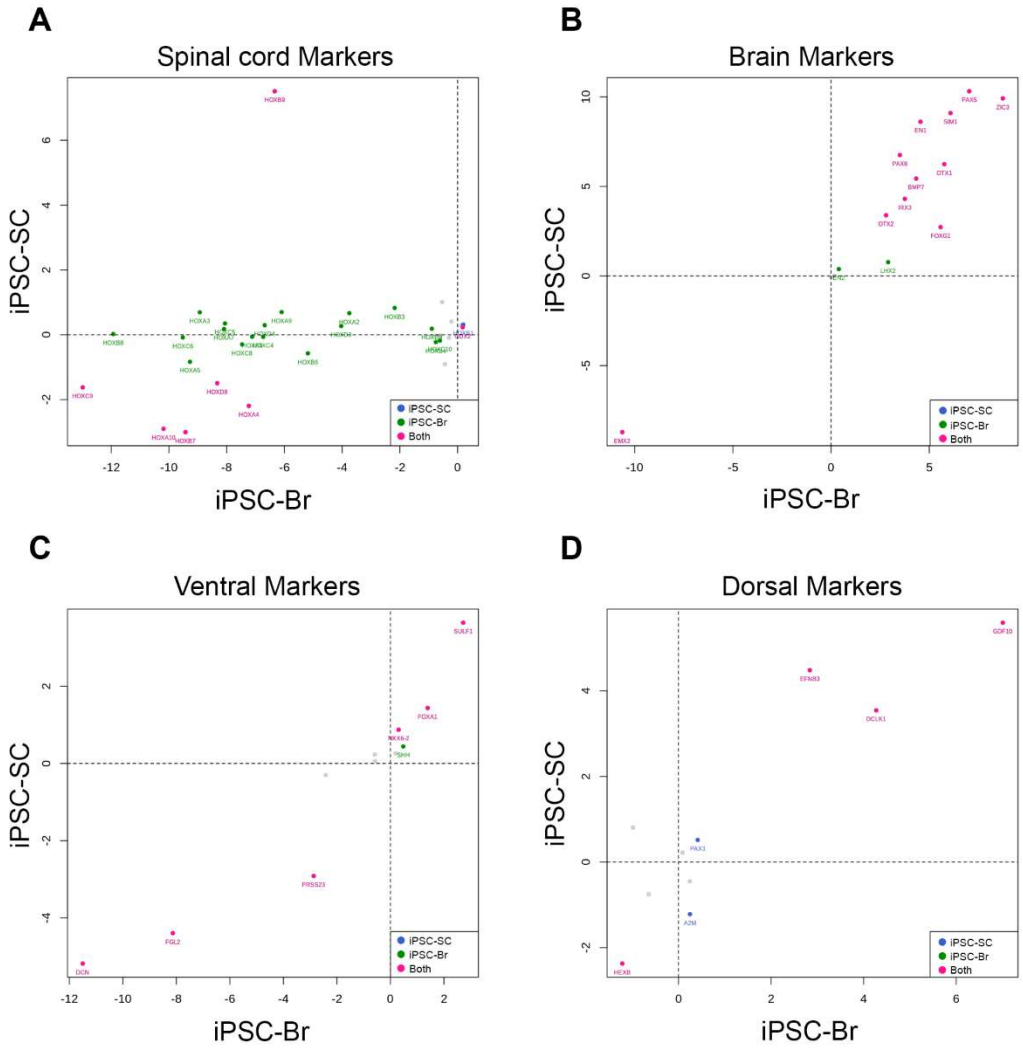

Figure 4.6 iPSC-Br and bona fide NSPCs express markers exclusive to their regional position in the CNS, while iPSC-SC NSPCs express markers for both the spinal cord and brain.

Scatter plots of DE genes exclusively in iPSC-SC, iPSC-Br, or both iPSC-derived NSPCs relative to bona fide NSPCs. A select number of genes that are markers for (A) spinal cord, (B) brain, (C) ventral, and (D) dorsal regions are shown**.** Genes that are DE with a fold change≥2 or ≤2 and a q-value <0.05 are indicated by colored dots**.** Blue dots indicate DE genes only in iPSC-SC NSPCs, blue dots indicate DE genes only in iPSC-Br NSPCs, and pink dots indicate DE genes in both iPSC-SC and -Br NSPCs. A heatmap and hierarchical clustering of the same genes are shown in Figure S4.3. n=6 bona fide, n=3 iPSC-SC, n=3 iPSC-Br.

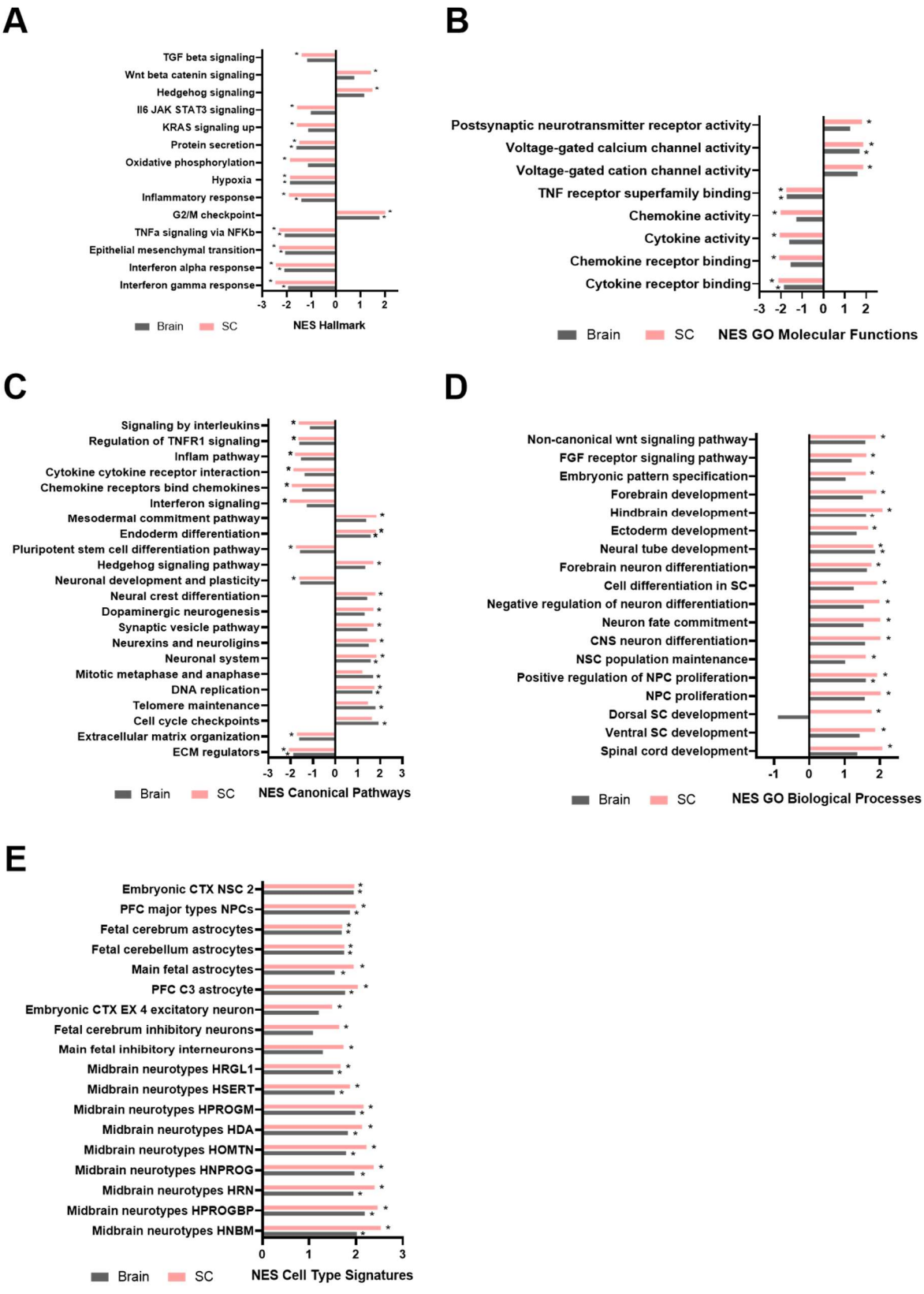
A
TGF beta signaling
Wnt beta catenin signaling
Hedgehog signaling
Il6 JAK STAT3 signaling
KRAS signaling up
Protein secretion
Oxidative phosphorylation
Hypoxia
Inflammatory response
G2/M checkpoint
TNFa signaling via NFKb
Epithelial mesenchymal transition
Interferon alpha response
Interferon gamma response
-3 -2 -1 0 1 2
Brain SC
NES Hallmark
B
Postsynaptic neurotransmitter receptor activity
Voltage-gated calcium channel activity
Voltage-gated cation channel activity
TNF receptor superfamily binding
Chemokine activity
Cytokine activity
Chemokine receptor binding
Cytokine receptor binding
-3 -2 -1 0 1 2
Brain SC
NES GO Molecular Functions
C
Signaling by interleukins
Regulation of TNFR1 signaling
Inflam pathway
Cytokine cytokine receptor interaction
Chemokine receptors bind chemokines
Interferon signaling
Mesodermal commitment pathway
Endoderm differentiation
Pluripotent stem cell differentiation pathway
Hedgehog signaling pathway
Neuronal development and plasticity
Neural crest differentiation
Dopaminergic neurogenesis
Synaptic vesicle pathway
Neurexins and neuroligins
Neuronal system
Mitotic metaphase and anaphase
DNA replication
Telomere maintenance
Cell cycle checkpoints
Extracellular matrix organization
ECM regulators
-3 -2 -1 0 1 2 3
Brain SC
NES Canonical Pathways
D
Non-canonical wnt signaling pathway
FGF receptor signaling pathway
Embryonic pattern specification
Forebrain development
Hindbrain development
Ectoderm development
Neural tube development
Forebrain neuron differentiation
Cell differentiation in SC
Negative regulation of neuron differentiation
Neuron fate commitment
CNS neuron differentiation
NSC population maintenance
Positive regulation of NPC proliferation
NPC proliferation
Dorsal SC development
Ventral SC development
Spinal cord development
-1 0 1 2
Brain SC
NES GO Biological Processes
E
Embryonic CTX NSC 2
PFC major types NPCs
Fetal cerebrum astrocytes
Fetal cerebellum astrocytes
Main fetal astrocytes
PFC C3 astrocyte
Embryonic CTX EX 4 excitatory neuron
Fetal cerebrum inhibitory neurons
Main fetal inhibitory interneurons
Midbrain neurotypes HRGL1
Midbrain neurotypes HSERT
Midbrain neurotypes HPROGM
Midbrain neurotypes HDA
Midbrain neurotypes HOMTN
Midbrain neurotypes HNPROG
Midbrain neurotypes HRN
Midbrain neurotypes HPROGBP
Midbrain neurotypes HNBM
0 1 2 3
Brain SC
NES Cell Type Signatures

Figure 4.7 iPSC-derived NSPCs express gene sets related to pathways, functions, cell type signatures, and biological processes that are similarly upregulated or downregulated relative to bona fide NSPCs

Gene set enrichment was analyzed using the GSEA preranked algorithm and ran against a subset of available gene sets from MSigDB. A normalized enrichment score (NES) was calculated for iPSC-SC and iPSC-Br NSPCs relative to bona fide NSPCs. The NES was used to compare gene sets for the categories (A) hallmark gene sets, (B) GO molecular functions, (C) canonical pathways, (D) GO biological processes, and (E) cell-type signatures. Gene sets with a significant positive or negative NES are indicated by *, representing a q-value<0.05. iPSC-SC and iPSC-Br are indicated by pink and grey bars, respectively. n=6 bona fide, n=3 iPSC-SC, n=3 iPSC-Br. The full report can be accessed here.

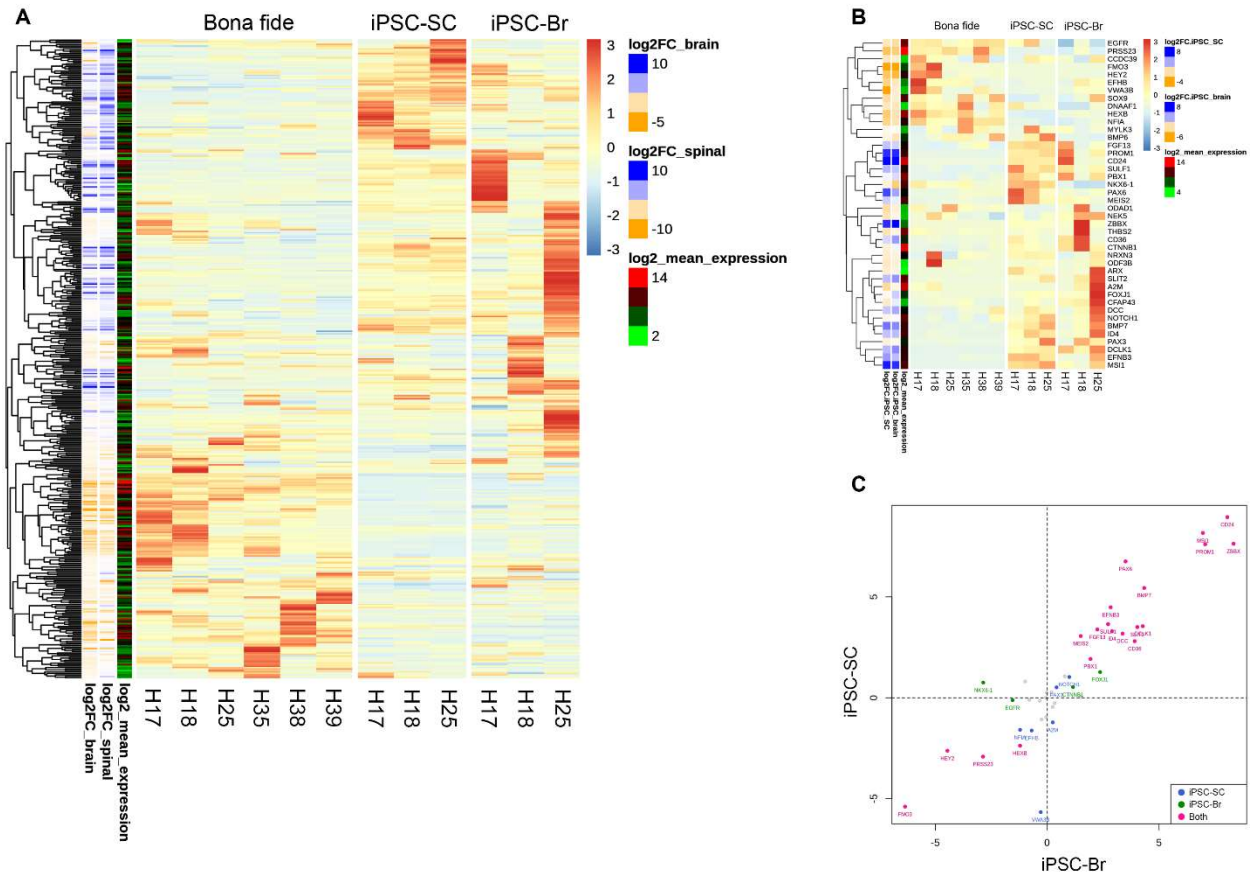

Figure 4.8 Adult human spinal cord ependymal cells undergo transcriptional changes when cultured *in vitro*.

(A) Heatmap and hierarchical clustering of DE ependymal-specific genes between bona fide, iPSC-SC, and -Br NSPCs. The dataset of ependymal genes was obtained from single nucleus RNA sequencing of the adult human spinal cord (n=7). The color scale indicates the relative expression: red represents an upregulation, and blue represents a downregulation relative to the ependymal cell's single nucleus RNA sequencing data. (B) Heatmap and hierarchical clustering of 42 genes that are markers for ependymal cells. The color scale indicates the relative expression: red represents an upregulation, and blue represents a downregulation. (C) Scatter plot of ependymal markers in (B) exclusively DE in iPSC-SC, iPSC-Br, or both iPSC-derived NSPCs relative to bona

fide NSPCs. Genes that are DE with a fold change≥2 or ≤2 and a q-value <0.05 are indicated by colored dots**.** Blue dots indicate DE genes only in iPSC-SC NSPCs, blue dots indicate DE genes only in iPSC-Br NSPCs, and pink dots indicate DE genes in both iPSC-SC and -Br NSPCs. n=6 bona fide, n=3 iPSC-SC, n=3 iPSC-Br.

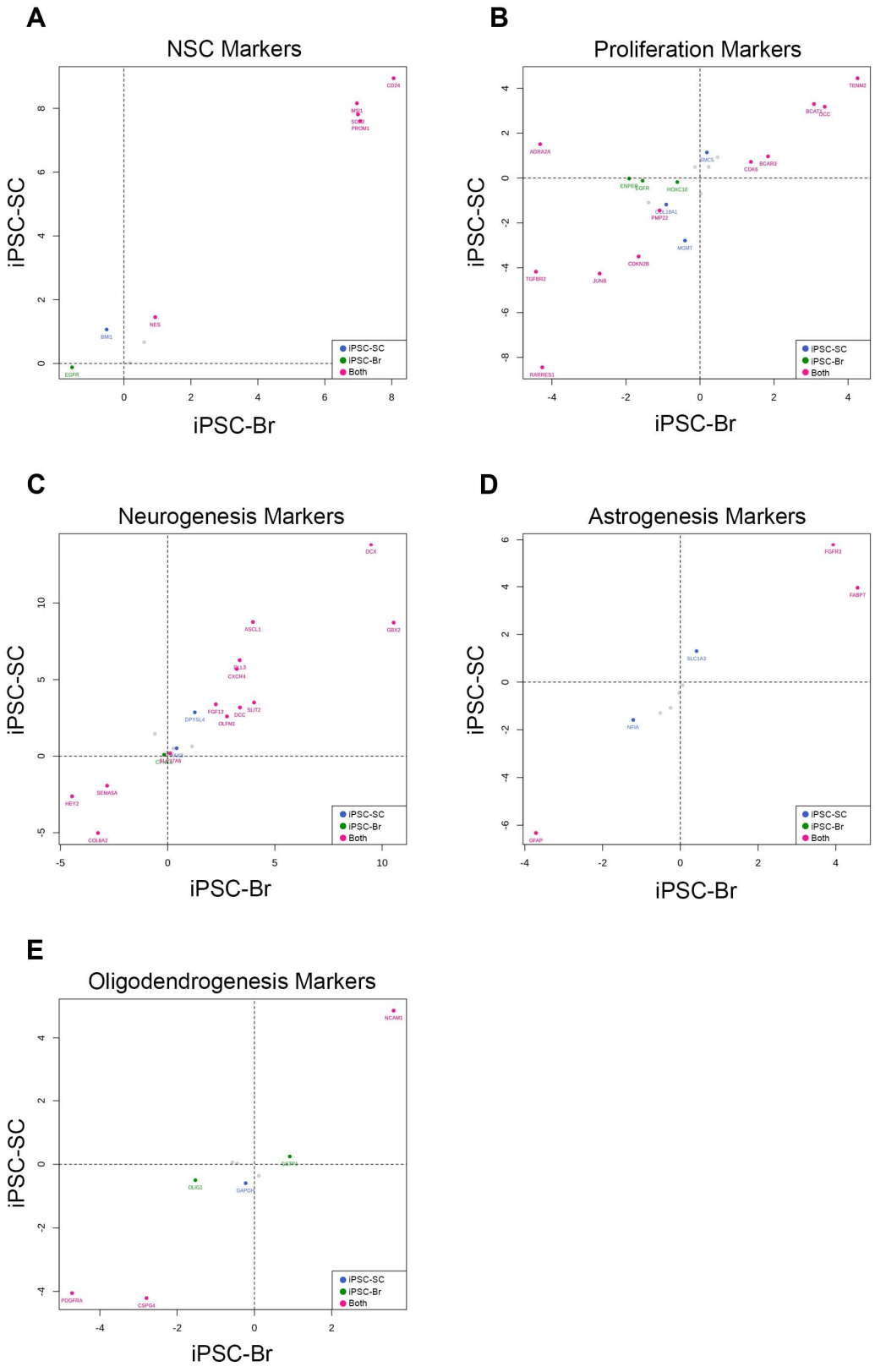
A
NSC Markers
iPSC-SC
iPSC-Br
CD24
MSI1
SOX2
PROM1
NES
BMI1
EGFR
iPSC-SC
iPSC-Br
Both
B
Proliferation Markers
iPSC-SC
iPSC-Br
TENM2
BCAT1
DCC
ADRA2A
BMCS
BCAR3
CDK6
ENPEP
EGFR
HOXC10
IL18A1
PMP22
MGMT
CDKN2B
TGFBR2
JUN8
RARRES1
iPSC-SC
iPSC-Br
Both
C
Neurogenesis Markers
iPSC-SC
iPSC-Br
DCX
ASCL1
GBX2
GJA1
CXCR4
FGF13
DCC
SLIT2
DPYSL4
OLFM1
SEMA5A
HEY2
COL6A2
iPSC-SC
iPSC-Br
Both
D
Astrogenesis Markers
iPSC-SC
iPSC-Br
FGFR3
FABP7
SLC1A3
NFIA
GFAP
iPSC-SC
iPSC-Br
Both
E
Oligodendrogenesis Markers
iPSC-SC
iPSC-Br
NCAM1
OLIG1
GAPDH
PDGFRA
CSPG4
iPSC-SC
iPSC-Br
Both

Figure 4.9 Genetic markers for NSPCs and their functional behaviour are differentially expressed between bona fide, iPSC-SC, and iPSC-Br NSPCs

Scatter plots of DE genes exclusively in iPSC-SC, iPSC-Br, or both iPSC-derived NSPCs relative to bona fide NSPCs. A select number of genes that are markers for (A) neural stem cells (NSCs), (B) proliferation, (C) neurogenesis, (D) astrogenesis, and (E) oligodendrogenesis are shown. Genes that are DE with a fold change≥2 or ≤2 and a q-value <0.05 are indicated by colored dots. Blue dots indicate DE genes only in iPSC-SC NSPCs, blue dots indicate DE genes only in iPSC-Br NSPCs, and pink dots indicate DE genes in both iPSC-SC and -Br NSPCs. A heatmap and hierarchical clustering of the same genes are shown in Figure S4.5. n=6 bona fide, n=3 iPSC-SC, n=3 iPSC-Br.

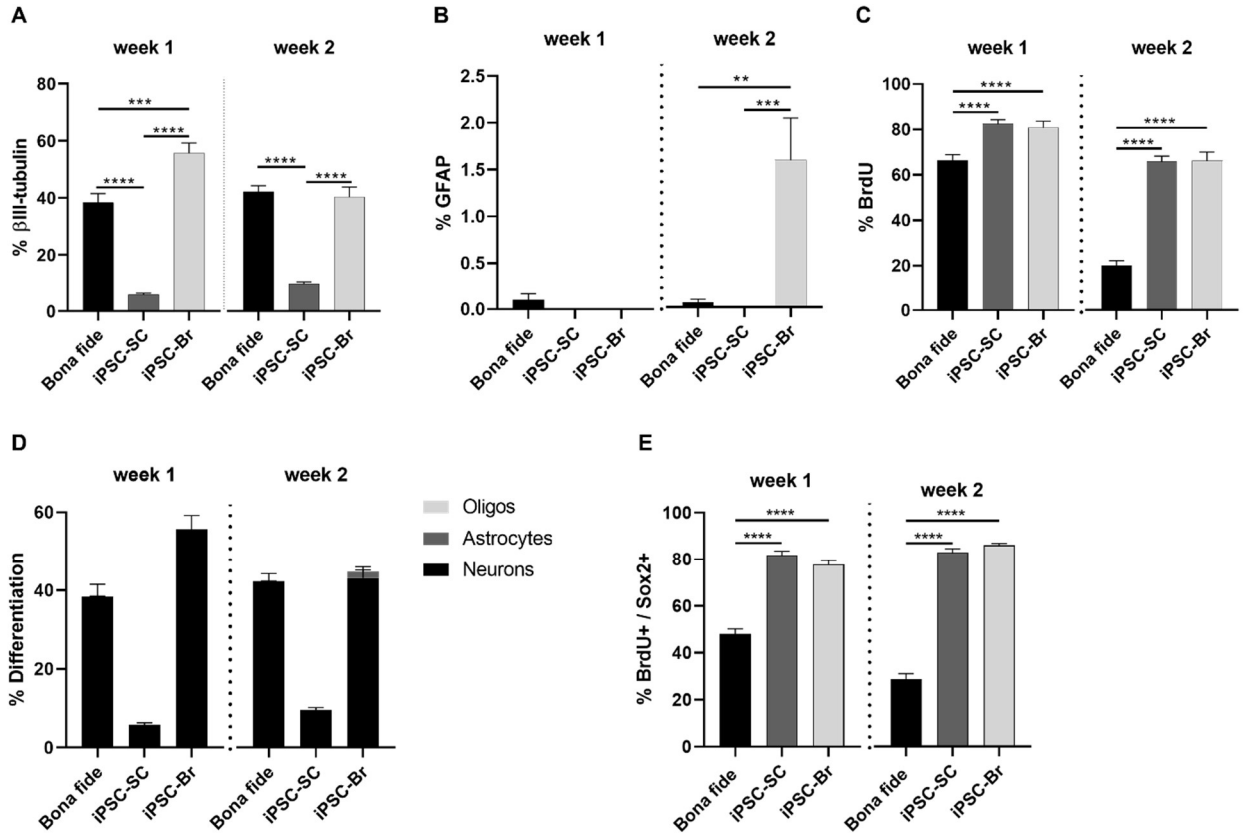

Figure 4.10 The differentiation and proliferation profiles of bona fide NSPCs are not recapitulated by iPSC-derived NSPCs

NSPCs were treated for one or two weeks in conditions that promote (A-D) differentiation or (E) proliferation. (A) The percentage of βiii tubulin$^+$ neurons generated from bona fide and iPSC-Br NSPCs was greater than iPSC-SC NSPCs. (B) percentage of GFAP$^+$ astrocytes generated from iPSC-Br NSPCs was greater than both bona fide and iPSC-SC NSPCs. (C) The percentage of BrdU$^+$ cells indicates that iPSC-derived NSPCs proliferate at a greater rate compared to bona fide NSPCs in differentiation conditions. (D) The overall differentiation profiles of bona fide, iPSC-SC, and -Br NSPCs. (E) The percentage of BrdU$^+$/Sox2$^+$ NSPCs indicates that both iPSC-derived NSPCs exhibited a higher self-renewal rate than bona fide NSPCs. mean ± s.e.m; **p<0.01, ***p<0.001, ****p<0.0001. n=3 bona fide, n=3 iPSC-SC, n=3 iPSC-Br.

Table 4.1 Organ donor demographic information including age, sex, cause of death, time from brain death to organ donation, and time from cardiac arrest to spinal cord harvest. M: male, F: female, CA: cardiac arrest, BD: brain death, SD: standard deviation

Age (mean ± SD, range)	Sex	Cause of death	Time from BD to organ donation (mean ± SD, range)	Time from CA to spinal cord harvest (mean ± SD, range)
37.3 ± 22.4, 22-63 years old	2M 1F	Traumatic brain injury Multicentered intracerebral hemorrhage Subdural hematoma	28.7 ± 10.2, 17-36 hours	133 ± 26.9, 103-155 minutes

Table 4.2 Description of the bona fide, iPSC-SC, and -Br NSPC samples used for RNA sequencing. M: male, F: female, DIV: days *in vitro*

Specimen	Age	Sex	Cell type	DIV
H17	66	M	Primary	68
			iPSC-Brain	28
			iPSC-Spinal Cord	28
H18	22	M	Primary	83
			iPSC-Brain	28
			iPSC-Spinal Cord	28
H25	27	F	Primary	35
			iPSC-Brain	28
			iPSC-Spinal Cord	28

Table 4.3 The number and percentage of differentially expressed (DE) genes between bona fide, iPSC-SC, and -Br NSPCs at a false discovery rate (q-value) of 5%. A total of 24,006 genes were used in this analysis.

	iPSC-Brain vs Primary	iPSC-SC vs Primary	iPSC-Brain vs iPSC-SC
Number of DE genes	5,555	8,737	2,015
% DE genes	23%	36%	8%

4.8 Supplementary Figures

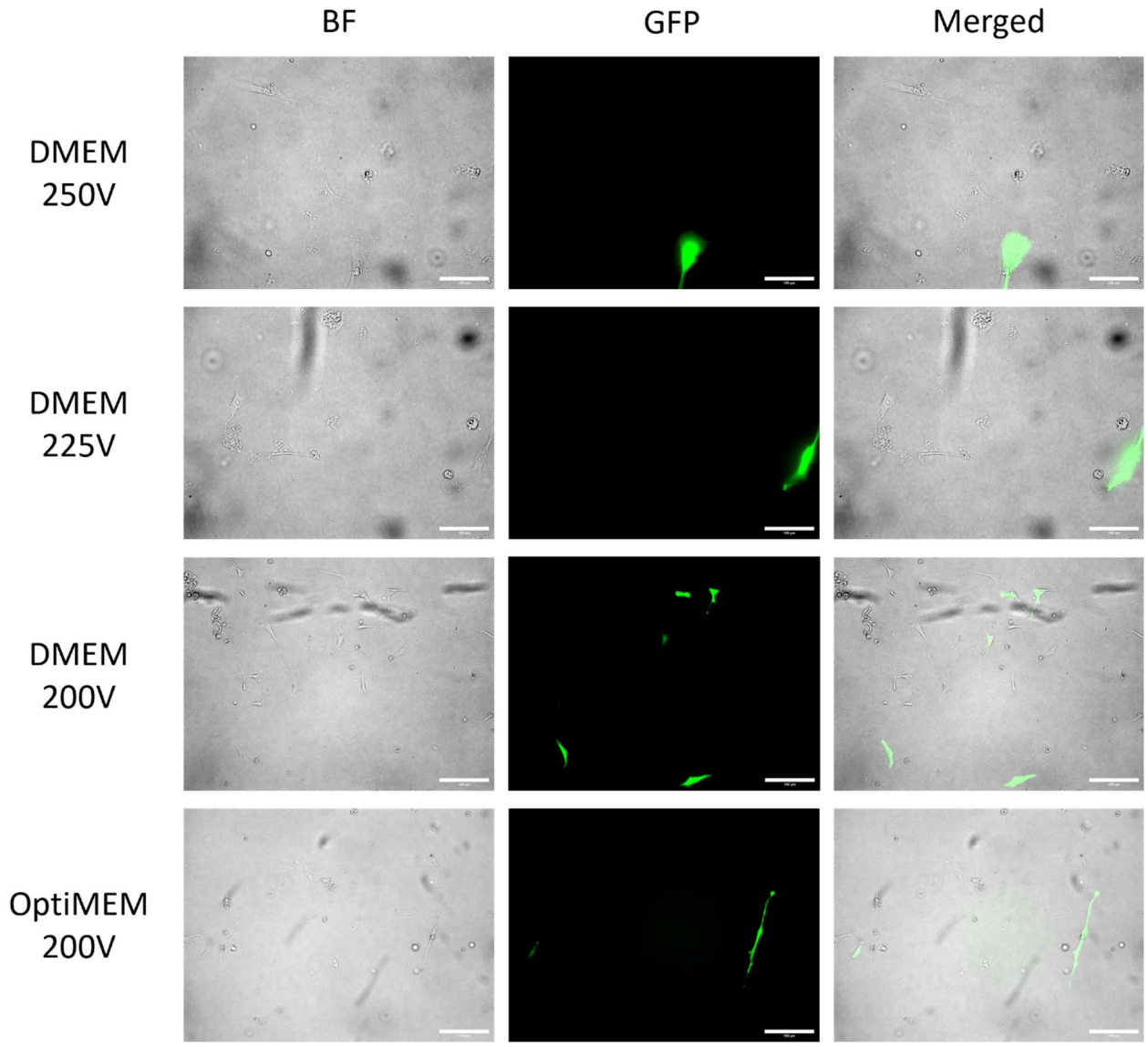

Figure S4.1 Optimization of electroporation parameters

Secondary dermal fibroblasts were electroporated to achieve episomal transfection. A plasmid concentration of 20 µg/mL was used while the voltage and electroporation buffer were altered for optimization. Either DMEM/F12 or Opti-MEM was used as an electroporation buffer. The electroporation voltage was tested at 200V, 225V, 250V, and 300V (not shown). Fibroblasts were

electroporated with two pulses lasting 20 ms each pulse. The left panels are bright field images, the middle panels are GFP, and the right panels are merged images. Scale bar = 100 μm

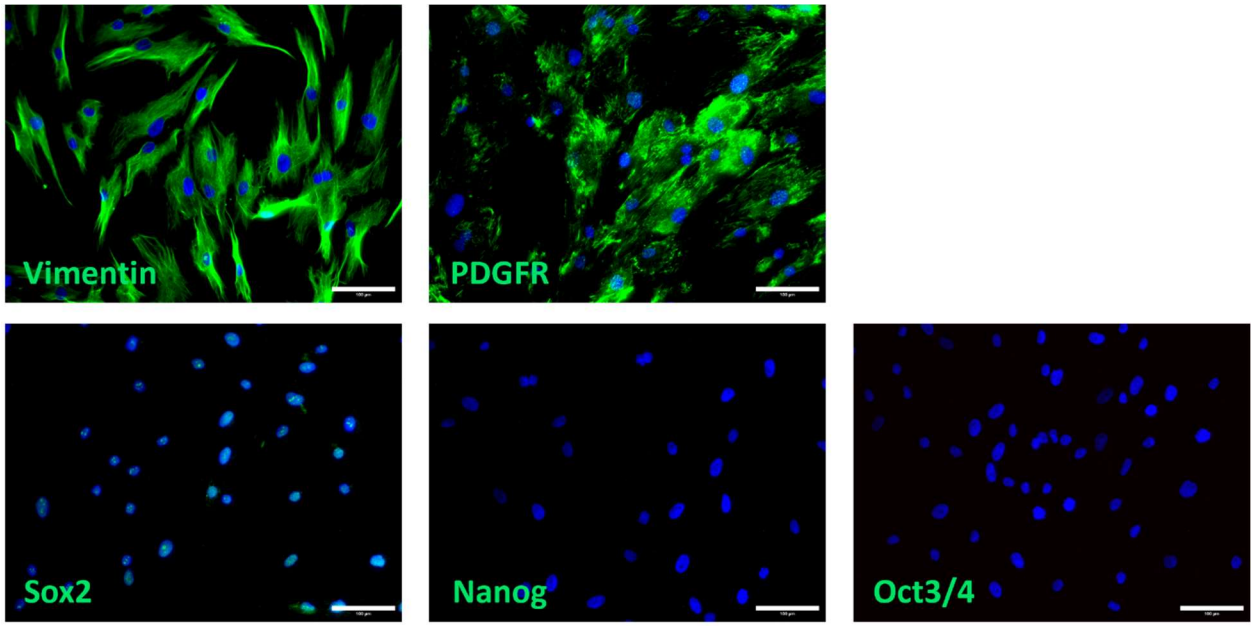

Figure S4.2 Positive and negative immunostaining of dermal fibroblasts

Secondary dermal fibroblasts were immunostained for markers of fibroblasts, including Vimentin and PDGFR (top panels), and markers of pluripotent stem cells, including Sox2, Nanog, and Oct3/4. Fibroblasts showed positive labeling for Vimentin, PDGFR, and Sox2 but negative for Nanog and Oct3/4.

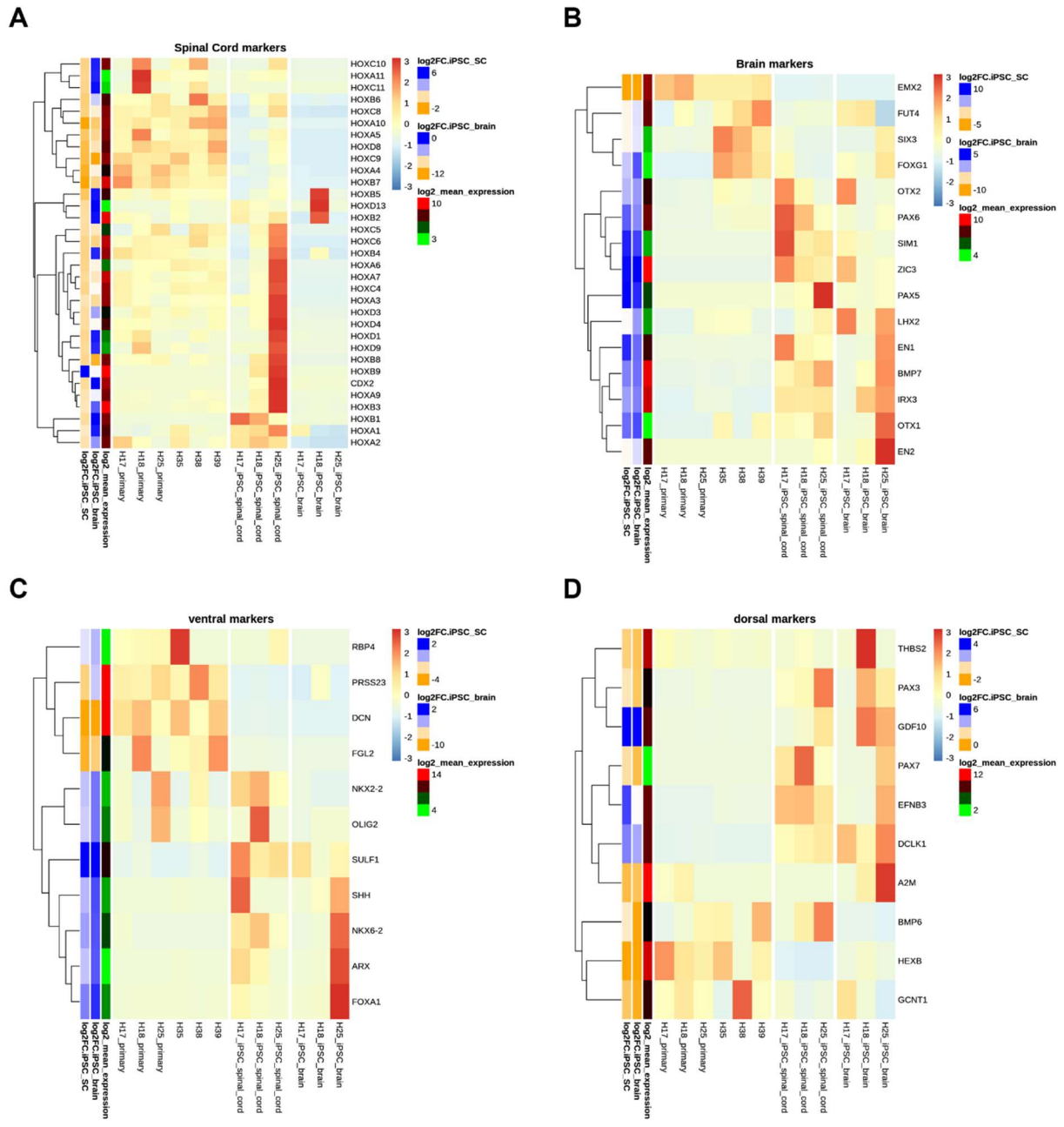

Figure S4.3 Relative expression of genes related to regionalization within the CNS

Heatmaps and hierarchical clustering of genes that are markers for (A) spinal cord, (B) brain, (C) ventral, and (D) dorsal regions are shown**.** The color scale indicates the relative expression: red represents an upregulation, and blue represents a downregulation. n=6 bona fide, n=3 iPSC-SC, n=3 iPSC-Br.

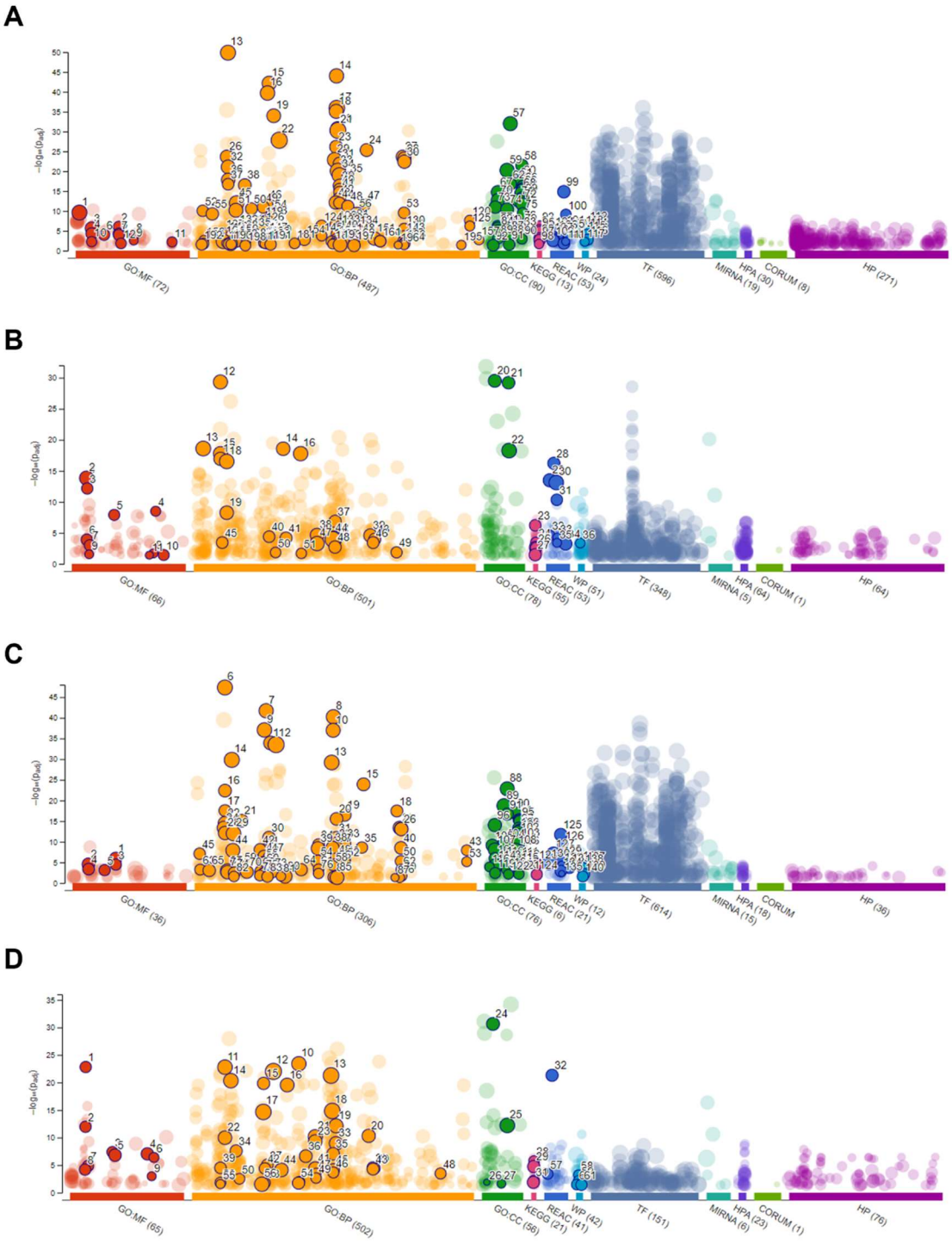
A
B
C
D
GO:MF (72)
GO:BP (487)
GO:CC (90)
KEGG (13)
REAC (53)
WP (24)
TF (596)
MIRNA (19)
HPA (30)
CORUM (8)
HP (271)
GO:MF (66)
GO:BP (501)
GO:CC (78)
KEGG (55)
REAC (53)
WP (51)
TF (348)
MIRNA (5)
HPA (64)
CORUM (1)
HP (64)
GO:MF (36)
GO:BP (306)
GO:CC (76)
KEGG (6)
REAC (21)
WP (12)
TF (614)
MIRNA (15)
HPA (18)
CORUM
HP (36)
GO:MF (65)
GO:BP (502)
GO:CC (56)
KEGG (21)
REAC (41)
WP (42)
TF (151)
MIRNA (6)
HPA (23)
CORUM (1)
HP (76)

Figure S4.4 Functional enrichment analysis of differentially expressed genes between bona fide, iPSC-SC, and -Br NSPCs

Gene set enrichment was analyzed using gProfiler for the 24,006 genes found in common among NSPCs. Gene sets related to the CNS are shown to be (A) upregulated in iPSC-SC NSPCs, (B) downregulated in iPSC-SC NSPCs, (C) upregulated in iPSC-Br NSPCs, (D) downregulated in iPSC-Br NSPCs. Bold numbered circles are gene sets that are DE with a $\log_2$FC greater than or less than two and a false discovery rate q-value<0.01. More information for each gene set can be seen in Tables S2 and S3 in the order they are listed. n=6 bona fide, n=3 iPSC-SC, n=3 iPSC-Br.

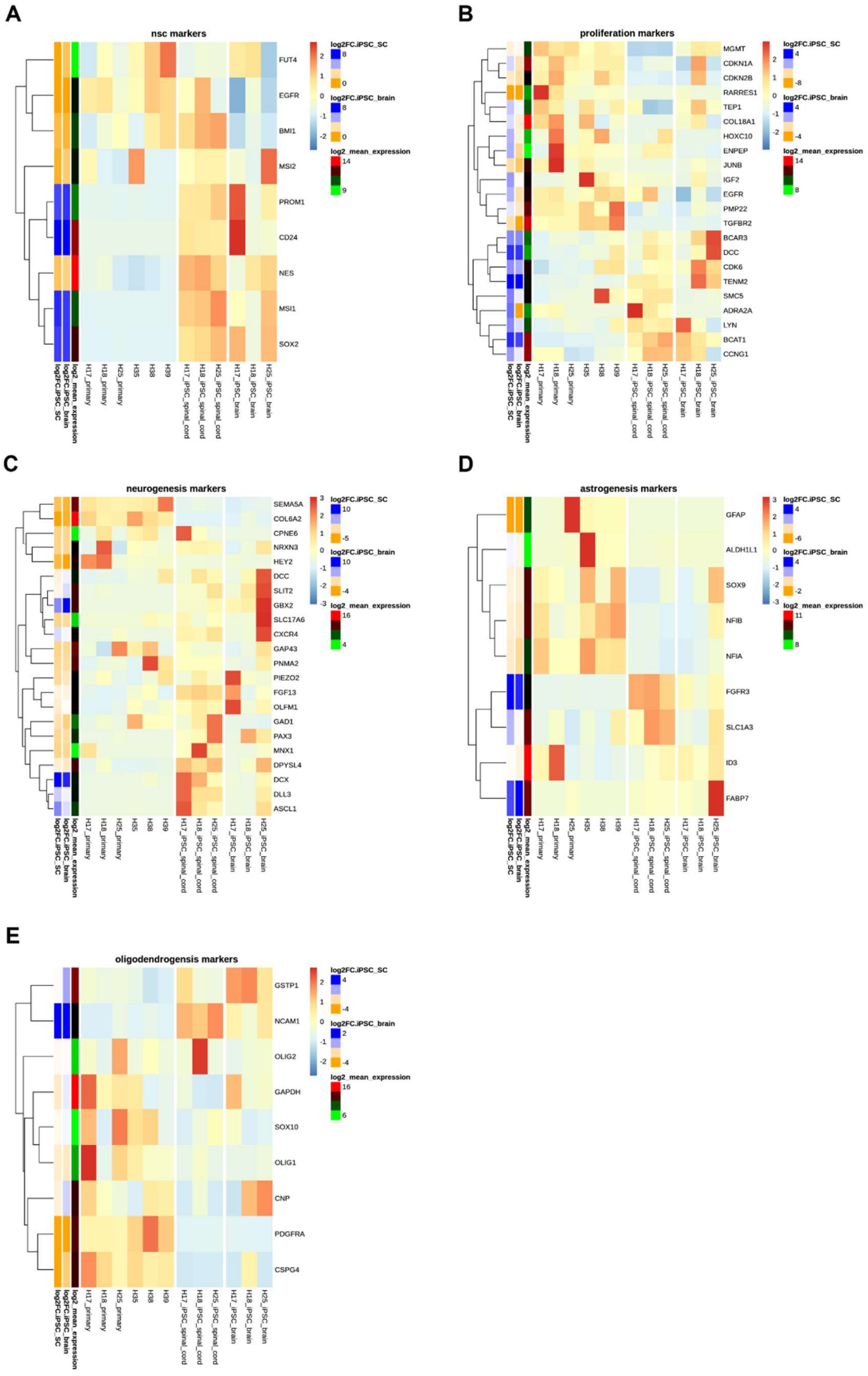
A
nsc markers
FUT4
EGFR
BMI1
MSI2
PROM1
CD24
NES
MSI1
SOX2
log2FC.iPSC_SC
log2FC.iPSC_brain
log2_mean_expression
B
proliferation markers
MGMT
CDKN1A
CDKN2B
RARRES1
TEP1
COL18A1
HOXC10
ENPEP
JUNB
IGF2
EGFR
PMP22
TGFBR2
BCAR3
DCC
CDK6
TENM2
SMC5
ADRA2A
LYN
BCAT1
CCNG1
C
neurogenesis markers
SEMA5A
COL6A2
CPNE6
NRXN3
HEY2
DCC
SLIT2
GBX2
SLC17A6
CXCR4
GAP43
PNMA2
PIEZO2
FGF13
OLFM1
GAD1
PAX3
MNX1
DPYSL4
DCX
DLL3
ASCL1
D
astrogenesis markers
GFAP
ALDH1L1
SOX9
NFIB
NFIA
FGFR3
SLC1A3
ID3
FABP7
E
oligodendrogensis markers
GSTP1
NCAM1
OLIG2
GAPDH
SOX10
OLIG1
CNP
PDGFRA
CSPG4
H17_primary
H18_primary
H25_primary
H35
H38
H39
H17_iPSC_spinal_cord
H18_iPSC_spinal_cord
H25_iPSC_spinal_cord
H17_iPSC_brain
H18_iPSC_brain
H25_iPSC_brain

Figure S4.5 Relative expression of genes characteristic of NSPCs and related functions

Heatmap and hierarchical clustering of genes that are characteristic of (A) neural stem cells (NSCs), (B) proliferation, (C) neurogenesis, (D) astrogenesis, and (E) oligodendrogenesis. The color scale indicates the relative expression: red represents an upregulation, and blue represents a downregulation. n=6 bona fide, n=3 iPSC-SC, n=3 iPSC-Br.

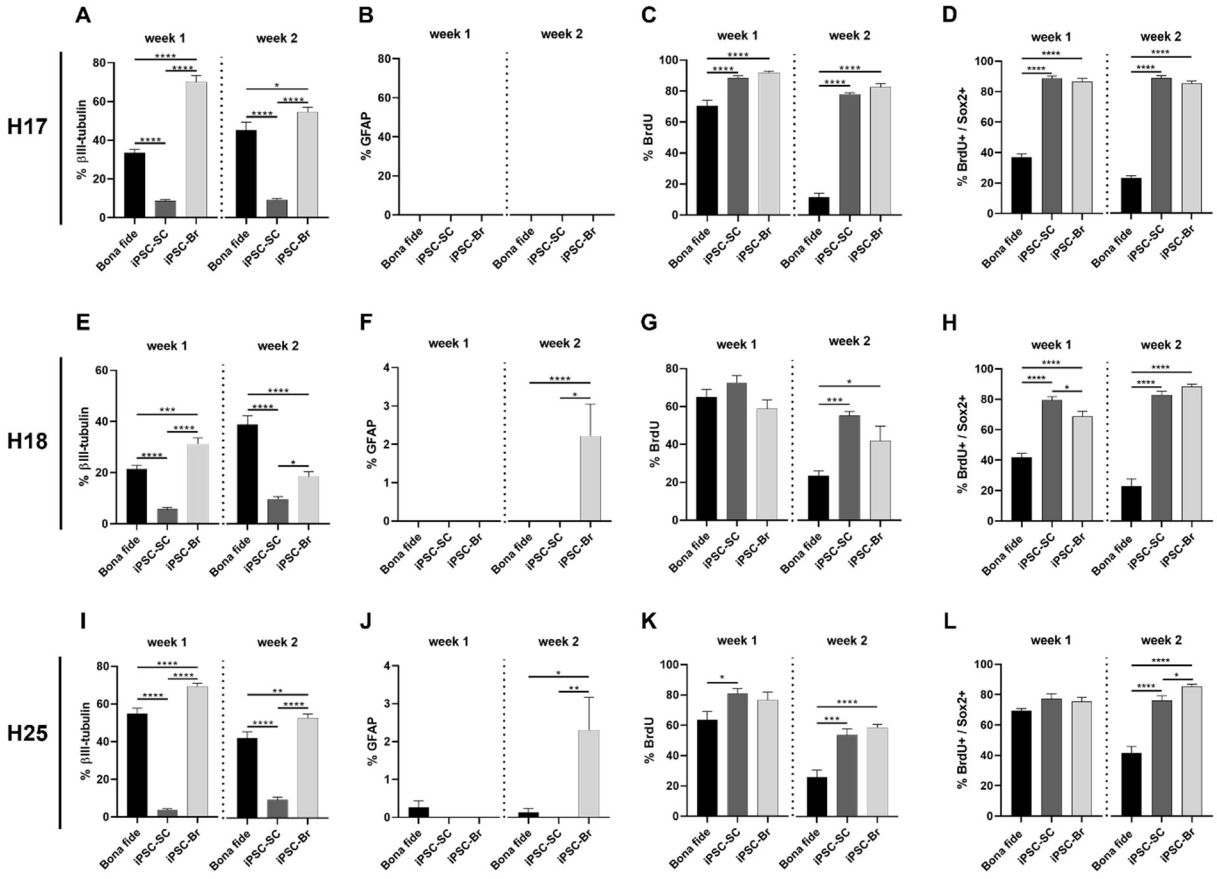

Figure S4.6 Functional characterization of bona fide, iPSC-SC, and -Br NSPCs from individual donors

Intra-donor comparisons of bona fide, iPSC-SC, and -Br NSPCs are shown for specimens (A-D) ”H17”, (E-H) “H18”, and (I-L) “H25”. NSPCs were treated for one or two weeks in conditions that promote (A-C, E-G, I-K) differentiation or (D, H, L) proliferation. (A, E, I) Percentage of βiii tubulin^{+} neurons, (B, F, J) Percentage of GFAP^{+} astrocytes, (C, G, K) Percentage of BrdU^{+} proliferating progenitors, and (D, H, L) percentage of BrdU^{+}/Sox2^{+} proliferating NSPCs. n=3 bona fide, n=3 iPSC-SC, n=3 iPSC-Br. Mean ± s.e.m; *p<0.05, **p<0.01, ***p<0.001, ****p<0.0001.

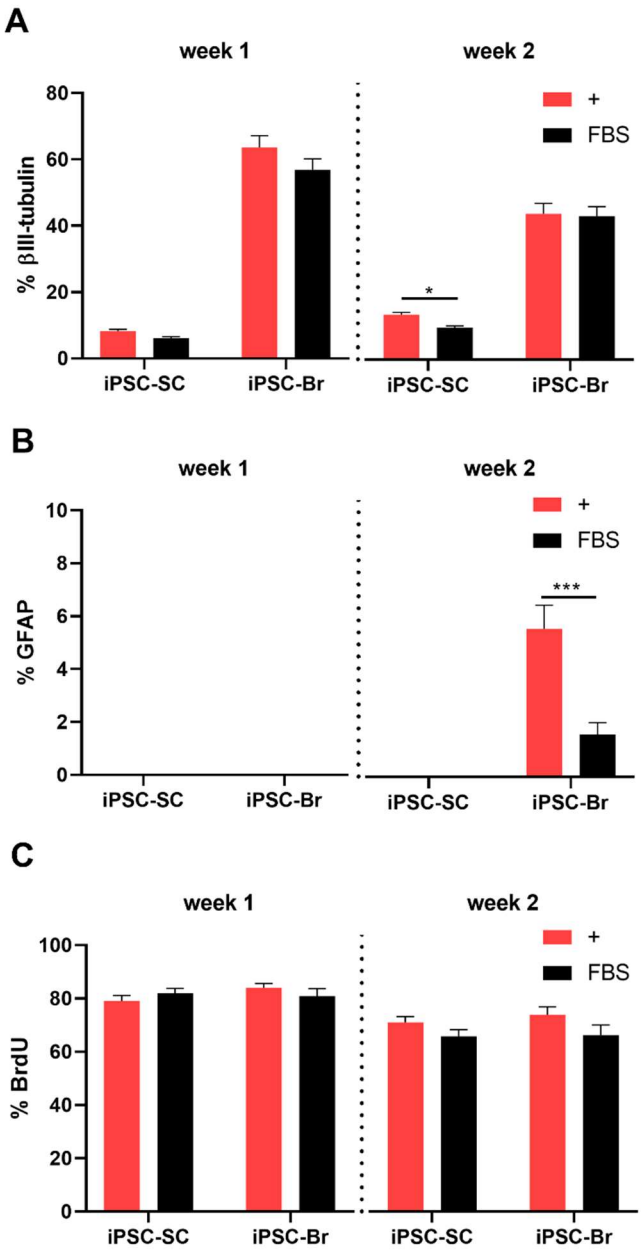

Figure S4.7 The effect of differentiation media on the differentiation and proliferation profiles of iPSC-derived NSPCs

iPSC-SC and -Br NSPCs were differentiated for one or two weeks using 1% FBS in neurobasal-A media ("FBS") or positive control ("+"). The positive control for iPSC-SC NSPCs consists of N2B27 media supplemented with dbcAMP and ascorbic acid. In contrast, the positive control for

iPSC-Br NSPCs consists of BrainPhys media™ supplemented with N2, SM1, dbcAMP, ascorbic acid, BDNF, and GDNF. The percentage of (A) βiii tubulin^{+} neurons, (B) GFAP+ astrocytes, and (C) BrdU^{+} proliferating progenitors. n=3 iPSC-SC, n=3 iPSC-Br. Mean ± s.e.m; *p<0.05.

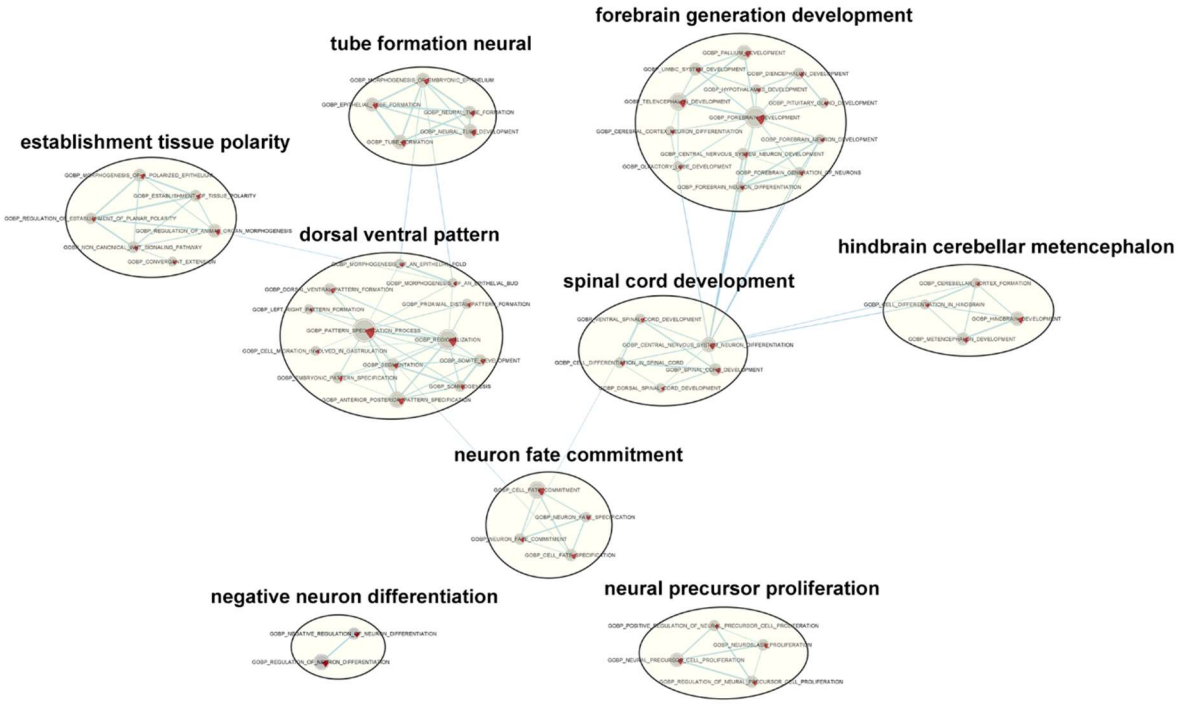

Figure S4.8 Enrichment map comparing iPSC-SC and bona fide NSPCs

Enrichment map for the GSEA GO biological processes analysis created in Cytoskape. Gene sets are represented by small circles, which are colored red or blue to depict a positive or negative normalized enrichment score. Links between enriched gene sets are represented by lines between circles identifying genes found in common between gene set pairs. Clusters of related gene sets are contained within larger circles annotated to describe that specific cluster. The complete list of gene sets and respective normalized enrichment scores are provided in Table S3.

Table S4.1 Complete list of gene sets for terms related to the CNS that are upregulated or downregulated in iPSC-SC NSPCs relative to bona fide NSPCs as analyzed using gProfiler. The complete report can be accessed here for upregulated and downregulated gene sets. GO = gene ontology, MF = molecular function, BP = biological pathway, CC = cellular component, KEGG = Kyoto Encyclopedia of Genes and Genomes, REAC = Reactome, WP = WikiPathways.

Upregulated in iPSC-SC vs. Primary			Downregulated in iPSC-SC vs. Primary		
Database	**Term**	**Adjusted p-value**	**Database**	**Term**	**Adjusted p-value**
GO: MF	DNA binding	2.52E-10	GO:MF	extracellular matrix structural constituent	1.43E-14
GO:MF	voltage-gated cation channel activity	9.86E-07	GO:MF	signaling receptor binding	1.47E-14
GO:MF	ion channel activity	2.25E-06	GO:MF	integrin binding	6.94E-13
GO:MF	voltage-gated ion channel activity	5.13E-05	GO:MF	extracellular matrix binding	3.26E-09
GO:MF	voltage-gated channel activity	6.13E-05	GO:MF	growth factor binding	1.26E-08
GO:MF	ligand-gated ion channel activity	1.03E-04	GO:MF	cytokine activity	1.25E-04
GO:MF	ligand-gated channel activity	1.03E-04	GO:MF	growth factor activity	9.86E-04
GO:MF	glutamate receptor binding	2.19E-04	GO:MF	transforming growth factor beta binding	2.05E-02
GO:MF	ionotropic glutamate receptor binding	3.00E-03	GO:MF	insulin-like growth factor binding	2.84E-02
GO:MF	extracellular ligand-gated ion channel activity	5.33E-03	GO:MF	growth factor receptor binding	3.73E-02
GO:MF	postsynaptic neurotransmitter receptor activity	6.13E-03	GO:MF	platelet-derived growth factor binding	3.93E-02
GO:MF	neurotransmitter receptor activity	1.50E-02	GO:BP	defense response	4.77E-30
GO:BP	nervous system development	1.40E-50	GO:BP	immune system process	2.54E-19

GO:BP	generation of neurons	9.60E-45	GO:BP	response to cytokine	2.75E-19
GO:BP	neuron differentiation	7.01E-43	GO:BP	immune response	1.69E-18
GO:BP	neurogenesis	2.00E-40	GO:BP	regulation of cell population proliferation	1.71E-18
GO:BP	system development	1.24E-36	GO:BP	inflammatory response	1.16E-17
GO:BP	neuron development	8.27E-36	GO:BP	cell population proliferation	3.08E-17
GO:BP	neuron projection development	1.07E-34	GO:BP	positive regulation of cell population proliferation	5.63E-09
GO:BP	neuron projection morphogenesis	1.56E-31	GO:BP	regulation of inflammatory response	1.36E-07
GO:BP	anatomical structure development	5.30E-31	GO:BP	positive regulation of cell differentiation	2.26E-05
GO:BP	developmental process	1.55E-28	GO:BP	response to growth factor	2.65E-05
GO:BP	cell morphogenesis involved in neuron differentiation	7.30E-27	GO:BP	regeneration	4.13E-05
GO:BP	axon development	4.59E-26	GO:BP	response to tumor necrosis factor	6.65E-05
GO:BP	axonogenesis	1.97E-24	GO:BP	cellular developmental process	9.23E-05
GO:BP	chemical synaptic transmission	2.23E-24	GO:BP	response to transforming growth factor beta	1.06E-04
GO:BP	anterograde trans-synaptic signaling	2.23E-24	GO:BP	system development	1.10E-04
GO:BP	trans-synaptic signaling	6.54E-24	GO:BP	transforming growth factor beta receptor signaling pathway	3.68E-04
GO:BP	cell development	1.38E-23	GO:BP	cellular response to tumor necrosis factor	3.72E-04
GO:BP	synaptic signaling	3.83E-23	GO:BP	regulation of cell differentiation	5.32E-04
GO:BP	synapse organization	1.13E-22	GO:BP	regulation of epithelial cell proliferation	1.92E-03
GO:BP	central nervous system development	8.21E-22	GO:BP	receptor signaling pathway via STAT	1.38E-02

GO:BP	cellular developmental process	8.50E-21	GO:BP	chemokine production	1.44E-02
GO:BP	regulation of developmental process	9.53E-20	GO:BP	tissue regeneration	2.02E-02
GO:BP	regulation of nervous system development	5.12E-19	GO:CC	extracellular matrix	3.07E-30
GO:BP	brain development	1.51E-18	GO:CC	collagen-containing extracellular matrix	6.27E-30
GO:BP	synapse assembly	1.84E-17	GO:CC	extracellular exosome	5.53E-19
GO:BP	regulation of neuron projection development	3.15E-17	KEGG	Cytokine-cytokine receptor interaction	6.15E-07
GO:BP	modulation of chemical synaptic transmission	3.93E-17	KEGG	TNF signaling pathway	3.75E-04
GO:BP	regulation of synapse structure or activity	3.39E-16	KEGG	PI3K-Akt signaling pathway	2.22E-03
GO:BP	regulation of synapse organization	1.89E-15	KEGG	JAK-STAT signaling pathway	2.58E-03
GO:BP	regulation of neurogenesis	8.55E-14	KEGG	MAPK signaling pathway	3.38E-02
GO:BP	embryonic morphogenesis	7.59E-13	REAC	Extracellular matrix organization	6.04E-17
GO:BP	regulation of axonogenesis	9.36E-13	REAC	Cytokine Signaling in Immune system	3.36E-14
GO:BP	tissue development	9.90E-13	REAC	Immune System	7.86E-14
GO:BP	central nervous system neuron differentiation	2.16E-12	REAC	Interferon Signaling	4.62E-11
GO:BP	neural precursor cell proliferation	2.41E-12	REAC	Collagen formation	2.49E-05
GO:BP	positive regulation of nervous system development	6.41E-12	REAC	Laminin interactions	5.84E-05
GO:BP	telencephalon development	1.10E-11	REAC	Interleukin-6 family signaling	4.00E-04
GO:BP	dendrite development	2.83E-11	REAC	Signaling by Interleukins	5.74E-04
GO:BP	embryo development	6.72E-11	WP	Pluripotent stem cell differentiation pathway	4.39E-04

GO:BP	neuron migration	8.94E-11			
GO:BP	postsynapse organization	2.81E-10			
GO:BP	hindbrain development	3.96E-10			
GO:BP	regionalization	5.44E-10			
GO:BP	epithelium development	7.02E-10			
GO:BP	central nervous system neuron development	1.48E-08			
GO:BP	spinal cord development	2.41E-08			
GO:BP	regulation of neural precursor cell proliferation	2.60E-08			
GO:BP	positive regulation of synapse assembly	6.11E-08			
GO:BP	regulation of developmental growth	3.59E-07			
GO:BP	negative regulation of neurogenesis	3.96E-07			
GO:BP	regulation of neuron differentiation	6.11E-07			
GO:BP	positive regulation of neural precursor cell proliferation	6.29E-07			
GO:BP	cerebellum development	7.22E-07			
GO:BP	negative regulation of axonogenesis	7.74E-07			
GO:BP	negative regulation of nervous system development	1.11E-06			
GO:BP	synaptic membrane adhesion	1.87E-06			
GO:BP	regulation of postsynapse organization	2.76E-06			
GO:BP	negative regulation of neuron projection development	2.81E-06			

GO:BP	anterior/posterior pattern specification	3.18E-06			
GO:BP	positive regulation of neurogenesis	3.52E-06			
GO:BP	mesenchyme development	6.45E-06			
GO:BP	Wnt signaling pathway	2.26E-05			
GO:BP	cerebral cortex development	5.49E-05			
GO:BP	neurotransmitter transport	5.64E-05			
GO:BP	dorsal/ventral pattern formation	6.03E-05			
GO:BP	central nervous system projection neuron axonogenesis	6.34E-05			
GO:BP	mesenchymal cell differentiation	8.12E-05			
GO:BP	forebrain neuron differentiation	1.22E-04			
GO:BP	neurotransmitter secretion	1.50E-04			
GO:BP	presynapse organization	1.60E-04			
GO:BP	neuron recognition	1.72E-04			
GO:BP	negative regulation of neuron differentiation	1.79E-04			
GO:BP	central nervous system neuron axonogenesis	2.06E-04			
GO:BP	neural tube development	2.49E-04			
GO:BP	regulation of postsynaptic membrane potential	4.19E-04			
GO:BP	negative regulation of axon extension	6.38E-04			
GO:BP	glial cell differentiation	8.72E-04			
GO:BP	response to growth factor	9.02E-04			

GO:BP	neuron fate commitment	9.54E-04			
GO:BP	ventral spinal cord development	1.10E-03			
GO:BP	gliogenesis	1.42E-03			
GO:BP	cerebellar cortex development	1.49E-03			
GO:BP	cell differentiation in spinal cord	1.70E-03			
GO:BP	regulation of neuron migration	2.02E-03			
GO:BP	postsynaptic membrane organization	2.31E-03			
GO:BP	stem cell development	3.87E-03			
GO:BP	cellular response to BMP stimulus	4.08E-03			
GO:BP	response to BMP	4.08E-03			
GO:BP	regulation of Wnt signaling pathway	4.11E-03			
GO:BP	regulation of neurotransmitter secretion	4.52E-03			
GO:BP	ion transport	4.56E-03			
GO:BP	regulation of action potential	4.84E-03			
GO:BP	hindbrain morphogenesis	5.08E-03			
GO:BP	axon extension	5.41E-03			
GO:BP	neural crest cell development	6.25E-03			
GO:BP	excitatory postsynaptic potential	6.35E-03			
GO:BP	embryonic pattern specification	6.92E-03			
GO:BP	neuron fate specification	6.98E-03			
GO:BP	cell differentiation in hindbrain	8.02E-03			
GO:BP	forebrain neuron development	8.20E-03			
GO:BP	postsynapse assembly	9.43E-03			

GO:BP	spinal cord dorsal/ventral patterning	9.65E-03			
GO:BP	regulation of dendrite development	1.09E-02			
GO:BP	stem cell differentiation	1.16E-02			
GO:BP	neuroblast proliferation	1.27E-02			
GO:BP	negative regulation of Wnt signaling pathway	1.35E-02			
GO:BP	neuron cell-cell adhesion	1.36E-02			
GO:BP	non-canonical Wnt signaling pathway	1.44E-02			
GO:BP	spinal cord patterning	1.56E-02			
GO:BP	chemical synaptic transmission, postsynaptic	1.59E-02			
GO:BP	neural tube formation	1.77E-02			
GO:BP	positive regulation of cell population proliferation	1.88E-02			
GO:BP	forebrain cell migration	1.97E-02			
GO:BP	cerebellar cortex formation	1.99E-02			
GO:BP	regulation of neuronal synaptic plasticity	2.08E-02			
GO:BP	mesoderm development	2.09E-02			
GO:BP	fibroblast growth factor receptor signaling pathway	2.42E-02			
GO:BP	BMP signaling pathway	2.71E-02			
GO:BP	action potential	2.79E-02			
GO:BP	nervous system process	3.23E-02			

GO:BP	regulation of presynapse organization	3.78E-02			
GO:BP	regulation of presynapse assembly	3.78E-02			
GO:BP	postsynaptic membrane assembly	3.97E-02			
GO:BP	canonical Wnt signaling pathway	4.90E-02			
GO:BP	neural crest cell differentiation	4.99E-02			
GO:CC	synapse	1.01E-32			
GO:CC	glutamatergic synapse	3.31E-22			
GO:CC	neuron projection	5.84E-21			
GO:CC	postsynapse	1.57E-18			
GO:CC	synaptic membrane	4.78E-18			
GO:CC	postsynaptic membrane	1.69E-17			
GO:CC	integral component of synaptic membrane	5.57E-17			
GO:CC	intrinsic component of synaptic membrane	2.38E-16			
GO:CC	intrinsic component of postsynaptic membrane	3.38E-16			
GO:CC	integral component of postsynaptic membrane	3.68E-16			
GO:CC	axon	1.79E-15			
GO:CC	presynapse	3.34E-15			
GO:CC	postsynaptic specialization	5.08E-14			
GO:CC	dendrite	1.87E-13			
GO:CC	dendritic tree	2.35E-13			
GO:CC	neuron to neuron synapse	1.85E-12			
GO:CC	postsynaptic density	1.09E-11			
GO:CC	neuronal cell body	4.12E-11			

GO:CC	postsynaptic specialization membrane	3.56E-10			
GO:CC	postsynaptic density membrane	1.89E-07			
GO:CC	growth cone	6.65E-07			
GO:CC	intrinsic component of postsynaptic density membrane	1.47E-06			
GO:CC	integral component of presynaptic membrane	1.53E-06			
GO:CC	site of polarized growth	1.79E-06			
GO:CC	presynaptic membrane	3.04E-06			
GO:CC	ion channel complex	3.07E-06			
GO:CC	intrinsic component of presynaptic membrane	8.98E-06			
GO:CC	extracellular matrix	1.20E-05			
GO:CC	excitatory synapse	5.19E-05			
GO:CC	axon terminus	7.05E-05			
GO:CC	neuron projection terminus	1.04E-04			
GO:CC	axonal growth cone	5.52E-04			
GO:CC	synaptic vesicle membrane	8.00E-04			
GO:CC	GABA-ergic synapse	1.08E-03			
GO:CC	neuron spine	2.98E-02			
GO:CC	synaptic vesicle	4.33E-02			
KEGG	Axon guidance	8.17E-07			
KEGG	Neuroactive ligand-receptor interaction	8.90E-06			
KEGG	Signaling pathways regulating pluripotency of stem cells	1.81E-05			
KEGG	Cell cycle	7.69E-04			

KEGG	Wnt signaling pathway	2.24E-03			
KEGG	DNA replication	2.05E-02			
REAC	Neuronal System	1.45E-15			
REAC	Protein-protein interactions at synapses	7.55E-10			
REAC	Neurexins and neuroligins	3.10E-06			
REAC	Transcriptional regulation of pluripotent stem cells	1.60E-05			
REAC	Cell Cycle	1.74E-05			
REAC	POU5F1 (OCT4), SOX2, NANOG activate genes related to proliferation	2.07E-05			
REAC	Nervous system development	6.56E-05			
REAC	Developmental Biology	1.63E-04			
REAC	Axon guidance	3.55E-04			
REAC	DNA Replication	1.22E-03			
REAC	Cell Cycle Checkpoints	2.77E-03			
REAC	Presynaptic depolarization and calcium channel opening	5.00E-03			
REAC	Neurotransmitter receptors and postsynaptic signal transmission	1.45E-02			
WP	Mesodermal commitment pathway	3.78E-07			
WP	Endoderm differentiation	4.31E-06			
WP	Neural crest differentiation	1.53E-05			
WP	Ectoderm differentiation	1.07E-04			

WP	Embryonic stem cell pluripotency pathways	1.66E-03			
WP	Dopaminergic neurogenesis	5.55E-03			

Table S4.2 Complete list of gene sets for terms related to the CNS that are upregulated or downregulated in iPSC-Br NSPCs relative to bona fide NSPCs as analyzed using gProfiler. The complete report can be accessed here for upregulated and downregulated gene sets. GO = gene ontology, MF = molecular function, BP = biological pathway, CC = cellular component, KEGG = Kyoto Encyclopedia of Genes and Genomes, REAC = Reactome, WP = WikiPathways.

Upregulated in iPSC-Brain vs Primary			**Downregulated in iPSC-Brain vs Primary**		
Database	**Term**	**Adjusted p-value**	**Database**	**Term**	**Adjusted p-value**
GO:MF	gated channel activity	1.01E-06	GO:MF	extracellular matrix structural constituent	1.54E-23
GO:MF	ion channel activity	2.89E-05	GO:MF	integrin binding	1.09E-12
GO:MF	voltage-gated cation channel activity	3.40E-05	GO:MF	growth factor binding	4.12E-08
GO:MF	voltage-gated ion channel activity	4.23E-04	GO:MF	receptor ligand activity	8.97E-08
GO:MF	channel regulator activity	7.37E-04	GO:MF	signaling receptor activator activity	1.52E-07
GO:BP	nervous system development	4.58E-48	GO:MF	extracellular matrix binding	4.02E-07
GO:BP	neuron differentiation	1.95E-42	GO:MF	growth factor activity	1.37E-05
GO:BP	generation of neurons	5.59E-41	GO:MF	cytokine activity	6.48E-05
GO:BP	neurogenesis	8.69E-38	GO:MF	transforming growth factor beta binding	1.05E-03
GO:BP	neuron development	1.07E-37	GO:BP	regulation of cell population proliferation	3.91E-24

GO:BP	neuron projection development	1.23E-34	GO:BP	cell population proliferation	1.60E-23
GO:BP	developmental process	3.11E-34	GO:BP	developmental process	9.51E-23
GO:BP	anatomical structure morphogenesis	1.52E-30	GO:BP	system development	5.34E-22
GO:BP	cell development	6.48E-30	GO:BP	tissue development	4.63E-21
GO:BP	axon development	1.28E-24	GO:BP	extracellular matrix organization	1.45E-20
GO:BP	axonogenesis	4.30E-23	GO:BP	tube development	2.83E-20
GO:BP	axon guidance	2.92E-18	GO:BP	cellular developmental process	1.46E-15
GO:BP	neuron projection guidance	3.60E-18	GO:BP	cell differentiation	2.19E-15
GO:BP	regulation of nervous system development	3.12E-17	GO:BP	positive regulation of developmental process	7.24E-13
GO:BP	synapse organization	2.91E-16	GO:BP	response to growth factor	4.79E-11
GO:BP	regulation of neuron projection development	7.76E-16	GO:BP	regulation of cell differentiation	6.94E-11
GO:BP	central nervous system development	3.56E-15	GO:BP	positive regulation of cell population proliferation	1.05E-10
GO:BP	anterograde trans-synaptic signaling	4.31E-14	GO:BP	positive regulation of cell differentiation	5.04E-10
GO:BP	chemical synaptic transmission	4.31E-14	GO:BP	negative regulation of developmental process	1.11E-09
GO:BP	synaptic signaling	7.16E-14	GO:BP	epithelial cell migration	2.61E-08
GO:BP	trans-synaptic signaling	8.81E-14	GO:BP	epithelial cell proliferation	8.67E-08
GO:BP	synapse assembly	6.39E-13	GO:BP	positive regulation of MAPK cascade	2.35E-07
GO:BP	brain development	7.75E-13	GO:BP	regeneration	8.94E-06
GO:BP	tissue development	1.03E-12	GO:BP	cellular response to transforming growth factor beta stimulus	2.89E-05
GO:BP	forebrain development	9.90E-12	GO:BP	transforming growth factor beta receptor signaling pathway	3.05E-05
GO:BP	regulation of neurogenesis	1.12E-11	GO:BP	response to BMP	3.76E-05

GO:BP	regulation of synapse organization	2.07E-10	GO:BP	negative regulation of cell differentiation	3.87E-05
GO:BP	positive regulation of nervous system development	2.48E-10	GO:BP	BMP signaling pathway	3.99E-05
GO:BP	regulation of neuron differentiation	5.00E-10	GO:BP	response to transforming growth factor beta	5.26E-05
GO:BP	neural precursor cell proliferation	2.46E-09	GO:BP	regulation of inflammatory response	7.11E-05
GO:BP	regulation of axonogenesis	2.61E-09	GO:BP	response to cytokine	7.45E-05
GO:BP	modulation of chemical synaptic transmission	2.87E-09	GO:BP	positive regulation of inflammatory response	2.13E-04
GO:BP	developmental growth	3.13E-09	GO:BP	positive regulation of glial cell differentiation	2.75E-04
GO:BP	regulation of trans-synaptic signaling	3.16E-09	GO:BP	regulation of cellular response to transforming growth factor beta stimulus	3.26E-04
GO:BP	positive regulation of cell differentiation	4.18E-09	GO:BP	regulation of glial cell differentiation	2.23E-03
GO:BP	central nervous system neuron development	6.97E-09	GO:BP	regulation of gliogenesis	3.03E-03
GO:BP	telencephalon development	7.95E-09	GO:BP	tissue regeneration	9.63E-03
GO:BP	regulation of neural precursor cell proliferation	1.15E-08	GO:BP	epidermal growth factor receptor signaling pathway	1.50E-02
GO:BP	embryo development	1.25E-08	GO:BP	regulation of BMP signaling pathway	1.65E-02
GO:BP	neuron migration	7.94E-08	GO:BP	gliogenesis	1.81E-02
GO:BP	central nervous system neuron differentiation	2.87E-07	GO:BP	regulation of epidermal growth factor-activated receptor activity	2.74E-02
GO:BP	hindbrain development	5.17E-07	GO:BP	neurogenesis	2.97E-02
GO:BP	negative regulation of neurogenesis	1.13E-06	GO:CC	extracellular matrix	2.28E-31
GO:BP	negative regulation of nervous system development	2.53E-06	GO:CC	extracellular exosome	6.19E-13

GO:BP	postsynapse organization	5.22E-06	GO:CC	interleukin-6 receptor complex	1.27E-02
GO:BP	forebrain neuron differentiation	5.45E-06	GO:CC	synaptic cleft	2.35E-02
GO:BP	regulation of synapse assembly	5.45E-06	KEGG	ECM-receptor interaction	1.74E-06
GO:BP	positive regulation of neural precursor cell proliferation	6.75E-06	KEGG	PI3K-Akt signaling pathway	1.79E-05
GO:BP	negative regulation of cell differentiation	6.94E-06	KEGG	TGF-beta signaling pathway	6.28E-03
GO:BP	neural tube development	1.11E-05	KEGG	MAPK signaling pathway	1.31E-02
GO:BP	positive regulation of neurogenesis	2.87E-05	REAC	Extracellular matrix organization	4.89E-22
GO:BP	forebrain generation of neurons	6.11E-05	REAC	Collagen formation	3.94E-04
GO:BP	neuron fate commitment	6.13E-05	WP	Pluripotent stem cell differentiation pathway	5.67E-04
GO:BP	negative regulation of neuron projection development	9.74E-05	WP	Spinal cord injury	7.13E-03
GO:BP	cerebral cortex development	1.23E-04	WP	Complement system in neuronal development and plasticity	3.39E-02
GO:BP	positive regulation of neuron differentiation	4.78E-04	WP	Neuroinflammation and glutamatergic signaling	3.84E-02
GO:BP	presynapse organization	4.99E-04			
GO:BP	neural tube formation	5.51E-04			
GO:BP	gliogenesis	5.84E-04			
GO:BP	regionalization	8.77E-04			
GO:BP	forebrain neuron fate commitment	1.13E-03			
GO:BP	cell population proliferation	1.26E-03			
GO:BP	central nervous system projection neuron axonogenesis	1.31E-03			

GO:BP	cerebellum development	1.42E-03			
GO:BP	Wnt signaling pathway	2.05E-03			
GO:BP	central nervous system neuron axonogenesis	2.07E-03			
GO:BP	positive regulation of cell population proliferation	2.32E-03			
GO:BP	regulation of nervous system process	2.46E-03			
GO:BP	glial cell differentiation	3.52E-03			
GO:BP	forebrain cell migration	4.07E-03			
GO:BP	negative regulation of neuron differentiation	4.84E-03			
GO:BP	spinal cord development	1.51E-02			
GO:BP	forebrain neuron development	1.60E-02			
GO:BP	chemical synaptic transmission, postsynaptic	1.76E-02			
GO:BP	synaptic transmission, glutamatergic	1.99E-02			
GO:BP	ion transmembrane transport	2.28E-02			
GO:BP	nuclear DNA replication	2.35E-02			
GO:BP	dorsal/ventral pattern formation	2.55E-02			
GO:BP	BMP signaling pathway	2.71E-02			
GO:BP	mesenchymal cell differentiation	3.93E-02			
GO:BP	nervous system process	4.75E-02			
GO:BP	presynaptic membrane organization	4.87E-02			
GO:CC	synapse	1.53E-23			

GO:CC	neuron projection	1.92E-19			
GO:CC	synaptic membrane	9.67E-18			
GO:CC	postsynaptic membrane	2.10E-17			
GO:CC	integral component of synaptic membrane	3.97E-16			
GO:CC	intrinsic component of postsynaptic membrane	4.08E-16			
GO:CC	integral component of postsynaptic membrane	6.04E-16			
GO:CC	intrinsic component of synaptic membrane	1.09E-15			
GO:CC	integral component of postsynaptic membrane	9.05E-15			
GO:CC	intrinsic component of synaptic membrane	5.68E-14			
GO:CC	axon	1.08E-13			
GO:CC	glutamatergic synapse	2.95E-13			
GO:CC	postsynaptic specialization membrane	5.64E-13			
GO:CC	postsynaptic specialization	1.32E-12			
GO:CC	postsynapse	7.81E-12			
GO:CC	intrinsic component of postsynaptic specialization membrane	1.48E-10			
GO:CC	presynapse	3.05E-10			
GO:CC	neuron to neuron synapse	7.57E-10			
GO:CC	neuronal cell body	7.78E-09			
GO:CC	postsynaptic density	8.06E-09			
GO:CC	postsynaptic density membrane	9.38E-09			

GO:CC	dendrite	1.03E-06			
GO:CC	dendritic tree	2.83E-06			
GO:CC	growth cone	3.03E-06			
GO:CC	presynaptic membrane	9.45E-06			
GO:CC	integral component of postsynaptic density membrane	3.18E-05			
GO:CC	intrinsic component of postsynaptic density membrane	4.85E-05			
GO:CC	ion channel complex	6.78E-05			
GO:CC	extracellular matrix	1.24E-04			
GO:CC	intrinsic component of presynaptic membrane	5.23E-04			
GO:CC	voltage-gated calcium channel complex	6.47E-04			
GO:CC	neuronal dense core vesicle	3.72E-03			
GO:CC	axonal growth cone	3.81E-03			
GO:CC	synaptic vesicle membrane	7.18E-03			
GO:CC	intrinsic component of synaptic vesicle membrane	7.56E-03			
GO:CC	GABA-ergic synapse	2.51E-05			
GO:CC	excitatory synapse	8.77E-03			
KEGG	Axon guidance	1.92E-12			
KEGG	Signaling pathways regulating pluripotency of stem cells	5.28E-10			
REAC	Neuronal System	8.88E-08			
REAC	Protein-protein interactions at synapses	1.64E-06			
REAC	Developmental Biology	2.13E-06			

REAC	Nervous system development	1.56E-05			
REAC	Neurexins and neuroligins	2.67E-05			
REAC	Axon guidance	4.46E-05			
REAC	Transcriptional regulation of pluripotent stem cells	1.72E-04			
REAC	POU5F1 (OCT4), SOX2, NANOG activate genes related to proliferation	1.23E-03			
REAC	Transmission across Chemical Synapses	5.17E-03			
REAC	Neurotransmitter receptors and postsynaptic signal transmission	4.70E-05			
REAC	POU5F1 (OCT4), SOX2, NANOG repress genes related to differentiation	6.23E-05			
WP	Endoderm differentiation	2.39E-04			
WP	Mesodermal commitment pathway	6.86E-03			
WP	Ectoderm differentiation	2.55E-02			
WP	Neural crest differentiation	1.01E-06			
WP	Wnt signaling	2.89E-05			

Table S4.3 Complete list of gene sets used to generate the enrichment map between bona fide and iPSC-SC NSPCs shown in Figure S4.9. GO = gene ontology, BP = biological pathway, NES = normalized enrichment score

Term Name	q-value	NES
GOBP_ANTERIOR_POSTERIOR_PATTERN_SPECIFICATION	1.88E-02	1.7125
GOBP_CELL_DIFFERENTIATION_IN_HINDBRAIN	3.81E-02	1.6289
GOBP_CELL_DIFFERENTIATION_IN_SPINAL_CORD	1.40E-03	1.9291
GOBP_CELL_FATE_COMMITMENT	1.32E-02	1.7457
GOBP_CELL_FATE_SPECIFICATION	5.80E-03	1.8169
GOBP_CELL_MIGRATION_INVOLVED_IN_GASTRULATION	1.86E-02	1.7123
GOBP_CENTRAL_NERVOUS_SYSTEM_NEURON_DEVELOPMENT	2.30E-03	1.8932
GOBP_CENTRAL_NERVOUS_SYSTEM_NEURON_DIFFERENTIATION	5.00E-04	2.0174
GOBP_CEREBELLAR_CORTEX_FORMATION	4.60E-02	1.6046
GOBP_CEREBRAL_CORTEX_NEURON_DIFFERENTIATION	1.43E-02	1.7379
GOBP_CONVERGENT_EXTENSION	3.31E-02	1.6447
GOBP_DIENCEPHALON_DEVELOPMENT	0.00E+0	2.1304
GOBP_DORSAL_SPINAL_CORD_DEVELOPMENT	9.60E-03	1.7715
GOBP_DORSAL_VENTRAL_PATTERN_FORMATION	1.20E-03	1.9479
GOBP_EMBRYONIC_PATTERN_SPECIFICATION	4.60E-02	1.6038
GOBP_EPITHELIAL_TUBE_FORMATION	5.80E-03	1.8126
GOBP_ESTABLISHMENT_OF_TISSUE_POLARITY	5.90E-03	1.8235
GOBP_FOREBRAIN_DEVELOPMENT	2.00E-03	1.9053
GOBP_FOREBRAIN_GENERATION_OF_NEURONS	6.10E-03	1.8082
GOBP_FOREBRAIN_NEURON_DEVELOPMENT	1.46E-02	1.736
GOBP_FOREBRAIN_NEURON_DIFFERENTIATION	1.15E-02	1.7595
GOBP_HINDBRAIN_DEVELOPMENT	0.00E+0	2.0728
GOBP_HYPOTHALAMUS_DEVELOPMENT	3.55E-02	1.6363
GOBP_LEFT_RIGHT_PATTERN_FORMATION	2.85E-02	1.6646
GOBP_LIMBIC_SYSTEM_DEVELOPMENT	1.83E-02	1.7159
GOBP_METENCEPHALON_DEVELOPMENT	1.50E-03	1.9307
GOBP_MORPHOGENESIS_OF_AN_EPITHELIAL_BUD	2.20E-02	1.6942

GOBP_MORPHOGENESIS_OF_AN_EPITHELIAL_FOLD	3.60E-03	1.8546
GOBP_MORPHOGENESIS_OF_A_POLARIZED_EPITHELIUM	8.50E-03	1.7836
GOBP_MORPHOGENESIS_OF_EMBRYONIC_EPITHELIUM	1.23E-02	1.7535
GOBP_NEGATIVE_REGULATION_OF_NEURON_DIFFERENTIATION	4.00E-04	1.9873
GOBP_NEURAL_PRECURSOR_CELL_PROLIFERATION	6.00E-04	2.0247
GOBP_NEURAL_TUBE_DEVELOPMENT	5.80E-03	1.8161
GOBP_NEURAL_TUBE_FORMATION	2.59E-02	1.6784
GOBP_NEUROBLAST_PROLIFERATION	3.70E-03	1.8579
GOBP_NEURON_FATE_COMMITMENT	4.00E-04	2.0113
GOBP_NEURON_FATE_SPECIFICATION	2.40E-03	1.8935
GOBP_NON_CANONICAL_WNT_SIGNALING_PATHWAY	3.00E-03	1.8811
GOBP_OLFACTORY_LOBE_DEVELOPMENT	3.23E-02	1.6491
GOBP_PALLIUM_DEVELOPMENT	3.28E-02	1.6456
GOBP_PATTERN_SPECIFICATION_PROCESS	3.30E-03	1.8706
GOBP_PITUITARY_GLAND_DEVELOPMENT	3.00E-04	2.0026
GOBP_POSITIVE_REGULATION_OF_NEURAL_PRECURSOR_CELL_PROLIFERATION	1.60E-03	1.9219
GOBP_PROXIMAL_DISTAL_PATTERN_FORMATION	5.90E-03	1.8189
GOBP_REGIONALIZATION	3.60E-03	1.8625
GOBP_REGULATION_OF_ANIMAL_ORGAN_MORPHOGENESIS	4.67E-02	1.6019
GOBP_REGULATION_OF_ESTABLISHMENT_OF_PLANAR_POLARITY	1.20E-03	1.9475
GOBP_REGULATION_OF_NEURAL_PRECURSOR_CELL_PROLIFERATION	1.20E-03	1.9431
GOBP_REGULATION_OF_NEURON_DIFFERENTIATION	5.80E-03	1.8133
GOBP_SEGMENTATION	2.60E-02	1.6788
GOBP_SOMITE_DEVELOPMENT	9.30E-03	1.776
GOBP_SOMITOGENESIS	1.10E-02	1.7624
GOBP_SPINAL_CORD_DEVELOPMENT	0.00E+0	2.0717

GOBP_TELENCEPHALON_DEVELOPMENT	1.42E-02	1.74
GOBP_TUBE_FORMATION	2.68E-02	1.6708
GOBP_VENTRAL_SPINAL_CORD_DEVELOPMENT	3.60E-03	1.8652

Chapter 5: Integrated Discussion

5.1 Introduction

5.1.1 Summary of findings

Regenerative strategies for treating SCI include stimulating endogenous NSPCs or transplanting genetically reprogrammed NSPCs (de Freria et al., 2021; S. Liu & Chen, 2019). These strategies have demonstrated promise in animal models of SCI but are yet to be successfully replicated in humans (Yamazaki et al., 2020). Therefore, to improve the translation of stem cell therapies, we characterized the molecular and functional attributes of adult human spinal cord NSPCs compared to animal model NSPCs and genetically reprogrammed NSPCs.

We began by developing a reproducible *in vitro* assay that would allow the direct comparison of primary NSPCs from humans, pigs, and rats. We first demonstrated a novel means to harvest viable spinal cord tissue from all three species and micro-dissect NSPCs from the central canal. We found that primary cultures were enriched in multi-potent NSPCs that could be propagated for several passages. We then cultured NSPCs from all three species under identical conditions to induce proliferation or differentiation and demonstrated a means to characterize NSPC behaviour.

Next, we used our *in vitro* assay to examine whether mechanisms of pathophysiology and regeneration are conserved between human, pig, and rat NSPCs. We first discovered that human NSPCs are neurogenic, while animal model NSPCs are astrogenic under standard differentiation conditions. We found that in response to SCI-induced inflammatory factors, animal model NSPCs exhibited glial scarring mechanisms but not human NSPCs. We also found that human NSPCs require different treatments with regenerative factors than rat NSPCs to direct NSPC fate into neurons, oligodendrocytes, and astrocytes in a predictable manner. In addition, we sequenced

primary NSPCs from all three species and correlated their transcriptomes and functional profiles. We found an expression of genes and gene sets that correlate with the observed differentiation and proliferation trends among species, including enhanced oligodendrocyte differentiation and self-renewal in rat NSPCs.

Lastly, we generated iPSC-derived NSPCs bearing a spinal cord (iPSC-SC) or brain (iPSC-Br) phenotype to examine their molecular and functional homology to isogenic primary NSPCs. We found that iPSC-Br NSPCs portrayed the expected dorsal forebrain phenotype while iPSC-SC NSPCs embodied a spinal cord regionalization with features of neuromesodermal progenitors. At a functional level, we observed that primary and iPSC-Br NSPCs were most similar, given their propensity to differentiate into neurons and astrocytes. However, the proliferation rate was greater from iPSC-derived NSPCs than primary NSPCs, which is reflected in their early and adult developmental stages, respectively.

5.1.2 Significance of findings

The work in this thesis provides three significant contributions to the field of stem cell therapy for SCI, which are discussed below. Before this study, there was a gap in the literature that provides a comprehensive characterization of stem cells from the adult human spinal cord. As such, our understanding of endogenous spinal cord NSPC pathophysiology and targeted regeneration stemmed largely from rodent models of SCI. Also, it was unclear whether genetically reprogrammed NSPCs exhibit a resemblance to adult human spinal cord NSPCs. Therefore, we speculated that an improved understanding of spinal cord NSPCs would improve translational outcomes for stem cell treatments that target endogenous NSPCs and transplant genetically reprogrammed NSPCs.

The first significant contribution of this thesis entails the development of an *in vitro* assay that could directly compare the functional behaviour of spinal cord NSPCs between human and animal models of SCI (Galuta et al., 2020). Only two research groups have previously attempted to characterize adult human spinal cord NSPCs *in vitro,* but neither group has made a comparison to animal model NSPCs (Dromard et al., 2008; A. J. Mothe et al., 2011). Comparing human and animal model NSPCs is helpful since *in vitro* studies may produce artifacts in NSPC behaviour, potentially rendering a characterization of human NSPCs irrelevant to their *in vivo* behaviour (Gil-Perotín et al., 2013; Soares et al., 2021). The inclusion of animal model NSPCs in our study enables the cross-reference of human NSPC behaviour to animal model NSPCs *in vivo* since animal models have been studied in an *in vivo* context. This assay demonstrated that human NSPCs are intrinsically driven toward neuronal fates. In contrast, animal model NSPCs favor glial fates, suggesting cell-intrinsic differences exist between human and animal model NSPCs. Ultimately, we hope this method will pave the way for future experiments that evaluate species-dependent cell behaviour in response to exogenous factors, such as testing the effectiveness of drugs or regenerative factors on human NSPCs.

This thesis's second significant contribution involves using our *in vitro* assay to determine possible mechanisms influencing the pathophysiology of human spinal cord NSPCs and their responses to regenerative factors that have known effects in animal models. Previously, two research groups have sought to discover the response of adult human spinal cord NSPCs to traumatic SCI with contradictory results. Cawsey and colleagues (2015) observed an increase in $Nestin^{+}$ cells around the central canal that correlated with injury severity and time post-injury. However, Paniagua-Torija and colleagues (2018) did not see an increase in ependymal cell proliferation at any level of

the spinal cord or time post-injury. A common drawback in both studies is the use of post-mortem tissue which invariably differs from one sample to the next, thus necessitating a large sample size.

Our study, assessing the effects of SCI-induced inflammatory factors, represents the first functional assay to determine causal mechanisms of pathophysiology from human NSPCs. We found that pig and rat NSPCs were induced to undergo reactive astrogliosis *in vitro* similarly to their *in vivo* counterparts following an SCI (Barnabé-Heider et al., 2010; Meletis et al., 2008; Sabelström et al., 2013). However, our finding that human NSPCs do not undergo reactive astrogliosis contradicts the notion that glial scarring is a pathological feature of human SCI and cautions against the direct translation of strategies that target the glial scar.

In a separate assay, assessing the effects of regenerative factors, we determined that human NSPCs cannot be directed to differentiate into neurons, oligodendrocytes, and astrocytes using the same conditions for rat NSPCs. These findings imply that treating human NSPCs with regenerative factors first requires testing and optimization, which can be conducted using an *in vitro* assay like the one developed in our study. Ultimately, the *in vitro* characterization of adult human spinal cord NSPCs and comparison to animal model NSPCs may improve our understanding of pathophysiological mechanisms in human SCI and the translation of regenerative treatments.

Our final contribution involved determining the molecular and functional homology between genetically reprogrammed NSPCs and isogenic bona fide spinal cord NSPCs. It was previously demonstrated in rodent models of SCI that the transplant of genetically reprogrammed NSPCs with a spinal cord phenotype produced the most effective neurological repair compared to other stem cell grafts (Kadoya et al., 2016; Kajikawa et al., 2020; Kumamaru, Kadoya, et al., 2018). Therefore, it is likely that genetically reprogrammed NSPCs that phenocopy bona fide spinal cord NSPCs will yield better clinical outcomes.

Our study characterized bona fide spinal cord NSPCs *in situ* and *in vitro*, representing inactivated and activated states. Importantly, our study is the first to characterize genetically reprogrammed NSPCs that are isogenic with bona fide spinal cord NSPCs, thus mitigating the influence of genetic variation between donors. This approach allowed us to distinguish genetically reprogrammed NSPCs and bona fide spinal cord NSPCs with respect to their regional, developmental, and functional properties. It also permitted us to evaluate the reproducibility of iPSC differentiation protocols in generating NSPCs with consistent features, which will be necessary for personalized medicine applications. Ultimately, we were able to provide a "blueprint" for bona fide spinal cord NSPCs that may be used as a target for future iPSC differentiation protocols and evaluating the homology with genetically reprogrammed NSPCs.

5.2 Small and large animal models as stepping stones to clinical translation

Animal models have been instrumental in understanding SCI mechanisms and developing experimental treatments (Cheriyan et al., 2014; Kjell & Olson, 2016; Schomberg et al., 2017). Rodents are the most studied animal model for SCI and for developing NSPC strategies, given that they are relatively inexpensive, available, and possess similarities in functional, electrophysiological, and morphological outcomes to humans (Cheriyan et al., 2014; Kjell & Olson, 2016). Mice have been particularly useful for conducting spatial- and temporal-specific genetic manipulations to determine *in vivo* causal inferences. As such, studies in mice have managed to lineage trace spinal cord NSPCs to reveal aspects of their lineage potential, pathophysiological response, and function (Barnabé-Heider et al., 2010; Cusimano et al., 2018; Meletis et al., 2008; Sabelström et al., 2013; Stenudd et al., 2022). On the other hand, rats more closely mimic human pathophysiology and behavioral outcome assessments (Kjell & Olson, 2016;

Metz et al., 2000). Therefore, most mechanistic studies are performed with mice, while pre-clinical SCI studies use rats.

Following pre-clinical validation in rodents, promising SCI repair strategies may be tested in larger animals, including pigs, cats, dogs, and non-human primates (Kwon et al., 2015; J. H. T. Lee et al., 2013b; Rosenzweig et al., 2018). This translational step is believed to be crucial because it is yet to be demonstrated that a safe and effective intervention in rodent models can be translated directly to clinical trials and convincingly show efficacy (Kwon et al., 2015). Indeed, large animal models may be more relevant to humans concerning the spinal cord anatomy, pathophysiology, and functional assessments (Kwon et al., 2015; Nout et al., 2012; Schomberg et al., 2017). For instance, to assess long-distance axonal regeneration for human spinal cord repair, strategies that promote axonal regeneration can be studied in larger animals rather than rodents, given the similarities in the spinal cord and lesion size between humans and larger animal models (Kjell & Olson, 2016). Furthermore, SCI repair strategies, such as the intrathecal administration of drugs or cell transplantation, differ significantly in large animals and humans compared to rodents due to anatomical differences in the spinal cord (K. T. Kim et al., 2018).

In particular, the porcine model of SCI has been advocated as a critical translational intermediate between rodents and humans (K. T. Kim et al., 2018; J. H. T. Lee et al., 2013b; Schomberg et al., 2017). Porcine models are more readily available and ethically feasible to study than non-human primates (Kwon et al., 2015; Schomberg et al., 2017). In some cases, the porcine model may be more relevant to humans than non-human primate models considering the anatomy of the thoracic spinal cord is more like that of humans (Sheng, Wang, Xu, Zhu, & Zhou, 2010). There are also physiological and genetic similarities between porcine and humans in SCI. For instance, pathophysiological markers (e.g., Il-6, tau, S100β, and GFAP) correlate with SCI severity and

outcome measures consistently between porcine and humans (Dalkilic et al., 2018; Kwon et al., 2017). This could lead to the development of biomarkers to stratify injury severity in humans which will aid in weighing the risks and benefits of a particular treatment during the acute phase of SCI. In addition, porcine may be helpful in screening and optimizing pre-clinical treatments before their clinical application. For instance, a study by Streijger and colleagues (2016) failed to reproduce the therapeutic effects of magnesium chloride within a polyethylene glycol formulation in a porcine model that previously demonstrated beneficial outcomes in rodents. Therefore, using larger animal models, such as the porcine model, may improve our understanding of human pathophysiological mechanisms and the translation of promising experimental treatments.

Although there is more significant homology between humans and larger animal models compared to humans and smaller animal models, species differences still exist on the molecular, cellular, and gross level (Alfaro-Cervello et al., 2014; Becker et al., 2018; Ghazale et al., 2019a; Metz et al., 2000; Sheng et al., 2010). For instance, humans' central canal ependymal cells are morphologically and molecularly distinct from macaques and rodents (Alfaro-Cervello et al., 2014). Even mice and rats have been shown to differ concerning their central canal anatomy and pathophysiological response to SCI (Sroga, Jones, Kigerl, McGaughy, & Popovich, 2003). Therefore, in addition to using larger animal models for SCI translational studies, cross-species comparisons must be conducted between large animal models and humans.

5.3 The importance and limitations of using human subjects and samples

The SCI field lacks translational studies examining humans and their cells or tissues (Cheriyan et al., 2014; K. T. Kim et al., 2018; Kwon et al., 2015). This is due to the technical and ethical factors limiting the scope of studying human spinal cord biology and pathophysiology. The methods

available to study living patients with an SCI include imaging techniques (e.g., magnetic resonance imaging or angiography, and computed tomography), assessing behavioral outcomes, and measuring blood/serum biomarkers (Dalkilic et al., 2018; Goldberg & Kershah, 2010). These techniques may provide helpful information about the prognosis of SCI outcomes but do not contribute to our understanding of the cellular and molecular mechanisms underlying secondary injury.

To understand the pathophysiology of human SCI, organ donor tissue from SCI patients can be studied using immunohistochemical techniques (Cawsey et al., 2015; Paniagua-Torija et al., 2018). However, this presents several challenges, including reproducibility, possible post-mortem artifacts, and scarcity of samples for study. It is practically impossible to conduct reproducible, controlled experiments using organ donor tissue since no two patients or their injuries are identical. This includes differences in donor age and sex, the type, severity and location of injury, medications used by the patient, post-mortem delay, comorbidities, injury treatment, and survival time.

One way to circumvent reproducibility issues of studying injured spinal cord tissue is to conduct *in vitro* assays using healthy donor spinal cord tissue (Dromard et al., 2008; A. J. Mothe et al., 2011). This would allow for the functional and causal study of NSPCs from different donors under identical conditions that avoids confounding variables associated with different SCIs. For instance, in our study, we treated primary human spinal cord NSPCs with inflammatory factors to address the occurrence of glial scarring. Similarly, NSPCs could be treated in other conditions that mimic aspects of SCI (e.g., co-culture with activated microglia) to predict their pathophysiological response (Ma et al., 2019). However, this may require large sample sizes to account for differences in donor demographics. Furthermore, cooperation among neurosurgical and neuroscientist

personnel is needed to harvest spinal cord tissue and immediately process the tissue for cell culture to maintain the viability of NSPCs (Galuta et al., 2020; A. Mothe & Tator, 2015). Therefore, given the technical limitations in studying living patients with SCI and the challenges associated with conducting *in vitro* functional assays, most clinicians and scientists have resorted to studying animal models (Alizadeh et al., 2019; Cheriyan et al., 2014).

5.4 Cross-species comparisons of NSPCs using *in vitro* models

The translation of NSPC targeted strategies could be improved by the *in vitro* study of primary NSPCs from humans compared to small and large animal models (Becker et al., 2018; Hodge et al., 2019). In this thesis, we developed an *in vitro* assay to culture NSPCs from humans, pigs, and rats under identical conditions, thus directly comparing species. This method allows for the functional analysis of human NSPCs and for determining cellular mechanisms that could occur *in vivo* in humans.

Before this thesis, no studies conducted a cross-species functional comparison of spinal cord NSPCs. Only a handful of *in situ* characterizations comparing adult human and animal ependymal cells have been performed (Alfaro-Cervello et al., 2014; Garcia-Ovejero et al., 2015; Ghazale et al., 2019a; González et al., 2020; Paniagua-Torija et al., 2015). However, these studies characterized ependymal cells in their quiescent state, which may not reflect the true regenerative potential of NSPCs. Furthermore, these studies do not allow for the functional analysis of NSPCs. On the other hand, *in vitro* studies could provide important information regarding the pathophysiological response of adult human NSPCs to secondary injury, which remains largely unknown (Cawsey et al., 2015; Paniagua-Torija et al., 2018).

We demonstrated in Chapter 3 that treating pig and rat spinal cord NSPCs with certain inflammatory factors (Il-6, TNFα, and TGFβ) induces reactive astrogliosis. These inflammatory factors also induce reactive astrogliosis from rodent NSPCs *in vivo* following an SCI, thus replicating our *in vitro* observations (M. K. Kang & Kang, 2008; Ma et al., 2019; Monje et al., 2002; Moreno-Manzano et al., 2009; S. Okada et al., 2004). In our study, treating human NSPCs with the same inflammatory factors did not increase reactive astrogliosis. Therefore, the same causal mechanisms that drive glial scarring in animal models of SCI do not apply to human NSPCs within the parameters tested. Since glial scarring has not been prominently observed in human post-mortem tissue, it may be possible that glial scarring is a feature exclusive to smaller animal models of SCI and not humans (Norenberg et al., 2004).

Besides examining potential pathophysiological mechanisms in humans, an *in vitro* assay could also be used to test regenerative factors in pre-clinical animal studies. It's been shown that rats treated with the mitogens EGF and FGF2 exhibit enhanced NSPC activation and proliferation following an SCI compared to non-treated controls (Jimenez Hamann et al., 2005; Kojima & Tator, 2002). Concomitantly, rats in the treatment group experienced a significant improvement in functional outcomes as early as two weeks post-injury. However, besides the increased activation and proliferation of NSPCs, there remained a substantial differentiation of astrocytes which may have contributed to glial scarring. Also, there was little differentiation into neurons and oligodendrocytes, which may have limited functional improvement. In a separate study, injured rats were treated with EGF, FGF2, and PDGF-AA to modulate the fate of NSPCs following their activation (Soheila Karimi-Abdolrezaee et al., 2012). In this case, there was an increase in NSPC proliferation, reduced astrocyte differentiation, and enhanced oligodendrocyte differentiation that

correlated with functional improvements. Therefore, it is possible to target and manipulate endogenous NSPCs to induce fates promoting regeneration and spinal cord repair.

Human NSPCs can also be induced to proliferate with EGF and FGF2 treatment (A. J. Mothe et al., 2011). However, we found that human NSPCs proliferate at a lower rate than rat NSPCs which may impact the application of EGF and FGF2 for humans *in vivo*. For instance, the concentration of mitogens or duration of application may need to be optimized for human NSPCs, which can be first assessed *in vitro*. Furthermore, we and others have shown that treating human NSPCs with PDGF-AA does not enhance oligodendrocyte differentiation despite PDGF-AA working effectively for rodent NSPCs (Fu et al., 2007; Iris Kulbatski & Tator, 2009; A. J. Mothe et al., 2011). A possible explanation could be that human NSPCs are not genetically primed to differentiate into oligodendrocytes. Our transcriptome analysis comparing human and rat NSPCs supports this idea, as we found genes and gene sets associated with oligodendrocyte development and differentiation enriched in rat NSPCs. This suggests that alternative growth factors may be required to induce oligodendrocyte fates from human NSPCs, which may be first tested *in vitro* before clinical translation.

5.5 Creating genetically reprogrammed NSPCs for transplant therapy

Cell transplantation for SCI is most beneficial when using NSPCs with a spinal cord phenotype that could faithfully integrate with the local neuroanatomy (Kadoya et al., 2016; Kajikawa et al., 2020; Kumamaru, Kadoya et al., 2018). Although bona fide human NSPCs are technically inaccessible for cell transplant, cell reprogramming protocols have allowed researchers to create spinal cord NSPCs that could be used instead (Chambers et al., 2009; Galiakberova & Dashinimaev, 2020; Kumamaru, Kadoya, et al., 2018; K. Takahashi & Yamanaka, 2006b). This

method of creating NSPCs also avoids the ethical concerns of using embryonic-derived cells. Importantly, genetically reprogrammed NSPCs have shown similar efficacy as bona fide spinal cord NSPCs in repairing the injured spinal cord (Kadoya et al., 2016). Thus, using genetically reprogrammed NSPCs represents a promising, technically, and ethically feasible approach for cell transplantation in SCI.

Many protocols claim to have created genetically reprogrammed NSPCs with a spinal cord phenotype (Bianchi et al., 2018a; Kajikawa et al., 2020; Kumamaru, Kadoya, et al., 2018; Olmsted et al., 2020). However, no studies have investigated the homology between genetically reprogrammed NSPCs and bona fide spinal cord NSPCs from adult humans. While some studies have compared reprogrammed NSPCs with embryonic- or fetal-derived spinal cord NSPCs, NSPCs from adult humans are developmentally distinct, bearing distinct molecular and functional profiles (Halliwell, 2017; Hofrichter et al., 2017; Kumamaru, Kadoya, et al., 2018). Therefore, it is unclear whether genetically reprogrammed NSPCs will be successful in their clinical application (Sugai et al., 2021).

Considering the imminent clinical application of genetically reprogrammed NSPCs for SCI, we characterized a subset of these cells with isogenic bona fide spinal cord NSPCs. We first created iPSCs using a clinically translatable method that does not involve foreign genomic integration. Then, we differentiated iPSCs into two distinct populations of NSPCs: one with a dorsal forebrain phenotype (iPSC-Br) and another with a spinal cord phenotype (iPSC-SC). iPSC-Br NSPCs were created using the dual SMAD inhibition protocol, a commonly used method of generating NSPCs from pluripotent stem cells (Chambers et al., 2009). On the other hand, iPSC-SC NSPCs were created via a distinct developmental route that involves a neuromesodermal progenitor state (Kumamaru, Kadoya et al., 2018). We confirmed the regional specificity of iPSC-Br and -SC

NSPCs to the brain and spinal cord using transcriptional analysis. Although iPSC-SC and bona fide NSPCs expressed a spinal cord regionalization, we found significant differences in their differentiation and proliferation profiles.

Moreover, there were more differentially expressed genes between iPSC-SC and bona fide NSPCs than between iPSC-Br and bona fide NSPCs. Our comparative analysis suggests that iPSC differentiation protocols have yet to produce a spinal cord NSPC population that closely resembles bona fide NSPCs. Therefore, iPSC differentiation protocols should be further optimized to enhance the homology between iPSC-SC and bona fide NSPCs. It remains to be seen whether alternative iPSC differentiation protocols can generate spinal cord NSPCs that are more homologous to bona fide NSPCs than the iPSC-SC NSPCs created in this study.

Besides iPSC differentiation, it is also possible to create genetically reprogrammed NSPCs via a direct transdifferentiation approach (Julian, McDonald, & Stanford, 2017; Shahbazi, Mirakhori, Ezzatizadeh, & Baharvand, 2018; D. Xiao et al., 2018). However, this method may carry over cellular defects from the original cell (Hu et al., 2015; Mertens et al., 2015, 2018). On the other hand, iPSC reprogramming induces genome-wide epigenetic changes that can "rejuvenate" a cell from functional defects (Mertens et al., 2015; Simpson, Olova, & Chandra, 2021). For instance, a previous study found that neuronal cells that were directly reprogrammed from fibroblasts display an age-associated decline in the function of a nuclear transporter (RanBP17). On the other hand, donor-matched neuronal cells derived from iPSCs did not show an age-associated drop of RanBP17 (Mertens et al., 2015). This rejuvenation phenomenon may be clinically significant, especially for an autologous transplant in aged patients in which high-quality NSPCs are preferred. For this reason, we utilized an iPSC reprogramming method for generating NSPCs in our study.

5.6 The ideal stem cell therapy: stimulate endogenous NSPCs or transplant exogenous NSPCs?

There are two main strategies by which NSPCs can be applied for regenerating the spinal cord: (1) stimulating endogenous NSPCs, or (2) transplanting exogenous NSPCs. The latter has been the most pursued, but each strategy has advantages and disadvantages. Several factors determining the ideal stem cell therapy include reproducibility, efficacy, safety, and ethical concerns (Assinck et al., 2017; Gilbert, Lakshman, Lau, & Morshead, 2022).

5.6.1 Reproducibility

Reproducibility is an essential concern for SCI treatments considering the range in age of afflicted patients. In Canada, 87% of SCI patients are below the age of 76 years old, and the incidence rate is similarly spread (19-26%) among age groups (16-30, 31-45, 46-60, and 61-75 years old) (Rhscir & Rhscir, 2009). Therefore, the ideal treatment would be effective across the age range. From this perspective, stimulating endogenous NSPCs may not be preferable, considering the effects of ageing on endogenous NSPC function, including senescence, reduced proliferation, and differentiation capacity (Ibrayeva et al., 2021; Xiaofei Li et al., 2016; Narbonne, 2018; Sorrells et al., 2018b). As such, a treatment that stimulates endogenous NSPCs in younger patients may not be as effective in elderly patients.

On the other hand, transplanting NSPCs may offer more reproducible outcomes, especially if a cell bank is used. In this case, a homogenous pool of NSPCs can be screened for the desired cell properties and applied across a range of SCI patients, a method currently being used in clinical trials (Sugai et al., 2021). However, using an allogenic cell bank is associated with a greater safety risk (discussed below).

5.6.2 Efficacy

There is debate about which strategy is the most efficacious treatment for SCI. Some studies have ruled out endogenous NSPCs as a source of effective regeneration in adult humans due to contrasting observations with rodent models (Garcia-Ovejero et al., 2015; Paniagua-Torija et al., 2018). These studies primarily observed an occluded central canal in post-mortem human spinal cord tissue and a lack of proliferation in the central canal region post-injury. The central canal is patent in rodents, and ependymal cells upregulate their proliferation in response to traumatic SCI (Blasko et al., 2012; Lacroix et al., 2014). However, others have observed a patent central canal in post-mortem human spinal cord tissue, including positive labeling for NSPCs markers (Cawsey et al., 2015; Dromard et al., 2008). Furthermore, we and others have been able to culture primary human spinal cord NSPCs and induce proliferation by applying mitogens (Dromard et al., 2008; Galuta et al., 2020; A. J. Mothe et al., 2011). Therefore, it appears that the human spinal cord NSPC niche has the potential to regenerate, but the conditions to promote regeneration *in vivo* are not clear.

Our study found several indicators that endogenous NSPCs may be suitable for targeted regeneration. First, we demonstrated that primary human spinal cord NSPCs are multi-potent by their potential to differentiate into neurons, oligodendrocytes, and astrocytes. NSPCs can also self-renew, as shown by their prolonged culture through successive passaging (A. J. Mothe et al., 2011). Interestingly, primary human NSPCs are primed toward neuronal differentiation even when treated with inflammatory factors. This feature, which was uniquely observed in humans but not pig or rat NSPCs, could be exploited to promote endogenous neurogenesis post-injury. In rodent models of SCI, inducing neurogenesis has been challenging due to the hostile and inhibitory nature of the injured spinal cord (Kojima & Tator, 2002; Meletis et al., 2008; Shihabuddin et al., 2000b).

However, our functional and transcriptional data suggest that human NSPCs may be better primed to differentiate into neurons than rat NSPCs. Lastly, we've demonstrated that human NSPCs can be directed to differentiate into lineage-restricted cells using growth factors. This implies endogenous NSPCs may be targeted and manipulated to control their fate *in vivo*.

By comparing human and animal model NSPCs, we also found several indicators that human NSPCs do not possess the same capacity to regenerate as rat NSPCs. For instance, a comparison of transcriptomes revealed that rat NSPCs portray more of a neural stem cell phenotype. Concurrently, rat NSPCs proliferate at a greater rate than human and pig NSPCs, which suggests that NSPCs from larger mammals may not be as capable of repopulating cells lost to SCI. Another significant difference between NSPCs of large (human and pig) and small (rat) mammals was their ability to differentiate into oligodendrocytes. Rat NSPCs readily differentiated into oligodendrocytes which could be further enhanced using PDGF-AA. On the contrary, human and pig NSPCs rarely or did not form any oligodendrocytes, which did not improve with PDGF-AA treatment. A transcriptome analysis revealed an enrichment of genes associated with oligodendrocyte development in rat NSPCs that may underlie their ability to differentiate into oligodendrocytes. As such, endogenous human NSPCs may not be a significant source of remyelination post-injury.

In a separate study, the regenerative potential of human NSPCs was evaluated by transplanting NSPCs in a rodent model of SCI (A. J. Mothe et al., 2011). However, the authors only reported immunohistochemical outcomes 1-week post-injury, including the integration of ~7.6% of grafted human NSPCs and their multi-lineage differentiation. Therefore, future experiments are needed to evaluate the regenerative potential of human NSPCs *in vivo,* including assessing functional outcomes at chronic time points.

Several lines of evidence implicate the transplant of genetically reprogrammed NSPCs as a more effective strategy than stimulating endogenous NSPCs. Our study found that iPSC-derived NSPCs were enriched in genes and gene networks associated with neurogenesis, proliferation, and NSPC maintenance relative to bona fide NSPCs. Furthermore, iPSC-derived NSPCs were highly proliferative, indicating a superior ability to repopulate cells after an SCI. However, the iPSC-SC NSPCs in our study did not differentiate into neurons to the same capacity as primary NSPCs. Given that previous studies have achieved significant neurogenesis *in vitro* and *in vivo* from iPSC-SC NSPCs, it may be possible that the cells in our study were at an early developmental stage and required further maturation (Kumamaru, Kadoya et al., 2018; Kumamaru, Lu, Rosenzweig, Kadoya, & Tuszynski Correspondence, 2019; Rosenzweig et al., 2018).

Another advantage of iPSC-derived NSPCs is that they may be differentiated into lineage-restricted precursors, such as glial-restricted precursors and neural-restricted precursors, before transplantation. This allows the grafting of specific cell types (e.g., neurons and oligodendrocytes), which can be used to promote particular mechanisms (e.g., neuronal relays and remyelination) (Davies et al., 2006; Kadoya et al., 2016). Despite these advantages, a study by Kadoya and colleagues (2016) demonstrated a similar efficacy of bona fide rodent NSPCs and human iPSC-SC NSPCs to repair the spinal cord. However, this study evaluated rat and not human bona fide NSPCs, rendering a direct comparison with human iPSC-SC NSPCs inadequate. To determine whether bona fide or genetically reprogrammed NSPCs possess the greatest regenerative capacity, transplanting isogenic pairs in a rodent model of SCI is needed.

5.6.3 Safety

From a safety perspective, stimulating endogenous regeneration may be the preferred option. Stimulating endogenous NSPCs can be achieved through minimally or non-invasive means,

including intrathecal injection of drugs, electrical stimulation, and diet (Y. Huang, Li, Chen, Zhou, & Tan, 2015; Soheila Karimi-Abdolrezaee et al., 2012; Kojima & Tator, 2002; Sefton et al., 2020; Streijger et al., 2013). On the other hand, the transplant of exogenous NSPCs is an invasive procedure that requires surgical intervention. Furthermore, transplanting allogeneic NSPCs will likely require immunosuppression to prevent graft rejection, possibly leading to secondary complications (Curtis et al., 2018b; Yousefifard et al., 2016). Indeed, it is possible to mitigate immunorejection and the use of immunosuppressants by transplanting autologous NSPCs (Khazaei et al., 2017). However, creating genetically reprogrammed NSPCs is time-consuming, which may limit the application of autologous transplants to chronic time points of SCI. Furthermore, transplanting autologous NSPCs in elderly patients may suffer from reproducibility issues due to age-related functional deficits in reprogrammed cells, which can impact differentiation and proliferation. (Lo Sardo et al., 2017b, 2017a).

5.6.4 Ethics

A primary ethical concern with stem cell treatments involves the use of embryonic or fetal-derived cells (Lo & Parham, 2009). Before the availability of genetic reprogramming technologies, embryonic stem cells were commonly used to produce nervous system stem cells, which can be used for transplant in SCI (Curtis et al., 2018b; Manley et al., 2017). However, researchers nowadays can create NSPCs from consenting adults using a skin or blood biopsy, thus mitigating the ethical concerns associated with using embryonic and fetal tissue (Khazaei et al., 2017). On the other hand, stimulating endogenous NSPCs poses fewer ethical concerns since it avoids using pluripotent stem cells altogether (Gilbert et al., 2022).

5.6.5 The verdict

Overall, stimulating endogenous NSPCs may be better suited for younger patients than the elderly, considering the safety profile of this strategy and that endogenous NSPCs from younger individuals are more inducible to regenerate (Ibrayeva et al., 2021; Xiaofei Li et al., 2016; Narbonne, 2018; Sorrells et al., 2018b). On the other hand, transplanting allogeneic genetically reprogrammed NSPCs may be better suited for the elderly population; unless autologous NSPCs can be genetically reprogrammed in a manner that is quick and overcomes the issues with reproducibility. Ultimately, it remains to be determined whether endogenous or genetically reprogrammed NSPCs bear the most significant potential for regeneration and would fare better in stem cell therapy for SCI. To this extent, we propose some experiments in Section 5.8 that may edge us closer to determining the ideal stem cell therapy.

5.7 Limitations of study

5.7.1 *In vitro* studies

The major limitation of the experiments conducted in this thesis involves using *in vitro* models to study human NSPC biology. The artificial conditions employed *in vitro* do not capture the entire nature and complexity of the spinal cord environment. As such, the physiology of NSPCs *in vitro* can be expected to deviate from their natural state *in vivo* (Gil-Perotín et al., 2013; Pfenninger, Steinhoff, Hertwig, & Nuber, 2011). For instance, NSPCs in healthy spinal cord tissue are dormant, but the culture of NSPCs induces their proliferation (Lacroix et al., 2014; Weiss et al., 1996). For this reason, we cannot confidently extrapolate that human NSPCs are neurogenic *in vivo* despite making these observations *in vitro*.

Similarly, we could not expect the response of NSPCs to inflammatory factors *in vitro* to fully recapitulate the pathophysiological response *in vivo*. To account for the differences between *in vitro* and *in vivo* environments, we compared human NSPCs with animal model NSPCs since the latter have been characterized *in vivo*. This allows us to cross-reference human NSPC behaviour *in vitro* with animal model NSPC behaviour *in vivo*.

Another limitation is that the longer NSPCs are cultured *in vitro*, the more their intrinsic biology will change to adapt to the culture conditions (Gil-Perotín et al., 2013; Soares et al., 2020, 2021; Yang et al., 2019). We found that rat NSPCs cultured for ten passages produce significantly more oligodendrocytes than primary NSPCs. Similarly, iPSC-Br NSPCs cultured for two more passages produced significantly more astrocytes. To circumvent this limitation in our study, we characterized primary NSPCs to minimize the time spent *in vitro* and, consequently, the influence of culture conditions. In doing so, we attempted to mitigate changes in the intrinsic biology of NSPCs from their *in vivo* state.

Lastly, the parameters used in *in vitro* assays will influence the observed outcomes (Gil-Perotín et al., 2013; Soares et al., 2021). Our study characterized NSPCs following only one or two weeks of treatment. Still, we may observe different outcomes if the assessment periods were extended. For example, we did not observe glial scarring in human NSPC cultures following two weeks of inflammatory treatment, although we did see a response from pig and rat NSPCs under the same conditions. However, it is possible that a more prolonged treatment was needed to induce glial scarring from human NSPCs. It is also possible that a different set of inflammatory factors which were not tested in our study could induce glial scarring in human NSPCs. Similarly, the low oligodendrocyte differentiation from human NSPCs may be due to insufficient time for oligodendrocytes to develop and/or using inadequate differentiation factors (Vogel et al., 2019).

Therefore, *in vitro* results must be interpreted cautiously since the parameters will influence the outcomes.

Despite these inherent limitations of *in vitro* models, the primary advantage is that it allows for the functional assessment of human NSPCs that would not be possible otherwise. The simple nature of an *in vitro* assay will enable us to model specific aspects of the *in vivo* state and determine causal mechanisms that may be occurring *in vivo*. For example, our inflammation assay treated NSPCs with inflammatory factors that are upregulated in SCI and have known causal effects on rat NSPCs *in vivo*. Therefore, we were able to assess whether the same causal mechanisms driving glial scarring in rats are also applicable to human NSPCs. Another advantage is that it permits the direct comparison of NSPCs among species by culturing cells under identical conditions. This could allow for the determination of species-specific mechanisms to improve our understanding of the differences between humans and pre-clinical animal models. Lastly, an *in vitro* assay could be used to test the effects of pre-clinical drugs on human NSPCs before their clinical application. It could also be used to optimize the dosage and duration of treatment that result in the most desirable outcomes (e.g., enhanced neuronal differentiation and survival).

5.7.2 Use of female animal models

The animals used in this study, including pigs and rats, were all female, thus limiting our understanding of sex differences concerning NSPC function. The field of basic science and pre-clinical research has predominately used young female rodents to study SCI and evaluate potential treatments (Stewart et al., 2020). However, most SCI patients are male, with a ratio of 4:1 males to females in Canada (Rhscir & Rhscir, 2009). Even within the female population of SCI patients, the least inflicted are young and elderly females (Furlan, Krassioukov, & Fehlings, 2005; McCaughey et al., 2016; Sipski, Jackson, Gómez-Marín, Estores, & Stein, 2004). Consequently,

the field of SCI research has primarily been using animal models that do not reflect the demographic profile of most SCI patients for biological sex and age.

Post-operative care is the primary reason for using young female rodents in SCI research. Fewer complications associated with the postoperative care of female rodents, such as bladder expression, reduce the chances of mortality and adverse health conditions (Stewart et al., 2020). There have been greater efforts to include male rats in SCI research. However, it is still not clear whether sex plays a significant role in SCI outcomes despite some evidence pointing towards a small neuroprotective effect in females (Datto et al., 2015; Farooque et al., 2006; Hauben, Mizrahi, Agranov, & Schwartz 2002). Sex differences concerning spinal cord NSPCs are even less known, although one study found that male NSPCs proliferate more and differentiate more into neurons *in vitro* (R. Li et al., 2012). Considering the wealth of *in vivo* and *in vitro* studies done using female rats, we used female rats to cross-reference our data with the literature. Female pigs were used in our study since they were provided to us by the Skills and Simulation Center (University of Ottawa).

5.7.3 Heterogeneity of iPSCs

Despite the advantage of rejuvenation during iPSC reprogramming, there remain some obstacles with the reproducibility of iPSC reprogramming. First, it's been shown that iPSC reprogramming can be incomplete, resulting in pluripotent clones with varying differentiation capacities (Brix, Zhou, & Luo, 2015). Therefore, there have been attempts to optimize iPSC reprogramming through epigenetic mechanisms such as using small molecules. Secondly, the epigenetic memory of the original cell may persist, which can affect the differentiation potential of iPSCs, including enhanced differentiation into the original cell type (Efrat, 2021). As such, it is important to determine the optimal cell type for reprogramming into NSPCs by performing a side-by-side

comparison of various easily accessible cell types. Lastly, inter-donor differences in iPSCs and their progeny may be due to the inherited genetic variation between donors. This could affect the regenerative characteristics of genetically reprogrammed NSPCs. For instance, Strano and colleagues (2020) found that the differentiation of iPSCs from different donors produced neurons with developmentally distinct spatial and regional axes. The observed divergence in neuronal progeny among donors was partly due to endogenous Wnt signaling. Correspondingly, the iPSC-Br and -SC NSPCs generated in our study exhibited functional and transcriptional variations between donors. Therefore, donor-dependent (e.g., genetic variability) and donor-independent (e.g., reprogramming method and original cell type) factors contribute to the reproducibility issues associated with iPSC reprogramming. These factors should be revised to improve the reproducibility of creating iPSC-derived NSPCs for autologous transplantation.

5.7.4 Human sample size

The study of human subjects and their cells or tissues typically requires a large sample size due to inherit genetic differences between humans (Hong & Park, 2012). This is particularly important when comparing human subjects but is less critical when making cross-species comparisons. For instance, our study comparing human and animal model NSPCs found significant differences in the average differentiation trends between species. Variability between humans was seen in the percentage of differentiated cells at specific time points, although the differentiation trends were the same (i.e., mostly neuron differentiation and little glial differentiation). Due to differences between donors, we attempted to find correlations between donor demographics (e.g., age and sex) and the doubling rate of NSPCs. However, we could not determine any significant statistical correlations in this case, likely due to our analysis's low statistical power. Therefore, a greater

sample size of humans is required to determine significant differences between donors, although it was not needed for our cross-species comparison.

5.8 Future directions

5.8.1 Enhance differentiation of primary human NSPCs

A primary goal of regenerative therapies has been to direct endogenous NSPCs along the neuronal lineage for cell replacement and the formation of neuronal relays (Becker et al., 2018; Gilbert et al., 2022; S. Liu & Chen, 2019). Our findings and previous studies suggest that human NSPCs possess neurogenic potential, which may be exploited *in vivo*. For instance, Mothe and colleagues (2011) found that primary human NSPCs differentiated approximately ten-fold more into neurons than glial cells. Neuronal differentiation was further enhanced 19-fold with the application of dbcAMP. Similarly, Jha and colleagues (2013) differentiated human NSPCs from the filum terminale. They reported a significant amount of neuronal differentiation (55%) that could be matured into motor neurons with the application of Shh, BDNF, GDNF, and CTNF. Another study treated human NSPCs from the filum terminale with PDGF-BB, which enhanced neuronal differentiation ten-fold (Arvidsson et al., 2011).

Our study found that primary human NSPCs spontaneously differentiate into a large proportion of neurons which could be further enhanced using retinoic acid treatment. In some experiments, we also demonstrated BDNF and GDNF's effectiveness in improving neuronal differentiation. However, our differentiation assays were only conducted for up to two weeks, thus necessitating extended differentiation periods to induce functionally mature neurons. Given the sparsity of studies on the differentiation of human spinal cord NSPCs into neurons, there is much to discover on the conditions that regulate and enhance this process (Dromard et al., 2008; A. J. Mothe et al.,

2011). Conducting a cross-species *in vitro* assay like the model presented in Chapter 2 could allow for determining and optimizing differentiation factors that could induce neuron differentiation from human NSPCs.

Another benefit of endogenous regeneration is the differentiation of spinal cord NSPCs into oligodendrocytes to improve remyelination post-injury. It's been demonstrated that endogenous NSPC differentiation into oligodendrocytes could be enhanced through pharmacological treatment or genetic manipulation in rodent models of SCI (Barnabé-Heider et al., 2010; Soheila Karimi-Abdolrezaee et al., 2012; Llorens-Bobadilla et al., 2020). However, our work and previous studies have demonstrated that human NSPCs bear little potential for oligodendrocyte differentiation (Arvidsson et al., 2011; Dromard et al., 2008; A. J. Mothe et al., 2011). Furthermore, human NSPCs have been refractory to treatments that promote oligodendrocyte differentiation in rodent NSPCs (Fu et al., 2007; Soheila Karimi-Abdolrezaee et al., 2012; Plemel et al., 2011). By understanding the differences in intracellular mechanisms between human and rat NSPCs, we may be able to induce oligodendrocytes successfully from human NSPCs.

Our transcriptome analysis revealed genes and gene networks associated with oligodendrocyte differentiation and development that were downregulated in humans compared to rat NSPCs. From this analysis, we can identify candidate genes in rat NSPCs that direct oligodendrocyte differentiation and overexpress these genes in human NSPCs (Llorens-Bobadilla et al., 2020). Alternatively, it may be possible to induce the expression of transcription factors that specify the oligodendrocyte lineage by activating associated signalling pathways using exogenous molecules (Vogel et al., 2019). Finding an effective method of differentiating human NSPCs into oligodendrocytes may pave the way for novel remyelination strategies for SCI.

5.8.2 Investigate the pathophysiology of human NSPCs in SCI

Developing treatments for SCI first necessitates understanding the pathophysiological mechanisms involved. Unfortunately, our understanding of the pathophysiological mechanisms mediated by endogenous NSPCs in human SCI is largely unknown. Previously, only two studies have attempted to decipher these mechanisms (Cawsey et al., 2015; Paniagua-Torija et al., 2018). Both studies examined post-mortem spinal cord tissue from SCI patients using immunohistochemical markers and obtained contradictory results. Cawsey and colleagues (2015) observed an upregulation of activated $Nestin^+$ NSPCs that correlated with post-injury time, while Paniagua-Torija and colleagues (2018) failed to observe an increase in NSPC proliferation following SCI.

Our study provides the first functional assay to understand the pathophysiological response of human NSPCs to secondary injury. Here, we treated NSPCs with inflammatory factors produced in SCI and assessed for markers of proliferation, neurogenesis, and glial scarring. However, the inflammatory factors tested here do not cover the complexity and scope of immune-NSPC interactions that are possibly occurring *in vivo*. To this extent, further exploration is needed to understand the effect of inflammation on human NSPCs during SCI.

This could be conducted similarly to the model presented in Chapter 3, which involves the treatment of NSPCs with inflammatory factors *in vitro*. To achieve more complex and realistic models of pathophysiology, human NSPCs could be co-cultured with activated microglia or other immune cells isolated from injured rodent spinal cord tissue. Alternatively, human NSPCs could be co-cultured with human microglia pre-treated to induce an activated pro-inflammatory state (Ma et al., 2019).

An exciting and relatively recent method entails *ex vivo* organotypic slices, which enable the study of human NSPCs in a three-dimensional model of the spinal cord. This method has been used to study secondary injury mechanisms and test the effects of pharmacological agents for neuroprotection and regeneration (Krassioukov et al., 2002; Sypecka, Koniusz, Kawalec, & Sarnowska, 2015). The advantage of this model over traditional two-dimensional cell culture models is that NSPCs maintain their original cell-to-cell contact within the spinal cord, thus possibly portraying *in vivo* behaviour more accurately.

In complement with *in vitro* and *ex vivo* functional assays, analyses of post-mortem spinal cord tissue from injured patients should also be conducted to support or reject predictions made using *in vitro* and *ex vivo* tests (Cawsey et al., 2015; Gonzalez-Fernandez et al., 2017; González et al., 2020; Paniagua-Torija et al., 2018). Indeed, these investigations require spinal cord tissue from healthy organ donors and SCI patients, which is not as easily accessible.

5.8.3 Evaluate the translational relevance of porcine NSPCs

The porcine SCI model has recently emerged as an important intermediary between rodents and humans and represents a more ethically feasible model to study than non-human primates (Kwon et al., 2015; Schomberg et al., 2017). Using porcine in SCI research has enabled the discovery of biomarkers that could predictably stratify SCI outcomes in humans and reject pre-clinical treatments that are ineffective in larger mammals (Dalkilic et al., 2018; Streijger et al., 2016; Wu et al., 2016). As such, the porcine model appears to be a vital contributor to translating pre-clinical SCI research. However, given the novelty of the porcine model, there is much yet to be discovered concerning endogenous NSPCs.

According to our knowledge, we have characterized adult porcine spinal cord NSPCs for the first time. Importantly, we noted functional and transcriptional distinctions between porcine and human NSPCs *in vitro*. Due to our lack of understanding of porcine NSPCs, further studies are required to assess the translational value of the porcine model. For instance, given that porcine NSPCs undergo reactive astrogliosis *in vitro* like rat NSPCs, it would be useful to determine whether porcine NSPCs also undergo reactive astrogliosis *in vivo*. Furthermore, given that porcine NSPCs proliferate at a similar rate as human NSPCs, it would be helpful to understand the proliferation rate of endogenous porcine NSPCs in a healthy and injured spinal cord. Answering these questions will shed light on the relevance of the porcine model to accurately depict human NSPC biology and the potential of studying porcine NSPCs as an alternative to human NSPCs.

5.8.4 Create iPSC-SC NSPCs

Ever since the discovery of iPSCs, there have been an increasing number of protocols that claim to generate NSPCs. In these protocols, iPSCs are differentiated in 2-D or 3-D using signaling molecules and inhibitors, epigenetic modifiers, and/or genetic manipulations of lineage-specific transcription factors (Galiakberova & Dashinimaev, 2020; H. C. Lin et al., 2021). Depending on the differentiation protocol used, the resulting NSPCs can vary in phenotype, including regional identities, developmental stages, molecular attributes, and functional behaviours. While most differentiation protocols have generated brain-regionalized NSPCs, protocols have been developed in recent years that aim to create caudalized NSPCs that mimic endogenous spinal cord NSPCs (Bianchi et al., 2018a; Chambers et al., 2009; Kumamaru, Kadoya, et al., 2018; Olmsted et al., 2020; Shimojo et al., 2015). Since spinal cord-homologous iPSC-derived NSPCs are preferred in SCI repair strategies, it's imperative to compare the phenotypes of iPSC-derived NSPCs with bona fide spinal cord NSPCs (Kadoya et al., 2016).

Our study differentiated a single iPSC clone into NSPCs bearing either a dorsal forebrain (iPSC-Br) or spinal cord (iPSC-SC) phenotype. We found that iPSC-SC NSPCs expressed regional markers of the spinal cord, such as *HOX* genes, at a much higher level than iPSC-Br NSPCs and a comparable level to bona fide NSPCs. Although iPSC-SC and bona fide NSPCs shared a regional homology, we found many discrepancies with respect to their transcriptomes and functional behaviour, including a reduced neurogenic potential of iPSC-SC NSPCs. As such, the iPSC-SC NSPCs generated in our study may not be suitable for clinical applications in SCI.

Based on our transcriptional and functional analysis, we hypothesize that the iPSC-SC NSPCs in our study may be at an early developmental stage. Since bona fide NSPCs are at an adult developmental stage, it would be worth culturing iPSC-SC NSPCs longer to create more developmentally mature NSPCs. This may enable the creation of iPSC-SC NSPCs that bear a greater resemblance to bona fide NSPCs.

Furthermore, considering the emergence of multiple iPSC differentiation protocols, it would be worth assessing the effectiveness of these protocols in generating iPSC-SC NSPCs (Bianchi et al., 2018a; Kajikawa et al., 2020; Olmsted et al., 2020). This could be conducted similarly to the method used in Chapter 4, whereby isogenic pairs of bona fide and iPSC-SC NSPCs are compared. These experiments could determine the most practical and effective protocol for generating spinal cord homologous iPSC-derived NSPCs. In the future, it would be interesting to identify candidate genes and gene networks in bona fide NSPCs that could be manipulated in iPSCs. Ultimately, the goal would be to create iPSC-derived NSPCs with the most significant molecular and functional resemblance to bona fide spinal cord NSPCs.

5.8.5 Assess the regenerative potential of human NSPCs

The primary goal of this thesis is to improve the translation of NSPC therapies for SCI, including targeting endogenous NSPCs and transplanting iPSC-derived NSPCs. We sought to achieve this goal by evaluating the regenerative properties of adult human spinal cord NSPCs and comparing them with animal models and iPSC-derived NSPCs. However, our evaluations consisted of *in vitro* characterizations that may not portray the true regenerative potential of human NSPCs *in vivo*.

To evaluate the regenerative potential of human NSPCs more accurately, it would be helpful to transplant primary human NSPCs in an SCI model. Previously, only one study reported the transplant of adult human NSPCs in a rodent model of SCI (A. J. Mothe et al., 2011). However, this study only evaluated immunohistochemical outcomes one-week post-grafting and did not assess any functional outcomes. Therefore, it's unclear whether human NSPCs bear the potential to repair the injured spinal cord.

To shed light on this matter, it would be interesting to transplant human NSPCs in a rodent model of SCI and evaluate both immunohistochemical and functional outcomes at chronic time points (>2 months). Furthermore, a controlled study involving the transplant of pig or rat NSPCs would enable a direct comparison of the regenerative potentials of human, pig, and rat NSPCs. The transplant of rat NSPCs has been demonstrated to improve neurological and functional outcomes (Brock et al., 2018; Soheila Karimi-Abdolrezaee et al., 2012; A. J. Mothe & Tator, 2008). Therefore, this experiment could answer questions regarding the regenerative capacity of endogenous NSPCs in humans to repair the injured spinal cord. This experiment could also allow the determination of factors (e.g., growth factors, drugs, biomaterials) that stimulate the proliferation, migration, differentiation, and survival of human NSPCs *in vivo*.

To improve the translation of iPSC-derived NSPC therapies for SCI, it would be helpful to transplant isogenic pairs of bona fide and iPSC-SC NSPCs in a small or large animal model of SCI. This experiment would better compare their regenerative potentials more accurately than our *in vitro* characterizations. Furthermore, it would be interesting to transplant iPSC-SC NSPCs derived from different aged donors to assess the effect of ageing on the regenerative potential of genetically reprogrammed NSPCs. This is an essential consideration for the autologous transplant of iPSC-SC NSPCs to ensure reproducible outcomes across patients.

5.9 Conclusion

In this collective work, we have begun to establish methods to guide future translational studies of stem cell strategies in SCI by evaluating the regenerative properties of human NSPCs *in vitro*. Primary spinal cord NSPCs from humans, pigs, and rats possess distinct proliferation and differentiation profiles reflected in their transcriptomes. Moreover, we observed species-specific responses of NSPCs to inflammatory and regenerative factors, which may improve our understanding of the pathophysiological mechanisms and conditions to promote regeneration in human SCI. We also compared the first-ever isogenic NSPCs derived from the adult human spinal cord and iPSCs. Primary spinal cord NSPCs differ from iPSC-derived NSPCs concerning their differentiation, proliferation, regional, developmental, and cellular phenotypes. Furthermore, we demonstrate that iPSC differentiation protocols are not reproducible across patients. In doing so, we are beginning to unravel the homology between iPSC-derived NSPCs and bona fide spinal cord NSPCs and evaluate the potential of autologous iPSC-derived NSPCs for transplant therapy in SCI. In the future, we hope this study will inspire investigations into human NSPC biology to ameliorate regenerative strategies targeting endogenous NSPCs or transplanting NSPCs for SCI repair.

Appendix A: Demographic Profile and Spinal Cord Region Influence Human NSPC Function

Abstract

Objectives: To characterize and compare the functional properties of human neural stem/progenitor cells (NSPCs) from multiple donors and different regions of the adult spinal cord neuroaxis.

Methods: Adult human primary NSPCs from the thoracic (n=21), lumbar (n=12), and conus medullaris (n=3) spinal cord were cultured using the Neurosphere assay. The yield and doubling rate of primary NSPCs were calculated upon passaging and correlated with donor demographics and medical history. Primary-derived NSPCs were treated for up to two weeks with either 1% fetal bovine serum (FBS) to induce differentiation or mitogens (EGF, FGF2) to induce proliferation. The differentiation and proliferation profiles were characterized by immunocytochemistry.

Results: The yield of primary NSPCs varied among donors and from different spinal cord regions of the same donor. Lumbar and conus-derived NSPCs from younger donors (≤51 years old) had significantly greater yield than thoracic-derived NSPCs. The primary NSPC doubling rate correlated linearly with cell culture parameters but not for donor demographics. The differentiation profile of NSPCs varied as lumbar-derived NSPCs generated the fewest neurons and most astrocytes over time. The proliferation rate was greatest from conus-derived NSPCs, yet the fold change in proliferation was greatest from lumbar-derived NSPCs.

Conclusions: The regional source of NSPCs and cell culture parameters may influence the yield and doubling rate of adult human spinal cord NSPCs. The regenerative potential of NSPCs varies along the spinal cord rostral-caudal axis, possibly due to cell-intrinsic differences or in the

composition of NSPCs (i.e., proportion of stem and progenitor cells). Therefore, differences in NSPCs along the rostral-caudal axis of the human spinal cord should be considered and further evaluated to optimize NSPC-targeted strategies for SCI repair.

Introduction

Neuro-regenerative strategies for spinal cord injury, including stem cell therapies, have not been reproducibly effective in humans despite pre-clinical success in animal models (Badhiwala et al., 2018; Courtine & Sofroniew, 2019; Yamazaki et al., 2020). The failure to translate can be partly attributed to the reliance on highly reproducible animal models that do not consider the heterogeneity of human spinal cord injuries, along with the lack of *in vitro* studies using human spinal cord tissue (Cheriyan et al., 2014; Dromard et al., 2008; K. T. Kim et al., 2018; A. J. Mothe et al., 2011; Silva et al., 2014). Furthermore, the effect of patient demographics and injury profiles on regenerative outcomes is poorly understood (Failli et al., 2021; Fehlings et al., 2017; J. R. Wilson et al., 2020). In contrast to the reproducible animal models used in most studies, spinal cord injury in humans is highly variable, including differences in a patient's age, sex, injury severity, and location (Norenberg et al., 2004; Silva et al., 2014). For this reason, further studies must be conducted in humans and using human samples that will consider the variability among patients.

A promising neuro-regenerative strategy that is relatively less invasive and immunogenic involves the stimulation of endogenous neural stem/progenitor cells (NSPCs) (Moore, 2016; Moreno-Manzano, 2020b). NSPCs have the potential to self-renew and differentiate, thereby repopulating cells that have died or degenerated as a result of injury (Temple, 2001). In addition, NSPCs have been shown to provide a growth-permissive environment that enhances endogenous regeneration

mechanisms, including remyelination, angiogenesis, and axonal growth (de Freria et al., 2021; Dulin & Lu, 2014; Hawryluk et al., 2012; Kumamaru, Lu, et al., 2018). For example, in lower vertebrates that can repair their spinal cord after injury, endogenous NSPCs differentiate into radial glia that provide paracrine and anatomical support for axon growth (Becker et al., 2018; Sîrbulescu & Zupanc, 2010). Therefore, understanding the mechanisms regulating NSPC behavior, including their self-renewal and differentiation, will be necessary for their application in neuro-regenerative strategies.

Rodents have been a resourceful pre-clinical animal model for studying endogenous spinal cord NSPCs and their potential as regenerative agents (Cheriyan et al., 2014; Yousefifard et al., 2016). It has been shown that NSPCs along the rostral-caudal neuroaxis of the spinal cord vary with respect to their molecular and functional properties (Blasko et al., 2012; Iris Kulbatski & Tator, 2009; Pfenninger et al., 2011; Sabourin et al., 2009b; Weiss et al., 1996). Therefore, the regional identity may affect how different NSPC populations are targeted and their regeneration capability. In addition to their regional identity, NSPCs vary depending on the donor demographic profile. For instance, NSPCs from young and aged animals vary in their self-renewal and differentiation properties which are directly correlated to different outcomes after spinal cord injury (Xiaofei Li et al., 2016; Sutherland, Mathews, Mao, Nguyen, & Gorrie, 2017). Therefore, it is likely that the regional identity and age of NSPCs will influence, to some degree, how they should be targeted for regenerative purposes.

Studies have demonstrated that human spinal cord NSPCs are unique compared to their animal model counterparts concerning their anatomy *in vivo*, functional behavior *in vitro*, and molecular profile (Alfaro-Cervello et al., 2014; Galuta et al., 2020; Garcia-Ovejero et al., 2015; Ghazale et al., 2019b; A. J. Mothe et al., 2011). However, these studies are relatively few, reinforcing the

notion of increasing and improving on the existing literature. As such, it is not known how adult human spinal cord NSPCs of different regional identities compare with respect to their functional properties.

We have previously demonstrated the ability to culture primary adult human spinal cord NSPCs and characterized their functional behavior (Galuta et al., 2020). In this study, we cultured primary human spinal cord NSPCs from the thoracic, lumbar, and conus regions in an identical manner. We assessed for direct relationships between the primary NSPC doubling rate to donor demographics, medical history, or cell culture parameters. Only cell culture parameters were determined to impose a significant influence on primary human spinal cord NSPC doubling rates. We also report distinct proliferation and differentiation profiles from regional NSPCs that may reflect cell-intrinsic differences or in the composition of NSPCs.

Methods

Ethics statement

For the harvesting of human spinal cord tissue, ethics approval for the study was obtained from the Ottawa Health Science Network Research Ethics Board and from the Trillium-Gift of Life Network (TGLN), which oversees organ donation in Ontario. Patients were identified to study personnel after neurologic determination of death (NDD) was assessed by TGLN. Informed written consent was obtained from the family of the deceased organ donor for tissue collection.

Spinal cord harvest and primary NSPC culture

Human spinal cords were harvested using an anterior approach, according to Galuta et al. (2020) (see Table 1 for donor demographics). Briefly, the spinal cord was exposed from the surrounding tissues and organs, and then transverse cuts were made at the L2 level of the spinal cord and the

most rostral level. Using a sternal saw angled 45° medially, transverse cuts were made in a caudal to rostral direction on both lateral sides of the spinal cord to remove the vertebral bodies. The harvested spinal cord was placed in cold, sterile dissection media: 1X Hank' Balanced Salt Solution (HBSS)+ 0.6% D-glucose + 2% penicillin-streptomycin (PS) (Gibco, 15140122) and processed immediately for micro-dissection. The central canal region was excised under a dissection microscope, leaving out contaminant surrounding grey and white matter, then dissociated using a papain dissociation kit (Worthington Biochemical Inc., LK003150) according to the manufacturer's instructions. Following purification, cells were re-suspended in a serum-free media (SFM), which consisted of: Neurobasal-A medium (ThermoFisher Scientific, 10888022), 2 mM L-glutamine (Gibco, A2916801), 100 U/mL PS, 1% B27-vitamin A (Gibco, 12587010), and 10% hormone mix (1:1 DMEM/F12 (Sigma, D8900), 0.6% glucose, 3 mM $NaHCO_3$, 5 mM HEPES, 25 µg/mL insulin, 100 µg/mL apo-transferrin, 10 µM putrescine, 30 nM selenium, and 20 nM progesterone in distilled water). Cells were seeded at 20 cells/µL onto matrigel (Corning™, 354230) coated six-well plates in a total of 4 mL of proliferation media (1X EFH): SFM + 20 ng/mL human epidermal growth factor (EGF) (Sigma, E9644) + 20 ng/mL human basic fibroblast growth factor (FGF2) (Sigma, F3685) + 2 µg/mL heparin (Sigma, H3149) and incubated at 37˚C, 5% CO_2, 20% O_2 for one week undisturbed. Cultures were fed every 2-3 days for 1-2 weeks by replacing half the culture medium with an equivalent amount of 2X EFH. Once adherent cultures were visibly expanding, cultures were fed by replacing the full media with 2 mL of 1X EFH. Cultures were fed this way before reaching confluence, at which point NSPCs were passaged and assessed.

Primary yield and doubling time calculation

The primary yield was calculated by dividing the total number of NSPCs counted during the primary passage by ten thousand initially seeded primary cells. The number of viable NSPCs was counted during seeding or passaging using Trypan Blue (1:1) and a hemacytometer. The doubling time (T_D), in days, was calculated using the equation: $T_D = (T_2 - T_1) \times [\ln(2) / \ln(P_2/P_1)$, where $T_2 - T_1$ represents the days *in vitro*, P_2 represents the number of NSPCs during primary passage, and P_1 represents the number of primary NSPCs seeded. P_1 was approximated to be 0.01% of the total number of cells seeded based on the neurosphere formation rate found in other studies (Dromard et al., 2008; Pfenninger et al., 2011; Sabourin et al., 2009b). A total of 22 subjects were included in the analysis.

Induction of NSPC differentiation and proliferation

Primary NSPC cultures were passaged using accutase (Gibco, A1110501) and incubated at 37ºC for 5 minutes. Lifted NSPCs were centrifuged at 300 xg for 5 minutes and resuspended in 1X EFH to calculate cell density. NSPCs were seeded onto matrigel-coated 96-well plates (150 µL/well) in 1X FH for two days before treatment. To assess the intrinsic NSPC differentiation potential, NSPCs were seeded at 1 cell/µL and induced to differentiate with 1% FBS (Corning™, 35015CV) in SFM. To induce regeneration, NSPCs were seeded at 5 cells/µL and directed to self-renew with 1X EFH. NSPCs were treated for one or two weeks, replacing the media every 2-3 days, then fixed with 4% paraformaldehyde (PFA) (Sigma, P6148) and characterized by immunocytochemistry. Cultures for which proliferation was assessed had bromodeoxyuridine (BrdU) (Sigma, B5002) administered 24 hours before being fixed.

Immunocytochemistry

Fixed cultures were blocked with 10% normal goat serum (NGS) (ThermoFisher Scientific, P131873) and permeabilized with 0.3% Triton-X in PBS for 30 minutes at room temperature. However, wells stained for O4 were only blocked and not permeabilized. Cultures were washed three times with PBS, then incubated with respective primary antibodies with 10% NGS in PBS overnight at 4 ºC. The following antibodies were used: mouse anti-O4 IgM (1:500) (Novus Biologicals, MAB1326) to label oligodendrocytes, mouse anti-β-iii tubulin IgG (1:500) (STEMCELL Technologies, 01409) (SantaCruz, 80005) to label immature neurons, rabbit anti-GFAP IgG (1:1000) (EMD Millipore, Ab5804) to label astrocytes, rabbit anti-Sox2 IgG (1:1000) (Abcam, ab97959) to label neural stem cells, and mouse anti-BrdU IgG (1:2000) (EMD Millipore, MAB4072) as a marker for proliferation. The following day, cultures were washed three times with PBS and incubated with respective species-matched secondary conjugated antibodies in PBS for 2 hours at room temperature. The following secondary antibodies were used: goat anti-mouse IgG Alexa Fluor 488 (1:300) (Abcam, Ab150113), goat anti-rabbit IgG Alexa Fluor 488 (1:500) (Abcam, Ab150077), goat anti-mouse IgG Alexa Fluor 594 (1:300) (Abcam, ab150116), goat anti-rabbit IgG Alexa Fluor 594 (1:500) (Abcam, ab150080), and goat anti-mouse IgM Alexa Fluor 594 (1:300) (ThermoFisher, A-21044). Cultures were washed three times with PBS, counterstained with Hoeschst (1:2000) (ThermoFisher, 62249), and processed for visualization.

NSPC characterization and statistical analysis

Immuno-stained cultures were visualized using a Nikon Ti Eclipse Epifluorescence. Ten images were taken for each well (n=3 wells per treatment). Images were analyzed using Image J software, from which the total number of immuno-positive cells was counted as a percentage of Hoechst-labeled nuclei. For induction of self-renewal, the fold change of $Sox2^{+}/BrdU^{+}$ immuno-positive

cells in 1X EFH was calculated relative to the control (SFM). Data are presented as a mean percent or fold change ± standard error. Statistical analyses were carried out using the Kruskal-Wallis test.

A Pearson correlation was conducted to analyze the doubling time correlation with demographic and cell culture parameters. Data is presented as a Pearson correlation coefficient "r" with respective p values. Only thoracic cultures (n=21 donors) were used in this analysis.

Results

Primary NSPC yield varies among humans and regions of the spinal cord

22 donors were used for this study, of which 15 were male and seven were female. The age of donors ranged from 18 to 72 years, and the mean age was 51.1 ± 17.2 years. The donors died due to hemorrhage in the head, traumatic brain injury, anoxic brain injury, or meningitis (Table 1).

Primary NSPCs from the thoracic (n=21), lumbar (n=12), and conus (n=3) regions of the spinal cord were passaged upon reaching confluence (4-10 weeks) and counted to determine the yield of NSPCs per ten thousand of primary cells seeded. At first glance, the yield between individual donors is variable (Figure 1 A). However, the pooled yield from the lumbar spinal cord was greater than the thoracic or conus regions, although this was not statistically significant. The yield of thoracic NSPCs was similar to conus NSPCs (Figure 1 B; Thoracic: 1906±346, Lumbar: 2893±1485, Conus: 1149±703 NSPCs per 10,000 cells seeded).

Human donors were also stratified by age according to the mean (51 years old). Here, NSPC cultures from younger donors (≤51 y/o) produced a greater yield than from older donors (>51 y/o) which was significant only for lumbar and conus-derived NSPCs (Figure 1 C; Young: 7186±5681, Old: 1644±616 NSPCs per 10,000 cells seeded, $p<0.05$). Thoracic-derived NSPCs from younger

donors also produced a greater yield than elderly donors, but this was not significant (Young: 2400±533, Elderly: 1602±447 NSPCs per 10,000 cells seeded).

Primary NSPC doubling rate is correlated with cell culture parameters

Due to the variability in NSPC yield among donors, we sought to address possible linear relationships between NSPC doubling rate and donor demographics using a Pearson's correlation (Table 2). There was no correlation between age and the doubling rate of NSPCs (Figure 2; r=0.2912, p=0.0892). The doubling rate of NSPCs from males (6.45 days) was greater than females (5.37 days) but not significantly different (p=0.2773). We did not find a significant correlation between the doubling rate and time from brain death (r=-0.2257, p=0.2193) or cross clamp (r=-0.0907, p=0.6687) to spinal cord harvest. However, the doubling rate increased with a shorter time from presentation to brain death (r=-0.5231, p=0.0001). Unexpectedly, there was no positive correlation between the doubling rate and the time from cross-clamp to spinal cord harvest (r=-0.0907, p=0.6687). The number of comorbidities does not appear to affect the doubling rate (r=-0.1204, p=0.5577). There was no significant difference in the doubling rate between donors with reported hypotension and no hypotension (6.37 vs. 6.05, respectively, p=0.7494). Expectedly, the doubling time for donors without hypoxia was less than those with hypoxia (5.99 vs. 7.25 days, respectively), although this was not statistically significant (p=0.0754).

Based on these statistical analyses, there does not appear to be a single demographic variable in our assessment that is linearly correlated with NSPC doubling time besides the time from presentation to brain death. However, we observed a negative correlation between the doubling rate and the number of primary NSPCs initially seeded (r=-0.3924, p=0.0110). Also, there was a positive correlation between the doubling rate and the time spent in culture (r=0.8864, p<0.0001).

Therefore, the yield of human NSPCs was influenced by cell culture parameters but was not linearly correlated with donor demographics.

Lumbar-derived NSPCs are most inducible to self-renew

Following the primary passage, an equal number of NSPCs from the thoracic (n=6), lumbar (n=4), and conus (n=3) spinal cord were treated with mitogens to induce self-renewal. The proliferation rate of NSPCs was similar from all regions after one week of mitogen treatment (thoracic: 47.8±2.5%, lumbar: 51.6±2.3%, Conus: 50.9±2.8% $BrdU^+/Sox2^+$). However, after two weeks of treatment, the proliferation rate increased in a rostral to caudal manner (thoracic: 26.8±2.0%, lumbar: 32.7±2.0%, Conus: 40.3±2.6% $BrdU^+/Sox2^+$) (Figure 3 A).

Given that NSPCs are heterogenous in composition, we measured the fold change in proliferation compared to cultures with no mitogen treatment to distinguish the proliferation due to stem or progenitor cells. The fold change in proliferation reflects the induction of stem cells to self-renew. Therefore, a greater stem-to-progenitor cell ratio will produce a more significant fold change. In this assessment, lumbar NSPCs had the most significant fold change in proliferation (2.5±0.2 and 10.4±1.8 fold after one and two weeks, respectively) compared to thoracic (1.7±0.1 and 1.3±0.1 fold after one and two weeks, respectively) and conus (1.1±0.1 and 2.4±0.2 fold after one and two weeks, respectively) NSPCs (Figure 3 B). Also, thoracic NSPCs had a significantly greater fold change in proliferation than conus NSPCs after one week ($p<0.05$).

Lumbar NSPCs are the least neurogenic and most astrogenic, while conus NSPCs had the least proliferation over time

Like the self-renewal assessment, an equal number of primary-derived NSPCs from each spinal cord region (n=6 thoracic, n=4 lumbar, n=3 conus) were treated with 1% FBS to induce

spontaneous differentiation (Figure 4). A similar trend in differentiation from the three regions was observed at one week; NSPCs had primarily differentiated into neurons (thoracic: 50.3±2.3%, lumbar: 46.5±2.2%, conus: 50.0±2.2% βiii tubulin^{+}) and little into astrocytes (thoracic: 0.33±0.11%, lumbar: 0.88±0.23%, conus: 0% GFAP^{+}). However, after two weeks of differentiation, lumbar NSPCs had significantly fewer neurons compared to NSPCs from either the thoracic ($p<0.05$) or conus ($p<0.01$) regions (thoracic: 50.6±2.1%, lumbar: 41.8±2.2%, conus: 54.6±2.5% βiii tubulin^{+}). When comparing rostral and caudal (lumbar/conus) NSPCs of the same donor, 5/6 donors followed this trend of reduced neuronal differentiation from caudal NSPCs over time (data not shown). Interestingly, concomitant with reduced neuronal differentiation, lumbar NSPCs differentiated significantly more into astrocytes compared to conus ($p<0.01$) NSPCs (thoracic: 0.36±0.11%, lumbar: 1.1±0.2%, conus: 0% GFAP^{+} at two weeks). No O4^{+} oligodendrocytes were observed from these donors.

The proliferation rate in 1% FBS, which reflects asymmetric division, was also measured (n=6 thoracic, n=4 lumbar, n=3 conus, Figure 4 C). After one week, the proliferation rate was not significantly different among thoracic, lumbar, or conus NSPCs (thoracic: 51.0±3.0%, lumbar: 57.6±2.1%, Conus: 63.0±2.2% BrdU^{+}). However, after two weeks of differentiation, conus NSPCs had the least proliferation, which was significantly less than thoracic ($p<0.01$) and lumbar ($p<0.01$) NSPCs (thoracic: 12.1±1.2%, lumbar: 12.3±1.2%, Conus: 5.3±0.9% BrdU^{+}). The proliferation rate was similar among thoracic and lumbar NSPCs throughout the differentiation treatment.

Discussion

This study characterized the primary yield, doubling rate, differentiation, and proliferation profiles of human NSPCs from the thoracic, lumbar, and conus spinal cords under identical conditions. It

also analyzed the possible linear relationships between NSPC doubling rate and donor demographic and cell culture parameters. It was determined that the primary yield and doubling rate of NSPCs varied among donors. Furthermore, the doubling rate did not correlate linearly with any donor demographic information except for a negative correlation with the time from presentation to brain death. NSPCs from the thoracic, lumbar, and conus regions are self-renewing and exhibit multi-lineage differentiation with a bias for neuronal over glial lineages. When controlling for cell-extrinsic parameters, lumbar-derived NSPCs possessed the greatest capacity for self-renewal, were the least neurogenic, and most astrogenic over time. This suggests differences in the self-renewal capability of NSPCs between donors and functional differences between NSPCs along the rostral-caudal axis of the spinal cord.

To culture adult human spinal cord NSPCs, we used a previously established protocol optimized for human NSPCs (A. Mothe & Tator, 2015). Using this method, the yield of primary NSPCs was calculated from 22 donors (n=21 thoracic, n=12 lumbar, and n=3 conus), which was found to vary in a manner that does not correlate linearly with age. Given the variability in yield among donors, it is likely that the combination of organ donor demographic variables will influence the yield of NSPCs. This was mirrored in the absence of linear correlations between the doubling time and donor demographic variables such as age, sex, medical background, cause of death, and time elapsed from cross-clamp to spinal cord harvest. However, there was a single negative correlation between the NSPC doubling rate and the time from presentation to brain death ($r=-0.5231$, $p=0.0001$), indicating that doubling time increased with a shorter time from presentation to brain death. A possible explanation is that a shorter time from presentation to brain death reflects a more severe morbidity which may have negatively affected the ability of NSPCs to self-renew. There was also a trend towards increased doubling time in patients who experienced hypoxia. Although

hypoxic conditions can ameliorate the self-renewal ability and proliferative index in pluripotent and adult stem cells *in vitro*, hypoxic conditions in organ donors may lead to reduced cell viability and function (Abdollahi et al., 2011). Notably, adult human spinal cord NSPCs have been shown to exhibit reduced proliferation in hypoxia relative to normoxia (A. J. Mothe et al., 2011).

In contrast to donor demographic variables, it was observed that cell culture parameters, such as the number of primary cells seeded and time spent in culture, can influence the doubling rate. Specifically, a smaller number of primary cells seeded and a more extended primary culture period resulted in a greater doubling rate. This information suggests that seeding more primary cells will reduce the doubling rate and produce greater yields within a period. This information also suggests an optimal time to passage primary NSPCs to obtain the greatest yield; too little time may not allow NSPCs to expand sufficiently, while extended periods may cause NSPCs to differentiate or attain confluency.

Several studies have shown that donor age and the rostral-caudal identity of NSPCs may affect the self-renewal capacity of NSPCs (Blasko et al., 2012; Iris Kulbatski & Tator, 2009; Xiaofei Li et al., 2016; Sabourin et al., 2009b; Weiss et al., 1996). A study of human filum terminale NSPCs observed higher growth rates and self-renewal capacity from young donors (1-7 years old) compared to older donors (42-60 years old) (Arvidsson et al., 2011). Another study observed a greater mitotic index for thoracic and lumbar NSPCs from a young donor (2 years old) compared to older donors (50 and 51 years old), albeit only being statistically significant for lumbar-derived NSPCs (A. J. Mothe et al., 2011).

These observations, as well as the results obtained in this study, coincide with rodent studies that demonstrate NSPCs from caudal regions of the spinal cord possess a greater mitotic index and capacity for self-renewal than more rostral regions (Blasko et al., 2012; Weiss et al., 1996). Also,

the self-renewal potential of rodent spinal cord NSPCs is dramatically reduced within the first two post-natal weeks, which gradually declines with aging (Xiaofei Li et al., 2016; Sabourin et al., 2009b). In our study, the yield of NSPCs from younger donors (≤ 51 years) was greater than from older donors (> 51 years), which was significant for lumbar but not thoracic NSPCs. Therefore, the lumbar spinal cord may contain a greater proportion of NSPCs or NSPCs with a greater self-renewal capacity relative to more rostral regions in younger populations.

It is known that NSPCs are a heterogenous population consisting of stem and progenitor cells that can both contribute to proliferation (Hamilton et al., 2009; Sabourin et al., 2009b). However, it is unclear whether the observed differences in proliferation activity among regional NSPCs are due to cell-intrinsic properties or the composition of NSPCs (i.e., proportion of stem and progenitor cells). Therefore, to address potential differences in NSPC composition along the rostral-caudal axis of the human spinal cord, we characterized their proliferation behavior.

Adult stem cells can self-renew for relatively long periods; meanwhile, progenitors have a limited self-renewal capacity but a greater proliferation rate. As such, progenitors approach terminal differentiation sooner than adult stem cells (Temple, 2001). Using these criteria, conus NSPCs behaved more like progenitors than thoracic and lumbar NSPCs when induced to differentiate or self-renew. For instance, asymmetric division for conus NSPCs decreased most significantly after two weeks of differentiation, reflecting their limited ability to proliferate and the presence of progenitors that are approaching terminal differentiation. When conus NSPCs were stimulated to self-renew with mitogens, the proliferation rate was not drastically greater than the control (lacking mitogens), supporting the notion that proliferation is largely due to progenitor activity.

Conversely, asymmetric division of lumbar NSPCs was longer-lasting and significantly greater than that of conus NSPCs, suggesting the presence of adult stem cells that have yet to terminally

differentiate. Furthermore, upon mitogen stimulation, the proliferation rate of self-renewing lumbar NSPCs was drastically increased relative to control and significantly greater than that of thoracic and conus NSPCs, suggesting that lumbar NSPCs consist more of self-renewing adult stem cells. Therefore, differences in proliferation behavior among regional NSPCs suggest they may vary with respect to the composition (abundance and type) of stem and progenitor cells.

NSPCs along the rostral-caudal axis of the spinal cord also vary with respect to their differentiation profile (R. Covacu et al., 2014; Iris Kulbatski & Tator, 2009; Sabourin et al., 2009b; Weiss et al., 1996). It's been previously shown that human NSPCs possess a high potential for neurogenesis but little potential for gliogenesis (Arvidsson et al., 2011; Galuta et al., 2020; Jha et al., 2013; A. J. Mothe et al., 2011). We further characterized human NSPCs derived from the thoracic, lumbar, and conus spinal cords and observed significant differences in the differentiation profiles over time. NSPCs from all regions differentiated predominately into neurons and only a few into astrocytes. Notably, we found that human lumbar NSPCs exhibited reduced neurogenesis over time concurrent with increased astrogenesis compared to thoracic and conus NSPCs.

In rodents, lumbar NSPCs tend to differentiate more into neurons, oligodendrocytes, and radial glia than cervical NSPCs, which tend to generate more astrocytes (Iris Kulbatski & Tator, 2009). Another study in rodents found that thoracic NSPCs produced more neurons than cervical and lumbar NSPCs (R. Covacu et al., 2014). Therefore, it is apparent that regional NSPCs vary in their functional properties, which should be considered when targeting a specific population.

Although we determined functional differences between thoracic, lumbar, and conus NSPCs in this study, it is unclear whether these descriptions are translatable to bona fide NSPCs in the human spinal cord. A possible solution would be to perform single-cell RNA sequencing of flash-frozen spinal cord tissue, as this would capture NSPCs in a state that most closely resembles their

endogenous nature (Rosenberg et al., 2018; Russ et al., 2021; Spaethling et al., 2017). From this data, it would be possible to tease apart the cells that constitute the ependymal layer and compare regional NSPCs (Yadav et al., 2022).

However, NSPCs in the intact spinal cord are quiescent and bear distinct molecular and functional profiles than activated NSPCs following SCI or *in vitro* culture (Moreno-Manzano et al., 2009; Pfenninger et al., 2011; Stenudd et al., 2022). Therefore, it may not be possible to determine functional differences among regional NSPCs *in vivo* unless terminally ill SCI patients are administered BrdU. Still, this approach would unlikely be ethically approved (Eriksson, Perfilieva, et al., 1998). Another limitation is that human NSPCs exhibit inter-donor functional variability, which may complicate the comparison of regional NSPCs among donors. One can use a large sample size to mitigate possible confounding effects of inter-donor variability. Alternatively, one may compare thoracic, lumbar, and conus NSPCs derived from the same donor to establish a isogenic comparison among NSPCs.

In our results, 5/6 donors followed the same trend in which lumbar NSPCs were the least neurogenic and most astrogenic over time. Therefore, it can be argued that the functional differences among regional NSPCs in our study are consistent across donors. Lastly, our study assessed for linear correlations between the NSPC doubling rate and donor demographics. Still, we found no significant correlations besides the time from presentation to brain death. Although donor demographics cannot be controlled for, a larger sample size of donors may elucidate how different factors, including age and sex, influence NSPCs which will be important for the application of regenerative treatments. Also, conducting a multivariate regression analysis may help determine such correlations between NSPC function and donor demographics.

In summary, we determined cell-intrinsic variability among donor NSPCs in primary culture. However, our sample size did not capture significant correlations between the NSPC doubling rate and donor demographics. We also cultured NSPCs from the thoracic, lumbar, and conus regions of the human spinal cord. We reported functional differences among regional NSPCs, which may be in part due to the composition of stem and progenitor cells. Lumbar NSPCs possessed the greatest capacity for self-renewal, were most astrogenic, and least neurogenic over time compared to thoracic or conus NSPCs. It is proposed that spinal cord regeneration and repair can be induced by targeting and stimulating endogenous NSPCs. Our study suggests that targeting endogenous NSPCs requires understanding the cell-intrinsic variability of NSPCs among humans and different regions of the spinal cord. Therefore, further investigations like the one presented here are needed to improve the translation of regenerative modalities by accounting for the variability in NSPCs. Ultimately, the development of regenerative strategies targeting endogenous spinal cord NSPCs should be effective and reproducible in the face of human diversity.

Acknowledgements

We are grateful for the families that have consented to our study and permitted the donation of spinal cord tissue from their beloved ones to advance medical science research. We want to thank Dr. Eugene Wai for analysis of the doubling rate and statistical analysis and Dr. Raiff Rached for data acquisition of NSPC differentiation and proliferation. We also want to acknowledge the Ottawa Hospital Department of Surgery, Division of Neurosurgery, and TGLN for permitting spinal cord extractions from organ donors.

Figures and Tables

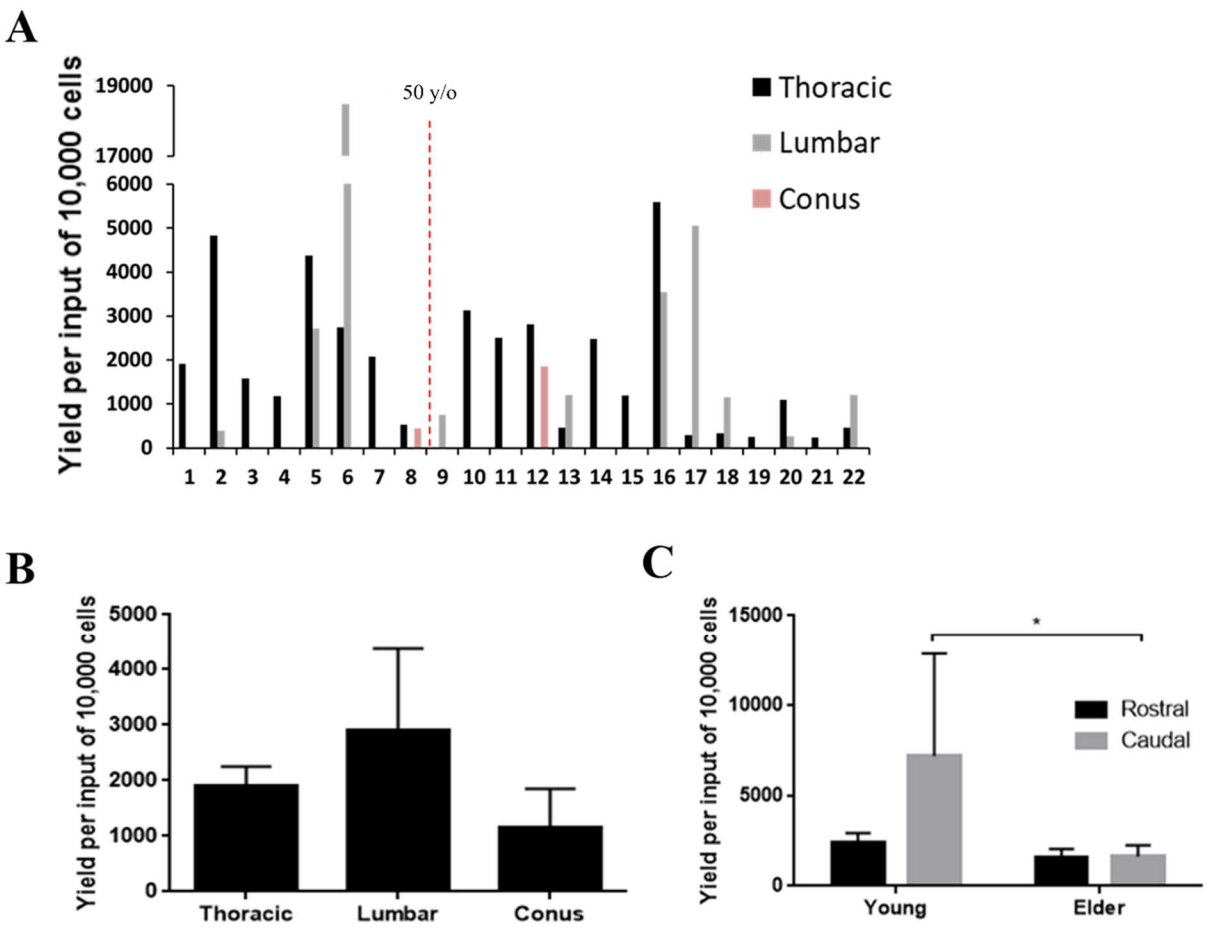

Appendix Figure 1. The yield of primary human NSPCs varies among donors, spinal cord regions, and donor age

Adult human spinal cords (n=22) were processed for primary culture using the mono-layer method. Upon attaining confluence, primary NSPCs were passaged and quantified. Yield per input was calculated by dividing the total number of cells obtained upon passaging per 10,000 cells seeded. (A) Yield per input of 10,000 cells for each donor. (B) Yield per input of 10,000 cells for thoracic (n=21), lumbar (n=12), and conus (n=3) NSPCs. (C) Yield per input of 10,000 cells from young (≤51 years old, n=8) and elderly (>51 years old, n=14) donors. Mean ± s.e.m; *$p<0.05$.

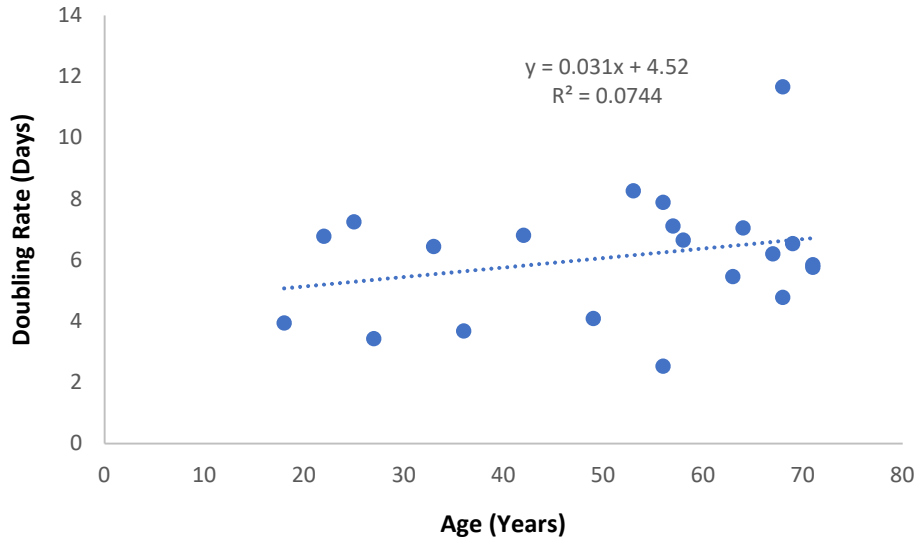

Appendix Figure 2. Linear correlation between NSPC doubling rate and donor age

Adult human thoracic spinal cord NSPCs (n=21) were cultured and passaged upon attaining confluence. A scatter plot between the doubling rate of NSPCs (days) and donor age (years) reveals a poor linear correlation (R^2=0.0744) between the two data sets. The doubling rate (DR) was calculated using the equation: DR = (T2 – T1) x [ln(2) / ln(P2/P1), where T2 – T1 represents the days in vitro, P2 represents the number of NSPCs counted during primary passage, and P1 represents the number of primary NSPCs that were initially seeded.

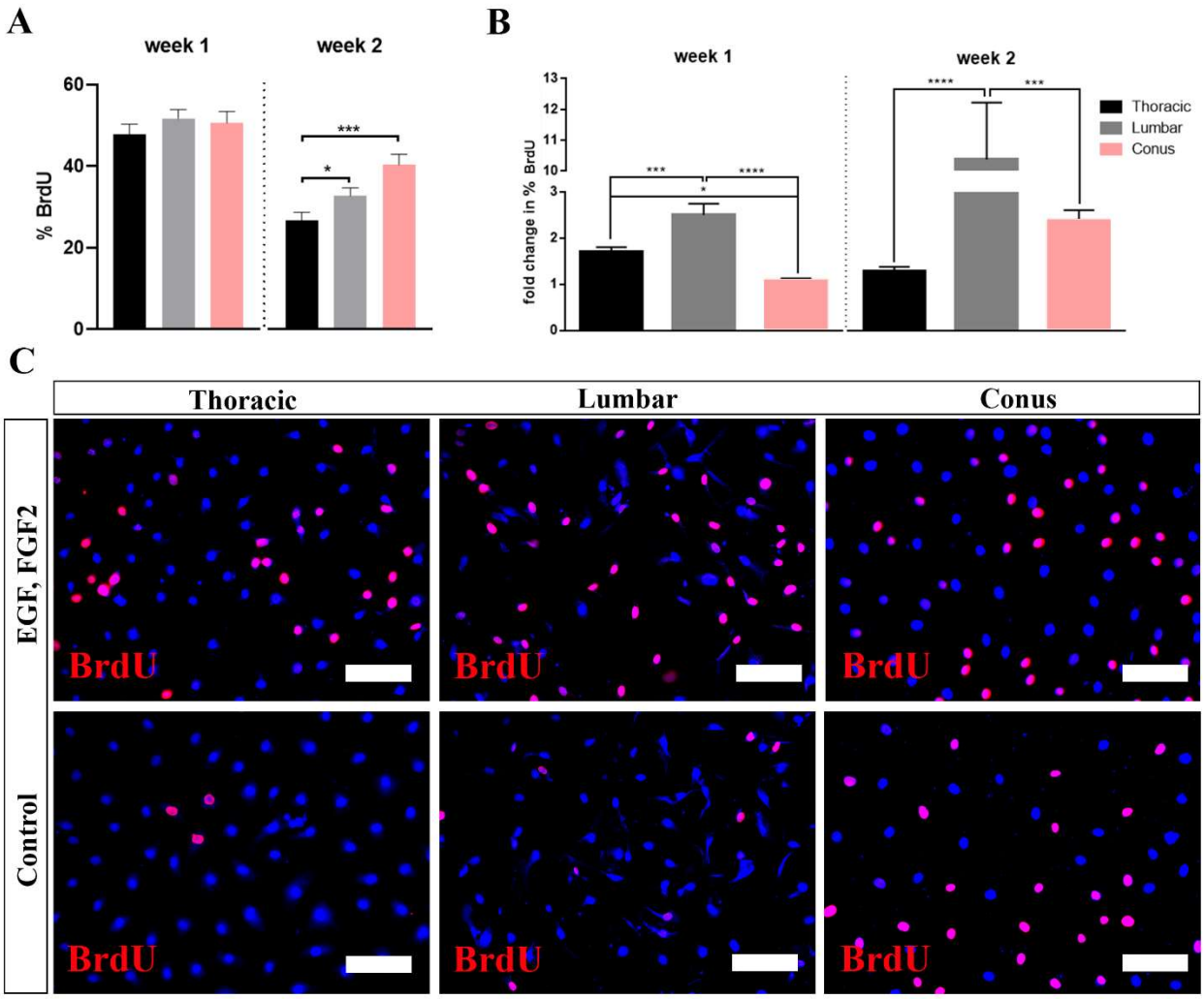

Appendix Figure 3. Conus NSPCs have the greatest absolute proliferation rate, but lumbar NSPCs are most inducible to self-renew

(A) The proliferation rate of thoracic, lumbar, and conus NSPCs that were treated with mitogens increased in a rostral to caudal manner over time. (B) The fold change in proliferation from lumbar NSPCs was greater than thoracic and conus NSPCs. (C) Representative images of thoracic, lumbar, and conus NSPCs treated with mitogens (top row) or serum-free media (bottom row). The proliferation rate was measured within the last 24 hours of mitogen treatment by immuno-staining

for BrdU. Red = BrdU, Blue = DAPI. n= 6 thoracic, 4 lumbar, 3 conus. Mean ± s.e.m; *p<0.05, ***p<0.001, ****p<0.0001. Scale bar = 100 µm

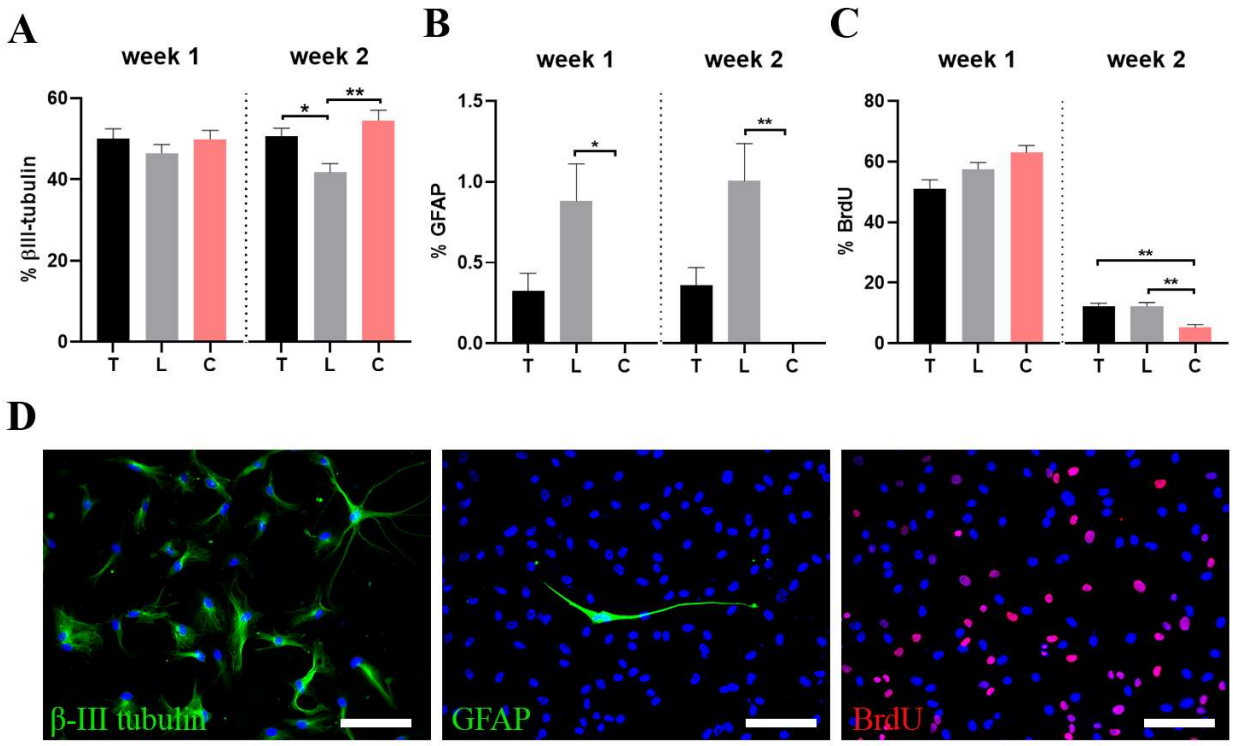

Appendix Figure 4. NSPCs along the rostral-caudal neuroaxis reveal unique signatures in their differentiation and proliferation over time

Primary-derived NSPCs from the thoracic, lumbar, and conus spinal cord were differentiated in 1% FBS for one or two weeks and characterized by immuno-staining. (A) Neuron differentiation was least from lumbar NSPCs after two weeks of differentiation. (B) Astrocyte differentiation was greatest from lumbar NSPCs. (C) Asymmetric division was least from conus NSPCs after two weeks of differentiation. BrdU was administered within the last 24 hours of culture. n= 6 thoracic, 4 lumbar, 3 conus. Mean ± s.e.m; *p<0.05, ***p<0.001. Scale bar = 100 µm.

Appendix Table 1. Organ donor demographic information, including mean age, sex, and cause of death. M, Male; F, Female.

Mean age ± standard deviation	**Sex**
51.1 ± 17.2	15M, 7F
Cause of death	**frequency**
Traumatic brain injury	5
Hemorrhage - intracerebral	3
Hemorrhage - subarachnoid	5
Hemorrhage - intracranial	4
Hemorrhage - subdural	5
Anoxic brain injury	3
Meningitis	1

Appendix Table 2. Correlation of doubling time with various parameters pertaining to cell culture and organ donors.

Variable	**Pearson Correlation**	**P value**
Initial number of cells	-0.3924	0.0110
Days *in vitro*	0.8864	< 0.0001
Age	0.2912	0.0892
Number of comorbidities	-0.1204	0.5577
Charlson comorbidity score	-0.1459	0.4657
Time from presentation to brain death	-0.5231	0.0001
Time from brain death to organ donation	-0.2257	0.2193
Time from aortic cross-clamp to harvest	-0.0907	0.6687
Variable	**Average Doubling Time**	**P value**
Males	6.45	0.2773
Females	5.37	
Chronic comorbidity as defined by Charlson	6.15	0.9851

No Charlson comorbidity	6.13	
Hypotension	6.37	0.7494
No hypotension or not reported	6.05	
Hypoxia	7.25	0.0754
No hypoxia or not reported	5.99	

Bibliography

1. Abdollahi, H., Harris, L. J., Zhang, P., McIlhenny, S., Srinivas, V., Tulenko, T., & Dimuzio, P. J. (2011). The role of hypoxia in stem cell differentiation and therapeutics. *Journal of Surgical Research*. https://doi.org/10.1016/j.jss.2009.09.057
2. Agrawal, S. K., & Fehlings, M. G. (1996). Mechanisms of Secondary Injury to Spinal Cord Axons In Vitro: Role of Na+, Na+-K+-ATPase, the Na+-H+ Exchanger, and the Na+-Ca*+ Exchanger. *The Journal of Neuroscience*, *16*(2), 545–552.
3. Alfaro-Cervello, C., Cebrian-Silla, A., Soriano-Navarro, M., Garcia-Tarraga, P., Matías-Guiu, J., Gomez-Pinedo, U., … Garcia-Verdugo, J. M. (2014). The adult macaque spinal cord central canal zone contains proliferative cells and closely resembles the human. *Journal of Comparative Neurology*, *522*(8), 1800–1817. https://doi.org/10.1002/cne.23501
4. Alfaro-Cervello, C., Soriano-Navarro, M., Mirzadeh, Z., Alvarez-Buylla, A., & Garcia-Verdugo, J. M. (2012). Biciliated ependymal cell proliferation contributes to spinal cord growth. *Journal of Comparative Neurology*, *520*(15), 3528–3552. https://doi.org/10.1002/cne.23104
5. Alizadeh, A., Dyck, S. M., & Karimi-Abdolrezaee, S. (2019). Traumatic Spinal Cord Injury: An Overview of Pathophysiology, Models and Acute Injury Mechanisms. *Frontiers in Neurology*, *10*(March), 1–25. https://doi.org/10.3389/fneur.2019.00282
6. All, A. H., Bazley, F. A., Gupta, S., Pashai, N., Hu, C., Pourmorteza, A., & Kerr, C. (2012). Human Embryonic Stem Cell-Derived Oligodendrocyte Progenitors Aid in Functional Recovery of Sensory Pathways following Contusive Spinal Cord Injury. *PLoS ONE*, *7*(10). https://doi.org/10.1371/journal.pone.0047645
7. Allen, A. R. (1911). SURGERY OF EXPERIMENTAL LESION OF SPINAL CORD

EQUIVALENT TO CRUSH INJURY OF FRACTURE DISLOCATION OF SPINAL COLUMN. *JAMA*, (57), 878– 80.

8. Almad, A., Sahinkaya, F. R., & McTigue, D. M. (2011). Oligodendrocyte Fate after Spinal Cord Injury. *Neurotherapeutics*. https://doi.org/10.1007/s13311-011-0033-5
9. Altman, J., & Das, G. D. (1965). Autoradiographic and histological evidence of postnatal hippocampal neurogenesis in rats. *Journal of Comparative Neurology*, *124*(3), 319–335. https://doi.org/10.1002/CNE.901240303
10. Anderson, A. J., Piltti, K. M., Hooshmand, M. J., Nishi, R. A., & Cummings, B. J. (2017). Preclinical Efficacy Failure of Human CNS-Derived Stem Cells for Use in the Pathway Study of Cervical Spinal Cord Injury. *Stem Cell Reports*, *8*(2), 249–263. https://doi.org/10.1016/j.stemcr.2016.12.018
11. Anderson, K. D., Guest, J. D., Dietrich, W. D., Bartlett Bunge, M., Curiel, R., Dididze, M., … Levi, A. D. (2017). Safety of Autologous Human Schwann Cell Transplantation in Subacute Thoracic Spinal Cord Injury. *Journal of Neurotrauma*, *34*(21), 2950–2963. https://doi.org/10.1089/neu.2016.4895
12. Anderson, M. A., Burda, J. E., Ren, Y., Ao, Y., O'Shea, T. M., Kawaguchi, R., … Sofroniew, M. V. (2016). Astrocyte scar formation AIDS central nervous system axon regeneration. *Nature*, *532*(7598), 195–200. https://doi.org/10.1038/nature17623
13. Andreatta, M., & Carmona, S. J. (2021). UCell: Robust and scalable single-cell gene signature scoring. *Computational and Structural Biotechnology Journal*, *19*, 3796–3798. https://doi.org/10.1016/j.csbj.2021.06.043
14. Anwar, M. A., Al Shehabi, T. S., & Eid, A. H. (2016, April 13). Inflammogenesis of secondary spinal cord injury. *Frontiers in Cellular Neuroscience*. Frontiers Media SA.

https://doi.org/10.3389/fncel.2016.00098

15. Arvidsson, L., Fagerlund, M., Jaff, N., Ossoinak, A., Jansson, K., Hägerstrand, A., … Svensson, M. (2011). Distribution and characterization of progenitor cells within the human filum terminale. *PLoS ONE*, *6*(11). https://doi.org/10.1371/journal.pone.0027393
16. Assinck, P., Duncan, G. J., Hilton, B. J., Plemel, J. R., & Tetzlaff, W. (2017). Cell transplantation therapy for spinal cord injury. *Nature Neuroscience*, *20*(5), 637–647. https://doi.org/10.1038/nn.4541
17. Assunção-Silva, R. C., Gomes, E. D., Sousa, N., Silva, N. A., & Salgado, A. J. (2015). Hydrogels and Cell Based Therapies in Spinal Cord Injury Regeneration. *Stem Cells International*, *2015*. https://doi.org/10.1155/2015/948040
18. Azari, H., Louis, S. A., Sharififar, S., Vedam-Mai, V., & Reynolds, B. A. (2011). Neural-colony forming cell assay: An assay to discriminate bona fide neural stem cells from neural progenitor cells. *Journal of Visualized Experiments*, (49), 2639. https://doi.org/10.3791/2639
19. Azari, M. F., Profyris, C., Zang, D. W., Petratos, S., & Cheema, S. S. (2005). Induction of endogenous neural precursors in mouse models of spinal cord injury and disease. *European Journal of Neurology*, *12*(8), 638–648. https://doi.org/10.1111/j.1468-1331.2005.01066.x
20. Badhiwala, J. H., Wilson, J. R., Kwon, B. K., Casha, S., & Fehlings, M. G. (2018). A Review of Clinical Trials in Spinal Cord Injury Including Biomarkers. *Journal of Neurotrauma*. https://doi.org/10.1089/neu.2018.5935
21. Barkho, B. Z., Song, H., Aimone, J. B., Smrt, R. D., Kuwabara, T., Nakashima, K., … Zhao, X. (2006). In Focus: Neural Stem Cells Identification of Astrocyte-expressed Factors That Modulate Neural Stem/Progenitor Cell Differentiation. *Stem Cells and Development*, *421*, 407–421.

22. Barnabé-Heider, F., Göritz, C., Sabelström, H., Takebayashi, H., Pfrieger, F. W., Meletis, K., & Frisén, J. (2010). Origin of new glial cells in intact and injured adult spinal cord. *Cell Stem Cell*, *7*(4), 470–482. https://doi.org/10.1016/j.stem.2010.07.014

23. Baron, V., Adamson, E. D., Calogero, A., Ragona, G., & Mercola, D. (2006, February). The transcription factor Egr1 is a direct regulator of multiple tumor suppressors including TGFβ1, PTEN, p53, and fibronectin. *Cancer Gene Therapy*. Cancer Gene Ther. https://doi.org/10.1038/sj.cgt.7700896

24. Beattie, M. S., Farooqui, A. A., & Bresnahan, J. C. (2009). Review of Current Evidence for Apoptosis After Spinal Cord Injury. *Https://Home.Liebertpub.Com/Neu*, *17*(10), 915–925. https://doi.org/10.1089/NEU.2000.17.915

25. Beattie, M. S., Hermann, G. E., Rogers, R. C., & Bresnahan, J. C. (2002). Cell death in models of spinal cord injury. *Progress in Brain Research*, *137*, 37–47. https://doi.org/10.1016/S0079-6123(02)37006-7

26. Beck, K. D., Nguyen, H. X., Galvan, M. D., Salazar, D. L., Woodruff, T. M., & Anderson, A. J. (2010). Quantitative analysis of cellular inflammation after traumatic spinal cord injury: evidence for a multiphasic inflammatory response in the acute to chronic environment. *Brain*, *133*(2), 433. https://doi.org/10.1093/BRAIN/AWP322

27. Becker, C. G., & Becker, T. (2015). Neuronal Regeneration from Ependymo-Radial Glial Cells: Cook, Little Pot, Cook! *Developmental Cell*, *32*(4), 516–527. https://doi.org/10.1016/j.devcel.2015.01.001

28. Becker, C. G., Becker, T., & Hugnot, J. P. (2018). The spinal ependymal zone as a source of endogenous repair cells across vertebrates. *Progress in Neurobiology*, *170*(April), 67–80. https://doi.org/10.1016/j.pneurobio.2018.04.002

29. Beers, J., Linask, K. L., Chen, J. A., Siniscalchi, L. I., Lin, Y., Zheng, W., … Chen, G. (2015). A cost-effective and efficient reprogramming platform for large-scale production of integration-free human induced pluripotent stem cells in chemically defined culture. *Scientific Reports*, *5*(June), 1–9. https://doi.org/10.1038/srep11319

30. Bergmann, O., Spalding, K. L., & Frisén, J. (2015). Adult neurogenesis in humans. *Cold Spring Harbor Perspectives in Medicine*, *5*(8), 1–13. https://doi.org/10.1101/cshperspect.a018994

31. Bhowmick, S., & Abdul-Muneer, P. M. (2021). PTEN Blocking Stimulates Corticospinal and Raphespinal Axonal Regeneration and Promotes Functional Recovery After Spinal Cord Injury. *Journal of Neuropathology and Experimental Neurology*, *80*(2), 169–181. https://doi.org/10.1093/jnen/nlaa147

32. Bianchi, F., Malboubi, M., Li, Y., George, J. H., Jerusalem, A., Szele, F., … Ye, H. (2018a). Rapid and efficient differentiation of functional motor neurons from human iPSC for neural injury modelling. *Stem Cell Research*, *32*, 126–134. https://doi.org/10.1016/j.scr.2018.09.006

33. Bianchi, F., Malboubi, M., Li, Y., George, J. H., Jerusalem, A., Szele, F., … Ye, H. (2018b). Rapid and efficient differentiation of functional motor neurons from human iPSC for neural injury modelling. *Stem Cell Research*, *32*, 126–134. https://doi.org/10.1016/j.scr.2018.09.006

34. Bible, E. (2013, July 9). Neuro-oncology: BCAT1 promotes cell proliferation in aggressive gliomas. *Nature Reviews Neurology*. Nature Publishing Group. https://doi.org/10.1038/nrneurol.2013.135

35. Birbrair, A., Zhang, T., Files, D. C., Mannava, S., Smith, T., Wang, Z. M., … Delbono, O. (2014). Type-1 pericytes accumulate after tissue injury and produce collagen in an organ-dependent manner. *Stem Cell Research and Therapy*, *5*(6), 1–18.

https://doi.org/10.1186/scrt512

36. Björklund, M. (2019, March 1). Cell size homeostasis: Metabolic control of growth and cell division. *Biochimica et Biophysica Acta - Molecular Cell Research*. Elsevier B.V. https://doi.org/10.1016/j.bbamcr.2018.10.002
37. Blasko, J., Martoncikova, M., Lievajova, K., Saganova, K., Korimova, A., & Racekova, E. (2012). Regional differences of proliferation activity in the spinal cord ependyma of adult rats. *Central European Journal of Biology*, *7*(3), 397–403. https://doi.org/10.2478/s11535-012-0027-2
38. Blesch, A., & Tuszynski, M. H. (2007). Transient growth factor delivery sustains regenerated axons after spinal cord injury. *Journal of Neuroscience*, *27*(39), 10535–10545. https://doi.org/10.1523/JNEUROSCI.1903-07.2007
39. Boldrini, M., Fulmore, C. A., Tartt, A. N., Simeon, L. R., Pavlova, I., Poposka, V., … Mann, J. J. (2018). Human Hippocampal Neurogenesis Persists throughout Aging. *Cell Stem Cell*, *22*(4), 589-599.e5. https://doi.org/10.1016/j.stem.2018.03.015
40. Bonizzato, M., & Martinez, M. (2021). An intracortical neuroprosthesis immediately alleviates walking deficits and improves recovery of leg control after spinal cord injury. *Science Translational Medicine*, *13*(586). https://doi.org/10.1126/scitranslmed.abb4422
41. Bonner, J. F., & Steward, O. (2015). Repair of spinal cord injury with neuronal relays: From fetal grafts to neural stem cells. *Brain Research*, *1619*, 115–123. https://doi.org/10.1016/j.brainres.2015.01.006
42. Bordoni, M., Fantini, V., Pansarasa, O., & Cereda, C. (2018). From Neuronal Differentiation of iPSCs to 3D Neural Organoids: Modeling of Neurodegenerative Diseases. *International Journal of Molecular Sciences*, *19*(12). https://doi.org/10.5772/intechopen.80055

43. Bradbury, E. J., & Burnside, E. R. (2019). Moving beyond the glial scar for spinal cord repair. *Nature Communications*. https://doi.org/10.1038/s41467-019-11707-7

44. Bradbury, E. J., Moon, L. D. F., Popat, R. J., King, V. R., Bennett, G. S., Patel, P. N., … McMahon, S. B. (2002). Chondroitinase ABC promotes functional recovery after spinal cord injury. *Nature*, *416*(6881), 636–640. https://doi.org/10.1038/416636A

45. Braga, T. T., Agudelo, J. S. H., & Camara, N. O. S. (2015). Macrophages During the Fibrotic Process: M2 as Friend and Foe. *Frontiers in Immunology*, *6*(NOV). https://doi.org/10.3389/FIMMU.2015.00602

46. Brennan, F. H., & Popovich, P. G. (2018). Emerging targets for reprograming the immune response to promote repair and recovery of function after spinal cord injury. *Current Opinion in Neurology*, *31*(3), 334–344. https://doi.org/10.1097/WCO.0000000000000550

47. Briona, L. K., Poulain, F. E., Mosimann, C., & Dorsky, R. I. (2015). Wnt/ß-catenin signaling is required for radial glial neurogenesis following spinal cord injury. *Developmental Biology*, *403*(1), 15–21. https://doi.org/10.1016/J.YDBIO.2015.03.025

48. Brix, J., Zhou, Y., & Luo, Y. (2015, December 20). The Epigenetic Reprogramming Roadmap in Generation of iPSCs from Somatic Cells. *Journal of Genetics and Genomics*. Elsevier. https://doi.org/10.1016/j.jgg.2015.10.001

49. Brock, J. H., Graham, L., Staufenberg, E., Im, S., & Tuszynski, M. H. (2018). Rodent Neural Progenitor Cells Support Functional Recovery after Cervical Spinal Cord Contusion. *Journal of Neurotrauma*, *35*(9), 1069–1078. https://doi.org/10.1089/neu.2017.5244

50. Cafferty, W. B. J., Yang, S. H., Duffy, P. J., Li, S., & Strittmatter, S. M. (2007). Functional Axonal Regeneration through Astrocytic Scar Genetically Modified to Digest Chondroitin Sulfate Proteoglycans. *Journal of Neuroscience*, *27*(9), 2176–2185.

https://doi.org/10.1523/JNEUROSCI.5176-06.2007

51. Cambray, N., & Wilson, V. (2007). Two distinct sources for a population of maturing axial progenitors. *Development (Cambridge, England)*, *134*(15), 2829–2840. https://doi.org/10.1242/DEV.02877

52. Canadian Institutes of Health Research, N. S. and R. C. of C. and S. S. and H. R. C. (2018). *Tri-Council Policy Statement: Ethical Conduct for Research Involving Humans*.

53. Cao, Q. lin, Zhang, Y. P., Howard, R. M., Walters, W. M., Tsoulfas, P., & Whittemore, S. R. (2001). Pluripotent Stem Cells Engrafted into the Normal or Lesioned Adult Rat Spinal Cord Are Restricted to a Glial Lineage. *Experimental Neurology*, *167*(1), 48–58. https://doi.org/10.1006/EXNR.2000.7536

54. Castro, R. F., Jackson, K. A., Goodell, M. A., Robertson, C. S., Liu, H., & Shine, H. D. (2002). Failure of bone marrow cells to transdifferentiate into neural cells in vivo. *Science (New York, N.Y.)*, *297*(5585), 1299. https://doi.org/10.1126/SCIENCE.297.5585.1299

55. Cawsey, T., Duflou, J., Weickert, C. S., & Gorrie, C. A. (2015). Nestin-Positive Ependymal Cells Are Increased in the Human Spinal Cord after Traumatic Central Nervous System Injury. *Journal of Neurotrauma*, *32*(18), 1393–1402. https://doi.org/10.1089/neu.2014.3575

56. Cekanaviciute, E., & Buckwalter, M. S. (2016). Astrocytes: Integrative Regulators of Neuroinflammation in Stroke and Other Neurological Diseases. *Neurotherapeutics*, *13*(4), 685. https://doi.org/10.1007/S13311-016-0477-8

57. CelluBridge - Spiderwort. (n.d.). Retrieved May 26, 2022, from https://spiderwortbio.com/product/cellubridge/

58. Cera, A. A., Cacci, E., Toselli, C., Cardarelli, S., Bernardi, A., Gioia, R., … Biagioni, S. (2018). Egr-1 maintains NSC proliferation and its overexpression counteracts cell cycle exit

triggered by the withdrawal of epidermal growth factor. *Developmental Neuroscience*, *40*(3), 223–233. https://doi.org/10.1159/000489699

59. Ceto, S., Sekiguchi, K. J., Takashima, Y., Nimmerjahn, A., & Tuszynski, M. H. (2020). Neural Stem Cell Grafts Form Extensive Synaptic Networks that Integrate with Host Circuits after Spinal Cord Injury. *Cell Stem Cell*, *27*(3), 430-440.e5. https://doi.org/10.1016/j.stem.2020.07.007
60. Chamak, B., Morandi, V., & Mallat, M. (1994). Brain macrophages stimulate neurite growth and regeneration by secreting thrombospondin. *Journal of Neuroscience Research*, *38*(2), 221–233. https://doi.org/10.1002/JNR.490380213
61. Chambers, S. M., Fasano, C. A., Papapetrou, E. P., Tomishima, M., Sadelain, M., & Studer, L. (2009). Highly efficient neural conversion of human ES and iPS cells by dual inhibition of SMAD signaling. *Nature Biotechnology*, *27*(3), 275–280. https://doi.org/10.1038/nbt.1529
62. Chen, G., Gulbranson, D. R., Hou, Z., Bolin, J. M., Probasco, M. D., Smuga-otto, K., … Thomson, J. a. (2011). Chemically defined conditions for human iPS cell derivation and culture. *Nature Methods*, *8*(5), 424–429. https://doi.org/10.1038/nmeth.1593.Chemically
63. Chen, N. ning, Wei, F., Wang, L., Cui, S., Wan, Y., & Liu, S. (2016). Tumor Necrosis Factor Alpha Induces Neural Stem Cell Apoptosis Through Activating p38 MAPK Pathway. *Neurochemical Research*, *41*(11), 3052–3062. https://doi.org/10.1007/s11064-016-2024-8
64. Cheriyan, T., Ryan, D. J., Weinreb, J. H., Cheriyan, J., Paul, J. C., Lafage, V., … Errico, T. J. (2014). Spinal cord injury models: A review. *Spinal Cord*, *52*(8), 588–595. https://doi.org/10.1038/sc.2014.91
65. Chhabra, H. S., & Sarda, K. (2017a). Clinical translation of stem cell based interventions for spinal cord injury — Are we there yet ? ☆. *Advanced Drug Delivery Reviews*, *120*, 41–49.

https://doi.org/10.1016/j.addr.2017.09.021

66. Chhabra, H. S., & Sarda, K. (2017b). Clinical translation of stem cell based interventions for spinal cord injury — Are we there yet? *Advanced Drug Delivery Reviews*. https://doi.org/10.1016/j.addr.2017.09.021

67. Cizkova, D., Nagyova, M., Slovinska, L., Novotna, I., Radonak, J., Cizek, M., … Vanicky, I. (2009). Response of ependymal progenitors to spinal cord injury or enhanced physical activity in adult rat. *Cellular and Molecular Neurobiology*, *29*(6–7), 999–1013. https://doi.org/10.1007/s10571-009-9387-1

68. Čížková, D., Rosocha, J., Vanický, I., Jergová, S., & Čížek, M. (2006). Transplants of human mesenchymal stem cells improve functional recovery after spinal cord injury in the rat. *Cellular and Molecular Neurobiology*, *26*(7–8), 1167–1180. https://doi.org/10.1007/s10571-006-9093-1

69. Cole, A. E., Murray, S. S., & Xiao, J. (2016). Bone Morphogenetic Protein 4 Signalling in Neural Stem and Progenitor Cells during Development and after Injury. *Stem Cells International*. https://doi.org/10.1155/2016/9260592

70. Courtine, G., & Sofroniew, M. V. (2019). Spinal cord repair: advances in biology and technology. *Nature Medicine*. https://doi.org/10.1038/s41591-019-0475-6

71. Covacu, R., Perez Estrada, C., Arvidsson, L., Svensson, M., & Brundin, L. (2014). Change of Fate Commitment in Adult Neural Progenitor Cells Subjected to Chronic Inflammation. *Journal of Neuroscience*, *34*(35), 11571–11582. https://doi.org/10.1523/JNEUROSCI.0231-14.2014

72. Covacu, Ruxandra, & Brundin, L. (2015). Effects of Neuroinflammation on Neural Stem Cells. *Neuroscientist*, *23*(1), 27–39. https://doi.org/10.1177/1073858415616559

73. Cregg, J. M., DePaul, M. A., Filous, A. R., Lang, B. T., Tran, A., & Silver, J. (2014). Functional regeneration beyond the glial scar. *Experimental Neurology*, *253*, 197–207. https://doi.org/10.1016/j.expneurol.2013.12.024

74. Crowe, M. J., Bresnahan, J. C., Shuman, S. L., Masters, J. N., & Beattie, M. S. (1997). Apoptosis and delayed degeneration after spinal cord injury in rats and monkeys. *Nature Medicine 1997 3:1*, *3*(1), 73–76. https://doi.org/10.1038/nm0197-73

75. Curtis, E., Martin, J. R., Gabel, B., Sidhu, N., Rzesiewicz, T. K., Mandeville, R., … Ciacci, J. D. (2018a). A First-in-Human, Phase I Study of Neural Stem Cell Transplantation for Chronic Spinal Cord Injury. *Cell Stem Cell*, *22*(6). https://doi.org/10.1016/j.stem.2018.05.014

76. Curtis, E., Martin, J. R., Gabel, B., Sidhu, N., Rzesiewicz, T. K., Mandeville, R., … Ciacci, J. D. (2018b). A First-in-Human, Phase I Study of Neural Stem Cell Transplantation for Chronic Spinal Cord Injury. *Cell Stem Cell*, *22*(6), 941-950.e6. https://doi.org/10.1016/j.stem.2018.05.014

77. Cusimano, M., Brambilla, E., Capotondo, A., De Feo, D., Tomasso, A., Comi, G., … Martino, G. (2018). Selective killing of spinal cord neural stem cells impairs locomotor recovery in a mouse model of spinal cord injury. *Journal of Neuroinflammation*, *15*(1), 1–14. https://doi.org/10.1186/s12974-018-1085-9

78. Dalkilic, T., Fallah, N., Noonan, V. K., Salimi Elizei, S., Dong, K., Belanger, L., … Kwon, B. K. (2018). Predicting Injury Severity and Neurological Recovery after Acute Cervical Spinal Cord Injury: A Comparison of Cerebrospinal Fluid and Magnetic Resonance Imaging Biomarkers. *Journal of Neurotrauma*, *35*(3), 435–445. https://doi.org/10.1089/neu.2017.5357

79. Datto, J. P., Bastidas, J. C., Miller, N. L., Shah, A. K., Arheart, K. L., Marcillo, A. E., …

Pearse, D. D. (2015). Female Rats Demonstrate Improved Locomotor Recovery and Greater Preservation of White and Gray Matter after Traumatic Spinal Cord Injury Compared to Males. *Journal of Neurotrauma*, *32*(15), 1146–1157. https://doi.org/10.1089/neu.2014.3702

80. David, S., & Kroner, A. (2011). Repertoire of microglial and macrophage responses after spinal cord injury. *Nature Reviews. Neuroscience*, *12*(7), 388–399. https://doi.org/10.1038/NRN3053
81. Davies, J. E., Huang, C., Proschel, C., Noble, M., Mayer-Proschel, M., & Davies, S. J. (2006). Astrocytes derived from glial-restricted precursors promote spinal cord repair. *Journal of Biology*, *5*. https://doi.org/10.1186/jbiol35
82. de Freria, C. M., Van Niekerk, E., Blesch, A., & Lu, P. (2021). Neural stem cells: Promoting axonal regeneration and spinal cord connectivity. *Cells*. https://doi.org/10.3390/cells10123296
83. De Vellis, J., & Cole, R. (2012). Preparation of mixed glial cultures from postnatal rat brain. *Methods in Molecular Biology (Clifton, N.J.)*, *814*, 49–59. https://doi.org/10.1007/978-1-61779-452-0_4
84. Decimo, I., Bifari, F., Rodriguez, F. J., Malpeli, G., Dolci, S., Lavarini, V., … Fumagalli, G. (2011). Nestin-and doublecortin-positive cells reside in adult spinal cord meninges and participate in injury-induced parenchymal reaction. *Stem Cells*, *29*(12), 2062–2076. https://doi.org/10.1002/stem.766
85. Deneen, B., Ho, R., Lukaszewicz, A., Hochstim, C. J., Gronostajski, R. M., & Anderson, D. J. (2006). The Transcription Factor NFIA Controls the Onset of Gliogenesis in the Developing Spinal Cord. *Neuron*, *52*(6), 953–968. https://doi.org/10.1016/j.neuron.2006.11.019

86. Denny, C. A., Kheirbek, M. A., Alba, E. L., Tanaka, K. F., Brachman, R. A., Laughman, K. B., … Hen, R. (2014). Hippocampal memory traces are differentially modulated by experience, time, and adult neurogenesis. *Neuron*, *83*(1), 189–201. https://doi.org/10.1016/J.NEURON.2014.05.018

87. Dias, D. O., Kim, H., Holl, D., Werne Solnestam, B., Lundeberg, J., Carlén, M., … Frisén, J. (2018). Reducing Pericyte-Derived Scarring Promotes Recovery after Spinal Cord Injury. *Cell*, *173*(1), 153-165.e22. https://doi.org/10.1016/j.cell.2018.02.004

88. Diaz Quiroz, J. F., Tsai, E., Coyle, M., Sehm, T., & Echeverri, K. (2014). Precise control of miR-125b levels is required to create a regeneration-permissive environment after spinal cord injury: A cross-species comparison between salamander and rat. *DMM Disease Models and Mechanisms*, *7*(6), 601–611. https://doi.org/10.1242/dmm.014837

89. Djenoune, L., Khabou, H., Joubert, F., Quan, F. B., Figueiredo, S. N., Bodineau, L., … Wyart, C. (2014). Investigation of spinal cerebrospinal fluid-contacting neurons expressing PKD2L1: Evidence for a conserved system from fish to primates. *Frontiers in Neuroanatomy*, *8*(MAY), 26. https://doi.org/10.3389/fnana.2014.00026

90. Donnelly, D. J., & Popovich, P. G. (2008, February). Inflammation and its role in neuroprotection, axonal regeneration and functional recovery after spinal cord injury. *Experimental Neurology*. NIH Public Access. https://doi.org/10.1016/j.expneurol.2007.06.009

91. Dorschner, R. A., Lee, J., Cohen, O., Costantini, T., Baird, A., & Eliceiri, B. P. (2020). ECRG4 regulates neutrophil recruitment and CD44 expression during the inflammatory response to injury. *Science Advances*, *6*(11). https://doi.org/10.1126/sciadv.aay0518

92. Drazin, D., & Boakye, M. (2014). Spontaneous Recovery Patterns and Prognoses after Spinal

Cord Injury. In *Essentials of Spinal Cord Injury*. https://doi.org/10.1055/b-0034-83849

93. Dromard, C., Guillon, H., Rigau, V., Ripoll, C., Sabourin, J. C., Perrin, F. E., … Bauchet, L. (2008). Adult human spinal cord harbors neural precursor cells that generate neurons and glial cells in vitro. *Journal of Neuroscience Research*, *86*(9), 1916–1926. https://doi.org/10.1002/jnr.21646
94. Dulin, J. N., & Lu, P. (2014, February 1). Bridging the injured spinal cord with neural stem cells. *Neural Regeneration Research*. Wolters Kluwer -- Medknow Publications. https://doi.org/10.4103/1673-5374.128212
95. Duncan, I. D., Aguayo, A. J., Bunge, R. P., & Wood, P. M. (1981). Transplantation of rat Schwann cells grown in tissue culture into the mouse spinal cord. *Journal of the Neurological Sciences*, *49*(2), 241–252. https://doi.org/10.1016/0022-510X(81)90082-4
96. Dunkelberger, N., Schearer, E. M., & O'Malley, M. K. (2020, June 1). A review of methods for achieving upper limb movement following spinal cord injury through hybrid muscle stimulation and robotic assistance. *Experimental Neurology*. Academic Press. https://doi.org/10.1016/j.expneurol.2020.113274
97. Dyck, S., Kataria, H., Alizadeh, A., Santhosh, K. T., Lang, B., Silver, J., & Karimi-Abdolrezaee, S. (2018). Perturbing chondroitin sulfate proteoglycan signaling through LAR and PTPσ receptors promotes a beneficial inflammatory response following spinal cord injury. *Journal of Neuroinflammation*, *15*(1). https://doi.org/10.1186/S12974-018-1128-2
98. Edgerton, V. R., Tillakaratne, N. J. K., Bigbee, A. J., De Leon, R. D., & Roy, R. R. (2004). Plasticity of the spinal neural circuitry after injury. *Annual Review of Neuroscience*, *27*, 145–167. https://doi.org/10.1146/ANNUREV.NEURO.27.070203.144308
99. Efrat, S. (2021, January 19). Epigenetic Memory: Lessons From iPS Cells Derived From

Human β Cells. *Frontiers in Endocrinology*. Frontiers Media S.A. https://doi.org/10.3389/fendo.2020.614234

100. Elkabes, S., DiCicco-Bloom, E. M., & Black, I. B. (1996). Brain microglia/macrophages express neurotrophins that selectively regulate microglial proliferation and function. *The Journal of Neuroscience : The Official Journal of the Society for Neuroscience*, *16*(8), 2508–2521. https://doi.org/10.1523/JNEUROSCI.16-08-02508.1996

101. Eriksson, P. S., Perfilieva, E., Björk-Eriksson, T., Alborn, A. M., Nordborg, C., Peterson, D. A., & Gage, F. H. (1998). Neurogenesis in the adult human hippocampus. *Nature Medicine*, *4*(11), 1313–1317. https://doi.org/10.1038/3305

102. Eriksson, P. S., Perrfilieva, E., BJörk-Eriksson, T., Alborn, A.-M., Nordborg, C., Peterson, D. A., & Cage, F. H. (1998). Neurogenesis in the adult human hippocampus. *Nature Medicine*, *4*(11), 1313–1317.

103. Failli, V., Kleitman, N., Lammertse, D. P., Hsieh, J. T. C., Steeves, J. D., Fawcett, J. W., … Blight, A. R. (2021). Experimental treatments for Spinal Cord Injury: What you should know. *Topics in Spinal Cord Injury Rehabilitation*, *27*(2), 50–73. https://doi.org/10.46292/sci2702-50

104. Falk, S., Wurdak, H., Ittner, L. M., Ille, F., Sumara, G., Schmid, M. T., … Sommer, L. (2008). Brain Area-Specific Effect of TGF-β Signaling on Wnt-Dependent Neural Stem Cell Expansion. *Cell Stem Cell*, *2*(5), 472–483. https://doi.org/10.1016/j.stem.2008.03.006

105. Farooque, M., Suo, Z., Arnold, P. M., Wulser, M. J., Chou, C. T., Vancura, R. W., … Festoff, B. W. (2006). Gender-related differences in recovery of locomotor function after spinal cord injury in mice. *Spinal Cord*, *44*(3), 182–187. https://doi.org/10.1038/sj.sc.3101816

106. Faulkner, J. R., Herrmann, J. E., Woo, M. J., Tansey, K. E., Doan, N. B., & Sofroniew, M. V. (2004). Reactive Astrocytes Protect Tissue and Preserve Function after Spinal Cord Injury. *Journal of Neuroscience*, *24*(9), 2143–2155. https://doi.org/10.1523/JNEUROSCI.3547-03.2004

107. Fehlings, M. G., Chen, Y., Aarabi, B., Ahmad, F., Anderson, K. D., Dumont, T., … McKerracher, L. (2021). A randomized controlled trial of local delivery of a rho inhibitor (VX-210) in patients with acute traumatic cervical spinal cord injury. *Journal of Neurotrauma*, *38*(15), 2065–2072. https://doi.org/10.1089/NEU.2020.7096/ASSET/IMAGES/LARGE/NEU.2020.7096_FIGURE2.JPEG

108. Fehlings, M. G., Tetreault, L. A., Wilson, J. R., Kwon, B. K., Burns, A. S., Martin, A. R., … Harrop, J. S. (2017, September 1). A Clinical Practice Guideline for the Management of Acute Spinal Cord Injury: Introduction, Rationale, and Scope. *Global Spine Journal*. Global Spine J. https://doi.org/10.1177/2192568217703387

109. Fei, J. F., Schuez, M., Tazaki, A., Taniguchi, Y., Roensch, K., & Tanaka, E. M. (2014). CRISPR-mediated genomic deletion of Sox2 in the axolotl shows a requirement in spinal cord neural stem cell amplification during tail regeneration. *Stem Cell Reports*, *3*(3), 444–459. https://doi.org/10.1016/j.stemcr.2014.06.018

110. Frisén, J., Hægerstrand, A., Risling, M., Fried, K., Johansson, C. B., Hammarberg, H., … Cullheim, S. (1995). Spinal axons in central nervous system scar tissue are closely related to laminin-immunoreactive astrocytes. *Neuroscience*, *65*(1), 293–304. https://doi.org/10.1016/0306-4522(94)00467-J

111. Frisén, Jonas, Johansson, C. B., Török, C., Risling, M., & Lendahl, U. (1995). Rapid,

widespread, and longlasting induction of nestin contributes to the generation of glial scar tissue after CNS injury. *Journal of Cell Biology*, *131*(2), 453–464. https://doi.org/10.1083/jcb.131.2.453

112. Fu, S. L., Hu, J. G., Li, Y., Wang, Y. X., Jin, J. Q., Xu, X. M., & Lu, P. H. (2007). A simplified method for generating oligodendrocyte progenitor cells from neural precursor cells isolated from the E16 rat spinal cord. *Acta Neurobiologiae Experimentalis*, *67*(4), 367–377.

113. Fuller, M. L., DeChant, A. K., Rothstein, B., Caprariello, A., Wang, R., Hall, A. K., & Miller, R. H. (2007). Bone morphogenetic proteins promote gliosis in demyelinating spinal cord lesions. *Annals of Neurology*, *62*(3), 288–300. https://doi.org/10.1002/ana.21179

114. Furlan, J. C., Krassioukov, A. V., & Fehlings, M. G. (2005). The effects of gender on clinical and neurological outcomes after acute cervical spinal cord injury. *Journal of Neurotrauma*, *22*(3), 368–381. https://doi.org/10.1089/neu.2005.22.368

115. Gabellini, D., Colaluca, I. N., Vodermaier, H. C., Biamonti, G., Giacca, M., Falaschi, A., … Peverali, F. A. (2003). Early mitotic degradation of the homeoprotein HOXC10 is potentially linked to cell cycle progression. *EMBO Journal*, *22*(14), 3715–3724. https://doi.org/10.1093/emboj/cdg340

116. Galiakberova, A. A., & Dashinimaev, E. B. (2020). Neural Stem Cells and Methods for Their Generation From Induced Pluripotent Stem Cells in vitro. *Frontiers in Cell and Developmental Biology*. https://doi.org/10.3389/fcell.2020.00815

117. Galuta, A., Sandarage, R., Ghinda, D., Auriat, A. M., Chen, S., Kwan, J. C. S., & Tsai, E. C. (2020). A Guide to Extract Spinal Cord for Translational Stem Cell Biology Research: Comparative Analysis of Adult Human, Porcine, and Rodent Spinal Cord Stem Cells. *Frontiers in Neuroscience*, *14*. https://doi.org/10.3389/fnins.2020.00607

118. Garcia-Ovejero, D., Arevalo-Martin, A., Paniagua-Torija, B., Florensa-Vila, J., Ferrer, I., Grassner, L., & Molina-Holgado, E. (2015). The ependymal region of the adult human spinal cord differs from other species and shows ependymoma-like features. *Brain*, *138*(6), 1583–1597. https://doi.org/10.1093/brain/awv089

119. Garriock, R. J., Chalamalasetty, R. B., Kennedy, M. W., Canizales, L. C., Lewandoski, M., & Yamaguchi, T. P. (2015). Lineage tracing of neuromesodermal progenitors reveals novel wnt-dependent roles in trunk progenitor cell maintenance and differentiation. *Development (Cambridge)*, *142*(9), 1628–1638. https://doi.org/10.1242/dev.111922

120. Gazdic, M., Volarevic, V., Randall Harrell, C., Fellabaum, C., Jovicic, N., Arsenijevic, N., & Stojkovic, M. (2018). Stem cells therapy for spinal cord injury. *International Journal of Molecular Sciences*. https://doi.org/10.3390/ijms19041039

121. Ghazale, H., Ripoll, C., Leventoux, N., Jacob, L., Azar, S., Mamaeva, D., … Hugnot, J. P. (2019a). RNA Profiling of the Human and Mouse Spinal Cord Stem Cell Niches Reveals an Embryonic-like Regionalization with MSX1+ Roof-Plate-Derived Cells. *Stem Cell Reports*, *12*(5), 1159–1177. https://doi.org/10.1016/j.stemcr.2019.04.001

122. Ghazale, H., Ripoll, C., Leventoux, N., Jacob, L., Azar, S., Mamaeva, D., … Hugnot, J. P. (2019b). RNA Profiling of the Human and Mouse Spinal Cord Stem Cell Niches Reveals an Embryonic-like Regionalization with MSX1+ Roof-Plate-Derived Cells. *Stem Cell Reports*, *12*(5), 1159–1177. https://doi.org/10.1016/j.stemcr.2019.04.001

123. Giger, R. J., Hollis, E. R., & Tuszynski, M. H. (2010). Guidance molecules in axon regeneration. *Cold Spring Harbor Perspectives in Biology*, *2*(7), 1–21. https://doi.org/10.1101/cshperspect.a001867

124. Gil-Perotín, S., Duran-Moreno, M., Cebrián-Silla, A., Ramírez, M., García-Belda, P., &

García-Verdugo, J. M. (2013). Adult neural stem cells from the subventricular zone: A review of the neurosphere assay. *Anatomical Record*, *296*(9), 1435–1452. https://doi.org/10.1002/ar.22746

125. Gilbert, E. A. B., Lakshman, N., Lau, K. S. K., & Morshead, C. M. (2022). Regulating Endogenous Neural Stem Cell Activation to Promote Spinal Cord Injury Repair. *Cells*, *11*(5), 1–26. https://doi.org/10.3390/cells11050846

126. Gill, M. L., Grahn, P. J., Calvert, J. S., Linde, M. B., Lavrov, I. A., Strommen, J. A., … Zhao, K. D. (2018). Neuromodulation of lumbosacral spinal networks enables independent stepping after complete paraplegia. *Nature Medicine 2018 24:11*, *24*(11), 1677–1682. https://doi.org/10.1038/s41591-018-0175-7

127. Ginhoux, F., Lim, S., Hoeffel, G., Low, D., & Huber, T. (2013). Origin and differentiation of microglia. *Frontiers in Cellular Neuroscience*, *0*(MAR), 45. https://doi.org/10.3389/FNCEL.2013.00045/BIBTEX

128. Glennie, R. A., Bailey, C. S., Tsai, E. C., Noonan, V. K., Rivers, C. S., Fourney, D. R., … Dvorak, M. F. (2017). An analysis of ideal and actual time to surgery after traumatic spinal cord injury in Canada. *Spinal Cord 2017 55:6*, *55*(6), 618–623. https://doi.org/10.1038/sc.2016.177

129. Global Newswire. (2019, January 24). Asterias Provides Top Line 12 Month Data Update for its OPC1 Phase 1/2a Clinical Trial in Severe Spinal Cord Injury. Retrieved May 26, 2022, from https://www.globenewswire.com/en/news-release/2019/01/24/1704757/0/en/Asterias-Provides-Top-Line-12-Month-Data-Update-for-its-OPC1-Phase-1-2a-Clinical-Trial-in-Severe-Spinal-Cord-Injury.html

130. Goldberg, A. L., & Kershah, S. M. (2010). INVITED REVIEW Advances in Imaging of

Vertebral and Spinal Cord Injury. *J Spinal Cord Med*, *33*(2), 105–116.

131. Goldman, S. A., & Kuypers, N. J. (2015). How to make an oligodendrocyte. *Development (Cambridge)*, *142*(23), 3983–3995. https://doi.org/10.1242/dev.126409

132. Goldshmit, Y., Sztal, T. E., Jusuf, P. R., Hall, T. E., Nguyen-Chi, M., & Currie, P. D. (2012). Fgf-Dependent Glial Cell Bridges Facilitate Spinal Cord Regeneration in Zebrafish. *Journal of Neuroscience*, *32*(22), 7477–7492. https://doi.org/10.1523/JNEUROSCI.0758-12.2012

133. Gonzalez-Fernandez, C., Arevalo-Martin, A., Paniagua-Torija, B., Ferrer, I., Rodriguez, F. J., & Garcia-Ovejero, D. (2017). Wnts Are Expressed in the Ependymal Region of the Adult Spinal Cord. *Molecular Neurobiology*, *54*(8), 6342–6355. https://doi.org/10.1007/s12035-016-0132-8

134. González, P., González-Fernández, C., Campos-Martín, Y., Mollejo, M., Carballosa-Gautam, M., Marcillo, A., … Rodríguez, F. J. (2020). Spatio-temporal and Cellular Expression Patterns of PTK7 in the Healthy and Traumatically Injured Rat and Human Spinal Cord. *Cellular and Molecular Neurobiology*, *40*(7), 1087–1103. https://doi.org/10.1007/s10571-020-00794-6

135. Gopalakrishnan, S., Hor, P., & Ichida, J. K. (2017). New approaches for direct conversion of patient fibroblasts into neural cells. *Brain Research*, *1656*, 2–13. https://doi.org/10.1016/j.brainres.2015.10.012

136. Göritz, C., Dias, D. O., Tomilin, N., Barbacid, M., Shupliakov, O., & Frisén, J. (2011). pericytes contribute to stromal deposition in scar tissue. *Science*.

137. Gouti, M., Delile, J., Stamataki, D., Wymeersch, F. J., Huang, Y., Kleinjung, J., … Briscoe, J. (2017). A Gene Regulatory Network Balances Neural and Mesoderm

Specification during Vertebrate Trunk Development. *Developmental Cell*, *41*(3), 243-261.e7. https://doi.org/10.1016/j.devcel.2017.04.002

138. Greenhalgh, A. D., & David, S. (2014). Differences in the Phagocytic Response of Microglia and Peripheral Macrophages after Spinal Cord Injury and Its Effects on Cell Death. *Journal of Neuroscience*, *34*(18), 6316–6322. https://doi.org/10.1523/JNEUROSCI.4912-13.2014

139. Grégoire, C.-A., Goldenstein, B. L., Floriddia, E. M., Barnabé-Heider, F., & Fernandes, K. J. L. (2015). Endogenous neural stem cell responses to stroke and spinal cord injury. *Glia*, *63*(8), 1469–1482. https://doi.org/10.1002/glia.22851

140. Grelat, A., Benoit, L., Wagner, S., Moigneu, C., Lledo, P. M., & Alonso, M. (2018). Adult-born neurons boost odor–reward association. *Proceedings of the National Academy of Sciences of the United States of America*, *115*(10), 2514–2519. https://doi.org/10.1073/PNAS.1716400115/SUPPL_FILE/PNAS.201716400SI.PDF

141. Groszer, M., Erickson, R., Scripture-Adams, D. D., Lesche, R., Trumpp, A., Zack, J. A., … Wu, H. (2001). Negative regulation of neural stem/progenitor cell proliferation by the Pten tumor suppressor gene in vivo. *Science*, *294*(5549), 2186–2189. https://doi.org/10.1126/science.1065518

142. Groszer, Matthias, Erickson, R., Scripture-Adams, D. D., Dougherty, J. D., Le Belle, J., Zack, J. A., … Wu, H. (2006). PTEN negatively regulates neural stem cell self-renewal by modulating G0-G1 cell cycle entry. *Proceedings of the National Academy of Sciences of the United States of America*, *103*(1), 111–116. https://doi.org/10.1073/pnas.0509939103

143. Gudz, T. I., Komuro, H., & Macklin, W. B. (2006). Glutamate Stimulates Oligodendrocyte Progenitor Migration Mediated via anαv Integrin/Myelin Proteolipid

Protein Complex. *The Journal of Neuroscience*, *26*(9), 2458. https://doi.org/10.1523/JNEUROSCI.4054-05.2006

144. Guest, J. D., Hiester, E. D., & Bunge, R. P. (2005). Demyelination and Schwann cell responses adjacent to injury epicenter cavities following chronic human spinal cord injury. *Experimental Neurology*, *192*(2), 384–393. https://doi.org/10.1016/J.EXPNEUROL.2004.11.033

145. Hachem, L. D., Mothe, A. J., & Tator, C. H. (2016). Glutamate Increases in Vitro Survival and Proliferation and Attenuates Oxidative Stress-Induced Cell Death in Adult Spinal Cord-Derived Neural Stem/Progenitor Cells via Non-NMDA Ionotropic Glutamate Receptors. *Stem Cells and Development*, *25*(16), 1223–1233. https://doi.org/10.1089/scd.2015.0389

146. Hachem, L. D., Mothe, A. J., & Tator, C. H. (2020, February 1). Unlocking the paradoxical endogenous stem cell response after spinal cord injury. *Stem Cells*. Wiley-Blackwell. https://doi.org/10.1002/stem.3107

147. Hagg, T., & Oudega, M. (2006). Degenerative and spontaneous regenerative processes after spinal cord injury. *Journal of Neurotrauma*. Mary Ann Liebert Inc. https://doi.org/10.1089/neu.2006.23.263

148. Halliwell, R. F. (2017). Electrophysiological properties of neurons derived from human stem cells and iNeurons in vitro. *Neurochemistry International*, *106*, 37–47. https://doi.org/10.1016/j.neuint.2016.10.003

149. Hamilton, L. K., Truong, M. K. V., Bednarczyk, M. R., Aumont, A., & Fernandes, K. J. L. (2009). Cellular organization of the central canal ependymal zone, a niche of latent neural stem cells in the adult mammalian spinal cord. *Neuroscience*, *164*(3), 1044–1056.

https://doi.org/10.1016/j.neuroscience.2009.09.006

150. Hauben, E., Mizrahi, T., Agranov, E., & Schwartz, M. (2002). Sexual dimorphism in the spontaneous recovery from spinal cord injury: A gender gap in beneficial autoimmunity? *European Journal of Neuroscience*, *16*(9), 1731–1740. https://doi.org/10.1046/j.1460-9568.2002.02241.x

151. Hawryluk, G. W. J., Mothe, A. J., Chamankhah, M., Wang, J., Tator, C., & Fehlings, M. G. (2012). In Vitro Characterization of Trophic Factor Expression in Neural Precursor Cells. *Stem Cells and Development*, *21*(3), 432–447. https://doi.org/10.1089/scd.2011.0242

152. Heinrich, P. C., Behrmann, I., Müller-Newen, G., Schaper, F., & Graeve, L. (1998). Interleukin-6-type cytokine signalling through the gp130/Jak/STAT pathway. *Biochemical Journal*, *334*(Pt 2), 297. https://doi.org/10.1042/BJ3340297

153. Henrique, D., Abranches, E., Verrier, L., & Storey, K. G. (2015). Neuromesodermal progenitors and the making of the spinal cord. *Development (Cambridge)*, *142*(17), 2864–2875. https://doi.org/10.1242/dev.119768

154. Herrmann, J. E., Imura, T., Song, B., Qi, J., Ao, Y., Nguyen, T. K., … Sofroniew, M. V. (2008). STAT3 is a Critical Regulator of Astrogliosis and Scar Formation after Spinal Cord Injury. *Journal of Neuroscience*, *28*(28), 7231–7243. https://doi.org/10.1523/JNEUROSCI.1709-08.2008

155. Hickey, R. J., Modulevsky, D. J., Cuerrier, C. M., & Pelling, A. E. (2018). Customizing the Shape and Microenvironment Biochemistry of Biocompatible Macroscopic Plant-Derived Cellulose Scaffolds. *ACS Biomaterials Science and Engineering*, *4*(11), 3726–3736. https://doi.org/10.1021/acsbiomaterials.8b00178

156. Hildebrand, M. E., Smith, P. L., Bladen, C., Eduljee, C., Xie, J. Y., Chen, L., … Snutch,

T. P. (2011). A novel slow-inactivation-specific ion channel modulator attenuates neuropathic pain. *Pain*, *152*(4), 833–843. https://doi.org/10.1016/j.pain.2010.12.035

157. Hodge, R. D., Bakken, T. E., Miller, J. A., Smith, K. A., Barkan, E. R., Graybuck, L. T., … Lein, E. S. (2019). Conserved cell types with divergent features in human versus mouse cortex. *Nature*, *573*(7772), 61–68. https://doi.org/10.1038/s41586-019-1506-7

158. Hofrichter, M., Nimtz, L., Tigges, J., Kabiri, Y., Schröter, F., Royer-Pokora, B., … Fritsche, E. (2017). Comparative performance analysis of human iPSC-derived and primary neural progenitor cells (NPC) grown as neurospheres in vitro. *Stem Cell Research*, *25*, 72–82. https://doi.org/10.1016/j.scr.2017.10.013

159. Hong, E. P., & Park, J. W. (2012). Sample Size and Statistical Power Calculation in Genetic Association Studies. *Genomics & Informatics*, *10*(2), 117. https://doi.org/10.5808/gi.2012.10.2.117

160. Hu, W., Qiu, B., Guan, W., Wang, Q., Wang, M., Li, W., … Pei, G. (2015). Direct Conversion of Normal and Alzheimer's Disease Human Fibroblasts into Neuronal Cells by Small Molecules. *Cell Stem Cell*, *17*(2), 204–212. https://doi.org/10.1016/j.stem.2015.07.006

161. Huang, W. L., King, V. R., Curran, O. E., Dyall, S. C., Ward, R. E., Lal, N., … Michael-Titus, A. T. (2007). A combination of intravenous and dietary docosahexaenoic acid significantly improves outcome after spinal cord injury. *Brain : A Journal of Neurology*, *130*(Pt 11), 3004–3019. https://doi.org/10.1093/BRAIN/AWM223

162. Huang, Y., Li, Y., Chen, J., Zhou, H., & Tan, S. (2015, October 19). Electrical stimulation elicits neural stem cells activation: New perspectives in CNS repair. *Frontiers in Human Neuroscience*. Frontiers Media S. A. https://doi.org/10.3389/fnhum.2015.00586

163. Huebner, E. A., & Strittmatter, S. M. (2009). Axon regeneration in the peripheral and

central nervous systems. *Results and Problems in Cell Differentiation*, *48*, 339–351. https://doi.org/10.1007/400_2009_19

164. Hui, S. P., Nag, T. C., & Ghosh, S. (2015). Characterization of Proliferating Neural Progenitors after Spinal Cord Injury in Adult Zebrafish. *PLoS ONE*, *10*(12), 1–27. https://doi.org/10.1371/journal.pone.0143595

165. Hunanyan, A. S., García-Alías, G., Alessi, V., Levine, J. M., Fawcett, J. W., Mendell, L. M., & Arvanian, V. L. (2010). Role of chondroitin sulfate proteoglycans in axonal conduction in Mammalian spinal cord. *The Journal of Neuroscience : The Official Journal of the Society for Neuroscience*, *30*(23), 7761–7769. https://doi.org/10.1523/JNEUROSCI.4659-09.2010

166. Hwan Yoon, S., Shik Shim, Y., Hoon Park, Y., Kwon Chung, J., Hyun Nam, J., Ok Kim, M., … Min, B. (2007). Complete Spinal Cord Injury Treatment Using Autologous Bone Marrow Cell Transplantation and Bone Marrow Stimulation with Granulocyte Macrophage-Colony Stimulating Factor: Phase I/II Clinical Trial. *Stem Cells*, *25*(8), 2066–2073. https://doi.org/10.1634/STEMCELLS.2006-0807

167. Ibrayeva, A., Bay, M., Pu, E., Jörg, D. J., Peng, L., Jun, H., … Bonaguidi, M. A. (2021). Early stem cell aging in the mature brain. *Cell Stem Cell*, *28*(5), 955-966.e7. https://doi.org/10.1016/j.stem.2021.03.018

168. Iida, T., Okano, H., Sugai, K., Yamaguchi, R., Isoda, M., Ohkubo, T., … Itakura, G. (2018). Concise Review: Laying the Groundwork for a First-In-Human Study of an Induced Pluripotent Stem Cell-Based Intervention for Spinal Cord Injury. *STEM CELLS*, *37*(1), 6–13. https://doi.org/10.1002/stem.2926

169. Inanici, F., Brighton, L. N., Samejima, S., Hofstetter, C. P., & Moritz, C. T. (2021).

Transcutaneous Spinal Cord Stimulation Restores Hand and Arm Function after Spinal Cord Injury. *IEEE Transactions on Neural Systems and Rehabilitation Engineering*, *29*, 310–319. https://doi.org/10.1109/TNSRE.2021.3049133

170. Jha, R. M., Liu, X., Chrenek, R., Madsen, J. R., & Cardozo, D. L. (2013). The postnatal human filum terminale is a source of autologous multipotent neurospheres capable of generating motor neurons. *Neurosurgery*, *72*(1), 118–128. https://doi.org/10.1227/NEU.0b013e318276b445

171. Jimenez Hamann, M. C., Tator, C. H., & Shoichet, M. S. (2005). Injectable intrathecal delivery system for localized administration of EGF and FGF-2 to the injured rat spinal cord. *Experimental Neurology*, *194*(1), 106–119. https://doi.org/10.1016/j.expneurol.2005.01.030

172. Jones, T., McDaniel, E., & Popovich, P. (2005). Inflammatory-Mediated Injury and Repair in the Traumatically Injured Spinal Cord. *Current Pharmaceutical Design*, *11*(10), 1223–1236. https://doi.org/10.2174/1381612053507468

173. Jovanovic, L. I., Kapadia, N., Zivanovic, V., Rademeyer, H. J., Alavinia, M., McGillivray, C., … Marquez-Chin, C. (2021). Brain–computer interface-triggered functional electrical stimulation therapy for rehabilitation of reaching and grasping after spinal cord injury: a feasibility study. *Spinal Cord Series and Cases*, *7*(1), 1–11. https://doi.org/10.1038/s41394-020-00380-4

174. Julian, L. M., McDonald, A. C., & Stanford, W. L. (2017). Direct reprogramming with SOX factors: masters of cell fate. *Current Opinion in Genetics and Development*, *46*, 24–36. https://doi.org/10.1016/j.gde.2017.06.005

175. Kadoya, K., Lu, P., Nguyen, K., Lee-Kubli, C., Kumamaru, H., Yao, L., … Tuszynski, M. H. (2016). Spinal cord reconstitution with homologous neural grafts enables robust

corticospinal regeneration. *Nature Medicine*, *22*(5), 479–487. https://doi.org/10.1038/nm.4066

176. Kajikawa, K., Imaizumi, K., Shinozaki, M., Shibata, S., Shindo, T., Kitagawa, T., … Okano, H. (2020). Cell therapy for spinal cord injury by using human iPSC-derived region-specific neural progenitor cells. *Molecular Brain*, *13*(1), 120. https://doi.org/10.1186/s13041-020-00662-w

177. Kakuta, Y., Adachi, A., Yokohama, M., Horii, T., Mieda, T., Iizuka, Y., … Nakamura, K. (2019). Spontaneous functional full recovery from motor and sensory deficits in adult mice after mild spinal cord injury. *Heliyon*, *5*(6), e01847. https://doi.org/10.1016/j.heliyon.2019.e01847

178. Kandasamy, M., Lehner, B., Kraus, S., Sander, P. R., Marschallinger, J., Rivera, F. J., … Aigner, L. (2014). TGF-beta signalling in the adult neurogenic niche promotes stem cell quiescence as well as generation of new neurons. *Journal of Cellular and Molecular Medicine*, *18*(7), 1444–1459. https://doi.org/10.1111/jcmm.12298

179. Kandasamy, M., Reilmann, R., Winkler, J., Bogdahn, U., & Aigner, L. (2011). Transforming growth factor-beta signaling in the neural stem cell niche: A therapeutic target for Huntington's disease. *Neurology Research International*, *2011*. https://doi.org/10.1155/2011/124256

180. Kandel, E. R., Schwartz, J. H., Jessell, T. M., Siegelbaum, S. A., Hudspeth, A. J., & Mack, S. (2013). *Principles of Neuroscience* (5th ed.). New York. N.Y.: McGraw-Hill Education LLC.

181. Kang, M. K., & Kang, S. K. (2008). Interleukin-6 induces proliferation in adult spinal cord-derived neural progenitors via the JAK2/STAT3 pathway with EGF-induced MAPK

phosphorylation. *Cell Proliferation*, *41*(3), 377–392. https://doi.org/10.1111/j.1365-2184.2008.00537.x

182. Kang, Y., Ding, H., Zhou, H., Wei, Z., Liu, L., Pan, D., & Feng, S. (2017). Epidemiology of worldwide spinal cord injury: a literature review. *Journal of Neurorestoratology*, *Volume 6*(1), 1–9. https://doi.org/10.2147/jn.s143236

183. Kanno, H., Ozawa, H., Sekiguchi, A., Yamaya, S., Tateda, S., Yahata, K., & Itoi, E. (2012). The role of mTOR signaling pathway in spinal cord injury. *Cell Cycle*, *11*(17), 3175. https://doi.org/10.4161/CC.21262

184. Káradóttir, R., & Attwell, D. (2007). Neurotransmitter receptors in the life and death of oligodendrocytes. *Neuroscience*. https://doi.org/10.1016/j.neuroscience.2006.08.070

185. Karimi-Abdolrezaee, S., Eftekharpour, E., Wang, J., Schut, D., & Fehlings, M. G. (2010). Synergistic Effects of Transplanted Adult Neural Stem/Progenitor Cells, Chondroitinase, and Growth Factors Promote Functional Repair and Plasticity of the Chronically Injured Spinal Cord. *Journal of Neuroscience*, *30*(5), 1657–1676. https://doi.org/10.1523/JNEUROSCI.3111-09.2010

186. Karimi-Abdolrezaee, Soheila, Eftekharpour, E., Wang, J., Morshead, C. M., & Fehlings, M. G. (2006). Delayed transplantation of adult neural precursor cells promotes remyelination and functional neurological recovery after spinal cord injury. *Journal of Neuroscience*, *26*(13), 3377–3389. https://doi.org/10.1523/JNEUROSCI.4184-05.2006

187. Karimi-Abdolrezaee, Soheila, Schut, D., Wang, J., & Fehlings, M. G. (2012). Chondroitinase and growth factors enhance activation and Oligodendrocyte differentiation of endogenous neural precursor cells after spinal cord injury. *PLoS ONE*, *7*(5), 37589. https://doi.org/10.1371/journal.pone.0037589

188. Karsten, S. L., Kudo, L. C., Jackson, R., Sabatti, C., Kornblum, H. I., & Geschwind, D. H. (2003). Global analysis of gene expression in neural progenitors reveals specific cell-cycle, signaling, and metabolic networks. *Developmental Biology*, *261*(1), 165–182. https://doi.org/10.1016/S0012-1606(03)00274-4

189. Kawaja, M. D., & Gage, F. H. (1991). Reactive astrocytes are substrates for the growth of adult CNS axons in the presence of elevated levels of nerve growth factor. *Neuron*, *7*(6), 1019–1030. https://doi.org/10.1016/0896-6273(91)90346-2

190. Khazaei, M., Ahuja, C. S., & Fehlings, M. G. (2017). Induced Pluripotent Stem Cells for Traumatic Spinal Cord Injury. *Frontiers in Cell and Developmental Biology*, *4*(January), 1–9. https://doi.org/10.3389/fcell.2016.00152

191. Kigerl, K. A., Gensel, J. C., Ankeny, D. P., Alexander, J. K., Donnelly, D. J., & Popovich, P. G. (2009). Identification of Two Distinct Macrophage Subsets with Divergent Effects Causing either Neurotoxicity or Regeneration in the Injured Mouse Spinal Cord. *The Journal of Neuroscience*, *29*(43), 13435. https://doi.org/10.1523/JNEUROSCI.3257-09.2009

192. Kim, E., Hwang, S. U., Yoon, J. D., Kim, H., Lee, G., & Hyun, S. H. (2018). Isolation and characterization of GFAP-positive porcine neural stem/progenitor cells derived from a GFAP-CreER T2 transgenic piglet. *BMC Veterinary Research*, *14*(1), 1–10. https://doi.org/10.1186/s12917-018-1660-4

193. Kim, K. T., Streijger, F., Manouchehri, N., So, K., Shortt, K., Okon, E. B., … Kwon, B. K. (2018). Review of the UBC porcine model of traumatic spinal cord injury. *Journal of Korean Neurosurgical Society*. https://doi.org/10.3340/jkns.2017.0276

194. Kim, S. M., Lim, K. T., Kwak, T. H., Lee, S. C., Im, J. H., Hali, S., … Han, D. W. (2016). Induced neural stem cells from distinct genetic backgrounds exhibit different

reprogramming status. *Stem Cell Research*, *16*(2), 460–468. https://doi.org/10.1016/j.scr.2016.02.025

195. Kirshblum, S. C., Waring, W., Biering-Sorensen, F., Burns, S. P., Johansen, M., Schmidt-Read, M., … Krassioukov, A. (2011). Reference for the 2011 revision of the International Standards for Neurological Classification of Spinal Cord Injury. *Journal of Spinal Cord Medicine*. https://doi.org/10.1179/107902611X13186000420242

196. Kjell, J., & Olson, L. (2016). Rat models of spinal cord injury: From pathology to potential therapies. *DMM Disease Models and Mechanisms*. https://doi.org/10.1242/dmm.025833

197. Klapka, N., & Müller, H. W. (2006). Collagen matrix in spinal cord injury. *Journal of Neurotrauma*, *23*(3–4), 422–435. https://doi.org/10.1089/NEU.2006.23.422

198. Kobayashi, Y., Okada, Y., Itakura, G., Iwai, H., Nishimura, S., Yasuda, A., … Okano, H. (2012). Pre-Evaluated Safe Human iPSC-Derived Neural Stem Cells Promote Functional Recovery after Spinal Cord Injury in Common Marmoset without Tumorigenicity. *PLoS ONE*, *7*(12), 52787. https://doi.org/10.1371/journal.pone.0052787

199. Köhler, S., Winkler, U., & Hirrlinger, J. (2021). Heterogeneity of Astrocytes in Grey and White Matter. *Neurochemical Research*, *46*(1), 3–14. https://doi.org/10.1007/s11064-019-02926-x

200. Kojima, A., & Tator, C. H. (2002). *Intrathecal Administration of Epidermal Growth Factor and Fibroblast Growth Factor 2 Promotes Ependymal Proliferation and Functional Recovery after Spinal Cord Injury in Adult Rats*. *JOURNAL OF NEUROTRAUMA* (Vol. 19).

201. Kokaia, Z., Martino, G., Schwartz, M., & Lindvall, O. (2012). Cross-talk between neural stem cells and immune cells: the key to better brain repair? *Nature Neuroscience*, *15*(8),

1078–1087. https://doi.org/10.1038/nn.3163

202. Krassioukov, A. V., Ackery, A., Schwartz, G., Adamchik, Y., Liu, Y., & Fehlings, M. G. (2002). An in vitro model of neurotrauma in organotypic spinal cord cultures from adult mice. *Brain Research Protocols*, *10*(2), 60–68. https://doi.org/10.1016/S1385-299X(02)00180-0

203. Kroner, A., Greenhalgh, A. D., Zarruk, J. G., PassosdosSantos, R., Gaestel, M., & David, S. (2014). TNF and increased intracellular iron alter macrophage polarization to a detrimental M1 phenotype in the injured spinal cord. *Neuron*, *83*(5), 1098–1116. https://doi.org/10.1016/J.NEURON.2014.07.027

204. Kucher, K., Johns, D., Maier, D., Abel, R., Badke, A., Baron, H., … Curt, A. (2018). First-in-Man Intrathecal Application of Neurite Growth-Promoting Anti-Nogo-A Antibodies in Acute Spinal Cord Injury. *Neurorehabilitation and Neural Repair*, *32*(6–7), 578–589. https://doi.org/10.1177/1545968318776371

205. Kuhn, S., Gritti, L., Crooks, D., & Dombrowski, Y. (2019, November 1). Oligodendrocytes in development, myelin generation and beyond. *Cells*. Multidisciplinary Digital Publishing Institute (MDPI). https://doi.org/10.3390/cells8111424

206. Kulbatski, I., Mothe, A., Nomura, H., & Tator, C. (2005). Endogenous and Exogenous CNS Derived Stem / Progenitor Cell Approaches for Neurotrauma. *Current Drug Targets*, *6*(1), 111–126. https://doi.org/10.2174/1389450053345037

207. Kulbatski, Iris, & Tator, C. H. (2009). Region-specific differentiation potential of adult rat spinal cord neural stem/precursors and their plasticity in response to in vitro manipulation. *Journal of Histochemistry and Cytochemistry*, *57*(5), 405–423. https://doi.org/10.1369/jhc.2008.951814

208. Kumamaru, H., Kadoya, K., Adler, A. F., Takashima, Y., Graham, L., Coppola, G., & Tuszynski, M. H. (2018). Generation and post-injury integration of human spinal cord neural stem cells. *Nature Methods*, *15*(9), 723–731. https://doi.org/10.1038/s41592-018-0074-3

209. Kumamaru, H., Lu, P., Rosenzweig, E. S., Kadoya, K., & Tuszynski Correspondence, M. H. (2019). Regenerating Corticospinal Axons Innervate Phenotypically Appropriate Neurons within Neural Stem Cell Grafts. *Cell Reports*, *26*. https://doi.org/10.1016/j.celrep.2019.01.099

210. Kumamaru, H., Lu, P., Rosenzweig, E. S., Kadoya, K., & Tuszynski, M. H. (2019). Regenerating Corticospinal Axons Innervate Phenotypically Appropriate Neurons within Neural Stem Cell Grafts. *Cell Reports*, *26*(9), 2329-2339.e4. https://doi.org/10.1016/j.celrep.2019.01.099

211. Kumamaru, H., Lu, P., Rosenzweig, E. S., & Tuszynski, M. H. (2018). Activation of Intrinsic Growth State Enhances Host Axonal Regeneration into Neural Progenitor Cell Grafts. *Stem Cell Reports*, *11*(4), 861–868. https://doi.org/10.1016/j.stemcr.2018.08.009

212. Kuscha, V., Barreiro-Iglesias, A., Becker, C. G., & Becker, T. (2012). Plasticity of tyrosine hydroxylase and serotonergic systems in the regenerating spinal cord of adult zebrafish. *Journal of Comparative Neurology*, *520*(5), 933–951. https://doi.org/10.1002/CNE.22739

213. Kuscha, V., Frazer, S. L., Dias, T. B., Hibi, M., Becker, T., & Becker, C. G. (2012). Lesion-induced generation of interneuron cell types in specific dorsoventral domains in the spinal cord of adult zebrafish. *The Journal of Comparative Neurology*, *520*(16), 3604–3616. https://doi.org/10.1002/CNE.23115

214. Kwon, B. K., Okon, E. B., Tsai, E., Beattie, M. S., Bresnahan, J. C., Magnuson, D. K., …

Tetzlaff, W. (2011). A Grading System To Evaluate Objectively the Strength of Pre-Clinical Data of Acute Neuroprotective Therapies for Clinical Translation in Spinal Cord Injury. *Journal of Neurotrauma*, *28*(8), 1525–1543. https://doi.org/10.1089/neu.2010.1296

215. Kwon, B. K., Streijger, F., Fallah, N., Noonan, V. K., Bélanger, L. M., Ritchie, L., … Dvorak, M. F. (2017). Cerebrospinal Fluid Biomarkers To Stratify Injury Severity and Predict Outcome in Human Traumatic Spinal Cord Injury. *Journal of Neurotrauma*, *34*, 567–580. https://doi.org/10.1089/neu.2016.4435

216. Kwon, B. K., Streijger, F., Hill, C. E., Anderson, A. J., Bacon, M., Beattie, M. S., … Tetzlaff, W. (2015). Large animal and primate models of spinal cord injury for the testing of novel therapies. *Experimental Neurology*, *269*, 154–168. https://doi.org/10.1016/j.expneurol.2015.04.008

217. Lacroix, S., Chang, L., Rose-John, S., & Tuszynski, M. H. (2002). Delivery of hyper-interleukin-6 to the injured spinal cord increases neutrophil and macrophage infiltration and inhibits axonal growth. *The Journal of Comparative Neurology*, *454*(3), 213–228. https://doi.org/10.1002/CNE.10407

218. Lacroix, S., Hamilton, L. K., Vaugeois, A., Beaudoin, S., Breault-Dugas, C., Pineau, I., … Fernandes, K. J. L. (2014). Central canal ependymal cells proliferate extensively in response to traumatic spinal cord injury but not demyelinating lesions. *PLoS ONE*, *9*(1). https://doi.org/10.1371/journal.pone.0085916

219. Lau, L. W., Keough, M. B., Haylock-Jacobs, S., Cua, R., Döring, A., Sloka, S., … Yong, V. W. (2012). Chondroitin sulfate proteoglycans in demyelinated lesions impair remyelination. *Annals of Neurology*, *72*(3), 419–432. https://doi.org/10.1002/ANA.23599

220. Le Dréau, G., & Martí, E. (2013). The multiple activities of BMPs during spinal cord

development. *Cellular and Molecular Life Sciences*. https://doi.org/10.1007/s00018-013-1354-9

221. Lech, M., & Anders, H. J. (2013). Macrophages and fibrosis: How resident and infiltrating mononuclear phagocytes orchestrate all phases of tissue injury and repair. *Biochimica et Biophysica Acta*, *1832*(7), 989–997. https://doi.org/10.1016/J.BBADIS.2012.12.001

222. Lee, J. H. T., Jones, C. F., Okon, E. B., Anderson, L., Tigchelaar, S., Kooner, P., … Kwon, B. K. (2013a). A Novel porcine model of traumatic thoracic spinal cord injury. *Journal of Neurotrauma*, *30*(3), 142–159. https://doi.org/10.1089/neu.2012.2386

223. Lee, J. H. T., Jones, C. F., Okon, E. B., Anderson, L., Tigchelaar, S., Kooner, P., … Kwon, B. K. (2013b). A Novel porcine model of traumatic thoracic spinal cord injury. *Journal of Neurotrauma*, *30*(3), 142–159. https://doi.org/10.1089/neu.2012.2386

224. Lee, J. K., Geoffroy, C. G., Chan, A. F., Tolentino, K. E., Crawford, M. J., Leal, M. A., … Zheng, B. (2010). Assessing spinal axon regeneration and sprouting in Nogo-, MAG-, and OMgp-deficient mice. *Neuron*, *66*(5), 663–670. https://doi.org/10.1016/J.NEURON.2010.05.002

225. Li, R., Strykowski, R., Meyer, M., Mulcrone, P., Krakora, D., & Suzuki, M. (2012). Male-Specific Differences in Proliferation, Neurogenesis, and Sensitivity to Oxidative Stress in Neural Progenitor Cells Derived from a Rat Model of ALS. *PLoS ONE*, *7*(11), e48581. https://doi.org/10.1371/journal.pone.0048581

226. Li, S., & Stys, P. K. (2001). Na+-K+-ATPase inhibition and depolarization induce glutamate release via reverse Na+-dependent transport in spinal cord white matter. *Neuroscience*, *107*(4), 675–683. https://doi.org/10.1016/S0306-4522(01)00385-2

227. Li, W. L., Chu, M. W., Wu, A., Suzuki, Y., Imayoshi, I., & Komiyama, T. (2018). Adult-born neurons facilitate olfactory bulb pattern separation during task engagement. *ELife*, *7*. https://doi.org/10.7554/ELIFE.33006

228. Li, Xiaofei, Floriddia, E. M., Toskas, K., Fernandes, K. J. L., Guérout, N., & Barnabé-heider, F. (2016). Regenerative Potential of Ependymal Cells for Spinal Cord Injuries Over Time. *EBIOM*, *13*, 55–65. https://doi.org/10.1016/j.ebiom.2016.10.035

229. Li, Xiaoran, Fan, C., Xiao, Z., Zhao, Y., Zhang, H., Sun, J., … Dai, J. (2018). A collagen microchannel scaffold carrying paclitaxel-liposomes induces neuronal differentiation of neural stem cells through Wnt/β-catenin signaling for spinal cord injury repair. *Biomaterials*, *183*, 114–127. https://doi.org/10.1016/j.biomaterials.2018.08.037

230. Li, Xiaoran, Xiao, Z., Han, J., Chen, L., Xiao, H., Ma, F., … Dai, J. (2013). Promotion of neuronal differentiation of neural progenitor cells by using EGFR antibody functionalized collagen scaffolds for spinal cord injury repair. *Biomaterials*, *34*(21), 5107–5116. https://doi.org/10.1016/j.biomaterials.2013.03.062

231. Li, Xing, Zhao, Y., Cheng, S., Han, S., Shu, M., Chen, B., … Dai, J. (2017). Cetuximab modified collagen scaffold directs neurogenesis of injury-activated endogenous neural stem cells for acute spinal cord injury repair. *Biomaterials*, *137*, 73–86. https://doi.org/10.1016/j.biomaterials.2017.05.027

232. Liard, O., Segura, S., Pascual, A., Gaudreau, P., Fusai, T., & Moyse, E. (2009). In vitro isolation of neural precursor cells from the adult pig subventricular zone. *Journal of Neuroscience Methods*, *182*(2), 172–179. https://doi.org/10.1016/j.jneumeth.2009.06.008

233. Liddelow, S. A., & Barres, B. A. (2016). Not everything is scary about a glial scar. *Nature*, *532*(7598), 182–183. https://doi.org/10.1038/nature17318

234. Lim, D. A., & Alvarez-Buylla, A. (2016). The adult ventricular–subventricular zone (V-SVZ) and olfactory bulb (OB) neurogenesis. *Cold Spring Harbor Perspectives in Biology*, *8*(5), 18820–18821. https://doi.org/10.1101/cshperspect.a018820

235. Lim, S. N., Huang, W., Hall, J. C. E., Michael-Titus, A. T., & Priestley, J. V. (2013). Improved outcome after spinal cord compression injury in mice treated with docosahexaenoic acid. *Experimental Neurology*, *239*(1), 13–27. https://doi.org/10.1016/J.EXPNEUROL.2012.09.015

236. Lima, C., Pratas-Vital, J., Escada, P., Hasse-Ferreira, A., Capucho, C., & Peduzzi, J. D. (2016). Olfactory Mucosa Autografts in Human Spinal Cord Injury: A Pilot Clinical Study. *Http://Dx.Doi.Org/10.1080/10790268.2006.11753874*, *29*(3), 191–203. https://doi.org/10.1080/10790268.2006.11753874

237. Lin, H. C., He, Z., Ebert, S., Schörnig, M., Santel, M., Nikolova, M. T., … Treutlein, B. (2021). NGN2 induces diverse neuron types from human pluripotency. *Stem Cell Reports*, *16*(9), 2118–2127. https://doi.org/10.1016/j.stemcr.2021.07.006

238. Lin, X. Y., Lai, B. Q., Zeng, X., Che, M. T., Ling, E. A., Wu, W., & Zeng, Y. S. (2016). Cell Transplantation and Neuroengineering Approach for Spinal Cord Injury Treatment: A Summary of Current Laboratory Findings and Review of Literature. *Cell Transplantation*, *25*(8), 1425–1438. https://doi.org/10.3727/096368916X690836

239. Lineage Cell Therapeutics. (2021, July 14). Dose Escalation Study of AST-OPC1 in Spinal Cord Injury. Retrieved May 26, 2022, from https://clinicaltrials.gov/ct2/show/NCT02302157

240. Lippmann, E. S., E.williams, C., Ruhl, D. A., Estevez-Silva, M. C., Chapman, E. R., Coon, J. J., & Ashton, R. S. (2015). Deterministic HOX patterning in human pluripotent stem

cell-derived neuroectoderm. *Stem Cell Reports*, *4*(4), 632–644. https://doi.org/10.1016/j.stemcr.2015.02.018

241. Liu, S., & Chen, Z. (2019). Employing Endogenous NSCs to Promote Recovery of Spinal Cord Injury. *Stem Cells International*, *2019*, 1–10. https://doi.org/10.1155/2019/1958631

242. Liu, X. Z., Xu, X. M., Hu, R., Du, C., Zhang, S. X., McDonald, J. W., … Choi, D. W. (1997). Neuronal and Glial Apoptosis after Traumatic Spinal Cord Injury. *The Journal of Neuroscience*, *17*(14), 5395. https://doi.org/10.1523/JNEUROSCI.17-14-05395.1997

243. Lledo, P. M., & Saghatelyan, A. (2005). Integrating new neurons into the adult olfactory bulb: joining the network, life-death decisions, and the effects of sensory experience. *Trends in Neurosciences*, *28*(5), 248–254. https://doi.org/10.1016/J.TINS.2005.03.005

244. Llorens-Bobadilla, E., Chell, J. M., Le Merre, P., Wu, Y., Zamboni, M., Bergenstråhle, J., … Frisén, J. (2020). A latent lineage potential in resident neural stem cells enables spinal cord repair. *Science*, *370*(6512). https://doi.org/10.1126/science.abb8795

245. Lo, B., & Parham, L. (2009, May). Ethical issues in stem cell research. *Endocrine Reviews*. The Endocrine Society. https://doi.org/10.1210/er.2008-0031

246. Lo Sardo, V., Ferguson, W., Erikson, G. A., Topol, E. J., Baldwin, K. K., & Torkamani, A. (2017a). Influence of donor age on induced pluripotent stem cells. *Nature Biotechnology*, *35*(1), 69–74. https://doi.org/10.1038/nbt.3749

247. Lo Sardo, V., Ferguson, W., Erikson, G. A., Topol, E. J., Baldwin, K. K., & Torkamani, A. (2017b). The effect of aging on human induced pluripotent stem cells Valentina. *Nature Biotechnology*, *35*(1), 69–74. https://doi.org/10.1038/nbt.3749

248. Lois, C., García-Verdugo, J. M., & Alvarez-Buylla, A. (1996). Chain migration of neuronal precursors. *Science (New York, N.Y.)*, *271*(5251), 978–981.

https://doi.org/10.1126/SCIENCE.271.5251.978

249. Long, J., Federico, P., & Perez, M. A. (2017). A novel cortical target to enhance hand motor output in humans with spinal cord injury. *Brain : A Journal of Neurology*, *140*(6), 1619–1632. https://doi.org/10.1093/BRAIN/AWX102

250. Louis, D. N., Ohgaki, H., Wiestler, O. D., Cavenee, W. K., Burger, P. C., Jouvet, A., … Kleihues, P. (2007, August). The 2007 WHO classification of tumours of the central nervous system. *Acta Neuropathologica*. Springer. https://doi.org/10.1007/s00401-007-0243-4

251. Lu, P., Wang, Y., Graham, L., Mchale, K., Gao, M., Wu, D., … Tuszynski, M. H. (2013). Long-Distance Growth and Connectivity of Neural Stem Cells After Severe Spinal Cord Injury. *Cell*, *150*(6), 1264–1273. https://doi.org/10.1016/j.cell.2012.08.020.Long-Distance

252. Lu, P., Wang, Y., Graham, L., McHale, K., Gao, M., Wu, D., … Tuszynski, M. H. (2012). Long-distance growth and connectivity of neural stem cells after severe spinal cord injury. *Cell*, *150*(6), 1264–1273. https://doi.org/10.1016/j.cell.2012.08.020

253. Luskin, M. B. (1993). Restricted proliferation and migration of postnatally generated neurons derived from the forebrain subventricular zone. *Neuron*, *11*(1), 173–189. https://doi.org/10.1016/0896-6273(93)90281-U

254. Ma, Y., Deng, M., & Liu, M. (2019). Effect of Differently Polarized Macrophages on Proliferation and Differentiation of Ependymal Cells from Adult Spinal Cord. *Journal of Neurotrauma*, *36*(15), 2337–2347. https://doi.org/10.1089/neu.2018.6133

255. Mackay-Sim, A., Féron, F., Cochrane, J., Bassingthwaighte, L., Bayliss, C., Davies, W., … Geraghty, T. (2008). Autologous olfactory ensheathing cell transplantation in human paraplegia: A 3-year clinical trial. *Brain*, *131*(9), 2376–2386. https://doi.org/10.1093/brain/awn173

256. Manley, N. C., Priest, C. A., Denham, J., Wirth, E. D., & Lebkowski, J. S. (2017). Human Embryonic Stem Cell-Derived Oligodendrocyte Progenitor Cells: Preclinical Efficacy and Safety in Cervical Spinal Cord Injury. *Stem Cells Translational Medicine*, *6*(10), 1917–1929. https://doi.org/10.1002/sctm.17-0065

257. Marcuzzo, S., Isaia, D., Bonanno, S., Malacarne, C., Cavalcante, P., Zacheo, A., … Bernasconi, P. (2019). FM19G11-Loaded Gold Nanoparticles Enhance the Proliferation and Self-Renewal of Ependymal Stem Progenitor Cells Derived from ALS Mice. *Cells*, *8*(3), 279. https://doi.org/10.3390/cells8030279

258. Marichal, N., García, G., Radmilovich, M., Trujillo-Cenóz, O., & Russo, R. E. (2012). Spatial domains of progenitor-like cells and functional complexity of a stem cell niche in the neonatal rat spinal cord. *Stem Cells*, *30*(9), 2020–2031. https://doi.org/10.1002/stem.1175

259. Martello, G., & Smith, A. (2014). The Nature of Embryonic Stem Cells. *Http://Dx.Doi.Org/10.1146/Annurev-Cellbio-100913-013116*, *30*(1), 647–675. https://doi.org/10.1146/ANNUREV-CELLBIO-100913-013116

260. Martínez-Cerdeño, V., & Noctor, S. C. (2018, December 6). Neural progenitor cell terminology. *Frontiers in Neuroanatomy*. Frontiers Media S.A. https://doi.org/10.3389/fnana.2018.00104

261. Matuzelski, E., Bunt, J., Harkins, D., Lim, J. W. C., Gronostajski, R. M., Richards, L. J., … Piper, M. (2017). Transcriptional regulation of Nfix by NFIB drives astrocytic maturation within the developing spinal cord. *Developmental Biology*, *432*(2), 286–297. https://doi.org/10.1016/j.ydbio.2017.10.019

262. McAdoo, D. J., Hughes, M. G., Nie, L., Shah, B., Clifton, C., Fullwood, S., & Hulsebosch, C. E. (2005). The effect of glutamate receptor blockers on glutamate release

following spinal cord injury. Lack of evidence for an ongoing feedback cascade of damage → glutamate release → damage → glutamate release → etc. *Brain Research*, *1038*(1), 92–99. https://doi.org/10.1016/j.brainres.2005.01.024

263. McCaughey, E. J., Purcell, M., Mclean, A. N., Fraser, M. H., Bewick, A., Borotkanics, R. J., & Allan, D. B. (2016). Changing demographics of spinal cord injury over a 20-year period: A longitudinal population-based study in Scotland. *Spinal Cord*, *54*(4), 270–276. https://doi.org/10.1038/sc.2015.167

264. McDonough, A., & Martínez-Cerdeño, V. (2012). Endogenous proliferation after spinal cord injury in animal models. *Stem Cells International*, *2012*. https://doi.org/10.1155/2012/387513

265. McKerracher, L., & Guertin, P. (2013). Rho as a target to promote repair: translation to clinical studies with cethrin. *Current Pharmaceutical Design*, *19*(24), 4400–4410. https://doi.org/10.2174/1381612811319240007

266. Meletis, K., Barnabé-Heider, F., Carlén, M., Evergren, E., Tomilin, N., Shupliakov, O., & Frisén, J. (2008). Spinal cord injury reveals multilineage differentiation of ependymal cells. *PLoS Biology*, *6*(7), 1494–1507. https://doi.org/10.1371/journal.pbio.0060182

267. Mertens, J., Paquola, A. C. M., Ku, M., Hatch, E., Böhnke, L., Ladjevardi, S., … Gage, F. H. (2015). Directly Reprogrammed Human Neurons Retain Aging-Associated Transcriptomic Signatures and Reveal Age-Related Nucleocytoplasmic Defects. *Cell Stem Cell*, *17*(6), 705–718. https://doi.org/10.1016/j.stem.2015.09.001

268. Mertens, J., Reid, D., Lau, S., Kim, Y., & Gage, F. H. (2018). Aging in a dish: IPSC-derived and directly induced neurons for studying brain aging and age-related neurodegenerative diseases. *Annual Review of Genetics*. https://doi.org/10.1146/annurev-

genet-120417-031534

269. Metz, G. A. S., Curt, A., Van De Meent, H., Klusman, I., Schwab, M. E., & Dietz, V. (2000). Validation of the weight-drop contusion model in rats: A comparative study of human spinal cord injury. *Journal of Neurotrauma*, *17*(1), 1–17. https://doi.org/10.1089/neu.2000.17.1

270. Metzis, V., Steinhauser, S., Pakanavicius, E., Gouti, M., Stamataki, D., Ivanovitch, K., … Briscoe, J. (2018). Nervous System Regionalization Entails Axial Allocation before Neural Differentiation. *Cell*, *175*(4), 1105-1118.e17. https://doi.org/10.1016/j.cell.2018.09.040

271. Min-Te Choo, A., Liu, J., Liu, Z., Dvorak, M., Tetzlaff, W., & Oxland, T. R. (2009). Modeling spinal cord contusion, dislocation, and distraction: Characterization of vertebral clamps, injury severities, and node of Ranvier deformations. *Journal of Neuroscience Methods*, *181*, 6–17. https://doi.org/10.1016/j.jneumeth.2009.04.007

272. Mokalled, M. H., Patra, C., Dickson, A. L., Endo, T., Stainier, D. Y. R., & Poss, K. D. (2016). Injury-induced ctgfa directs glial bridging and spinal cord regeneration in zebrafish. *Science (New York, N.Y.)*, *354*(6312), 630. https://doi.org/10.1126/SCIENCE.AAF2679

273. Monje, M. L., Mizumatsu, S., Fike, J. R., & Palmer, T. D. (2002). Irradiation induces neural precursor-cell dysfunction. *Nature Medicine*, *8*(9), 955–962. https://doi.org/10.1038/nm749

274. Moore, S. A. (2016). The Spinal Ependymal Layer in Health and Disease. *Veterinary Pathology*, *53*(4), 746–753. https://doi.org/10.1177/0300985815618438

275. Morales, A. V., & Mira, H. (2019). Adult neural stem cells: Born to last. *Frontiers in Cell and Developmental Biology*. Frontiers Media S.A. https://doi.org/10.3389/fcell.2019.00096

276. Morante-Redolat, J. M., & Porlan, E. (2019). Neural stem cell regulation by adhesion

molecules within the subependymal niche. *Frontiers in Cell and Developmental Biology*. Frontiers Media S.A. https://doi.org/10.3389/fcell.2019.00102

277. Moreno-Manzano, V. (2020a, February 1). Ependymal cells in the spinal cord as neuronal progenitors. *Current Opinion in Pharmacology*. Elsevier Ltd. https://doi.org/10.1016/j.coph.2019.11.008

278. Moreno-Manzano, V. (2020b, February 1). Ependymal cells in the spinal cord as neuronal progenitors. *Current Opinion in Pharmacology*. Elsevier Ltd. https://doi.org/10.1016/j.coph.2019.11.008

279. Moreno-Manzano, V., Rodriguez-Jimenez, F. J., Garcia-Rosello, M., Lainez, S., Erceg, S., Calvo, M. T., … Stojkovic, M. (2009). Activated spinal cord ependymal stem cells rescue neurological function. *Stem Cells*, *27*(3), 733–743. https://doi.org/10.1002/stem.24

280. Morizur, L., Chicheportiche, A., Gauthier, L. R., Daynac, M., Boussin, F. D., & Mouthon, M. A. (2018). Distinct Molecular Signatures of Quiescent and Activated Adult Neural Stem Cells Reveal Specific Interactions with Their Microenvironment. *Stem Cell Reports*, *11*(2), 565–577. https://doi.org/10.1016/j.stemcr.2018.06.005

281. Mortazavi, M. M., Jaber, M., Adeeb, N., Deep, A., Hose, N., Rezaei, M., … Tubbs, R. S. (2015). Engraftment of neural stem cells in the treatment of spinal cord injury. *Translational Research in Anatomy*, *1*, 11–16. https://doi.org/10.1016/j.tria.2015.10.002

282. Mothe, A. J., & Tator, C. H. (2008). Transplanted neural stem/progenitor cells generate myelinating oligodendrocytes and Schwann cells in spinal cord demyelination and dysmyelination. *Experimental Neurology*, *213*(1), 176–190. https://doi.org/10.1016/j.expneurol.2008.05.024

283. Mothe, A. J., Zahir, T., Santaguida, C., Cook, D., & Tator, C. H. (2011). Neural

stem/progenitor cells from the adult human spinal cord are multipotent and self-renewing and differentiate after transplantation. *PLoS ONE*, *6*(11). https://doi.org/10.1371/journal.pone.0027079

284. Mothe, A., & Tator, C. H. (2015). Isolation of Neural Stem/Progenitor Cells from the Periventricular Region of the Adult Rat and Human Spinal Cord. *Journal of Visualized Experiments*, (99), 1–8. https://doi.org/10.3791/52732

285. Musk, E. (2019). An integrated brain-machine interface platform with thousands of channels. *Journal of Medical Internet Research*, *21*(10), e16194. https://doi.org/10.2196/16194

286. Nagoshi, N., Khazaei, M., Ahlfors, J. E., Ahuja, C. S., Nori, S., Wang, J., … Fehlings, M. G. (2018). Human Spinal Oligodendrogenic Neural Progenitor Cells Promote Functional Recovery After Spinal Cord Injury by Axonal Remyelination and Tissue Sparing. *Stem Cells Translational Medicine*, *7*(11), 806–818. https://doi.org/10.1002/sctm.17-0269

287. Nagoshi, N., Tsuji, O., Nakamura, M., & Okano, H. (2019). Cell therapy for spinal cord injury using induced pluripotent stem cells. *Regenerative Therapy*. https://doi.org/10.1016/j.reth.2019.05.006

288. Nakamura, M., & Okano, H. (2013). Cell transplantation therapies for spinal cord injury focusing on induced pluripotent stem cells. *Cell Research*, *23*(1), 70–80. https://doi.org/10.1038/cr.2012.171

289. Namiki, J., & Tator, C. H. (1999). Cell proliferation and nestin expression in the ependyma of the adult rat spinal cord after injury. *Journal of Neuropathology and Experimental Neurology*, *58*(5), 489–498. https://doi.org/10.1097/00005072-199905000-00008

290. Narayanan, G., Yu, Y. H., Tham, M., Gan, H. T., Ramasamy, S., Sankaran, S., … Ahmed, S. (2016). Enumeration of Neural Stem Cells Using Clonal Assays. *Journal of Visualized Experiments*, (116), 1–8. https://doi.org/10.3791/54456

291. Narbonne, P. (2018). The effect of age on stem cell function and utility for therapy. *Cell Medicine*, *10*, 215517901877375. https://doi.org/10.1177/2155179018773756

292. Nas, K., Yazmalar, L., Şah, V., Aydin, A., & Öneş, K. (2015). Rehabilitation of spinal cord injuries. *World Journal of Orthopedics*, *6*(1), 8–16. https://doi.org/10.5312/wjo.v6.i1.8

293. Navarrete-Opazo, A., Alcayaga, J., Sepúlveda, O., Rojas, E., & Astudillo, C. (2017). Repetitive Intermittent Hypoxia and Locomotor Training Enhances Walking Function in Incomplete Spinal Cord Injury Subjects: A Randomized, Triple-Blind, Placebo-Controlled Clinical Trial. *Journal of Neurotrauma*, *34*(9), 1803–1812. https://doi.org/10.1089/NEU.2016.4478

294. Neirinckx, V., Coste, C., Franzen, R., Gothot, A., Rogister, B., & Wislet, S. (2014, August 28). Neutrophil contribution to spinal cord injury and repair. *Journal of Neuroinflammation*. BioMed Central Ltd. https://doi.org/10.1186/s12974-014-0150-2

295. Netoff, T., Darrow, D., Phillips, A. A., Parr, A. M., Balser, D. Y., Samadani, U., & Krassioukov, A. V. (2019). Epidural Spinal Cord Stimulation facilitates immediate restoration of dormant motor and autonomic supraspinal pathways after chronic neurologically complete spinal cord injury. *Journal of Neurotrauma*, *36*, 1–12. https://doi.org/10.1089/neu.2018.6006

296. Norenberg, M. D., Smith, J., & Marcillo, A. (2004). The pathology of human spinal cord injury: defining the problems. *J.Neurotrauma*, *21*(0897-7151 (Print)), 429–440.

297. Nout, Y. S., Rosenzweig, E. S., Brock, J. H., Strand, S. C., Moseanko, R., Hawbecker, S.,

… Tuszynski, M. H. (2012). Animal Models of Neurologic Disorders: A Nonhuman Primate Model of Spinal Cord Injury. *Neurotherapeutics*. https://doi.org/10.1007/s13311-012-0114-0

298. O 'shea, T. M., Burda, J. E., & Sofroniew, M. V. (2017). Cell biology of spinal cord injury and repair. *J Clin Invest*, *127*(9), 3259–3270. https://doi.org/10.1172/JCI90608

299. Oberheim, N. A., Goldman, S. A., & Nedergaard, M. (2012). Heterogeneity of astrocytic form and function. *Methods in Molecular Biology*, *814*, 23–45. https://doi.org/10.1007/978-1-61779-452-0_3

300. Obernier, K., & Alvarez-Buylla, A. (2019, February 1). Neural stem cells: Origin, heterogeneity and regulation in the adult mammalian brain. *Development (Cambridge)*. Company of Biologists Ltd. https://doi.org/10.1242/dev.156059

301. Ogai, K., Nakatani, K., Hisano, S., Sugitani, K., Koriyama, Y., & Kato, S. (2014). Function of Sox2 in ependymal cells of lesioned spinal cords in adult zebrafish. *Neuroscience Research*, *88*, 84–87. https://doi.org/10.1016/J.NEURES.2014.07.010

302. Ohori, Y., Yamamoto, S. -i., Nagao, M., Sugimori, M., Yamamoto, N., Nakamura, K., & Nakafuku, M. (2006). Growth Factor Treatment and Genetic Manipulation Stimulate Neurogenesis and Oligodendrogenesis by Endogenous Neural Progenitors in the Injured Adult Spinal Cord. *Journal of Neuroscience*, *26*(46), 11948–11960. https://doi.org/10.1523/JNEUROSCI.3127-06.2006

303. Okada, S., Nakamura, M., Mikami, Y., Shimazaki, T., Mihara, M., Ohsugi, Y., … Okano, H. (2004). Blockade of Interleukin-6 Receptor Suppresses Reactive Astrogliosis and Ameliorates Functional Recovery in Experimental Spinal Cord Injury. *Journal of Neuroscience Research*, *76*(2), 265–276. https://doi.org/10.1002/jnr.20044

304. Okada, Seiji, Hara, M., Kobayakawa, K., Matsumoto, Y., & Nakashima, Y. (2018).

Astrocyte reactivity and astrogliosis after spinal cord injury. *Neuroscience Research*, *126*, 39–43. https://doi.org/10.1016/j.neures.2017.10.004

305. Olivera-Martinez, I., Harada, H., Halley, P. A., & Storey, K. G. (2012). Loss of FGF-dependent mesoderm identity and rise of endogenous retinoid signalling determine cessation of body axis elongation. *PLoS Biology*, *10*(10). https://doi.org/10.1371/JOURNAL.PBIO.1001415

306. Olmsted, Z. T., Stigliano, C., Scimemi, A., Marzullo, B., Wolfe, T., Cibelli, J., … Paluh, J. L. (2020). Neuromesodermal progenitors advance network formation of spinal neurons and support cells in neural ribbons in vitro and unprotected survival in a rat subacute contusion model. *BioRxiv*. https://doi.org/10.1101/2020.11.10.374876

307. Oyinbo, C. A. (2011). Secondary injury mechanisms in traumatic spinal cord injury a nugget. *Acta Neurobiologiae Experimentalis*, *71*(2), 281–299.

308. Pagin, M., Pernebrink, M., Giubbolini, S., Barone, C., Sambruni, G., Zhu, Y., … Nicolis, S. K. (2021). Sox2 Controls Neural Stem Cell Self-Renewal Through a Fos-Centered Gene Regulatory Network. *Stem Cells*, *39*(8), 1107–1119. https://doi.org/10.1002/STEM.3373

309. Panayiotou, E., & Malas, S. (2013). Adult spinal cord ependymal layer: a promising pool of quiescent stem cells to treat spinal cord injury. *Frontiers in Physiology*, *4*(November), 3–5. https://doi.org/10.3389/fphys.2013.00340

310. Pandya, J. D., Nukala, V. N., & Sullivan, P. G. (2013). Concentration dependent effect of calcium on brain mitochondrial bioenergetics and oxidative stress parameters. *Frontiers in Neuroenergetics*, *5*(DEC). https://doi.org/10.3389/fnene.2013.00010

311. Paniagua-Torija, B., Arevalo-Martin, A., Ferrer, I., Molina-Holgado, E., & Garcia-Ovejero, D. (2015). CB1 cannabinoid receptor enrichment in the ependymal region of the

adult human spinal cord. *Scientific Reports*, *5*, 17745. https://doi.org/10.1038/srep17745

312. Paniagua-Torija, B., Norenberg, M., Arevalo-Martin, A., Carballosa-Gautam, M. M., Campos-Martin, Y., Molina-Holgado, E., & Garcia-Ovejero, D. (2018). Cells in the adult human spinal cord ependymal region do not proliferate after injury. *Journal of Pathology*, *246*(4), 415–421. https://doi.org/10.1002/path.5151

313. Panter, S. S., Yum, S. W., & Faden, A. I. (1990). Alteration in extracellular amino acids after traumatic spinal cord injury. *Annals of Neurology*, *27*(1), 96–99. https://doi.org/10.1002/ANA.410270115

314. Paoletti, P., Bellone, C., & Zhou, Q. (2013). NMDA receptor subunit diversity: Impact on receptor properties, synaptic plasticity and disease. *Nature Reviews Neuroscience*. https://doi.org/10.1038/nrn3504

315. Paton, J. A., & Nottebohm, F. N. (1984). Neurons generated in the adult brain are recruited into functional circuits. *Science*, *225*(4666), 1046–1048. https://doi.org/10.1126/science.6474166

316. Pendleton, J. C., Shamblott, M. J., Gary, D. S., Belegu, V., Hurtado, A., Malone, M. L., & McDonald, J. W. (2013). Chondroitin sulfate proteoglycans inhibit oligodendrocyte myelination through PTPσ. *Experimental Neurology*, *247*, 113–121. https://doi.org/10.1016/J.EXPNEUROL.2013.04.003

317. Perry, V. H., & Teeling, J. (2013). Microglia and macrophages of the central nervous system: the contribution of microglia priming and systemic inflammation to chronic neurodegeneration. *Seminars in Immunopathology*, *35*(5), 601. https://doi.org/10.1007/S00281-013-0382-8

318. Petrosyan, H. A., Hunanyan, A. S., Alessi, V., Schnell, L., Levine, J., & Arvanian, V. L.

(2013). Neutralization of Inhibitory Molecule NG2 Improves Synaptic Transmission, Retrograde Transport, and Locomotor Function after Spinal Cord Injury in Adult Rats. *Journal of Neuroscience*, *33*(9), 4032–4043. https://doi.org/10.1523/JNEUROSCI.4702-12.2013

319. Pfeffer, D. B., Donner, D., Guo, J. D., Dunbar, H., & Yang, L. M. (1998). the Type 1 TNF Receptor Induction of Jak/STAT Signaling by Activation of.

320. Pfenninger, C. V., Steinhoff, C., Hertwig, F., & Nuber, U. A. (2011). Prospectively isolated CD133/CD24-positive ependymal cells from the adult spinal cord and lateral ventricle wall differ in their long-term in vitro self-renewal and in vivo gene expression. *Glia*, *59*(1), 68–81. https://doi.org/10.1002/glia.21077

321. Philippidou, P., & Dasen, J. S. (2013, October 2). Hox Genes: Choreographers in Neural Development, Architects of Circuit Organization. *Neuron*. https://doi.org/10.1016/j.neuron.2013.09.020

322. Piltti, K. M., Funes, G. M., Avakian, S. N., Salibian, A. A., Huang, K. I., Carta, K., … Anderson, A. J. (2017). Increasing Human Neural Stem Cell Transplantation Dose Alters Oligodendroglial and Neuronal Differentiation after Spinal Cord Injury. *Stem Cell Reports*, *8*(6), 1534–1548. https://doi.org/10.1016/j.stemcr.2017.04.009

323. Pineau, I., & Lacroix, S. (2007). Proinflammatory cytokine synthesis in the injured mouse spinal cord: Multiphasic expression pattern and identification of the cell types involved. *Journal of Comparative Neurology*, *500*(2), 267–285. https://doi.org/10.1002/CNE.21149

324. Pineau, I., Sun, L., Bastien, D., & Lacroix, S. (2010). Astrocytes initiate inflammation in the injured mouse spinal cord by promoting the entry of neutrophils and inflammatory

monocytes in an IL-1 receptor/MyD88-dependent fashion. *Brain, Behavior, and Immunity*, *24*(4), 540–553. https://doi.org/10.1016/J.BBI.2009.11.007

325. Plemel, J. R., Chojnacki, A., Sparling, J. S., Liu, J., Plunet, W., Duncan, G. J., … Tetzlaff, W. (2011). Platelet-derived growth factor-responsive neural precursors give rise to myelinating oligodendrocytes after transplantation into the spinal cords of contused rats and dysmyelinated mice. *Glia*, *59*(12), 1891–1910. https://doi.org/10.1002/glia.21232

326. Poiana, G., Gioia, R., Sineri, S., Cardarelli, S., Lupo, G., & Cacci, E. (2020). Transcriptional regulation of adult neural stem/ progenitor cells: Tales from the subventricular zone. *Neural Regeneration Research*. https://doi.org/10.4103/1673-5374.280301

327. Quinn, S. M., Walters, W. M., Vescovi, A. L., & Whittemore, S. R. (1999). Lineage restriction of neuroepithelial precursor cells from fetal human spinal cord. *Journal of Neuroscience Research*, *57*(5), 590–602. https://doi.org/10.1002/(SICI)1097-4547(19990901)57:5<590::AID-JNR2>3.0.CO;2-X

328. Raivich, G., Bohatschek, M., Da Costa, C., Iwata, O., Galiano, M., Hristova, M., … Behrens, A. (2004). The AP-1 transcription factor c-Jun is required for efficient axonal regeneration. *Neuron*, *43*(1), 57–67. https://doi.org/10.1016/J.NEURON.2004.06.005/ATTACHMENT/9AA5A705-4AB4-4D00-AA3C-1CB05E9B7CDD/MMC3.JPG

329. Ramakonar, H., & Fehlings, M. G. (2021, July 3). 'Time is Spine': new evidence supports decompression within 24 h for acute spinal cord injury. *Spinal Cord*. Nature Publishing Group. https://doi.org/10.1038/s41393-021-00654-0

330. Ramer, L. M., Ramer, M. S., & Bradbury, E. J. (2014). Restoring function after spinal

cord injury: Towards clinical translation of experimental strategies. *The Lancet Neurology*, *13*(12), 1241–1256. https://doi.org/10.1016/S1474-4422(14)70144-9

331. Reimer, M. M., Sörensen, I., Kuscha, V., Frank, R. E., Liu, C., Becker, C. G., & Becker, T. (2008). Motor neuron regeneration in adult zebrafish. *The Journal of Neuroscience : The Official Journal of the Society for Neuroscience*, *28*(34), 8510–8516. https://doi.org/10.1523/JNEUROSCI.1189-08.2008

332. Ren, Y., Ao, Y., O'Shea, T. M., Burda, J. E., Bernstein, A. M., Brumm, A. J., … Sofroniew, M. V. (2017). Ependymal cell contribution to scar formation after spinal cord injury is minimal, local and dependent on direct ependymal injury. *Scientific Reports*, *7*(January), 1–16. https://doi.org/10.1038/srep41122

333. Reynolds, B. A., & Rietze, R. L. (2005). Neural stem cells and neurospheres - Re-evaluating the relationship. *Nature Methods*, *2*(5), 333–336. https://doi.org/10.1038/nmeth758

334. Rhscir, & Rhscir. (2009). Rick Hansen Spinal Cord Injury Registry, facts and Statistics.

335. Ribeiro, A., Monteiro, J. F., Certal, A. C., Cristovão, A. M., & Saúde, L. (2017). Foxj1a is expressed in ependymal precursors, controls central canal position and is activated in new ependymal cells during regeneration in zebrafish. *Open Biology*, *7*(11). https://doi.org/10.1098/RSOB.170139

336. Richards, L. J., Kilpatrick, T. J., & Bartlett, P. F. (1992). De novo generation of neuronal cells from the adult mouse brain (neuronal precursors/fibroblast growth factor/neurofllament/differentiation). *Neurobiology*, *89*, 8591–8595.

337. Rivlin, A. S., & Tator, C. H. (1978). Regional spinal cord blood flow in rats after severe cord trauma. *Journal of Neurosurgery*, *49*(6), 844–853.

https://doi.org/10.3171/JNS.1978.49.6.0844

338. Rogulja-Ortmann, A., & Technau, G. M. (2008). Multiple roles for Hox genes in segment-specific shaping of CNS lineages. *Fly*, *2*(6), 316–319. https://doi.org/10.4161/fly.7464

339. Rosenberg, A. B., Roco, C. M., Muscat, R. A., Kuchina, A., Sample, P., Yao, Z., … Seelig, G. (2018). Single-cell profiling of the developing mouse brain and spinal cord with split-pool barcoding. *Science*, *360*(6385), 176–182. https://doi.org/10.1126/science.aam8999

340. Rosenzweig, E. S., Brock, J. H., Lu, P., Kumamaru, H., Salegio, E. A., Kadoya, K., … Tuszynski, M. H. (2018). Restorative effects of human neural stem cell grafts on the primate spinal cord. *Nature Medicine*, *24*(4), 484–490. https://doi.org/10.1038/nm.4502

341. Russ, D. E., Cross, R. B. P., Li, L., Koch, S. C., Matson, K. J. E., Yadav, A., … Levine, A. J. (2021). A harmonized atlas of mouse spinal cord cell types and their spatial organization. *Nature Communications*, *12*(1). https://doi.org/10.1038/s41467-021-25125-1

342. Sabelström, H., Stenudd, M., & Frisén, J. (2014). Neural stem cells in the adult spinal cord. *Experimental Neurology*, *260*, 44–49. https://doi.org/10.1016/j.expneurol.2013.01.026

343. Sabelström, H., Stenudd, M., Réu, P., Dias, D. O., Elfineh, M., Zdunek, S., … Frisén, J. (2013). Resident neural stem cells restrict tissue damage and neuronal loss after spinal cord injury in mice. *Science*, *342*(6158), 637–640. https://doi.org/10.1126/science.1242576

344. Sabourin, J. C., Ackema, K. B., Ohayon, D., Guichet, P. O., Perrin, F. E., Garces, A., … Hugnot, J. P. (2009a). A mesenchymal-like ZEB1+ niche harbors dorsal radial glial fibrillary acidic protein-positive stem cells in the spinal cord. *Stem Cells*, *27*(11), 2722–2733. https://doi.org/10.1002/stem.226

345. Sabourin, J. C., Ackema, K. B., Ohayon, D., Guichet, P. O., Perrin, F. E., Garces, A., …

Hugnot, J. P. (2009b). A mesenchymal-like ZEB1+ niche harbors dorsal radial glial fibrillary acidic protein-positive stem cells in the spinal cord. *Stem Cells*, *27*(11), 2722–2733. https://doi.org/10.1002/stem.226

346. Sambasivan, R., & Steventon, B. (2021, January 15). Neuromesodermal Progenitors: A Basis for Robust Axial Patterning in Development and Evolution. *Frontiers in Cell and Developmental Biology*. Frontiers. https://doi.org/10.3389/fcell.2020.607516

347. Schomberg, D. T., Miranpuri, G. S., Chopra, A., Patel, K., Meudt, J. J., Tellez, A., … Shanmuganayagam, D. (2017). Translational relevance of swine models of spinal cord injury. *Journal of Neurotrauma*. https://doi.org/10.1089/neu.2016.4567

348. Sefton, E., Iwasa, S. N., Morrison, T., Naguib, H. E., Popovic, M. R., & Morshead, C. M. (2020). Electric field application in vivo regulates neural precursor cell behavior in the adult mammalian forebrain. *ENeuro*, *7*(4), 1–12. https://doi.org/10.1523/ENEURO.0273-20.2020

349. Seijffers, R., Allchorne, A. J., & Woolf, C. J. (2006). The transcription factor ATF-3 promotes neurite outgrowth. *Molecular and Cellular Neuroscience*, *32*(1–2), 143–154. https://doi.org/10.1016/J.MCN.2006.03.005

350. Seo, B. J., Hong, Y. J., & Do, J. T. (2017). Cellular reprogramming using protein and cell-penetrating peptides. *International Journal of Molecular Sciences*. https://doi.org/10.3390/ijms18030552

351. Sevc, J., Matiasova, A., Kutna, V., & Daxnerova, Z. (2014). Evidence that the central canal lining of the spinal cord contributes to oligodendrogenesis during postnatal development and adulthood in intact rats. *Journal of Comparative Neurology*, *522*(14), 3194–3207. https://doi.org/10.1002/cne.23590

352. Shahbazi, E., Mirakhori, F., Ezzatizadeh, V., & Baharvand, H. (2018). Reprogramming

of somatic cells to induced neural stem cells. *Methods*. Elsevier Inc. https://doi.org/10.1016/j.ymeth.2017.09.007

353. Sheng, S. R., Wang, X. Y., Xu, H. Z., Zhu, G. Q., & Zhou, Y. F. (2010, January). Anatomy of large animal spines and its comparison to the human spine: A systematic review. *European Spine Journal*. Springer. https://doi.org/10.1007/s00586-009-1192-5

354. Shihabuddin, L. S., Horner, P. J., Ray, J., & Gage, F. H. (2000a). Adult spinal cord stem cells generate neurons after transplantation in the adult dentate gyrus. *The Journal of Neuroscience : The Official Journal of the Society for Neuroscience*, *20*(23), 8727–8735. https://doi.org/20/23/8727 [pii]

355. Shihabuddin, L. S., Horner, P. J., Ray, J., & Gage, F. H. (2000b). Adult Spinal Cord Stem Cells Generate Neurons after Transplantation in the Adult Dentate Gyrus. *The Journal of Neuroscience*, *20*(23), 8727. https://doi.org/10.1523/JNEUROSCI.20-23-08727.2000

356. Shimojo, D., Onodera, K., Doi-Torii, Y., Ishihara, Y., Hattori, C., Miwa, Y., … Okada, Y. (2015). Rapid, efficient, and simple motor neuron differentiation from human pluripotent stem cells. *Molecular Brain*, *8*(1). https://doi.org/10.1186/s13041-015-0172-4

357. Shin, J. C., Kim, K. N., Yoo, J., Kim, I.-S., Yun, S., Lee, H., … Park, K. I. (2015). Clinical Trial of Human Fetal Brain-Derived Neural Stem/Progenitor Cell Transplantation in Patients with Traumatic Cervical Spinal Cord Injury. *Neural Plasticity*, *2015*, 1–22. https://doi.org/10.1155/2015/630932

358. Shu, M., Xue, X., Nie, H., Wu, X., Sun, M., Qiao, L., … Dai, J. (2021). Single-cell RNA sequencing reveals Nestin+ active neural stem cells outside the central canal after spinal cord injury. *Science China Life Sciences*, *65*(2), 295–308. https://doi.org/10.1007/s11427-020-1930-0

359. Siddiqui, A. M., Khazaei, M., & Fehlings, M. G. (2015). Translating mechanisms of neuroprotection, regeneration, and repair to treatment of spinal cord injury. *Progress in Brain Research*, *218*. https://doi.org/10.1016/bs.pbr.2014.12.007

360. Silva, N. A., Sousa, N., Reis, R. L., & Salgado, A. J. (2014). From basics to clinical: A comprehensive review on spinal cord injury. *Progress in Neurobiology*, *114*, 25–57. https://doi.org/10.1016/j.pneurobio.2013.11.002

361. Silver, J., & Miller, J. H. (2004). Regeneration beyond the glial scar. *Nature Reviews Neuroscience*. Nature Publishing Group. https://doi.org/10.1038/nrn1326

362. Simpson, D. J., Olova, N. N., & Chandra, T. (2021, September 6). Cellular reprogramming and epigenetic rejuvenation. *Clinical Epigenetics*. BioMed Central. https://doi.org/10.1186/s13148-021-01158-7

363. Sipski, M. L., Jackson, A. B., Gómez-Marín, O., Estores, I., & Stein, A. (2004). Effects of gender on neurologic and functional recovery after spinal cord injury. *Archives of Physical Medicine and Rehabilitation*, *85*(11), 1826–1836. https://doi.org/10.1016/j.apmr.2004.04.031

364. Sîrbulescu, R. F., & Zupanc, G. K. H. (2010). Spinal cord repair in regeneration-competent vertebrates: Adult teleost fish as a model system. *Brain Research Reviews*, *67*(1–2), 73–93. https://doi.org/10.1016/j.brainresrev.2010.11.001

365. Soares, R., Ribeiro, F. F., Lourenço, D. M., Rodrigues, R. S., Moreira, J. B., Sebastião, A. M., … Xapelli, S. (2020). Isolation and expansion of neurospheres from postnatal (P1−3) mouse neurogenic niches. *Journal of Visualized Experiments*, *2020*(159), e60822. https://doi.org/10.3791/60822

366. Soares, R., Ribeiro, F., Lourenço, Di., Rodrigues, R., Moreira, J., Sebastião, A., … Xapelli, S. (2021, November 1). The neurosphere assay: An effective in vitro technique to

study neural stem cells. *Neural Regeneration Research*. Wolters Kluwer Medknow Publications. https://doi.org/10.4103/1673-5374.310678

367. Sofroniew, M. V. (2009). Molecular dissection of reactive astrogliosis and glial scar formation. *Trends in Neurosciences*. https://doi.org/10.1016/j.tins.2009.08.002

368. Sorrells, S. F., Paredes, M. F., Cebrian-Silla, A., Sandoval, K., Qi, D., Kelley, K. W., … Alvarez-Buylla, A. (2018a). Human hippocampal neurogenesis drops sharply in children to undetectable levels in adults. *Nature*, *555*(7696), 377–381. https://doi.org/10.1038/nature25975

369. Sorrells, S. F., Paredes, M. F., Cebrian-Silla, A., Sandoval, K., Qi, D., Kelley, K. W., … Alvarez-Buylla, A. (2018b). Human hippocampal neurogenesis drops sharply in children to undetectable levels in adults. *Nature*, *555*(7696), 377–381. https://doi.org/10.1038/nature25975

370. Spaethling, J. M., Na, Y. J., Lee, J., Ulyanova, A. V., Baltuch, G. H., Bell, T. J., … Eberwine, J. H. (2017). Primary Cell Culture of Live Neurosurgically Resected Aged Adult Human Brain Cells and Single Cell Transcriptomics. *Cell Reports*, *18*(3), 791–803. https://doi.org/10.1016/j.celrep.2016.12.066

371. Sroga, J. M., Jones, T. B., Kigerl, K. A., McGaughy, V. M., & Popovich, P. G. (2003). Rats and mice exhibit distinct inflammatory reactions after spinal cord injury. *Journal of Comparative Neurology*, *462*(2), 223–240. https://doi.org/10.1002/CNE.10736

372. Steinle, H., Weber, M., Behring, A., Mau-Holzmann, U., Schlensak, C., Wendel, H. P., & Avci-Adali, M. (2019). Generation of iPSCs by nonintegrative RNA-based reprogramming techniques: Benefits of Self-Replicating RNA versus Synthetic mRNA. *Stem Cells International*, *2019*. https://doi.org/10.1155/2019/7641767

373. Stenudd, M., Sabelström, H., Llorens-Bobadilla, E., Zamboni, M., Blom, H., Brismar, H., … Frisén, J. (2022). Identification of a discrete subpopulation of spinal cord ependymal cells with neural stem cell properties. *Cell Reports*, *38*(9). https://doi.org/10.1016/j.celrep.2022.110440

374. Stewart, A. N., MacLean, S. M., Stromberg, A. J., Whelan, J. P., Bailey, W. M., Gensel, J. C., & Wilson, M. E. (2020, August 5). Considerations for Studying Sex as a Biological Variable in Spinal Cord Injury. *Frontiers in Neurology*. Frontiers Media S.A. https://doi.org/10.3389/fneur.2020.597689

375. Stirling, D. P., Liu, S., Kubes, P., & Yong, V. W. (2009). Depletion of Ly6G/Gr-1 leukocytes after spinal cord injury in mice alters wound healing and worsens neurological outcome. *The Journal of Neuroscience : The Official Journal of the Society for Neuroscience*, *29*(3), 753–764. https://doi.org/10.1523/JNEUROSCI.4918-08.2009

376. Strano, A., Tuck, E., Stubbs, V. E., & Livesey, F. J. (2020a). Variable Outcomes in Neural Differentiation of Human PSCs Arise from Intrinsic Differences in Developmental Signaling Pathways. *Cell Reports*, *31*(10), 107732. https://doi.org/10.1016/j.celrep.2020.107732

377. Strano, A., Tuck, E., Stubbs, V. E., & Livesey, F. J. (2020b). Variable Outcomes in Neural Differentiation of Human PSCs Arise from Intrinsic Differences in Developmental Signaling Pathways. *Cell Reports*, *31*(10), 107732. https://doi.org/10.1016/j.celrep.2020.107732

378. Streijger, F., Lee, J. H. T., Manouchehri, N., Okon, E. B., Tigchelaar, S., Anderson, L. M., … Kwon, B. K. (2016). The Evaluation of Magnesium Chloride within a Polyethylene Glycol Formulation in a Porcine Model of Acute Spinal Cord Injury. *Journal of*

Neurotrauma, *33*(24), 2202–2216. https://doi.org/10.1089/neu.2016.4439

379. Streijger, F., Plunet, W. T., Lee, J. H. T., Liu, J., Lam, C. K., Park, S., … Tetzlaff, W. (2013). Ketogenic diet improves forelimb motor function after spinal cord injury in rodents. *PLoS ONE*, *8*(11), 78765. https://doi.org/10.1371/journal.pone.0078765

380. Stys, P. K., Waxman, S. G., & Ransom, B. R. (1992). Ionic mechanisms of anoxic injury in mammalian CNS white matter: Role of Na+ channels and Na+-Ca2+ exchanger. *Journal of Neuroscience*, *12*(2), 430–439. https://doi.org/10.1523/jneurosci.12-02-00430.1992

381. Su, Z., Niu, W., Liu, M. L., Zou, Y., & Zhang, C. L. (2014). In vivo conversion of astrocytes to neurons in the injured adult spinal cord. *Nature Communications*, *5*, 1–15. https://doi.org/10.1038/ncomms4338

382. Sugai, K., Sumida, M., Shofuda, T., Yamaguchi, R., Tamura, T., Kohzuki, T., … Okano, H. (2021). First-in-human clinical trial of transplantation of iPSC-derived NS/PCs in subacute complete spinal cord injury: Study protocol. *Regenerative Therapy*, *18*, 321–333. https://doi.org/10.1016/j.reth.2021.08.005

383. Sutherland, T. C., Mathews, K. J., Mao, Y., Nguyen, T., & Gorrie, C. A. (2017). Differences in the Cellular Response to Acute Spinal Cord Injury between Developing and Mature Rats Highlights the Potential Significance of the Inflammatory Response. *Frontiers in Cellular Neuroscience*, *10*(January), 1–18. https://doi.org/10.3389/fncel.2016.00310

384. Suzuki, H., Ahuja, C. S., Salewski, R. P., Li, L., Satkunendrarajah, K., Nagoshi, N., … Fehlings, M. G. (2017). Neural stem cell mediated recovery is enhanced by Chondroitinase ABC pretreatment in chronic cervical spinal cord injury. *PLoS ONE*, *12*(8). https://doi.org/10.1371/journal.pone.0182339

385. Sypecka, J., Koniusz, S., Kawalec, M., & Sarnowska, A. (2015). The organotypic

longitudinal spinal cord slice culture for stem cell study. *Stem Cells International*, *2015*. https://doi.org/10.1155/2015/471216

386. Takahashi, J. L., Giuliani, F., Power, C., Imai, Y., & Yong, V. W. (2003). Interleukin-1β promotes oligodendrocyte death through glutamate excitotoxicity. *Annals of Neurology*, *53*(5), 588–595. https://doi.org/10.1002/ANA.10519

387. Takahashi, K., & Yamanaka, S. (2006a). Induction of Pluripotent Stem Cells from Mouse Embryonic and Adult Fibroblast Cultures by Defined Factors. *Cell*, *126*(4), 663–676. https://doi.org/10.1016/j.cell.2006.07.024

388. Takahashi, K., & Yamanaka, S. (2006b). Induction of Pluripotent Stem Cells from Mouse Embryonic and Adult Fibroblast Cultures by Defined Factors. *Cell*, *126*(4), 663–676. https://doi.org/10.1016/j.cell.2006.07.024

389. Tanaka, E. M., & Ferretti, P. (2009). Considering the evolution of regeneration in the central nervous system. *Nature Reviews Neuroscience*, *10*(10), 713–723. https://doi.org/10.1038/nrn2707

390. Taoka, Y., Okajima, K., Uchiba, M., Murakami, K., Kushimoto, S., Johno, M., … Takatsuki, K. (1997). Role of neutrophils in spinal cord injury in the rat. *Neuroscience*, *79*(4), 1177–1182. https://doi.org/10.1016/S0306-4522(97)00011-0

391. Temple, S. (2001). The development of neural stem cells. *Nature*, *414*(6859), 112–117. https://doi.org/10.1038/35102174

392. Terada, N., Hamazaki, T., Oka, M., Hoki, M., Mastalerz, D. M., Nakano, Y., … Scott, E. W. (2002). Bone marrow cells adopt the phenotype of other cells by spontaneous cell fusion. *Nature*, *416*(6880), 542–545. https://doi.org/10.1038/NATURE730

393. Terranova, J. I., Ogawa, S. K., & Kitamura, T. (2019). Adult hippocampal neurogenesis

for systems consolidation of memory. *Behavioural Brain Research*, *372*(March). https://doi.org/10.1016/j.bbr.2019.112035

394. Theodore, N., Hlubek, R., Danielson, J., Neff, K., Vaickus, L., Ulich, T. R., & Ropper, A. E. (2016). First human implantation of a bioresorbable polymer scaffold for acute traumatic spinal cord injury: A clinical pilot study for safety and feasibility. *Neurosurgery*, *79*(2), E305–E312. https://doi.org/10.1227/NEU.0000000000001283

395. Tiwari, N., & Berninger, B. (2017). Transcriptional and Epigenetic Control of Astrogliogenesis. In *Essentials of Noncoding RNA in Neuroscience: Ontogenetics, Plasticity of the Vertebrate Brain* (pp. 177–195). https://doi.org/10.1016/B978-0-12-804402-5.00010-8

396. Toborek, M., Malecki, A., Garrido, R., Mattson, M. P., Hennig, B., & Young, B. (1999). Arachidonic acid-induced oxidative injury to cultured spinal cord neurons. *Journal of Neurochemistry*, *73*(2), 684–692. https://doi.org/10.1046/j.1471-4159.1999.0730684.x

397. Tönjes, M., Barbus, S., Park, Y. J., Wang, W., Schlotter, M., Lindroth, A. M., … Radlwimmer, B. (2013). BCAT1 promotes cell proliferation through amino acid catabolism in gliomas carrying wild-type IDH1. *Nature Medicine*, *19*(7), 901–908. https://doi.org/10.1038/nm.3217

398. Toyota, B., Carbonetto, S., & David, S. (1990). A dual laminin/collagen receptor acts in peripheral nerve regeneration (extracellular matrix/integrin). *Proc. Nati. Acad. Sci. USA*, *87*, 1319–1322.

399. Traynelis, S. F., Wollmuth, L. P., McBain, C. J., Menniti, F. S., Vance, K. M., Ogden, K. K., … Dingledine, R. (2010). Glutamate receptor ion channels: Structure, regulation, and function. *Pharmacological Reviews*. https://doi.org/10.1124/pr.109.002451

400. Trillium Gift of Life Network. (2015). Trillium Gift of Life Network - Ontario's Organ

and Tissue Donation Agency : Public Reporting. Retrieved November 28, 2019, from https://www.giftoflife.on.ca/en/professionals.htm

401. Trounson, A., & McDonald, C. (2015). Stem Cell Therapies in Clinical Trials: Progress and Challenges. *Cell Stem Cell*, *17*(1), 11–22. https://doi.org/10.1016/j.stem.2015.06.007

402. Tsai, E. C., Dalton, P. D., Shoichet, M. S., & Tator, C. H. (2004). Synthetic hydrogel guidance channels facilitate regeneration of adult rat brainstem motor axons after complete spinal cord transection. *Journal of Neurotrauma*, *21*(6), 789–804. https://doi.org/10.1089/0897715041269687

403. Tsai, E. C., Dalton, P. D., Shoichet, M. S., & Tator, C. H. (2006). Matrix inclusion within synthetic hydrogel guidance channels improves specific supraspinal and local axonal regeneration after complete spinal cord transection. *Biomaterials*, *27*(3), 519–533. https://doi.org/10.1016/j.biomaterials.2005.07.025

404. Tzouanacou, E., Wegener, A., Wymeersch, F. J., Wilson, V., & Nicolas, J. F. (2009). Redefining the Progression of Lineage Segregations during Mammalian Embryogenesis by Clonal Analysis. *Developmental Cell*, *17*(3), 365–376. https://doi.org/10.1016/J.DEVCEL.2009.08.002/ATTACHMENT/38DB3730-3B9F-4785-919E-BF8A7B962668/MMC1.PDF

405. Ung, R. V., Lapointe, N. P., Tremblay, C., Larouche, A., & Guertin, P. A. (2007). Spontaneous recovery of hindlimb movement in completely spinal cord transected mice: A comparison of assessment methods and conditions. *Spinal Cord*, *45*(5), 367–379. https://doi.org/10.1038/sj.sc.3101970

406. Van Der Laan, L. J. W., De Groot, C. J. A., Elices, M. J., & Dijkstra, C. D. (1997). Extracellular matrix proteins expressed by human adult astrocytes in vivo and in vitro: An

astrocyte surface protein containing the CS1 domain contributes to binding of lymphoblasts. *Journal of Neuroscience Research*, *50*(4), 539–548. https://doi.org/10.1002/(SICI)1097-4547(19971115)50:4<539::AID-JNR5>3.0.CO;2-F

407. Varghese, M., Olstorn, H., Berg-Johnsen, J., Moe, M. C., Murrell, W., & Langmoen, I. A. (2009). Isolation of Human Multipotent Neural Progenitors from Adult Filum Terminale. *Stem Cells and Development*. https://doi.org/10.1089/scd.2008.0144

408. Varma, A. K., Das, A., Wallace IV, G., Barry, J., Vertegel, A. A., Ray, S. K., & Banik, N. L. (2013). Spinal cord injury: A review of current therapy, future treatments, and basic science frontiers. *Neurochemical Research*, *38*(5), 895–905. https://doi.org/10.1007/s11064-013-0991-6

409. Verrier, L., Davidson, L., Gierliński, M., Dady, A., & Storey, K. G. (2018). Neural differentiation, selection and transcriptomic profiling of human neuromesodermal progenitor-like cells in vitro. *Development (Cambridge)*, *145*(16 Special Issue). https://doi.org/10.1242/dev.166215

410. Vogel, S., Schäfer, C., Hess, S., Folz-Donahue, K., Nelles, M., Minassian, A., … Aswendt, M. (2019). The in vivo timeline of differentiation of engrafted human neural progenitor cells. *Stem Cell Research*, *37*, 101429. https://doi.org/10.1016/j.scr.2019.101429

411. Wagner, F. B., Mignardot, J. B., Le Goff-Mignardot, C. G., Demesmaeker, R., Komi, S., Capogrosso, M., … Courtine, G. (2018). Targeted neurotechnology restores walking in humans with spinal cord injury. *Nature 2018 563:7729*, *563*(7729), 65–71. https://doi.org/10.1038/s41586-018-0649-2

412. Walker, T. L., & Kempermann, G. (2014). One Mouse, Two Cultures: Isolation and Culture of Adult Neural Stem Cells from the Two Neurogenic Zones of Individual Mice.

Journal of Visualized Experiments, (84), 1–9. https://doi.org/10.3791/51225

413. Waly, B. El, Macchi, M., Cayre, M., & Durbec, P. (2014). Oligodendrogenesis in the normal and pathological central nervous system. *Frontiers in Neuroscience*, *8*(8 JUN), 1–22. https://doi.org/10.3389/fnins.2014.00145

414. Wang, J., & Pearse, D. D. (2015). Therapeutic Hypothermia in Spinal Cord Injury: The Status of Its Use and Open Questions. *Int. J. Mol. Sci*, *16*, 16848–16879. https://doi.org/10.3390/ijms160816848

415. Wang, P., Wu, S., Zeng, X., Zhang, Y., Zhou, Y., Su, L., & Lin, W. (2018). BCAT1 promotes proliferation of endometrial cancer cells through reprogrammed BCAA metabolism. *International Journal of Clinical and Experimental Pathology*, *11*(12), 5536–5546.

416. Wang, S., He, Y., Zhang, H., Chen, L., Cao, L., Yang, L., … Li, Q. (2021). The Neural Stem Cell Properties of PKD2L1+ Cerebrospinal Fluid-Contacting Neurons in vitro. *Frontiers in Cellular Neuroscience*, *15*, 58. https://doi.org/10.3389/fncel.2021.630882

417. Wanner, I. B., Anderson, M. A., Song, B., Levine, J., Fernandez, A., Gray-Thompson, Z., … Sofroniew, M. V. (2013). Glial scar borders are formed by newly proliferated, elongated astrocytes that interact to corral inflammatory and fibrotic cells via STAT3-dependent mechanisms after spinal cord injury. *Journal of Neuroscience*, *33*(31), 12870–12886. https://doi.org/10.1523/JNEUROSCI.2121-13.2013

418. Waters, R L, Adkins, R. H., & Yakura, J. S. (1991). *Definition of Complete Spinal Cord Injury*. *Paraplegia* (Vol. 29). https://doi.org/10.1038/sc.1991.85

419. Waters, Robert L, & Adkins, R. H. (1994). Motor and Sensory Recovery Following Incomplete Tetraplegia. *Arch Phys Med Rehabil*, *75*.

420. Wehner, D., Tsarouchas, T. M., Michael, A., Haase, C., Weidinger, G., Reimer, M. M., … Becker, C. G. (2017). Wnt signaling controls pro-regenerative Collagen XII in functional spinal cord regeneration in zebrafish. *Nature Communications 2017 8:1*, *8*(1), 1–17. https://doi.org/10.1038/s41467-017-00143-0

421. Weidner, N., Rupp, R., & Tansey, K. E. (2017). *Neurological aspects of spinal cord injury*. *Neurological Aspects of Spinal Cord Injury*. https://doi.org/10.1007/978-3-319-46293-6

422. Weiss, S., Dunne, C., Hewson, J., Wohl, C., Wheatley, M., Peterson, A. C., & Reynolds, B. A. (1996). Multipotent CNS stem cells are present in the adult mammalian spinal cord and ventricular neuroaxis. *The Journal of Neuroscience : The Official Journal of the Society for Neuroscience*, *16*(23), 7599–7609. https://doi.org/10.1002/CNE.902890106

423. Wilson, J., Hashimoto, R., Dettori, J., & Fehlings, M. (2011). Spinal cord injury and quality of life: a systematic review of outcome measures. *Evidence-Based Spine-Care Journal*, *2*(01), 37–44. https://doi.org/10.1055/s-0030-1267085

424. Wilson, J. R., Cronin, S., Fehlings, M. G., Kwon, B. K., Badhiwala, J. H., Ginsberg, H. J., … Jaglal, S. (2020). Epidemiology and Impact of Spinal Cord Injury in the Elderly: Results of a Fifteen-Year Population-Based Cohort Study. *Journal of Neurotrauma*, *37*(15), 1740–1751. https://doi.org/10.1089/neu.2020.6985

425. Windle, W. F., Clemente, C. D., & Chambers, W. W. (1952). Inhibition of formation of a glial barrier as a means of permitting a peripheral nerve to grow into the brain. *The Journal of Comparative Neurology*, *96*(2), 359–369. https://doi.org/10.1002/CNE.900960207

426. Wu, Y., Streijger, F., Wang, Y., Lin, G., Christie, S., Mac-Thiong, J. M., … Li, L. (2016). Parallel Metabolomic Profiling of Cerebrospinal Fluid and Serum for Identifying

Biomarkers of Injury Severity after Acute Human Spinal Cord Injury. *Scientific Reports*. https://doi.org/10.1038/srep38718

427. Wurmser, A. E., & Gage, F. H. (2002). Cell fusion causes confusion. *Nature 2002 416:6880*, *416*(6880), 485–487. https://doi.org/10.1038/416485a

428. Xiao, D., Liu, X., Zhang, M., Zou, M., Deng, Q., Sun, D., … Xiang, M. (2018). Direct reprogramming of fibroblasts into neural stem cells by single non-neural progenitor transcription factor Ptf1a. *Nature Communications*, *9*(1). https://doi.org/10.1038/s41467-018-05209-1

429. Xiao, Q., Du, Y., Wu, W., & Yip, H. K. (2010). Bone morphogenetic proteins mediate cellular response and, together with Noggin, regulate astrocyte differentiation after spinal cord injury. *Experimental Neurology*, *221*(2), 353–366. https://doi.org/10.1016/j.expneurol.2009.12.003

430. Xiao, Z., Tang, F., Zhao, Y., Han, G., Yin, N., Li, X., … Dai, J. (2018). Significant Improvement of Acute Complete Spinal Cord Injury Patients Diagnosed by a Combined Criteria Implanted with NeuroRegen Scaffolds and Mesenchymal Stem Cells. *Cell Transplantation*, *27*(6), 907–915. https://doi.org/10.1177/0963689718766279

431. Xie, M., Tang, S., Li, K., & Ding, S. (2017). Pharmacological Reprogramming of Somatic Cells for Regenerative Medicine. *Accounts of Chemical Research*, *50*(5), 1202–1211. https://doi.org/10.1021/acs.accounts.7b00020

432. Xu, J., Du, Y., & Deng, H. (2015). Direct lineage reprogramming: Strategies, mechanisms, and applications. *Cell Stem Cell*. https://doi.org/10.1016/j.stem.2015.01.013

433. Yadav, A., Matson, K. J. E., Li, L., Hua, I., Gaur, P., Alkaslasi, M. R., … Levine, A. J. (2022). The Human Motoneuron Expression Signature is Defined by ALS-Related Genes.

BioRxiv, 2022.03.25.485808.

434. Yamazaki, K., Kawabori, M., Seki, T., & Houkin, K. (2020, June 1). Clinical trials of stem cell treatment for spinal cord injury. *International Journal of Molecular Sciences*. Multidisciplinary Digital Publishing Institute (MDPI). https://doi.org/10.3390/ijms21113994

435. Yang, S., Cao, Z., Zhu, J., Zhang, Z., Zhao, H., Zhao, L., … Wang, X. (2019). In Vitro Monolayer Culture of Dispersed Neural Stem Cells on the E-Cadherin-Based Substrate with Long-Term Stemness Maintenance. *ACS Omega*, *4*(19), 18136–18146. https://doi.org/10.1021/acsomega.9b02053

436. Yousefifard, M., Rahimi-Movaghar, V., Nasirinezhad, F., Baikpour, M., Safari, S., Saadat, S., … Hosseini, M. (2016). Neural stem/progenitor cells transplantation for spinal cord injury treatment; a systematic review and meta-analysis. *Neuroscience*, *322*(February), 377–397. https://doi.org/10.1016/j.neuroscience.2016.02.034

437. Yu, P., Wang, H., Katagiri, Y., & Geller, H. M. (2012). An in vitro model of reactive astrogliosis and its effect on neuronal growth. *Methods in Molecular Biology*, *814*, 327–340. https://doi.org/10.1007/978-1-61779-452-0_21

438. Yuan, X. B., Jin, Y., Haas, C., Yao, L., Hayakawa, K., Wang, Y., … Fischer, I. (2016). Guiding migration of transplanted glial progenitor cells in the injured spinal cord. *Scientific Reports*, *6*(March), 1–11. https://doi.org/10.1038/srep22576

439. Zakrzewski, W., Dobrzyński, M., Szymonowicz, M., & Rybak, Z. (2019). Stem cells: Past, present, and future. *Stem Cell Research and Therapy*, *10*(1), 1–22. https://doi.org/10.1186/S13287-019-1165-5/FIGURES/8

440. Zhang, F., Clarke, J. D. W., & Ferretti, P. (2000). FGF-2 up-regulation and proliferation of neural progenitors in the regenerating amphibian spinal cord in vivo. *Developmental*

Biology, *225*(2), 381–391. https://doi.org/10.1006/dbio.2000.9843

441. Zhang, J., & Jiao, J. (2015). Molecular Biomarkers for Embryonic and Adult Neural Stem Cell and Neurogenesis. *BioMed Research International*. https://doi.org/10.1155/2015/727542

442. Zhang, Q., Wu, X., Fan, Y., Jiang, P., Zhao, Y., Yang, Y., … Dai, J. (2021). Single-cell analysis reveals dynamic changes of neural cells in developing human spinal cord. *EMBO Reports*, *22*(11), e52728. https://doi.org/10.15252/embr.202152728

443. Zhou, X., He, X. J., & Ren, Y. (2014). Function of microglia and macrophages in secondary damage after spinal cord injury. *Neural Regeneration Research*, *9*(20), 1787–1795. https://doi.org/10.4103/1673-5374.143423

444. Zivkovic, S., Ayazi, M., Hammel, G., & Ren, Y. (2021). For Better or for Worse: A Look Into Neutrophils in Traumatic Spinal Cord Injury. *Frontiers in Cellular Neuroscience*, *15*(April), 1–10. https://doi.org/10.3389/fncel.2021.648076

445. Zukor, K., Belin, S., Wang, C., Keelan, N., Wang, X., & He, Z. (2013). Short hairpin RNA against PTEN enhances regenerative growth of corticospinal tract axons after spinal cord injury. *Journal of Neuroscience*, *33*(39), 15350–15361. https://doi.org/10.1523/JNEUROSCI.2510-13.2013